Airports as Energy Nodes (ÆNodes) Project Report

Darren Paschedag, Bryan Mentlik, Kevin Robby, Bhavesh Rathod, Myles Kelly, Bidur Poudel, Shubhasmita Pati, Bharatkumar Solanki, Rob Hovsapian, Scott Cary

National Laboratory of the Rockies

The National Laboratory of the Rockies is a national laboratory of the U.S. Department of Energy, Office of Critical Minerals and Energy Innovation, operated under Contract No. DE-AC36-08GO28308.

This report is available at no cost from the National Laboratory of the Rockies (NLR) at www.nlr.gov/publications.

Technical Report
NLR/TP-5R00-98503
July 2026

National Laboratory of the Rockies

Airports as Energy Nodes (ÆNodes) Project Report

Darren Paschedag, Bryan Mentlik, Kevin Robby, Bhavesh Rathod, Myles Kelly, Bidur Poudel, Shubhasmita Pati, Bharatkumar Solanki, Rob Hovsapian, Scott Cary

National Laboratory of the Rockies

Suggested Citation
Paschedag, Darren, Bryan Mentlik, Kevin Robby, Bhavesh Rathod, Myles Kelly, Bidur Poudel, Shubhasmita Pati, Bharatkumar Solanki, Rob Hovsapian, Scott Cary. 2026. *Airports as Energy Nodes (ÆNodes) Project Report.* Golden, CO: National Laboratory of the Rockies. NLR/TP-5R00-98503. https://www.nlr.gov/docs/fy26osti/98503.pdf.

The National Laboratory of the Rockies is a national laboratory of the U.S. Department of Energy, Office of Critical Minerals and Energy Innovation, operated under Contract No. DE-AC36-08GO28308.

This report is available at no cost from the National Laboratory of the Rockies (NLR) at www.nlr.gov/publications.

Technical Report
NLR/TP-5R00-98503
July 2026

National Laboratory of the Rockies
15013 Denver West Parkway
Golden, CO 80401
303-275-3000 • www.nlr.gov

NOTICE

This work was authored by the National Laboratory of the Rockies for the U.S. Department of Energy (DOE), operated under Contract No. DE-AC36-08GO28308. Funding provided by the National Aeronautics and Space Administration (NASA) under Agreement IAG-24-24860. The views expressed herein do not necessarily represent the views of the DOE or the U.S. Government.

This report is available at no cost from the National Laboratory of the Rockies (NLR) at www.nlr.gov/publications.

U.S. Department of Energy (DOE) reports produced after 1991 and a growing number of pre-1991 documents are available free via www.OSTI.gov.

Cover photo by Josh Bauer, National Laboratory of the Rockies 061725.

The National Laboratory of the Rockies prints on paper that contains recycled content.

Acknowledgments

The National Laboratory of the Rockies team thanks Nicholas Borer, Nathaniel Blaesser, Michael Patterson and everyone else on the Convergent Aeronautics Solutions project team at the National Aeronautics and Space Administration for their labor, guidance, and overall support of this work. The laboratory team would also like to thank NASA's Aeronautics Research Mission Directorate for financially supporting this work.

List of Acronyms

AAM	advanced air mobility
ÆNodes	Airports as Energy Nodes
AEU	annual energy used
ANOVA	analysis of variance
ARIES	Advanced Research on Integrated Energy Systems
BAU	business as usual
BCOC	break-even cost of charging
BESS	battery energy storage system
BLDG	building
BMS	battery management system
C	critical
CAPEX	capital expenditure
CCS	Combined Charging System
CHP	combined heat and power
CONUS	contiguous United States
DER	distributed energy resource
DISCO	Distribution Integration Solution Cost Options
EERC	Energy Escalation Rate Calculator
eGA	electric general aviation
eGSE	electric ground support equipment
eRAM9	9-passenger fixed-wing fully electric regional air mobility
ERP	Energy Resilience Performance
EV	electric vehicle
EVSE	electric vehicle supply equipment
eVTOL	electric vertical takeoff and landing
FAA	Federal Aviation Administration
FCR	fixed charge rate
FOC	fixed operating cost
GA	general aviation
GDT	generic digital twin
GEACS	Global Electric Aviation Charging System
GFL	grid following
GFM	grid forming
GS	general service
GSD	general service demand
GSE	ground support equipment
GST	general service time of use
GSTD	general service time-of-use demand
HIES	hydrogen-based integrated energy system
hRAM19	19-passenger fixed-wing hybrid regional air mobility
HVAC	heating, ventilation, and air conditioning
HVN	Tweed New Haven Airport
IFR	instrument flight rules
ITC	investment tax credit
kW	kilowatt

kWh	kilowatt-hour
LCC	life cycle cost
LCOE	levelized cost of energy
MCS	Megawatt Charging System
MW	megawatt
NASA	National Aeronautics and Space Administration
NC	noncritical
NIST	National Institute of Standards and Technology
NLR	National Laboratory of the Rockies
nmi	nautical mile
NPV	net present value
NSRDB	National Solar Radiation Database
O&M	operations and maintenance
OKV	Winchester Regional Airport
PCC	point of common coupling
PLL	phase-locked loop
PV	photovoltaics
RAM	regional air mobility
REC	renewable energy credit
RTDS	real-time digital simulation
SC	semicritical
SCADA	supervisory control and data acquisition
SMR	small modular reactor
SOC	state of charge
SRP	survival resilience period
TCC	total capital cost
UAM	urban air mobility
UI	United Illuminating
VALE	Voluntary Airport Low Emission Program
VARF	Virginia Airport Revolving Fund
VFR	visual flight rules

Executive Summary

Aviation is experiencing an influx of electrified aircraft in the advanced air mobility (AAM) space. The goal of the Airports as Energy Nodes (ÆNodes) project was to evaluate the impact of AAM and other advanced aircraft adoption growth on the electrical system of existing small to medium hub regional airports to better prepare them for the future while also enhancing resilience for the airports and the surrounding communities.

AAM small passenger air service encompasses vertical takeoff and landing, flight training and other general aviation (GA) operations, and 9- to 30-passenger conventional aircraft for regional air mobility (RAM) applications—all of which include electrically-, hybrid-electrically, or hydrogen-powered varieties. Some challenges that ÆNodes was trying to address include how to use the existing airport infrastructure in a way that is robust to meet the energy needs of AAM growth while also leveraging any airport-hosted energy assets for the surrounding community in emergency situations. Figure ES-1 illustrates an airport design at a high-level with installs of electric vehicle charging equipment and local energy generation (e.g., photovoltaics, battery storage, and hydrogen) to support AAM growth and community needs.

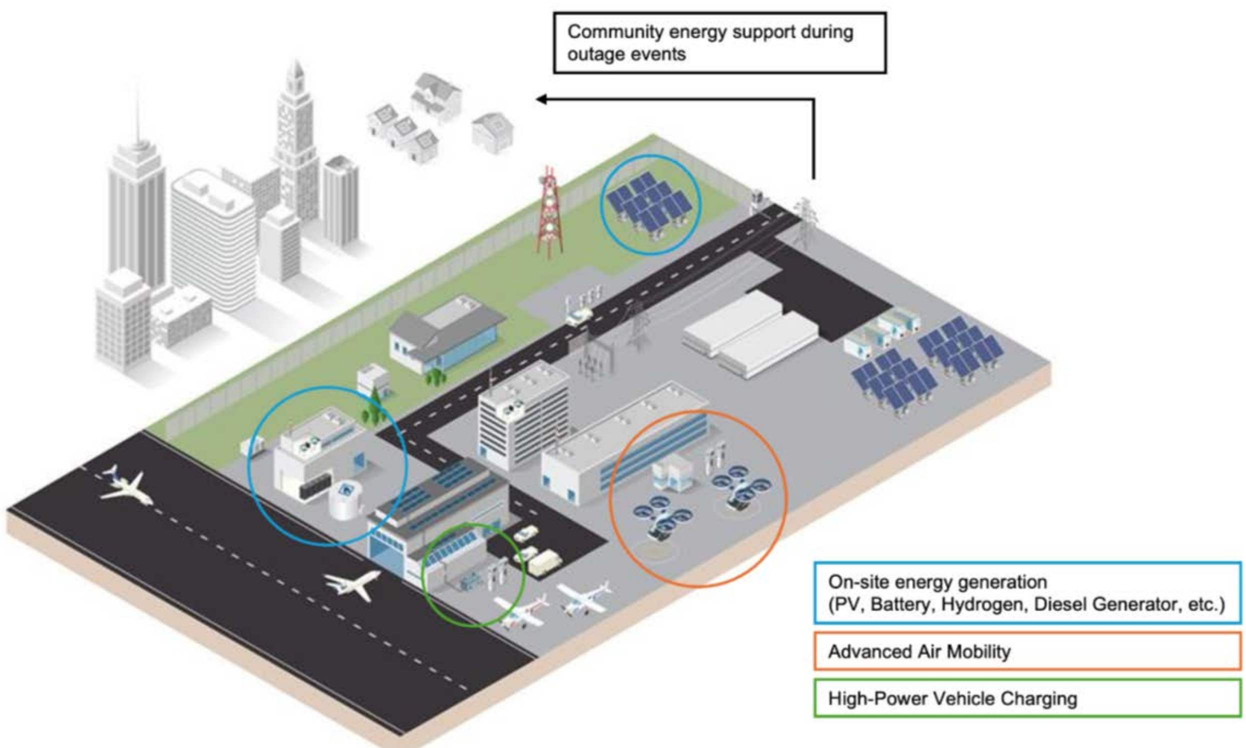

Figure ES-1. Example airport installation with electric aircraft and local energy generation.

Illustration by Anthony Castellano, National Laboratory of the Rockies

It is impossible to develop a generic airport representation to do this work due individual airport complexities so partnering with representative airports was paramount. Building partnerships was necessary for this study to succeed because the work requires a large amount of information sharing among partners. Figure ES-2 illustrates the organizational structure of the project. The National Aeronautics and Space Administration (NASA) led effort with the National Laboratory of the Rockies (NLR) as a key partner. This publication covers NLR's portion of the work; for NASA's portion please see (N. K. Borer et al., 2025).

The selected partner airports included Winchester Regional Airport (OKV), in Winchester, Virginia, near Washington, D.C., which is not a Part 139[1] airport and Tweed New Haven Airport (HVN), in New Haven, Connecticut, near the New York City metropolitan area and is a Part 139 airport. Each airport's electric utility provider also participated, Rappahannock Electric Cooperative for OKV and United Illuminating (UI) for HVN. OKV is a small airport that services primarily GA but also business aviation, charger flights, and cargo and flight training operations. HVN is a midsize airport with one commercial carrier.

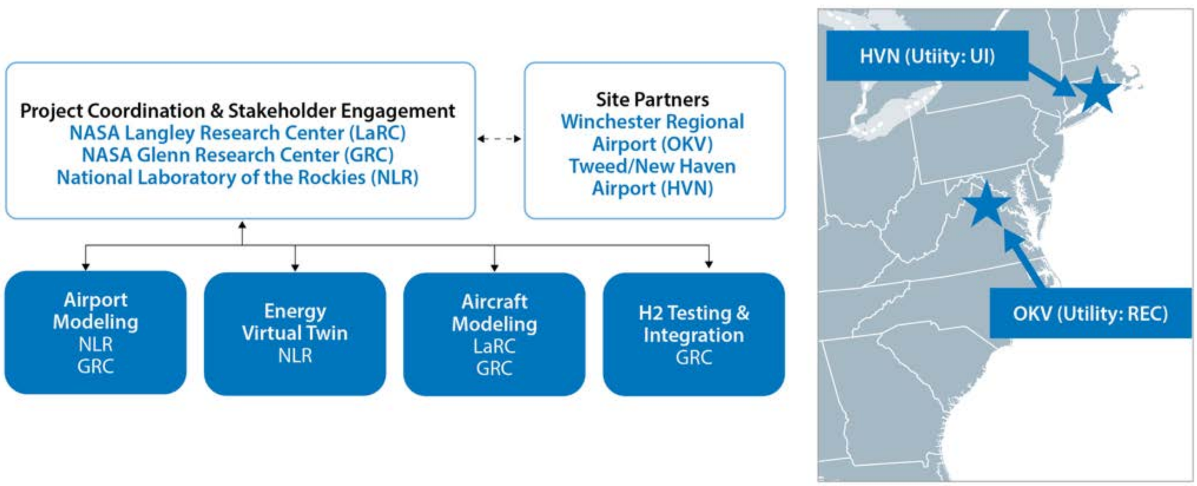

Figure ES-2. Project partnerships and airport locations.

Illustration by Anthony Castellano, National Laboratory of the Rockies

The work NASA and NLR performed for this project involved:

1. Forecasting advanced air traffic at both airports based on future projections.
2. Forecasting increased electric loads due to airport building electrification.
3. Estimating vehicle battery sizes for each aircraft type based on the energy needed to complete the forecasted routes.
4. Generating electrical demand associated with aircraft charging (also including ground support equipment and customer vehicles in addition to aircraft) using aircraft ground (dwell) time taken from existing flight schedules. Energy demand modeling was done modeling using a modified version of NLR's EVI-EnSite[2] tool.

[1] See https://www.faa.gov/airports/airport_safety/part139_cert
[2] See www.nlr.gov/transportation/evi-ensitepy.

5. Performing techno-economic and robustness analysis on each site using the vehicle charging power demand and existing site load demand with NLR's REopt®[3] model to determine cost metrics and recommended generation sources for each site.
6. Analyzing the grid interconnection potential of on-site generation with the local electric grid to provide community energy resilience in case of a regional outage.
7. Constructing a digital twin of OKV's power system to validate the operational viability of the REopt-identified generation sources to help inform the airport before procurement.

Throughout this work, NASA and NLR developed and applied models and tools to the partner airports to assist them in their AAM goals. In addition, the teams demonstrated a blueprint that can be applied to other regional airports or scaled to support the adoption of AAM aircraft at larger airports. The key achievements of this work include:

1. Developed realistic models of electrified aircraft schedules and energy models that represent future aircraft into the 2035 time horizon
2. Sized local generation installations using scenarios such as cost-efficiency and outage ride-through probability to give airport operators an idea of what sizes to target
3. Developed a new tool, called REopt-Insight, to further explore the robustness of a design and provide the airport operator key insights, such as what external factors will make an installation more viable
4. Developed an accurate digital twin of OKV that allowed for the placement and viability testing of the generation assets to highlight any issues or other required upgrades to the associated infrastructure before the airport operator starts a project.

This work found that the loads associated with AAM adoption are substantial and could surpass the current electric loads at smaller airports like OKV and HVN. The power demanded by AAM depends on the charge rate, with maximum charging powers ranging from 350 kW to greater than 1 MW per charger and can result in large peaks that could grow with the needs of AAM aircraft and the increasing flight scheduling complexity that comes with increasing AAM adoption. Energy usage for charging is also significant, with some projected aircraft using battery capacities up to 746 kWh each.

Airports can choose to engage their electric utility to serve existing loads and any anticipated AAM related loads; however, solely relying on the utility might not be the most expeditious or least-cost way of serving these electric loads. Therefore, it is critical that airports proactively work with their utilities to learn about electric tariff options and other programs that could provide cost savings. Choosing to wait to settle on the electricity supply for new EVSE loads can lock in the airport to excessively high electric utility bills and distribution infrastructure upgrade costs. Electrical utility connection issues can also arise that delay EVSE projects by many years, so advanced infrastructure planning can help to alleviate that.

The financial viability of supporting these loads is highly dependent on existing utility rate structures and government incentives which vary across the nation. Robust generation installations that can support outages were found to not be financially viable in general, but since the cost associated with outages are hard to model because they are highly dependent on the

---

[3] See reopt.nlr.gov/tool.

outage time value for a particular operator, it could become viable if that outage time cost is considered. When considering only robustness and the ability to ride through an outage, the land that a regional airport can build on holds great potential. Developing this space for local energy generation could enable the airports to serve the energy demands of the local community in emergency situations such as a natural disaster or other long-term outage thus turning the airport into an energy node for their communities. Enabling local community members to use an airport's facilities during an outage can be invaluable and could justify modest or poor economic projections from on-site generation systems.

If an airport chooses to maximize generation capability on their grounds to act as an energy source for their community, they could potentially dispatch substantial power to the local grid either during outages or during times of high electricity demand and help critical local facilities remain online. The value of a lost load for a nearby hospital, supermarket, or law enforcement center can be challenging to quantify for comparison against the cost incurred for system installation. Additionally, surplus generation from an airport installation can add flexibility in power generation to the local distribution feeder. The additional capacity can help reduce electrical capacity demand from the community and allow electric utilities to bring large-load customers (such as data centers) online faster compared to constructing new power plants.

Systems of this size require advanced planning which is where a digital twin of the airport infrastructure is most valuable. Using the airport digital twin the NLR team was able to test several generation combinations and AAM load scenarios to ensure that the installation would perform as intended and helped identify additional electrical system upgrades required to support the generation equipment.

Table of Contents

List of Figures

List of Tables

1 Project Overview

The Airports as Energy Nodes (ÆNodes) project has three goals:

1. Improve the viability of small to medium hub airports through the adoption of electric aircraft and understanding how the airports will adapt to these new substantial electric loads.
2. Identify locations at each airport for potential electric vehicle supply equipment (EVSE) siting and on-site energy generation to offset these new loads.
3. Understand the viability of using the airports as small regional nodes that could generate energy and export it to the nearby grid to maintain critical services in case of a regional power outage.

Small and regional airports are plentiful and spread across population centers in the contiguous United States (CONUS) (see Figure 1), totaling 4,059 (N. Borer, 2023), and often contain a large amount of open space that can be utilized for energy generation for both the flying and non-flying public. Recognizing this potential, the National Aeronautics and Space Administration (NASA) and the National Laboratory of the Rockies (NLR) partnered to determine the viability of on-site energy generation to offset increasing loads and build energy resilience at critical infrastructure and local communities. Preparing airports for these new aircraft involves a multiteam effort in vehicle scheduling and modeling, electric load generation, techno-economic analysis of generation sources, energy generation source sizing, and energy generation performance validation.

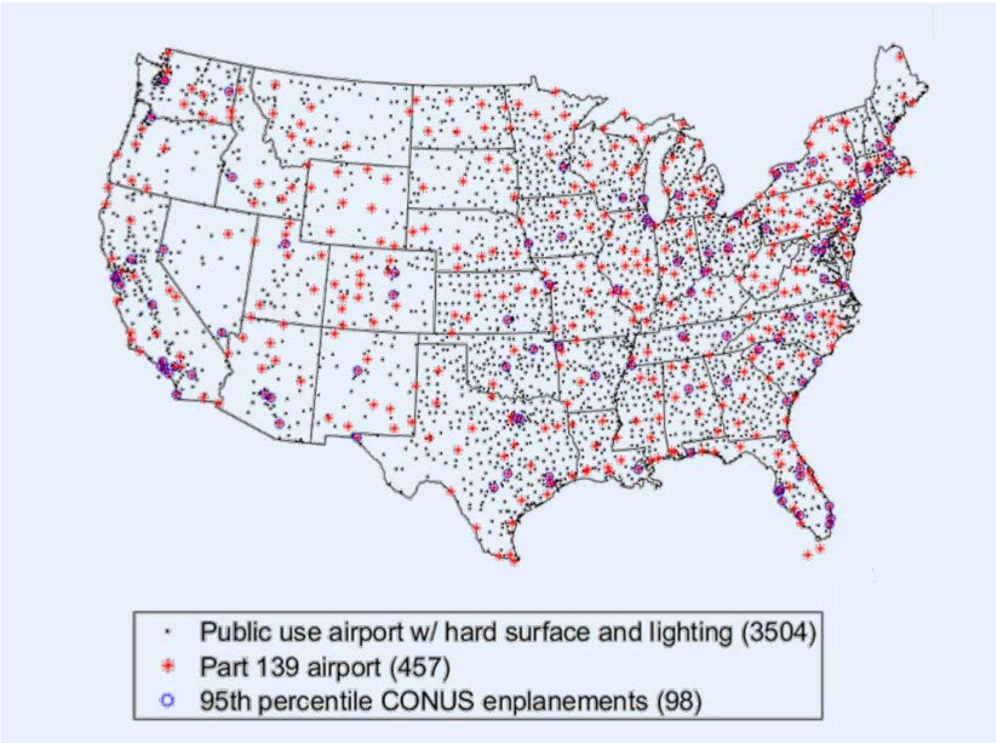

Figure 1. Map of CONUS small and regional airports.

Source: (N. Borer, 2023)

NASA's ÆNodes activity, under Aeronautics Research Mission Directorate (ARMD) Advanced Concepts group, partnered with NLR for this effort. The NASA team contributed aircraft models, adoption rates, and forecasted traffic, and the NLR team applied their energy modeling and techno-economic expertise. Two partner airports were chosen primarily based on their classification (Part 139 versus not), proximity to larger cities to support traffic demand, and existing partnerships with their electric utilities: Winchester Regional Airport (OKV), in Winchester, Virginia, and Tweed New Haven Airport (HVN), in New Haven, Connecticut, with Rappahannock Electric Cooperative and United Illuminating (UI), respectively.

Figure 2 illustrates the NLR-NASA workflow for this analysis. Future charging loads were generated using NLR's EVI-EnSite tool and the NASA-provided air traffic and energy requirement data along with ground vehicle charging expectations for each airport to generate a time-series power load. The power load was based on electric vehicle (EV) models, both aircraft and ground, sized to match the performance and capacity of the conventional vehicles they will replace.

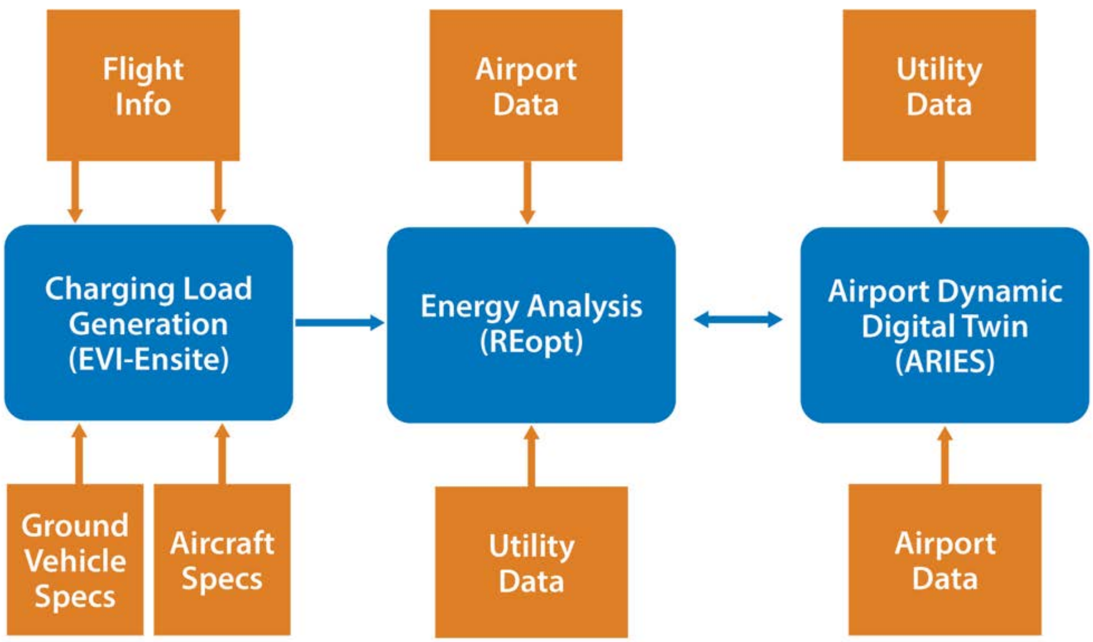

Figure 2. Project tool chain and data flow.

Illustration by Anthony Castellano, National Laboratory of the Rockies

The power load associated with vehicle charging was then incorporated with the existing building loads (and any future expansions shared by the airport) to perform the techno-economic analysis with NLR's REopt® tool, which sizes generation sources (e.g., photovoltaics (PV), battery energy storage systems (BESS), diesel generation) based on utility and airport data for different use case scenarios. These scenarios are then passed to a digital twin of the airport's electrical system that uses NLR's Advanced Research on Integrated Energy Systems (ARIES)[4]

[4] See www.nlr.gov/aries.

real-time simulation capability to model the generation sources for each scenario to de-risk an install by validating the performance of the assets and providing feedback on the physical placement and electrical connections. Any issues with energy source sizing, like inability to serve the load, resulted in the REopt team performing further analysis.

2 Data Sourcing

The modeling performed in this effort required a large amount of data from the participating airports, their utilities, and NASA. The data required from HVN and OKV and their utilities ranged from current utility electrical usage, to future upgrade plans, and the current airport utilization level. NASA provided air traffic forecasts for each airport (N. K. Borer et al., 2025) that enabled the charging load estimates to be performed.

The requested information fell into three categories: data on the airports, data specific to the utilities, and data on vehicles that operate at the airports.

2.1 Airport Data

Table 1 lists the requested information from each airport. Information on the physical layout and equipment in use at each airport as well as future expansion plans and market information was critical to this study.

Table 1. Data Requested from Airport Partners

Data	Description
Airport location	Latitude and longitude
On-site energy assets	PV, BESS, diesel or natural gas generators, etc.
Space available for generation sources	Rough estimate of land available for construction of new generation sources
Map of airport	With land use classifications to help with generation site selection
Airport critical loads	What loads are critical for airport operation, what is their peak load value, when does that peak load occur, and what meter(s) are they connected to?
List of any EVSE at the airport	Does the airport currently support vehicle charging for GSE or customers?
Airport use	What different areas does the airport serve (commercial, GA, cargo, flight training, etc.)?
Future upgrade plans	Any plans to upgrade airport terminal(s), vehicle charging, etc.?
List of ground support equipment (GSE)	List all GSE in use at the airport and any plans to electrify them.

2.2 Utility Data

Table 2 lists the requested information from each partner utility. The requested information focuses on load history, outage history, power system design, branch capacity, and existing or future tariffs specifically related to vehicle charging.

Table 2. Data Requested from Utility Partners

Data	Description
Airport power outage history	Time, duration, frequency, etc.
Network information	Single-line diagrams, current line utilization or capacity for additional load, current substation utilization, time period of peak network congestion, supervisory control and data acquisition (SCADA) data
Tariffs	Current rate tariffs and any plans for future changes in tariffs specifically targeting EV charging
Planned local distribution upgrades	Any local distribution upgrades planned by the utility
Existing network models	Any existing power system models of the current system
Meter information	Required for each meter: meter ID, associated tariff name, voltage level, 12 months of hourly or sub-hourly load data, 12 months of electric bills

2.3 Ground Vehicle Data

Table 3 lists the requested information from each airport regarding ground vehicles that operate at their airport.

Table 3. Data Requested from Airports on Ground Vehicles

Data	Description
Rental car offerings	Do rental car companies operate at the airport, and are they interested in electrification?
List of GSE and plans for future expansion	What GSE is currently operated at the airport, are there any plans for expansion in the future, and will that include electrification?
Customer vehicle charging	Do you have EVSE installed for customer vehicles? If so, how many, and what is their power capacity?

3 Considered Energy Sources

Energy asset planning for airports requires balancing cost, sustainability, resilience, and regulatory compliance. This section summarizes a high-level, initial review of emerging and available energy technologies which offer viable means of reducing the airport's utility costs while improving the site's robustness against utility outages. Table 4 summarizes the energy sources considered for this work. Not all sources listed here were used in the analysis. A detailed description of the analysis around each technology is presented in Appendix D.

Table 4. Possible Energy Generation Technologies

Technology	Maturity (2025)	Typical Capital Costs/ Financial Benefit	Energy Resilience Contribution	Key Challenges
Battery Storage	**Commercial**: Mainstream	**Medium**: $400–500/kWh (Cole, 2023) Can make variable energy sources more cost-effective Can reduce time-of-use and demand charges	**High:** Potentially fast response, limited duration	High capital expenditure (CAPEX)Degradation/ replacement after approx. 10 years Fire safety management and codes
Ground-source heat pumps	**Commercial**: Large projects are becoming more common.	**High:** ~$1,075/ton (RSMeans 2018 for 5-ton unit) Highly variable depending on drilling costs. Reduces heating and cooling costs Minimal maintenance costs once installed	**Low:** Could provide passive survivability benefits. Typically used for heating and cooling loads, not as an energy generator, requires power to function	High up-front cost vs. savings Need drilling and land area
Cold temperature storage	**Commercial:** Mainstream	**Low:** $1.9/gal (Glazer, 2019) Requires chillers and ice tanks Reduces cooling bills	**Medium:** Can potentially provide cooling during an outage, but pumps and fans are still required to operate and will use some energy	Requires space for tank Integration with heating, ventilating, and air-conditioning system

Solar PV	**Commercial:** Mainstream	**Low:** $1,000–2,000/kW (Ramasamy, 2023) Protects against utility bill increases No fuel required after initial CAPEX	**Medium:** Daytime power (nighttime needs would require energy storage), reduces grid reliance	Requires large land area or roof space Variable energy source Requires glare mitigation consideration
Natural gas combined heat and power (CHP)	**Commercial:** Mainstream	**Medium:** CAPEX: $1,600–3,400/kW (Desai, 2020), fuel cost: $5.60/MMBtu (January 2025) (EIA 2025) Natural gas is usually cheaper than electricity.	**Very high:** On-site generation can potentially maintain airport power during larger grid outages, if natural gas is available.	Needs reliable fuel (natural gas) Complex to maintain/operate
Hydrogen	**Early:** Pilot projects are underway.	**High:** Electrolyzers: $800–1,500/kW (DOE HFTO 2020), H_2 fuel: $5–6/kg (DOE HFTO 2020) Fuel cells, combustion turbines, or hydrogen-powered vehicles are also required at a high cost.	**High:** Similar benefits to CHP, but only if hydrogen is consistently available	Fuel infrastructure immature. Very costly fuel; price expected to decrease. Safety protocols and new regulations needed Low round-trip efficiency from electricity
Nuclear small modular reactor	**Research and development:** No currently operating plant	**Very high**: Current estimates are uncertain. Small modular reactors are unlikely to become cost-effective in the near future.	**Very high:** Continuous generation regardless of weather; minimal refueling required	Regulatory approval lengthy and uncertainPublic acceptance challenges Low technology readiness level; no market technologies High cost
Wind	**Commercial:** Mainstream	**Low:** <$2,000/kW (Stehly, Duffy, & Hernando, 2024)	**Medium:** Can be consistent in areas with a reliable wind resource	Tall turbines violate Federal Aviation Administration Part 77 May cause issues with turbulence, sightlines, and radar

Geothermal power generation	**Commercial:** Traditional **Emerging:** Enhanced	**Medium-High:** \$3,000–6,000/kW Highly variable depending on local resource availability (US Department of Energy, 2019)	**Very high:** Nonintermittent renewable resource	Highly location dependent Expensive/uncertain initial geological surveys required

[a] Typical capital costs and potential savings are estimates only.

[b] Resilience benefits can only be achieved if on-site generation resources are designed to be resilient (e.g., connected via a microgrid and operable during an outage).

This project primarily examines solar PV and battery storage as candidate technologies for airport energy systems due to their well-established market maturity, standardized deployment pathways, and relative ease of implementation. Note that a glare analysis will be needed for any solar installations at federally-funded airports; this was not considered in the designs presented in this report. Combined heat and power (CHP) was briefly evaluated during the preliminary analyses, with some scenarios indicating potential cost savings; however, these benefits were small and largely offset once the significant infrastructure requirements for additional natural gas lines were accounted for, along with the higher ongoing operations and maintenance costs associated with specialized staffing. Although CHP can provide substantial value at large hub airports, such as John F. Kennedy International Airport or Los Angeles International Airport, the scale of HVN and OKV is insufficient to justify its inclusion in later stages of the analysis.

Thermal energy storage was not considered because the analysis focused on EVSE loads rather than heating, ventilating, and air-conditioning-driven demand. Emerging technologies, such as hydrogen-based systems and small modular reactors, remain too early in their development to support reliable cost modeling and are unlikely to be commercially viable in the near term. Geothermal, hydro, wave, and tidal resources were excluded due to their strong location dependence and limited feasibility at the sites considered.

Finally, although wind power is a mature technology, the challenges of siting turbines near airports—particularly related to airspace, sightlines, and turbulence—make on-site deployment impractical. As a result, wind is best pursued through off-site procurement mechanisms, such as power purchase agreements, if they are included in an airport's energy portfolio.

4 EVI-EnSite Charging Load Generation

NLR's EVI-EnSite tool is used for charging station design, modeling, and analysis at a specific site. For this study, charging infrastructure was sized to meet critical operational turnaround times—defined as the shortest duration an aircraft spends at the gate between arrival and departure so that the inclusion of electrified aircraft in the operating cadence is easier by removing charging-related schedule shifts. Due to the relatively low flight volume at both airports in the study, only one charger per aircraft type was modeled for the charging scenarios. The different aircraft types with their battery details and their arrival schedules were provided by NASA researchers (N. K. Borer et al., 2025) and included the arrival state of charge (SOC), the dwell time or time on the ground before next departure, and the minimum energy required to meet the next flight mission. This section describes the methodology used in converting the aircraft details and arrival schedules into charging loads that could then be used in the techno-economic modeling and analysis to determine the cost-effective on-site generation and storage assets that would be needed to meet the new forecasted charging demand.

4.1 EVI-EnSite Modeling Requirements

The EVI-EnSite charging simulation tool requires a list of vehicle arrivals at a charging station with specific battery details provided for each type of EV in the arrival list. Details on the charging infrastructure, such as charger power and number of chargers, are also needed to model the charging station. The required vehicle battery details include the battery's energy capacity, the arrival SOC of the battery, the target departure SOC of the battery, and a charge acceptance curve for the appropriate charging rate.

4.2 Charger Background

EVSE power sizing ranges from less than 10 kW (Level 1 and Level 2 AC chargers) to tens or hundreds of kilowatts (DC fast chargers), to multiple megawatts per charger (Megawatt Charging Systems (MCS) chargers). Some aircraft original equipment manufacturers (OEMs) use existing automotive connectors and standards, such as the Combined Charging System (CCS) plug (using the International Electrotechnical Commission 62196 standard) and protocol. This typically allows for maximum power up to 350 kW and the use of existing automotive EVSE hardware or development of in-house CCS chargers, such as BETA's Charge Cube (BETA n.d.).

Current developments in heavy-duty charging have led to CharIN's MCS standard (CharIN 2025), which allows for a maximum power rating of 3.75 MW. Airframers can also consider this standard for aviation as well.

Electric vertical takeoff and landing (eVTOL) manufacturer Joby has been working on their own, aviation-specific charging system standard, called the Global Electric Aviation Charging System (GEACS) (Joby n.d.). It includes charging power, secure data transfer, and liquid cooling connectors in the same cable and allows for charging up to 300 kW.

4.3 Aircraft Types and Battery Details

The NASA-provided schedule of flight arrivals included four different types of electric and hybrid-electric aircraft (N. K. Borer et al., 2025). The battery capacities for the four aircraft types ranged between 140 kWh for the electric general aviation (eGA) aircraft and 746 kWh for the regional air mobility (RAM) 9-passenger fully electric fixed-wing aircraft (eRAM9), as shown in Table 5. The eVTOL aircraft for urban air mobility (UAM) operations included in the model had a battery capacity of 341 kWh, and the 19-passenger hybrid fixed-wing aircraft (hRAM19) had a battery capacity of 440 kWh. See (N. K. Borer et al., 2025) for more specific information on the aircraft models.

Table 5. Aircraft Battery Sizing

Aircraft Type	Maximum Battery Capacity
eGA	140 kWh
eRAM9 (9-passenger fully electric)	746 kWh
hRAM19 (19-passenger hybrid-electric)	440 kWh
eVTOL (UAM operations)	341 kWh

Charge acceptance curves, or power charging curves, describe the amount of power drawn from the charger as the aircraft battery's SOC increases. Charge acceptance curves for these hypothetical aircraft were estimated using a physics-based model written in MATLAB. Assuming a constant-current constant-voltage charging method with no battery management system (BMS), a theoretical charge acceptance curve was derived for each aircraft battery at various charging rates. The modeled charge acceptance curves are described in more detail in Section 4.5 Charging Infrastructure Analysis to determine the charger sizing.

4.4 Flight Schedules and Energy Requirements

A key component needed to model electric aircraft charging loads at the two airports is the flight arrival and departure schedules provided by the NASA research team. The NASA-provided flight data included a full year of energy and scheduling information (N. K. Borer et al., 2025). The forecasted flight data are generated using three separate methods, one for each aircraft type. The general aviation and flight training forecasts are based on actual 2024 flight and weather data at each airport. UAM operations, which refer to eVTOL flights, were forecasted by NASA researchers who developed a flight demand model specific for UAM operations. Finally, the 9-passenger full-electric and 19-passenger hybrid-electric demand were included from a previous Georgia Tech study (Justin et al., 2022), with adjustments to power requirements of 150% to align with updated technology projections and considering flight modifications due to weather or weekend traffic (N. K. Borer et al., 2025). The flight schedule for each airport included the arrival and departure times, the aircraft type, the arrival SOC, and the minimum energy required for the next flight. NASA provided schedules for three different time frames: a baseline 2024 flight schedule (ET1), an estimated traffic scenario forecasted for 2035–2040 (ET2), and a refined version of the 2035–2040 flight forecasts (ET2+). The refined ET2+ forecasts included improved weather data interpolation and used 2024 as the seed year in the model. A sample flight schedule for the OKV ET2+ scenario is presented in Table 6, with a description of the data column names included in Table 7.

Table 6. Sample OKV ET2+ Data

Aircraft Category	Arrival Time	Departure Time	Landing SOC (%)	Min. Energy Used (kWh)	Min. Energy Needed (kWh)	Outer Diameter (OD) Distance (nmi)	Aircraft Type
UAM	1/1/2035 12:23:45	1/1/2035 15:02:57	50	136.15	174.34	57.82	Lift + cruise
eRAM9	1/1/2035 8:43:45	1/1/2035 17:45:00	64	193.37	638.60	125.70	9-passenger
eRAM9	1/1/2035 9:43:45	1/1/2035 17:45:00	68	161.81	587.64	103.70	9-passenger
hRAM19	1/1/2035 9:08:06	1/1/2035 17:45:00	80	42.56	203.74	68.70	19-passenger

Table 7. Scenario Column Descriptions

Data	Description
Aircraft category	Category flag used to identify behavior/energy consumption.
Arrival time	Arrival time in UTC used to set the start of ground time. In all cases, the arrival time is assigned via quasi-random process because tail number continuity could not be established in the dataset, so detailed scrutiny could result in inconsistencies.
Departure time	Departure time in UTC used to set the end of ground time. This generally corresponds with an observed departure time in the Sherlock[5] dataset.
Landing SOC	Estimate of battery SOC for the aircraft upon landing. Assumes departing at 90% SOC and 100% state of health and using the "Min energy used (kWh)" assumption below. (This assumes that batteries at 90% state of health could depart at 100% SOC, etc.)
Min. energy used (kWh)	Estimate of minimum amount of onboard battery energy (in good weather, at 90% SOC/100% state of health at departure) the aircraft would consume prior to arrival. Does not account for significant routing variation or weather contingencies.
Min. energy needed (kWh)	Estimate of amount of onboard battery energy the aircraft would need to have onboard prior to departure, assuming the destination airport is in the same weather category as the departure (home) airport at the time of departure. Considers visual flight rules (VFR), VFR night, instrument flight rules (IFR), and IFR with alternative reserves.
OD distance (nmi)	Great circle distance between the point of departure (current airport) and the destination.

[5] See https://www.nasa.gov/ames/aviationsystems/sherlock-data-warehouse/

NLR modeled charging loads only for the ET2 and ET2+ forecasted scenarios due to the low volume of electrical flights in the ET1 scenario. The ET2+ scenario is discussed in this section. The baseline scenario is provided only as a reference point and does not include any electric or hybrid-electric flights. NASA assumed the following assumptions when developing the ET2+ scenario:

1. Fifty percent of GA flight operations with single-engine reciprocating aircraft that can meet the range and reserve requirements were converted to the electric trainer flights.
2. UAM flights depart VFR only and have an energy density of 400 Wh/kg.

The eRAM9 and hRAM19 flights were included from Georgia Tech's 2022 study with a power adjustment of 150% to align with this study (N. K. Borer et al., 2025).

Summaries of the ET2+ flight schedule data for OKV and HVN are presented in Table 8 and Table 9, respectively. The annual energy required represents the energy required at the vehicle input and does not include charger efficiency.

Table 8. OKV ET2+ Flight Schedule Summary Data

EV Type	Total Annual Flights	Avg. Daily Flights	Avg. OD Distance (nmi)	Avg. Landing SOC (%)	Max. Daily Flights	Annual Energy Required (MWh)	Avg. Energy Consumption per Flight (kWh)
Non-electric	6,576	18.2	--	--	96	0	0
eVTOL	2,964	8.9	50.1	43.4	24	581.0	196.0
RAM (electric& hybrid)	3,234	9.0	127.9	66.0	11	562.8	174.0
eGA	1,827	5.6	42.4	43.4	31	106.6	58.3

Table 9. HVN ET2+ Flight Schedule Summary Data

EV Type	Total Annual Flights	Avg. Daily Flights	Avg. OD Distance (nmi)	Avg. Landing SOC (%)	Max. Daily Flights	Annual Energy Required (MWh)	Avg. Energy Consumption per Flight (kWh)
Non-electric	7,837	21.6	--	--	51	0	0
eVTOL	2,844	8.7	44.8	46.7	21	599.6	210.8
RAM (electric & hybrid)	6,965	19.3	98.3	59.2	24	968.0	139.0
eGA	1,440	4.8	35.5	47.1	14	82.7	57.5

Figure 3 shows the arrival time-of-day distribution for each flight operation type that the study focused on: UAM arrivals of eVTOL, general aviation arrivals (denoted as SR), eRAM9, and hRAM19. The hourly distribution profiles can help inform when demand between different aircraft types might coincide, leading to higher charging peak demand. Conversely, the arrival distribution can also inform when the demand is low and thus allow operators to plan for managed charging events. For example, the early hours of the day between midnight and 10 a.m. have low demand for UAM and GA operations, making it ideal for the higher-power demand electric and hybrid-electric RAM aircraft to charge without amplifying the overall aircraft charging peak demand. This example ignores the peak demand from other airport energy consumption sources; airport operators should consider the overall airport energy demand needs when making decisions on when to charge high-power aircraft.

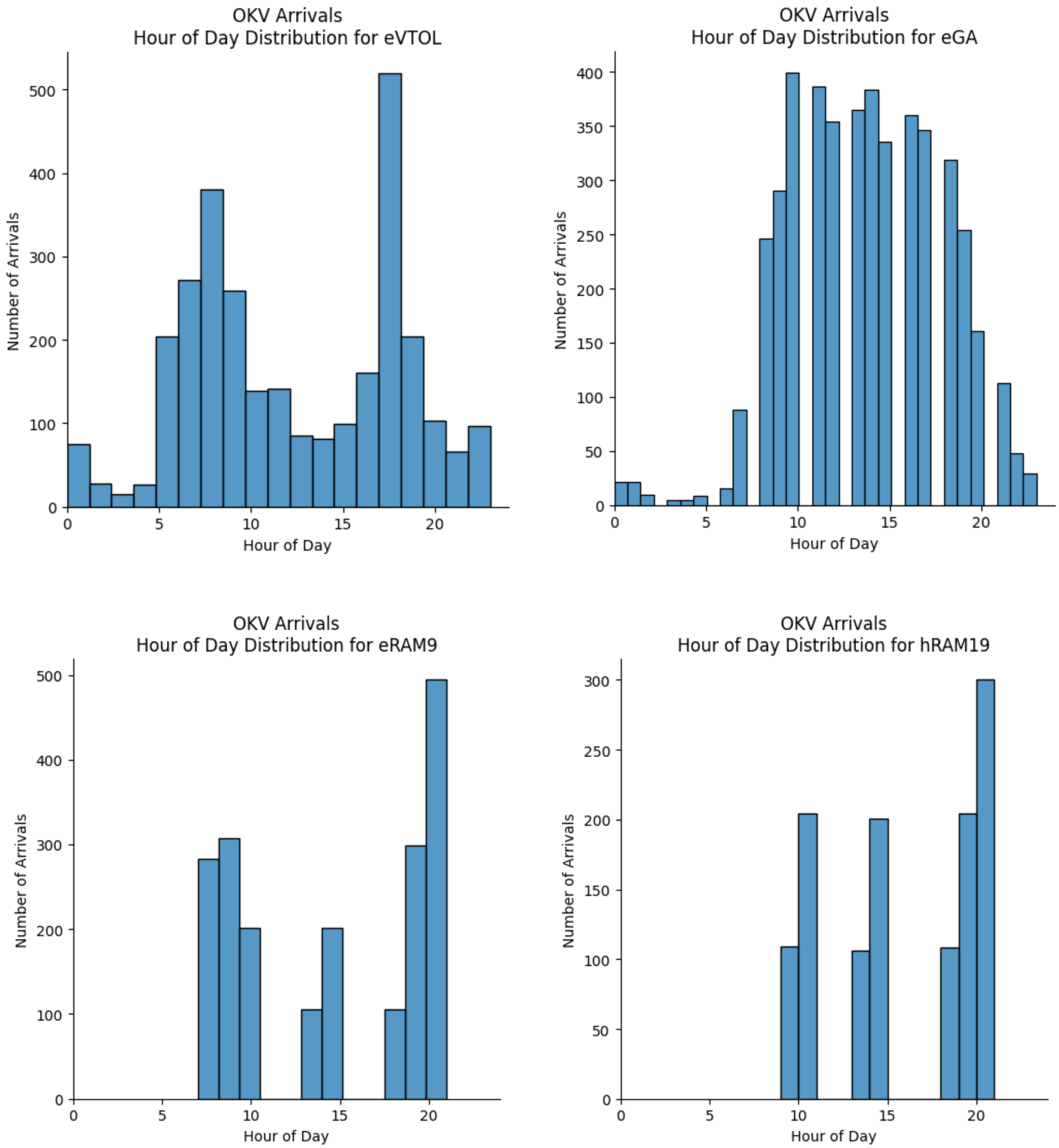

Figure 3. OKV aircraft arrival distributions

Arrivals are lowest in the early morning hours across all four flight operation types. These early hours could be used for overnight charging of electric ground support equipment (eGSE) that might only require one full charge per day, whereas electric aircraft typically require charging in between each flight operation. The flight schedules include the minimum energy needed to recharge the battery to a desired SOC to meet the next flight with enough reserves. The desired, or “target,” SOC is assumed to be 90% for all flights if time allows.

Figure 4 and Figure 5 show the total annual flight counts for each aircraft type, with the annual energy required to meet the all-electric and hybrid-electric flights in the flight schedule for OKV and HVN, respectively.

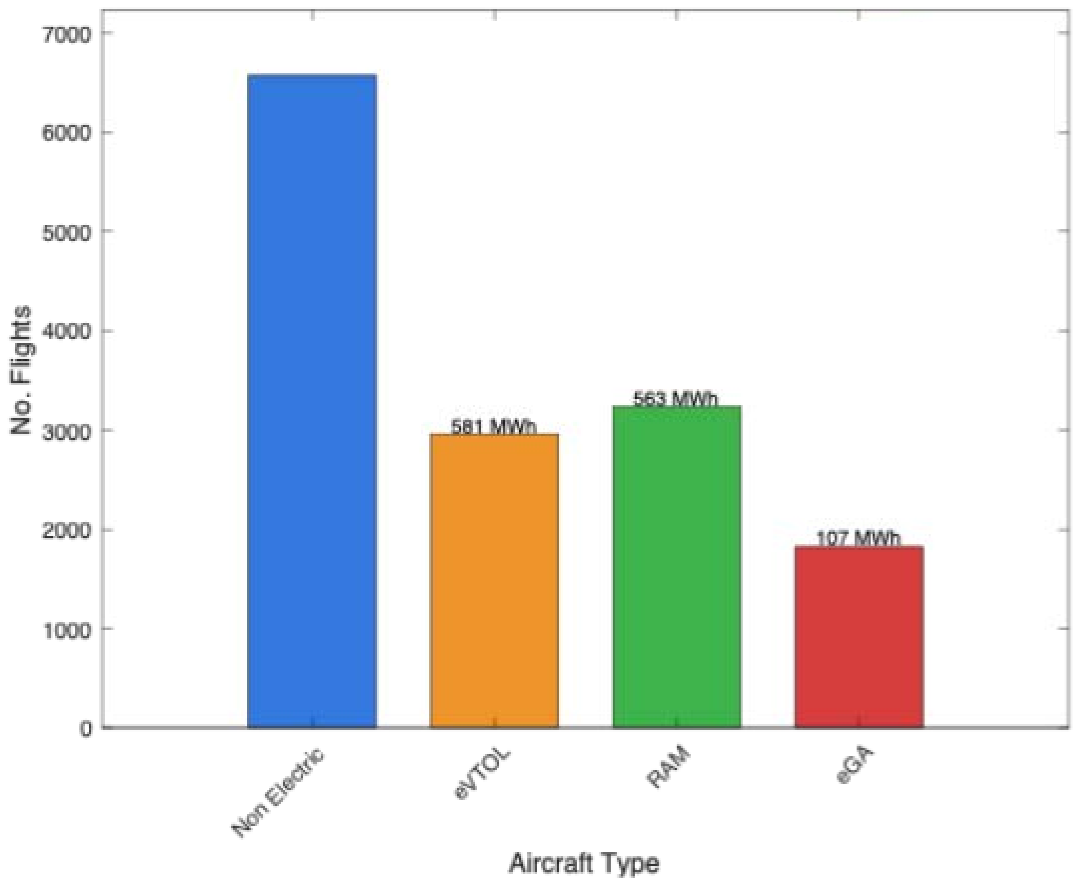

Figure 4. OKV annual flight demand distribution for ET2+

At OKV, the annual charging demand for the ET2+ UAM eVTOL operations of 581 MWh makes up almost half of the 1,251-MWh total estimated energy requirement from the all-electric and hybrid-electric aircraft combined.[6]

[6] This calculation assumes that vehicles charge to 90% SOC and does not consider efficiency, so actual consumption will be higher.

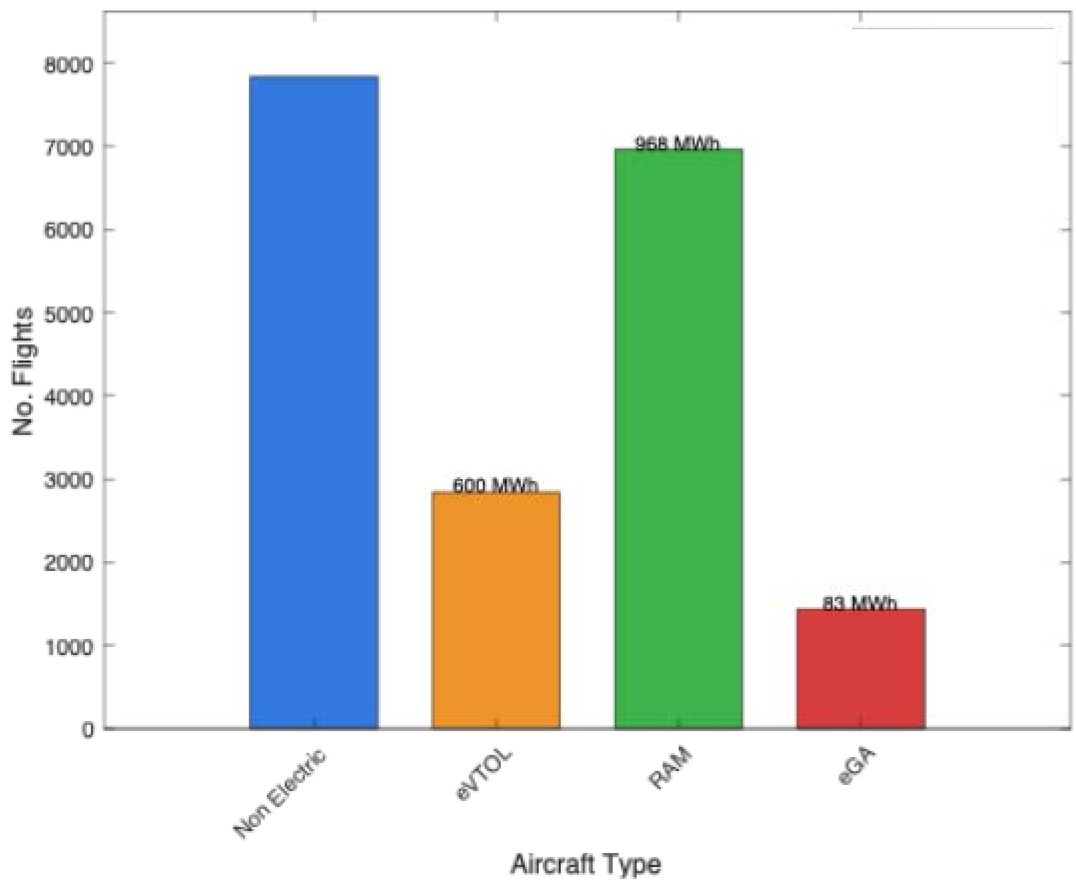

Figure 5. HVN annual flight demand distribution for ET2+

There were more than two times as many eRAM operations at HVN as there were at OKV, making eRAM aircraft operations the most significant portion, accounting for approximately 60% of the total annual electric aircraft charging energy requirement. Although some hybrid RAM operations occurred at HVN, none of the aircraft required additional energy capacity to meet their next flight with reserve capacity to spare.

Actual electricity consumption due to aircraft charging is expected to be greater than the aircraft charging energy requirements presented in this section due to efficiency losses at the charger. The charging model will account for losses and provide actual electricity consumption values to REopt as an input. The next section describes how the charging infrastructure was selected and how peak charging demand could be mitigated by careful selection of the charging infrastructure.

4.5 Charging Infrastructure Analysis

RAM operations, specifically eRAM, at HVN exceeded those at OKV by more than a factor of two. At HVN, these operations dominated traffic and accounted for approximately 59% of the total annual electric aircraft charging energy of 1,651 MWh. Although some hybrid RAM operations occurred at HVN, none of the aircraft required additional energy capacity to meet their next flight with reserve capacity to spare.

Aircraft charging loads are modeled with their associated charge acceptance curves, which map charging demand power with current battery SOC and ideally allow for EVI-EnSite to account for charging dynamics specific to a vehicle's BMS and charging hardware. These plots allow for proper charger sizing such that the proposed charging setup will meet the requirements of a given scenario.

Charging demand curves specific to OEM offerings were not available for this effort, so they were modeled based on lithium-ion cell test results. They do not include a BMS, so they are missing any dynamics related to BMS charge control; the charging demand curves strictly represent the constant-current constant-voltage charging of a lithium-ion pack.

4.5.1 eTrainer: 140 kWh

The charger sizes used to model the eTrainer charging demand were 150 kW, 350 kW, and 750 kW for the 1C, 2C, and 4C charging rates, respectively, with 1C being the slower charging rate and 4C being the fastest. Charging rates determine the speed at which a battery can accept charge, where a 1C charging rate corresponds to a 1-hour charge time from 0% to 100% SOC. As the charging rate increases, the time it takes to charge a battery from 0% SOC to 100% SOC decreases. A 2C charging rate corresponds to a 30-minute charge time from 0% to 100% SOC, and a 4C charging rate corresponds to a 15-minute charge time from 0% SOC to 100% SOC. Figure 6 shows the resulting charge acceptance curves used for the eTrainer aircraft.

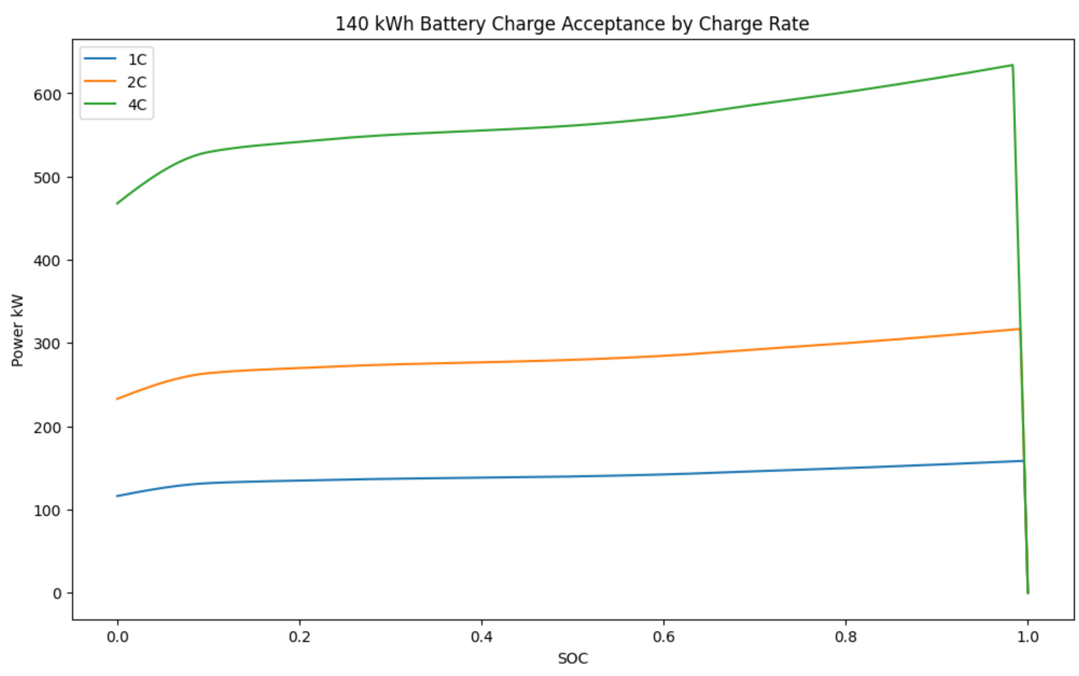

Figure 6. eTrainer (140 kWh) charge acceptance curves for the 1C, 2C, and 4C charge rates

Results from the EVI-EnSite modeling for the 140-kWh battery capacity eTrainer eGA are shown in Table 10 for each charging rate and charger size scenario. The peak demand for each charging scenario coincides with the charge acceptance curves. As expected, the higher charging rate scenarios have shorter charging durations; however, if the operational needs of the aircraft operator do not require extremely fast turnaround times, then the largest and fastest charging scenario might not be the best choice for that type of flight operation. For the OKV modeled charging scenarios, the critical turnaround time was 30 minutes and could be met with 2C charging and a 350-kW charger. Although all three charging scenarios were modeled in EVI-EnSite, only one charging scenario was used in the subsequent techno-economic modeling. The charging scenario selected for the downstream analysis was the charging scenario with the lowest power demand and a maximum charge duration that was lower than the critical turnaround time for the operation type. For the eTrainer, the 350-kW charger size at a 2C charging rate was used for the techno-economic analysis in Section 5.For these results, the starting SOC varied depending on the proceeding flight, but the final SOC was 90%.

Table 10. OKV eTrainer Charging Analysis Results

Charger Size (kW)	Charge Rate	Number of Chargers	Avg. Charge Duration (min.)	Max. Charge Duration (min.)	Peak Demand (kW)
150	1C	1	15.8	41.5	150
350	2C	1	7.9	20.5	304
750	4C	1	4.4	10.5	604

4.5.2 UAM eVTOL: 341 kWh

The charge acceptance curves for the 341-kWh UAM eVTOL aircraft battery (Figure 7) show peak power demands ranging from 350 kW for the 1C charging rate to more than 1.4 MW for the 4C charging rate. Charger sizes were based on existing and future standard charger sizes.

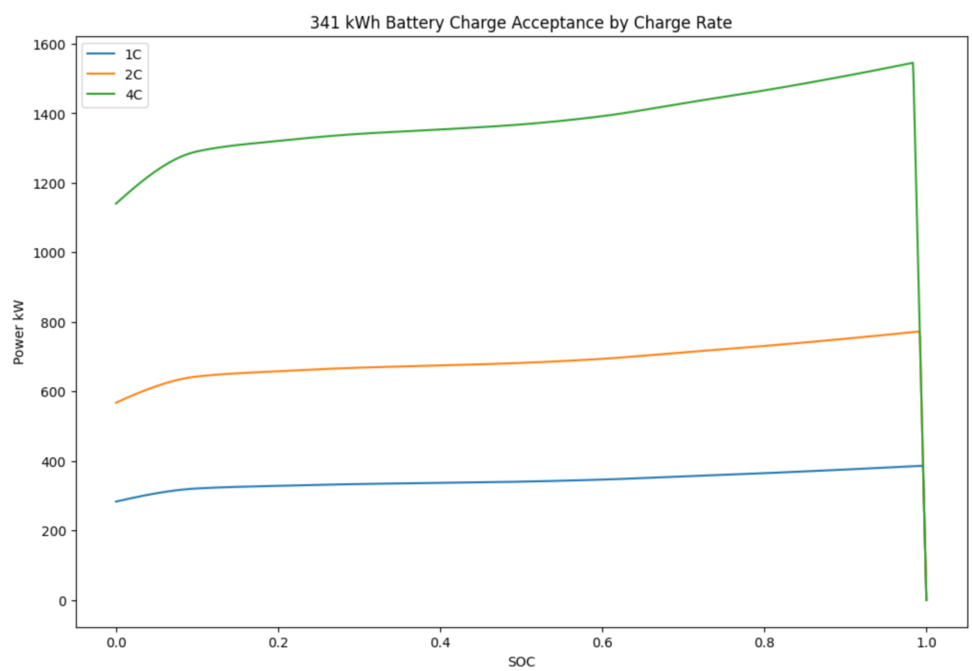

Figure 7. UAM eVTOL (341-kWh) charge acceptance curves for the 1C, 2C, and 4C charge rates

UAM operators must balance fast charging for increased daily operations with the higher peak demands and faster battery degradation rates that result from the faster charging rates. For this study, a critical turnaround time for UAM operations of 30 minutes was assumed due to the relatively low volume of daily operations at the modeled airports; however, future studies should consider looking further into the costs-benefits of faster charging for increased revenue and the operations and maintenance costs associated with higher charging rates.

Table 11 lists the results from the charger analysis for OKV. The peak demand for the 1C and 2C charging rate scenarios were limited by the charger size used. Although the theoretical charge acceptance curves for the 1C and 2C charging show the maximum power draws to be greater than 350 kW and 750 kW, respectively, these peaks appear between 90% to 100% SOC—the range where a BMS commonly slows down the charge rate and thus the maximum power requirement.

Table 11. OKV UAM eVTOL Charging Analysis Results

Charger Size (kW)	Charge Rate	Number of Chargers	Avg. Charge Duration (min.)	Max. Charge Duration (min.)	Peak Demand (kW)
350	1C	1	18.7	24.5	350
750	2C	1	9.4	12.5	750
1,750	4C	1	4.7	6.5	1,424

4.5.3 eRAM: 746 kWh and hRAM: 440 kWh

The charge acceptance curve shown in Figure 8 for the 746-kWh eRAM9 provides the required power to charge the battery at various SOCs. The charger sizes used for each charging rate scenario were 1 MW for the 1C rate, 1.75 MW for the 2C rate, and 3.75 MW for the 4C rate. These charger sizes were not based on any existing vehicle chargers; instead, the charger sizes were selected to ensure that maximum power draw by the aircraft battery was possible for each charging rate. Megawatt charging standards are being developed for the high-power-rated chargers that will be needed to meet charging demand quickly enough to sustain operations from larger electric aircraft.

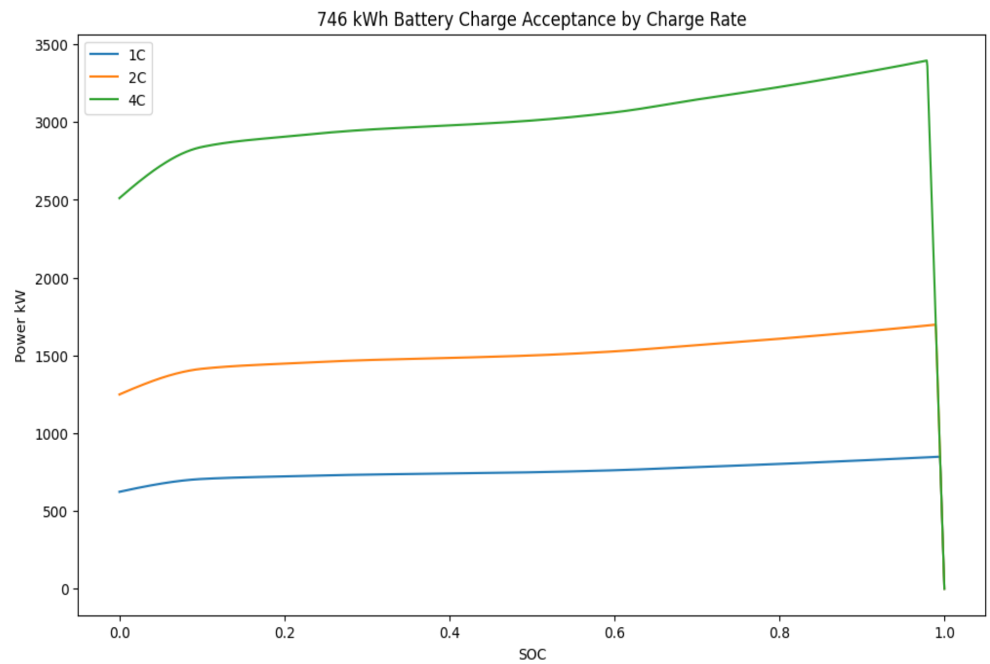

Figure 8. eRAM9 (746 kWh) charge acceptance curves for the 1C, 2C, and 4C charging rates

The hRAM19 charging (Figure 9) was modeled alongside the eRAM9 flight operations, with both aircraft types sharing the same chargers; therefore, the EVI-EnSite modeling results are for the combined charging operations from both electric and hybrid-electric RAM aircraft, with the larger eRAM9 aircraft battery being the driving force behind the charging infrastructure sizing.

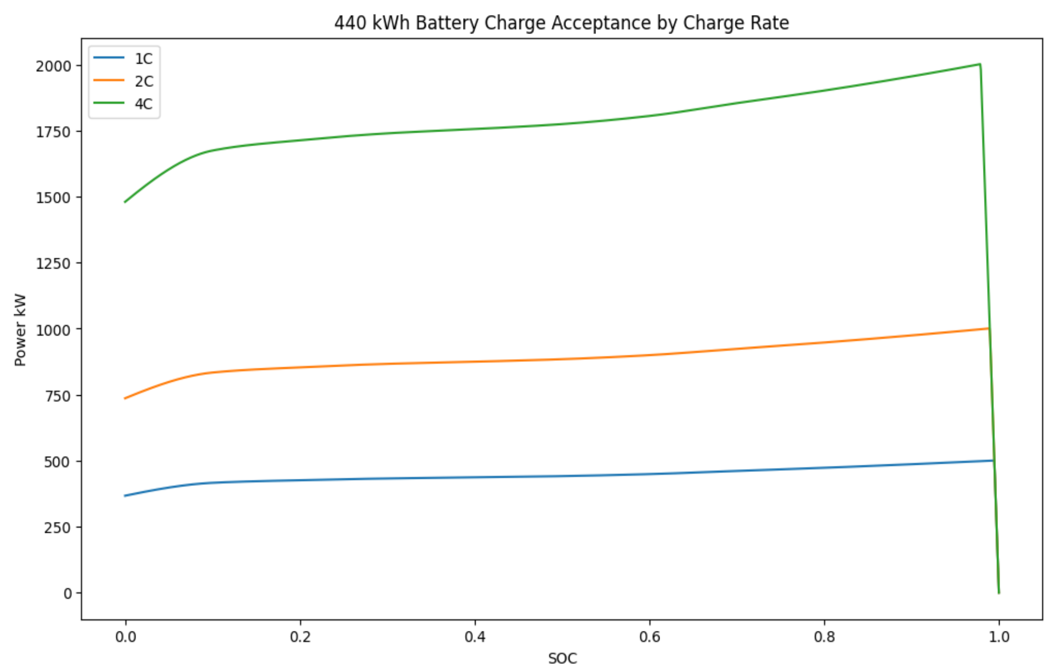

Figure 9. hRAM19 (440 kWh) charge acceptance curves for the 1C, 2C, and 4C charge rates

Table 12 features the EVI-EnSite modeling results from the combined charging operations of the electric and hybrid-electric RAM flights. The results indicate that a standard 1C charging rate should be sufficient to meet the forecasted operations within the 30-minute critical turnaround time while minimizing the overall peak demand from the aircraft charging.

Table 12. OKV eRAM9 and hRAM19 Charging Analysis Results

Charger Size (kW)	Charge Rate	Number of Chargers	Avg. Charge Duration (min.)	Max. Charge Duration (min.)	Peak Demand (kW)
1,000	1C	1	5.4	15.5	809
1,750	2C	1	2.6	7.5	1,606
3,750	4C	1	1.2	3.5	3,197

4.5.4 eGSE Load Modeling

Four types of vehicles were modeled for this effort: aircraft tugs, baggage tugs, cargo tugs, and water/lavatory trucks. Table 13 lists the specific details of each type used in this study.

Table 13. eGSE Vehicle Types Modeled

Vehicle Type	Battery Capacity (kWh)	Max. Charging Rate (kW)	Operating Duration per Aircraft (min.)	Modeled After
Aircraft tug	72	70	9–11	TREPEL aircraft tractor
Baggage tug	40	30	13–18	Charlatte baggage tractor
Lavatory/water truck	40	30	10–15	Charlatte baggage tractor
Cargo tug	50	22	20–30	Charlatte cargo tractor

The number of vehicles considered was based on the GSE list provided to NLR by each airport. The types and quantity of each vehicle will vary from one airport to another, depending on the flight volume and types of traffic the airport handles.

4.6 EVI-EnSite Modeling Results

This section summarizes the key results from the charging analysis performed with the EVI-EnSite modeling tool for the various scenarios and aircraft types. For each airport, we looked at both the ET2 and the ET2+ scenarios and selected the charging infrastructure that best suited each aircraft type, as described in the previous section. Generally, the same charging infrastructure was used for each aircraft type to the model charging loads because the critical turnaround times did not vary much between the ET2 and ET2+ flight forecasts.

4.6.1 Winchester Regional Airport Results

4.6.1.1 Aircraft

At OKV, the biggest peak load was due to RAM charging at a 1C charge rate on the 1-MW charger for both forecasted scenarios. The average charge duration for the RAM aircraft was approximately 14 minutes with a maximum charge duration of 18 minutes for the ET2 scenario. The ET2+ scenario had a 15-minute average charge duration with a maximum charge duration of almost 28 minutes. The longer maximum charge duration could be due to the higher energy demands required for the RAM aircraft in the ET2+ scenario compared to the ET2 scenario. Table 14 summarizes the results for all aircraft for both scenarios.

Table 14. Summary of Charging Analysis Results for OKV

ET Scenario	EV Type	Max Power (kW)	Charge Speed	Avg. Charge Duration (Minutes)	Maximum Charge Duration (Minutes)	Peak Power (kW)	Total Energy Consumed (MWh)
ET2	RAM	1,000	1C	14.2	18.2	825	474.3
ET2	eGA	350	2C	15.2	21	308	120.5
ET2	eVTOL	750	2C	14	17	750	438.6
ET2+	RAM	1,000	1C	15.5	27.7	825	562.8
ET2+	eGA	350	2C	15	21	308	106.6
ET2+	eVTOL	750	2C	15.1	20.3	750	581.0

The charge durations for the eGA aircraft did not vary as much between the ET2 and ET2+ scenarios because the energy requirements were similar. The eVTOL aircraft maximum charge duration increases by approximately 3 minutes between scenarios, with an additional energy requirement of approximately 140 MWh for the ET2+ scenario.

Overall, the charge durations between scenarios were relatively similar even though the energy requirements increased by more than 100 MWh for both the RAM and eVTOL aircraft. Peak demands remained the same across scenarios due to use of the same charging infrastructure.

4.6.1.2 eGSE

Figure 10 and Table 15 present the results of the eGSE modeling at OKV. The ET horizon (2 or 2+) did not have an impact on the eGSE number or load, so only one set of results is presented here. The resulting eGSE charging loads for OKV are small, approximately 66 MWh annually, compared with the aircraft charging loads shown in Table 14.

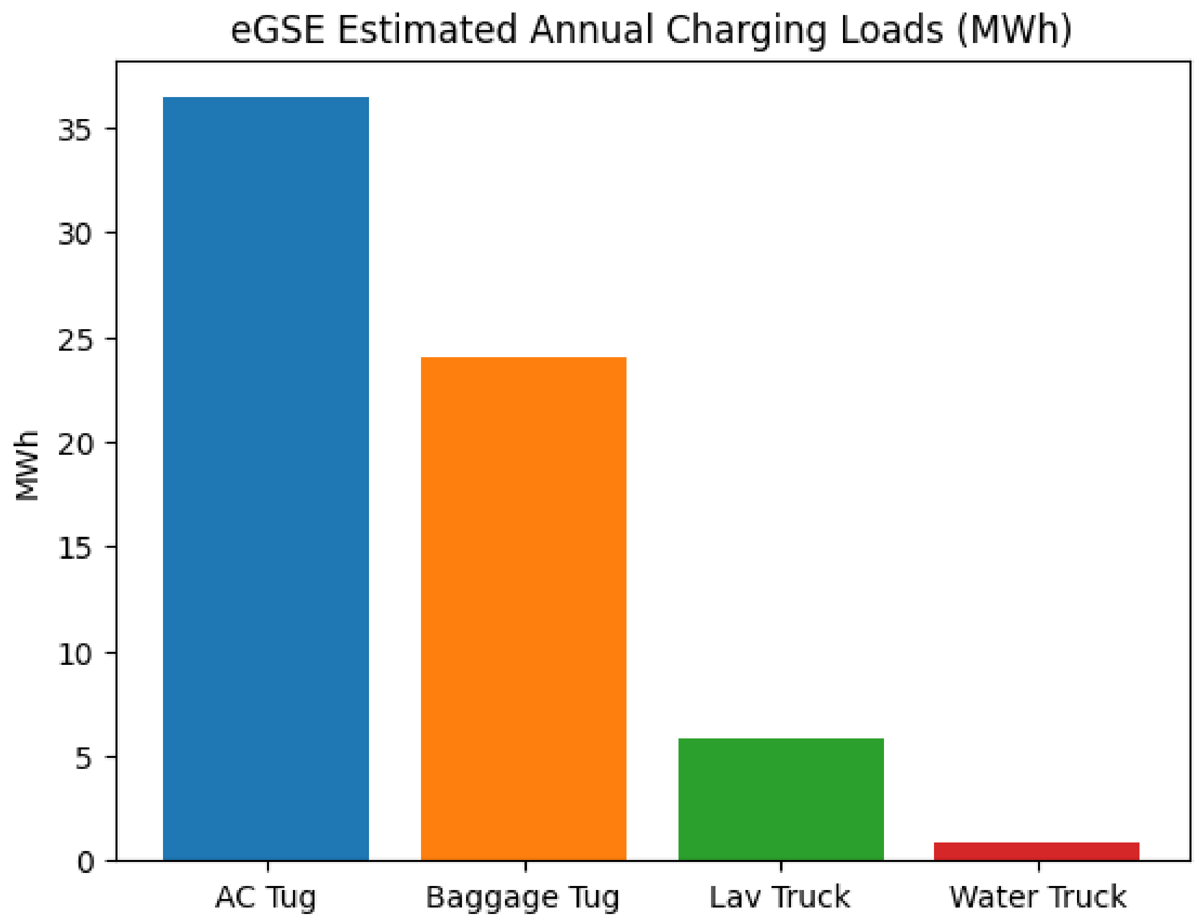

Figure 10. Annual eGSE charging demand at OKV

Table 15. Summary of eGSE Charging Demand at OKV

Vehicle Type	No. of Charging Events	Avg. Charging Demand (kWh)
Aircraft tug	784	46.4
Baggage tug	871	27.6
Lavatory truck	223	26.0
Water truck	32	26.0

4.6.2 Tweed New Haven Airport Results

4.6.2.1 Aircraft

Table 16 summarizes the charging analysis results for HVN. RAM aircraft charging had the highest peak demand at HVN for both the ET2 and ET2+ scenarios, followed by eVTOL charging demand and then the eGA aircraft charging. The maximum charge duration was the longest for the eGA aircraft in the ET2 scenario, but the RAM aircraft charging had the longest duration for the ET2+ scenario at HVN. The longer charge duration in the ET2+ scenario for the

RAM aircraft is expected due to the more than 100-MWh energy requirement for the ET2+ scenario.

Table 16. Summary of Charging Analysis Results for HVN

ET Scenario	Airport	EV Type	Max. Power (kW)	Charge Speed	Avg. Charge Duration (Minutes)	Max. Charge Duration (Minutes)	Peak Power (kW)	Total Energy Consumed (MWh)
ET2	HVN	RAM	1,000	1C	10.5	17.2	825	859.7
ET2	HVN	eGA	350	2C	13.8	21.1	308	86.9
ET2	HVN	eVTOL	750	2C	11.8	15.7	750	357.9
ET2+	HVN	RAM	1,000	1C	11.3	26.5	819	968.0
ET2+	HVN	eGA	350	2C	13.6	21.5	305	82.7
ET2+	HVN	eVTOL	750	2C	14	20.5	744	599.6

As with the modeled charging at OKV, the charge durations were relatively similar between scenarios, allowing for the use of the same-sized charging infrastructure for each aircraft type. Targeting shorter charging durations would require higher-powered charging infrastructure and would come with larger peak demand loads. Peak demand loads will also multiply if multiple chargers are required to be used in parallel to maintain the desired flight operations. This study shows the peak demand required for a single charger per aircraft type, which is suitable for the low-flight-volume operations at OKV and HVN.

4.6.2.2 eGSE

Figure 11 and Table 17 show the results of the eGSE modeling for HVN. HVN is larger, both in size and traffic volume, than OKV, so it makes sense that the total number of vehicle charging events increased as did the resulting annual energy (approximately 156 MWh annually). The eGSE power demand is still less significant than the sum of the aircraft (Table 16), but it is larger than the eGA power demand for both the ET2 and ET2+ scenarios. So, the eGSE load is increasing in this case, and it is expected to increase as larger, more trafficked airports are modeled.

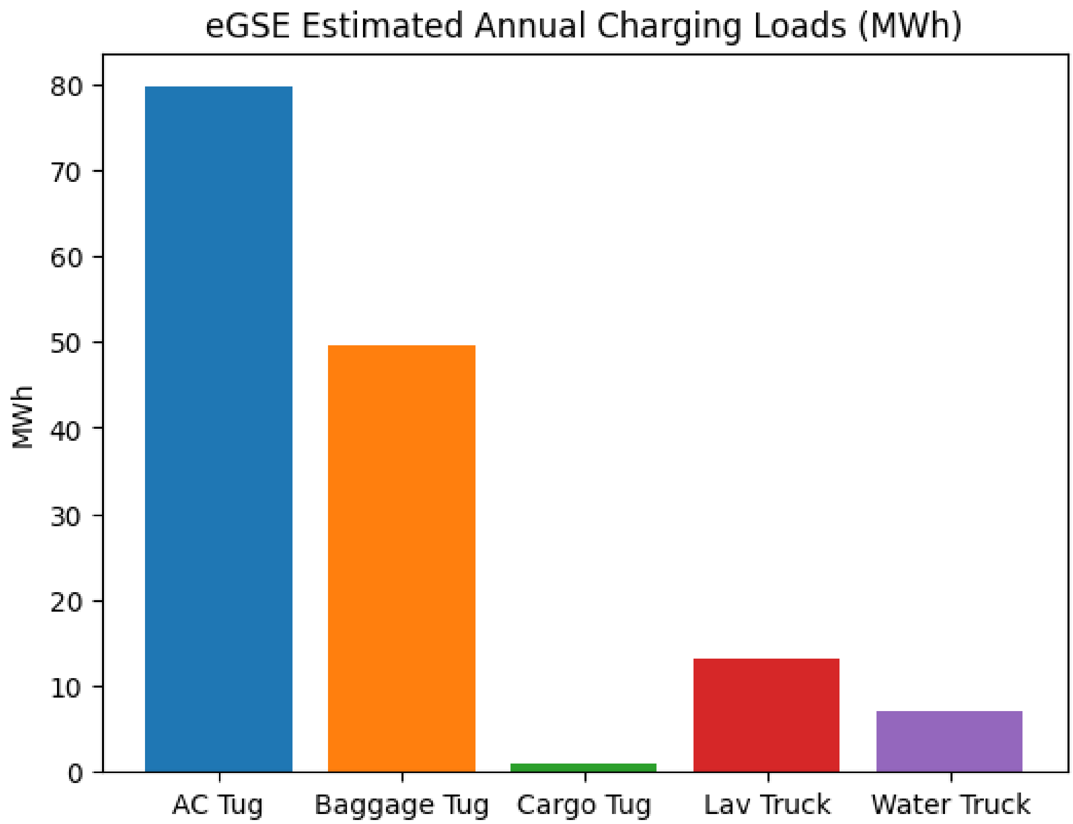

Figure 11. Annual eGSE charging demand at HVN

Table 17. Summary of eGSE Charging Demand at HVN

Vehicle Type	No. of Charging Events	Avg. Charging Demand (kWh)
Aircraft tug	1,655	48
Baggage tug	1,840	27
Cargo tug	27	32
Lavatory truck	509	26
Water truck	273	26

5 REopt Techno-Economic Analysis

The adoption of advanced air mobility (AAM) will require EVSE installation and forecasted aircraft charging at airports, resulting in new electric loads at these airports. These new electric loads must be served to maintain flight operations. There might be cases where placing on-site generation will allow an airport to reduce the net cost of serving these loads, thereby helping the airport save money compared to solely relying on the grid (i.e., business as usual [BAU]). These airports have existing backup diesel generators (see Table 18 for details) but do not have any onsite energy generation sources that could operate in parallel with the grid. Airports, specifically small regional airports, tend to have large amounts of available land that cannot be developed into other things like hangers or buildings. Such airports are uniquely positioned to use the available open land to install on-site generation to minimize the cost of serving electric loads.

An airport might also choose to maximize the total installed on-site generation capacity by using all open land parcels. The addition of on-site energy storage systems could allow excess on-site generation to be stored at the airport for use when electricity costs are high or in case of a power outage. Such configurations might not be cost-effective, but they could provide a variety of benefits[7] to the airport and its surrounding community:

1. This could increase reliability against short-duration outages and increase resilience against long-term outages. The airport might also be able to sustain critical loads within its vicinity by fully using its available land area and acting as a localized energy node. Such an investment might not be the most cost-effective solution, but it could provide critically needed energy resilience, which is difficult to value.
2. Although grid power is available, on-site generation can provide airports revenue streams by exporting power to the grid for compensation via available state- and utility-level mechanisms and by selling renewable energy credits (RECs) in states with renewable portfolio standards.
3. An airport that is an energy node could also partner with large loads, such as data centers, to help reduce their time to market or provide virtual capacity for the large load to rely on (DiGangi, 2025).
4. Surplus generation from an airport can provide flexibility in net load at the airport, allowing for demand response under extreme grid stress through energy arbitrage.

The methodologies and results presented in this section quantify the magnitude of electric utility bills and infrastructure upgrade costs associated with serving EVSE loads at regional airports. Information in this section also quantifies how on-site generation could augment existing backup generation sources and help the airport and its community serve critical loads during an outage. Key results for scenarios considered in this section identify system sizes, project economics, and dispatch strategies for on-site generation and storage at the analyzed airports. The latest version of NLR's REopt model (Cutler et al., 2017) was used to formulate and execute these scenarios.

[7] The airport might need to engage its electricity distribution utility to implement the necessary infrastructure and agree on a sequence of operations to allow power exports from the airport to its local distribution line to realize some of these benefits.

5.1 REopt Introduction

REopt is an NLR-developed open-source mathematical model. It is typically used to identify on-site generation and storage system size combinations that can minimize the cost of serving electric loads at a site. This work uses REopt to quantify the electricity costs associated with EVSE charging at Tweed New Haven Airport (HVN) and Winchester Regional Airport (OKV) (introduced in Project Overview and analyzed in subsequent sections). As part of this effort, relevant data were collected from the airports and their electric utilities, as detailed in Section 2. Figure 12 illustrates how REopt interfaces with upstream and downstream modeling tools.

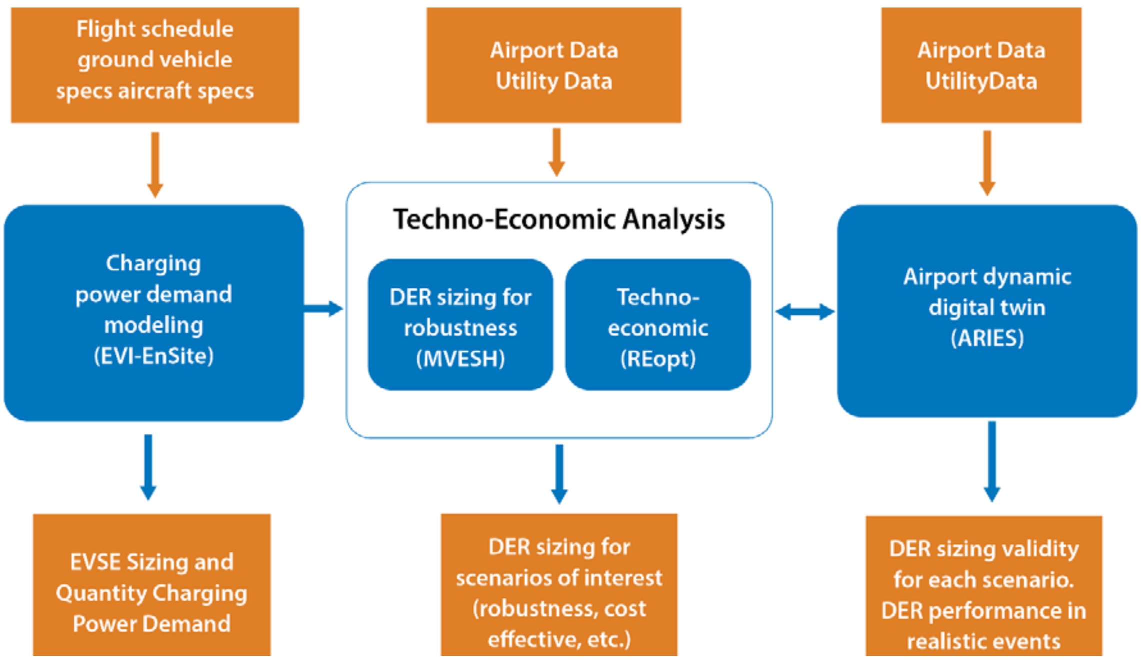

Figure 12. Overview of REopt's interactions with EVI-EnSite and ARIES.

Illustration by Anthony Castellano, National Laboratory of the Rockies

Forecasted EVSE power consumption profiles (exported from EVI-EnSite) and airport building load profiles at the analyzed airports were fed as electric load inputs and represent the load that must be served. All the load profiles were up-sampled or down-sampled to 15-minute-resolution (35,040 elements for a year) time-series data. Electric tariffs (or rate structures) represent how costly electricity is at each time step, and they are essential for the accurate calculation of modeled electric utility bills. These electric tariffs also form the basis of cost-effectiveness on-site generation and storage because higher tariffs might allow these systems to provide value and therefore be identified as cost-effective by the model. Because REopt performs a life cycle-based cost analysis, techno-economic inputs were provided to represent how costs change over the project span of 25 years.

Outputs from REopt included on-site generation system sizes that minimized the cost of serving electric loads over a 25-year time horizon, the net present value (NPV) of the cost savings, the dispatch strategy for these systems to maximize the cost savings, and other financial outputs.

This analysis was conducted programmatically in Julia programming language using REopt's Julia package.[8] A limited version of REopt can also be accessed online using the web tool.

For OKV, these system sizes were then implemented in a digital twin of OKV's electrical system (see Section 6) to check the validity of the generation size and the installation location for a given scenario. Due to project funding constraints, NLR was only able to build a full digital twin of OKV. On-site line upgrade costs are included because the generation asset locations are part of the digital twin, and these costs represent the added capital cost of including a new underground cable at the airport to carry power from the electric utility meter to the EVSE and from the generation assets (which could be placed in open areas near the airport) to the EVSE loads.

5.2 Key Model Inputs

The on-site generation analysis portion of this work continues to focus on OKV and HVN. Table 18 provides key airport information that is considered in REopt, such as the airport's electric utility, the total area available for solar PV, and the existing backup generation capacity.

Table 18. Key Airport Characteristics for On-Site Generation Analysis

Site Name	Type of Airport	Electric Utility	Area for Solar PV (80% of Total Available)	Location	Existing Backup Diesel Generator Capacity
OKV	Small general aviation	Rappahannock Electric Cooperative	Ground: 2,195,106 ft^2 or 203,931 m^2 or 50 acres	Winchester, VA	250 kW
HVN	Small hub	United Illuminating (UI) Constellation Direct Energy	Ground: 446,316 ft^2 or 41,464 m^2 or 10 acres Carport: 196,383 ft^2 or 18,245 m^2 or 4.5 acres	New Haven, CT	500 kW

5.2.1 Electric Loads

REopt focused on the existing airport infrastructure and the forecasted EVSE loads for both airports; therefore, the model considered the following electric loads at each airport:

1. Existing airport electrical infrastructure (building [BLDG] loads)
2. RAM-only EVSE loads (RAM loads)
3. Trainer-only EVSE loads (Trainer loads)
4. UAM-only EVSE loads (UAM loads)
5. RAM + Trainer + UAM loads (aggregated EVSE loads)
6. RAM + Trainer + UAM + BLDG loads (EVSE + BLDG loads).

[8] Julia (julialang.org/) is a programming language suitable for scientific computations and high-performance computing. REopt's underlying mathematical model is available as a Julia package for advanced users. This package offers more flexibility in modeling sites then the REopt web tool or the REopt application programming interface.

Electric loads were decomposed by their intended end use (BLDG vs. EVSE loads) to understand the electric utility bill implications of individual end use in isolation. The aggregation of the EVSE loads and the eventual aggregation with BLDG loads were also considered to help identify the synergistic effects of load aggregation on eventual on-site generation and storage system sizing. As loads are aggregated, the airport is modeled with all loads behind a single meter. The digital twin for OKV then considers power flow and any needed line upgrades throughout the airport.

5.2.2 Electric Tariff Inputs

For each airport, electric tariffs from their existing electric utilities were considered to serve the existing and forecasted electric loads. It is important to consider site-specific electric tariffs when working with REopt to ensure that the calculated electricity costs and the identified results are representative of what is possible at the airport. Table 19 details the applicable electric tariffs at OKV. All existing airport meters and forecasted EVSE loads were paired with Rappahannock Electric Cooperative's (REC's) Schedule B3 or LP1. Existing airport building loads are served under REC's Schedule B1 for very small meters and B3 (single phase and three phase) for other meters.

Table 19. Electric Utility Tariffs for Rappahannock Electric Cooperative

Electric Tariff	Description	Fixed Charges	Energy Charges	Demand Charges
Schedule B1 (RAPPAHANNOCK ELECTRIC COOPERATIVE, 2024b)	For customers whose peak demand is 25 kW or less.	$45 per month	$0.10816/kWh June – September $0.08242/kWh October - May	$0/kW
Schedule B3 (RAPPAHANNOCK ELECTRIC COOPERATIVE, 2024c)	For customers whose peak demand exceeds 25 kW but is less than 200 kW. Available as single-phase and three-phase rate	$44–$73 per month	$0.092565 /kWh	Summer: $3.11 per kW up to 100-kW demand then $11.21 per kW Winter: $2.11 per kW up to 100-kW demand then $10.21 per kW
Schedule LP1 (RAPPAHANNOCK ELECTRIC COOPERATIVE, 2024a)	For customers whose peak demand is at least 100 kW	$117 per month	$0.06748/kWh	Summer: $10.485 per kW Winter: $9.485 per kW
Net energy metering rider (RAPPAHANNOCK ELECTRIC COOPERATIVE, 2023)	Systems that use sunlight, biomass, energy from waste and are meant to offset customer's demand qualify	System size must be at most 1 MWac and generate up to 12 months of anticipated electricity consumption of the customer. Any excess generation is purchased by the cooperative at the hourly avoided wholesale electricity cost (a higher price can be negotiated).		

Note: Due to modeling limitations and small differences between costs, tiered energy and demand charges were averaged and used as a single value.

Although HVN's primary electric utility is UI, the airport is billed for electricity supply by third-party entities, such as Constellation Energy and Direct Energy (specifics are listed in Table 20). All airport meters that had sufficient data to be considered in the analysis received their electricity supply at market rates and paid for electricity transmission and distribution to UI under general service (GS), general service demand (GSD), general service time of use (GST), and general service time-of-use demand (GSTD) rates (UI: An Avangrid company, 2026). The airport's electricity supply was assumed to be from Direct Energy for simplification analysis and because all but two of HVN's existing meters (for which data were available) are serviced by Constellation Energy. This assumption does not impact the analysis because both companies charge HVN's energy supply on a day-ahead market rate basis (plus fixed adder, an unforced capacity charge, and the cost of renewable portfolio standards).

Table 20. Electric Utility Tariffs for HVN's Electric Utilities

	GS	GSD	GST	GSTD	GST-EV
Electricity Delivery Charges (Transmission and Delivery Charges)					
Fixed charges [$/month]	16.98	53.2	30.95	85.35	85.35
Energy charges	$0.211/kWh	$0.052/kWh	$0.350/kWh (10 a.m.–6 p.m.; all weekdays)	$0.063/kWh (10 a.m.–6 p.m.; all weekdays)	$0.073/kWh
Off-peak energy charges	N/A—no time-of-use component	N/A—no time-of-use component	$0.073/kWh (all remaining weekday hours and weekends)	$0.063/kWh (all remaining weekday hours and weekends)	N/A
Demand charges	$0/kW	$27.25/kW	$0/kW	$22.19/kW (applies to highest demand registered between 10 a.m.–6 p.m. on weekdays)	$3.17/kW (applies to highest demand registered between 10 a.m.–6 p.m. on weekdays)
Off-peak demand charges	N/A—no time-of-use component	N/A—no time-of-use component	$0/kW	$4.77/kW (see note)	$0.68/kW (see note)
Note:	GSDT and GST-EV tariffs have an off-peak demand charge that is charged on excess demand in a month (difference between peak demand registered for peak and off-peak hours). At present, this cannot be modeled in REopt and is not considered.				
Electricity Supply Charges					
Market charges	See Figure 13 for a plot of the total market charges.				
Fixed adder	$0.00279/kWh				
UCAP	$5.5/kW				
Renewable portfolio standard	$0.01436/kWh				

Figure 13 presents the day-ahead market rates for the Connecticut load zone in Independent System Operator New England that were used for HVN's electricity supply charges.

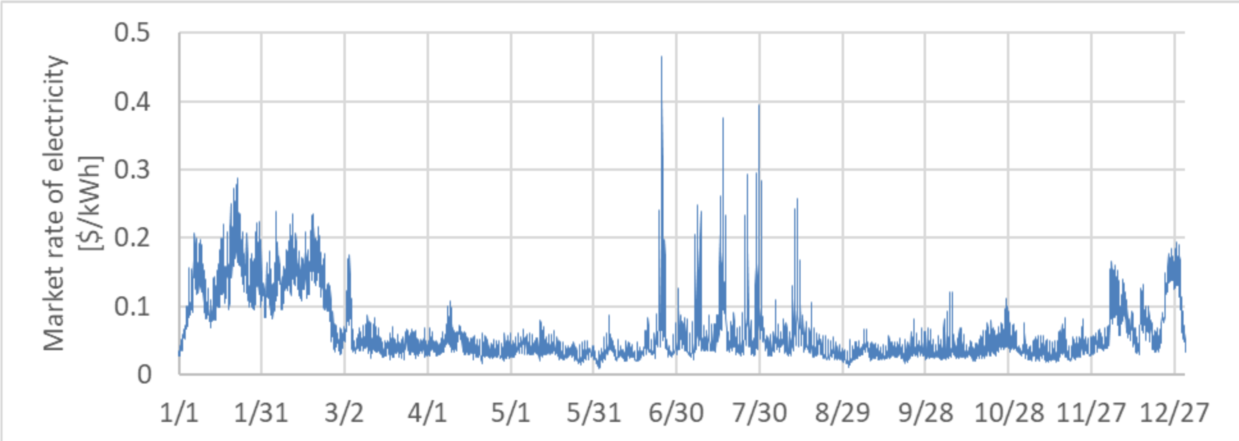

Figure 13. Day-ahead market rates for Connecticut load zone

This analysis does not consider RECs as a revenue stream. Both UI and Rappahannock Electric Cooperative offer their customers the option to purchase any RECs from on-site solar PV generation. Rappahannock Electric Cooperative requires its net metering customers to enter into a power purchase agreement where compensation for RECs is driven by the "CR" portion of Dominion Virginia Power's Rider G tariff (RAPPAHANNOCK ELECTRIC COOPERATIVE, 2023). Because the state of Connecticut has a solar carve-out in its renewable portfolio standard, a customer can choose to sell all their solar generation along with the RECs to UI at a flat compensation rate (Public Utilities Regulatory Authority, n.d.). The customer can also choose to sell net surplus solar PV generation to the utility at comparatively lower rates, thereby retaining any RECs for self-use or market resale. This analysis does not factor in REC values as part of the modeling and only focuses on grid exports from on-site generation.

5.2.3 REopt Analysis Scenarios

Scenarios executed using REopt to support this analysis and their motivations are described in Table 21. Further details for the ÆNodes, Robust, and Break-Even scenarios are provided in the respective supporting subsections (sections 5.6.4, 5.6.7, 5.7.4, 5.7.7, and 5.8).

Table 21. Description of Airport-Wide Scenarios

Scenario	Description	Loads Considered
Baseline	Calibrating model using existing site loads and electric tariffs. No new systems are sized. Missing data points might be identified in this step.	BLDG only
Grid-Only	Quantifying electric utility bill costs, grid electricity consumption, and peak power draw for serving electric loads. This can be treated as the BAU scenario for the Cost-Optimal scenario discussed in the next row. Any existing on-site energy systems are considered.	BLDG, RAM, Trainer, UAM, RAM + Trainer + UAM, RAM + Trainer + UAM + BLDG

Scenario	Description	Loads Considered
Cost-Optimal	Identifying DER on-site generation systems that minimize the cost of serving electric loads (purely financial benefit). Results from this scenario are compared against the Grid-Only scenario outcomes to calculate the NPV of the cost savings and project economics.	BLDG, RAM, Trainer, UAM, RAM + Trainer + UAM, RAM + Trainer + UAM + BLDG
Allowed PV (ÆNodes)	Identifying system sizes and performance while requiring solar PV buildout up to any net metering limits imposed by the utility (in absence of this information, building sufficient PV for the site to become grid neutral[9])	RAM + Trainer + UAM + BLDG
Maximum PV (ÆNodes)	Identifying system sizes and performance while requiring solar PV buildout to cover all suitable land/parking lots/rooftops on the airport	RAM + Trainer + UAM + BLDG
Resilient	Quantifying the chance of surviving an outage given the system sizes identified under the Cost-Optimal, Allowed PV, and Maximum PV (i.e., ÆNodes) systems	BLDG, RAM, Trainer, UAM, RAM + Trainer + UAM, RAM + Trainer + UAM + BLDG
Break-Even	Identifying the system size mixes that have the same life cycle costs of serving electric loads as the Grid-Only scenario	RAM + Trainer + UAM + BLDG
Robust	Identifying the system design parameters that are "future-proof" and can provide value despite uncertainties in future parameters	RAM + Trainer + UAM + BLDG

Throughout these scenarios, the model focuses on the buildout and installation of new solar PV and BESS. When resilience is considered, the model accounts for existing backup generator systems of fixed capacity with unlimited fuel reserves to identify how PV and BESS can augment existing diesel backup systems. This analysis primarily examines solar PV and battery storage as candidate technologies for airport energy systems due to their well-established market maturity, standardized deployment pathways, and relative ease of implementation. Appendix D details all potential on-site generation options and why they were or were not included in this study. Dispatchable technologies to operate parallel with the grid, such as prime generators, are also considered in the Cost-Optimal scenario (results are presented in Appendix B); however, this technology was not carried into further analysis steps because it was not cost-effective under all load types. When it was cost-effective, the savings were small, and the cost of operating the

[9] A grid-neutral system generates enough energy to offset grid electricity consumption on an annual basis.

plant and hiring trained mechanics within a year could be more than the money saved over 25 years.

5.2.4 ÆNodes Scenario Selection Rationale

The ÆNodes scenario (which consists of the Allowed PV and Maximum PV scenarios) identifies the system sizes and associated project economics where the airport is an energy node on its transmission-and-distribution network instead of being a conventional electricity consumer. During an event resulting in a regional power outage disaster or a blackout, an airport with sufficient generation capacity might be able to sustain its critical loads while exporting generation to support nearby critical infrastructure. This scenario estimates only the time series of surplus on-site generation that an airport might be able to supply to its electrical neighbors. The digital twin considers the electrical feasibility of such systems and factors in the estimated electric loads of the airport's electrical neighbors.

The system sizes identified under this scenario might not maximize cost savings and are intended to maximize on-site energy generation for the benefit of surplus power generation; financial considerations are secondary. This differs from other scenarios where the objective might be to maximize cost savings or to cost-effectively add resilience. This scenario assumes that both airports and their electric utilities are willing to allow the export of surplus energy; therefore, distribution grid upgrades are not factored in the life cycle cost calculations for these system configurations. Benefits of participation would be:

7. Electric utilities are working to build sufficient generation and distribution capacity to meet the increasing demand for electricity (US Energy Information Administration, 2025) in addition to planning upgrades for aging critical infrastructure (United States Department of Energy, 2024). The presence of an ÆNode within the vicinity of load growth zones can help the utility by creating a local power source (i.e., slack) to serve such loads. Additionally, if the ÆNode is designed to be reliable, the utility might be able to save money by avoiding noncritical transmission-and-distribution bottleneck upgrades for new loads within the vicinity of the airport. Such energy sources might also help the utility prioritize more pressing matters within its service territory.
8. The presence of surplus PV and BESS capacity instead of power sources with inertia could allow for quick responses to fluctuating demand from grid edge technologies and relieve stress on existing transmission-and-distribution infrastructure (OFFICE OF ELECTRICITY, 2023). Further, an ÆNode could also partner with large loads (such as data centers) to offer capacity to the grid at the right times to make money and support reliable grid operations. This is referred to as "bring your own capacity." It could allow large loads to come online more quickly than solely relying on grid upgrades or on-site installations (Brancucci et al., 2025).

This analysis considers a range of flat wholesale rates ($/kWh) for compensating the airport for any exports to the regional grid; however, the true benefit to the grid might vary depending on the time of day and the region of the country. For example, in a region with surplus rooftop area, solar PV can help alleviate the stresses of ramping up power plants in the evening (US Energy Information Administration, 2023). Similarly, a site within the vicinity of data centers might be able to assist in the case of a byte blackout, which consists of unstable grid conditions introduced to a system due to the behavior of large loads, such as data centers. In both cases, the grid might value an ÆNode more than routine operations (Grid Status, 2025).

5.3 Identifying Resilient System Design

As discussed in Section 5.2, the presence of on-site generation can augment the resilience provided by on-site backup diesel generators against outages. REopt was used to identify the range of system sizes that can provide the desired levels of resilience for a fixed outage duration. The execution of the Cost-Optimal (or financial) scenarios provides a combination of system sizes that maximize cost savings over analysis time horizon, but they do not factor in resilience against sustained power outages. Additionally, airports might experience outages that vary in duration and frequency. They might also wish to target a likelihood of surviving outages of varying durations (such as surviving 8-hour outages with 95% confidence levels).

Figure 14 details the methodology used for the resilience assessment in this study. First, it is important to identify the critical loads that must be served during an outage along with an outage duration that must be survived (A). These data inputs can be paired with REopt-identified system sizes (B) through REopt's Energy Resilience Performance (ERP) tool to assess the confidence of surviving an outage (C). If the system sizes are manually manipulated to improve the resulting numbers, they can then be run through REopt for a techno-economic assessment and life cycle cost quantification (D and E). Note that systems that provide resilience might not be sized to maximize cost savings and could result in a relatively higher up-front cost (i.e., negative NPV of cost savings).

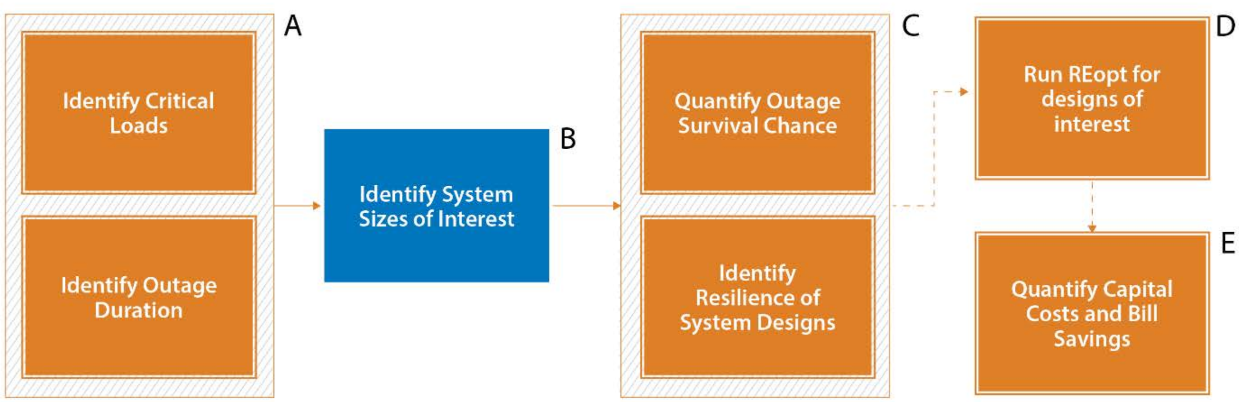

Figure 14. Resilience study design.

Illustration by Anthony Castellano, National Laboratory of the Rockies

This approach assists in translating system sizes to a resilience metric; however, airports might be interested in listing a variety of system size mixes that meet or exceed a predefined resilience threshold. Such translation of resilience goals into system design parameters is explained in Section 5.6.8 Robust Design Guidance for OKV.

5.4 Identifying Robust Designs: REopt-Insight

The REopt tool being used to identify system sizes in this analysis is a deterministic optimization model that cannot account for the impact of uncertainty in some assumptions, such as equipment costs, discount rates, and tariff prices. Many of these parameters can be highly variable and extremely impactful on the optimal system sizes and the financial and resilience outcomes of a design. Additionally, REopt is inherently a financial optimization tool, and it rarely deals with multi-objective optimization. This can make it difficult to evaluate the nonfinancial benefits of a system. To overcome these challenges, REopt-Insight was developed as an extension of the traditional REopt tool. The tool uses high-performance computing and statistical analysis to delve deeper into system performance. For a thorough overview of the methodology used in REopt-Insight and results for each airport, see Appendix A.1. REopt-Insight not only provides optimal system sizing but also aims to answer the following questions:

- How will a system be affected by external factors, such as inflation and variable hardware costs?
- Can a system be designed that performs consistently regardless of future market volatility?
- What is the trade-off of prioritizing resilience over cost savings?
- What is the lowest-cost investment strategy for developing a resilient energy system?
- What changes need to happen to allow a site to build a cost-effective on-site generation system?

We refer to these systems as robust designs—systems that have the highest probability of achieving their stated goals regardless of uncertainties. REopt-Insight has been developed to identify such designs.

Section 5.9 discusses the key takeaways from this analysis. These takeaways should be used to support investment strategies at HVN and OKV.

5.5 Validating Operability of REopt Results at Airports Using a Digital Twin

The scenarios described in the preceding sections are meant to identify system sizes that might meet the financial or resilience goals at either airport; however, these scenarios treat the entire airport as a single node where electricity demand and costs vary by scenario. The physical airport comprises multiple nodes with physical underground/aboveground cables connecting each node. True cost minimization of the airport will require placing EVSE and on-site generation across the airports such that the equipment can operate as intended while minimizing the costs of new installations and line upgrades. For example, if the airport has two large land parcels available for a solar PV system, on which land parcel could the system be placed to save costs on new underground cable? The digital twin for an airport can capture power flows across the airport's distribution lines and therefore can:

1. Give an accurate estimation of where EVSE and on-site generation can be safely placed.
2. Determine any resulting line upgrade requirements to ensure that power can flow through the airport in a safe manner.
3. Identify system designs that could require significant up-front infrastructure costs or are electrically infeasible with the airport, requiring reassessment using REopt.

More details on how digital twin considers electrical site constraints can be found in Section 6. Figure 15 captures the exchange of information between REopt and the digital twin that is required to make the modeling feedback loop work.

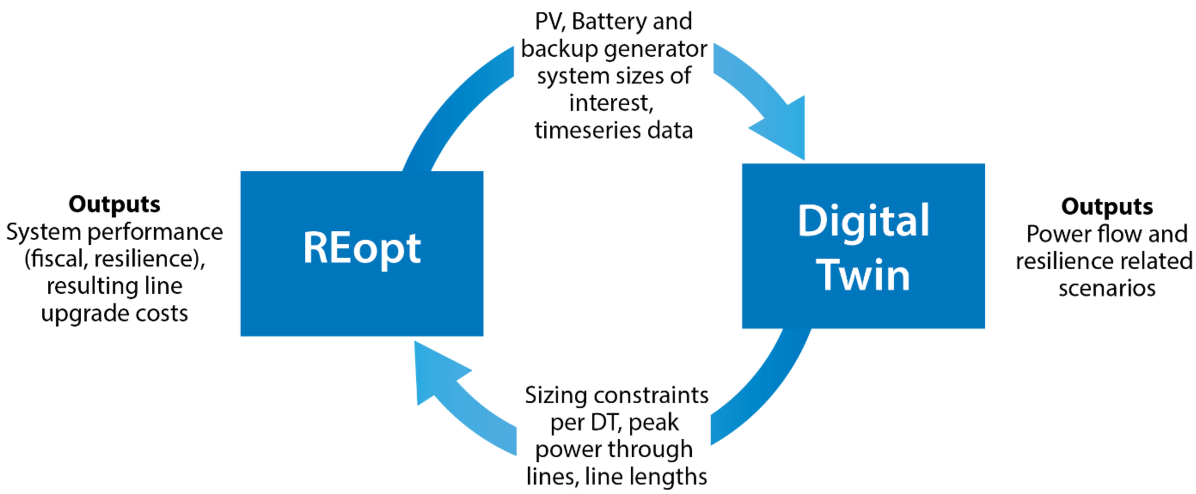

Figure 15. REopt and digital twin feedback loop.

Illustration by Anthony Castellano, National Laboratory of the Rockies

5.5.1 Detailed Techno-Economic Input Parameters

This section highlights key techno-economic input parameters used for identifying system sizes using REopt. As discussed, this analysis focused on OKV and HVN. The U.S. Department of Defense U.S. Army Corps of Engineers' area cost factors (US Army Corps of Engineers, n.d.) were used to scale the installed costs[10] by state to account for cost variations across the country. REopt analysis is a techno-economic analysis with a 25-year time horizon; therefore, the model relies on various economic inputs to calculate the project economics over these 25 years. This analysis considers only direct ownership of the identified systems across all scenarios. Per the National Institute of Standards and Technology (NIST), this analysis uses an inflation rate of 1.2%/year and a discount rate of 4.2%/year (Kneifel & Lavappa, 2024). Per NIST's Energy Escalation Rate Calculator (EERC) (National Institute of Standards and Technology, n.d.), nominal electricity cost escalation rates of 0.52%/year for OKV and 0.99%/year for HVN are employed. These escalation rates provide cost escalation for electricity purchased in either Virginia or Connecticut starting in 2026 for a 25-year contract where the annual inflation rate is 1.2%/year. It is also assumed that the airports pay a 0% tax rate because they are small publicly owned facilities.[11]

Note that due to load growth fueled by large-load buildout, electricity costs are rising across the United States at a quicker pace than the escalation rates assumed here. The REopt results do not

---

[10] Scaling was done for the closest military facility to OKV and HVN; cost factors for Quantico (107%) and the Stratford Army Engine Plant (109%) were used for OKV and HVN in Virginia and Connecticut, respectively.
[11] Winchester Regional Airport Authority Act: www.flyokv.com/home/showpublisheddocument/18682/637108891136100000.

consider a higher electricity cost escalation rate in response because the escalation rate is meant to represent an average rate of growth over 25 years. Electricity prices might escalate at higher rates in the short term, but there is uncertainty in their direction over the entirety of the analysis period. If electricity costs increase more quickly than the assumed input parameters, any on-site generation might become more cost-effective over the 25-year time horizon; therefore, using long-term escalation rates allows this analysis to take a conservative approach in how quickly electricity costs might rise at either airport.

Given uncertainties around the long-term cost of energy, REopt-Insight (discussed in Section 5.4) considers a wider range of electricity cost escalation rates to provide insights on a future with average escalation rates that are higher than anticipated.

Table 22 details the key techno-economic assumptions used for modeling in REopt. This analysis considers a standard PV module that is south facing. Values for system operations and maintenance costs and DC-to-AC ratio are obtained from NLR's 2024 Annual Technology Baseline data (National Renewable Energy Laboratory, n.d.-a).

Table 22. Economic Input Parameters

Parameter	Value
Technologies evaluated	Solar PV, BESS
Objective	Cost minimization, resilience, robust solutions
Ownership model	Direct airport ownership
Analysis period	25 years
Inflation rate	1.2%/year
Discount rate	4.2% nominal 6.38% nominal for nongovernmental entities per NLR's 2023 version (National Renewable Energy Laboratory, n.d.-a).
Electricity cost escalation rate	OKV: 0.52%year nominal HVN: 0.99%/year nominal
Effective tax rate	Assume 0%
Grid exports	Considered for both airports

Table 23 lists the model input parameters for solar PV. Because PV is AC connected with the load, its inverter efficiency is assumed to be 96%, while the PV modules are assumed to undergo 14% losses due to reasons such as soiling, snow, and connection losses (National Renewable Energy Laboratory, n.d.-b). System installed costs vary by state and PV panel type. The model does not consider investment tax credits or asset depreciation by default; however, a 30% investment tax credit is considered for scenarios of interest to showcase the impacts of such incentives in making specific scenarios more cost-effective. The model does not consider RECs based on generation from solar PV as part of the techno-economic analysis. This means that solar PV sizing is purely done to meet the financial or resilience goals for a scenario. Additionally, glare analysis for the identified solar PV installation is not considered as part of this modeling effort. Given the scale of the airports considered, the PV system installed costs in the table are for PV systems ranging from 25 kW–225 kW. These costs are conservative, and larger PV systems could see lower installed costs due to economies of scale. More details on installed cost derivation are in Table 9 (page 60) of (Anderson et al., n.d.).

Table 23. Solar PV Input Parameters

Parameter	Value
System operations and maintenance cost	$19/kW/year
PV module type	Standard
Azimuth	180 degrees
DC-to-AC ratio	1.2
Inverter efficiency	96%
Solar resource data	Yes, location-specific data were used.
System installed cost (scaled) and tilt for OKV	Rooftop: $1,915/kW at 20-degrees tilt Ground: $2,547/kW at 20-degrees tilt Carport: $3,772/kW at 15-degrees tilt
System installed cost (scaled) and tilt for HVN	Rooftop: $1,951/kW at 20-degrees tilt Ground: $2,595/kW at 20-degrees tilt Carport: $3,843/kW at 15-degrees tilt
Incentives	None considered by default. A 30% investment tax credit was considered for specific scenarios of interest.
Treatment of RECs	Not considered
Glare analysis	Not considered
Allowed PV system sizes	See airport-specific sections for calculated system sizes.
Maximum PV system sizes	See airport-specific sections for calculated system sizes.

Note: Rooftop PV price point is provided for reference only. At OKV, new PV capacity could only be installed on the ground whereas at HVN, new PV capacity could either be installed on the ground or as carport PV. Available areas are provided in Table 18.

REopt considers a lithium-ion battery as the BESS (Table 24 lists the battery model input parameters). This system is modeled with a round-trip efficiency of 89.9%, an initial SOC of 50%, and a minimum SOC of 20% (i.e., the battery can cycle from 100% down to 20% of its capacity). This analysis did not force the SOC to remain between the typical range of 10% and 90%. In lieu of costing the degradation of battery cells, the model assumes replacement in year 10 of the analysis with an identical battery. The replacement battery is assumed to last from year 11 through the end of the analysis due to forecasted improvements in battery technologies. Default capital costs for the new ($910/kW + $455/kWh) and replacement batteries ($715/kW + $318/kWh) presented in this table were scaled per the U.S. Department of Defense U.S. Army Corps of Engineers' area cost factors mentioned in (US Army Corps of Engineers, n.d.). This battery was modeled with standard capital costs, no cost constant, and no constraint on SOC in the final time step of the analysis.

Table 24. Battery Storage System Input Parameters

Parameter	Value
Battery type	Lithium-ion (REopt's default battery type—efficient and long-lasting)
AC-AC round-trip efficiency	89.9% (97.5% internal, 96% inverter, 96% rectifier)
Minimum SOC	20% (battery charge is managed to stay above this typical minimum)
Initial SOC	50% (charge at the start of the analysis period—before system charging begins)
Capital costs for OKV	$974/kW + $487/kWh
Capital costs for HVN	$992/kW + $496/kWh
Scheduled replacement costs for OKV	$768/kW + $340/kWh
Scheduled replacement costs for HVN	$779/kW + $347/kWh
Allow the utility grid to charge the battery along with PV?	Yes
Exports to the grid	False—battery export to the grid is not considered.
Incentives	None considered by default. A 30% investment tax credit is considered for specific scenarios of interest.

The line upgrade costs (see Table 25) used in this analysis are derived from an updated version of the Distribution Integration Solution Cost Options (DISCO) cost database (Horowitz, 2019). These costs are not representative of specific regions in the United States and are derived from various distinct data sources; hence, these are approximate line upgrade costs given the peak voltage, current, and spare capacity requirements for each line within the airport's distribution system.

Table 25. Line Upgrade Cost Parameters

Line Option	Line Capacity Rating (kVA)	Line Capacity Rating (kW)	Line Type	Line Cost ($/meter)	Voltage Rating (kV)	Ampere Rating (A)
1	38,244	34,419	Overhead	2,887	39.8	960
2	13,857	12,471	Overhead	2,887	14.4	960
3	6,912	6,221	Overhead	2,887	7.2	960
4	6,480	5,832	Overhead	2,756	7.2	900
5	6,480	5,832	Underground	3,576	7.2	900
6	4,284	3,856	Underground	2,789	7.2	595
7	4,258	3,832	Underground	2,034	14.4	295
8	4,140	3,726	Underground	2,756	7.2	575
9	3,960	3,564	Underground	2,690	7.2	550
10	3,780	3,402	Underground	2,625	7.2	525

Line Option	Line Capacity Rating (kVA)	Line Capacity Rating (kW)	Line Type	Line Cost ($/meter)	Voltage Rating (kV)	Ampere Rating (A)
11	3,456	3,110	Underground	2,493	7.2	480
12	3,420	3,078	Underground	2,493	7.2	475
13	3,348	3,013	Underground	2,461	7.2	465
14	3,204	2,884	Underground	2,428	7.2	445
15	2,808	2,527	Underground	2,264	7.2	390
16	2,664	2,398	Underground	2,231	7.2	370
17	2,124	1,912	Underground	2,034	7.2	295
18	1,185	1,066	Underground	2,001	4.2	285
19	332	299	Underground	4,364	0.3	1,200
20	152	137	Underground	2,690	0.3	550
21	102	92	Underground	2,231	0.3	370
22	79	71	Underground	2,001	0.3	285

The resilience assessment conducted as part of this analysis, using parameters listed in Table 26, focused on the performance of the REopt-identified system sizes in serving critical loads. The critical loads were assumed to be either 25% of the scenario loads (assuming only emergency loads are served) or 100% of the scenario loads (including EVSE loads, if any). The resilience assessment can also use backup generators at either airport. One additional backup generator was considered at each airport to highlight improvements in the reliability metrics from these assets. Each outage began with an initial battery SOC of 70%, assuming the battery is not operated conservatively during routine operations.

Table 26. Resilience Input Parameters

Parameter	Value
Outage duration	Up to 96 hours
Critical loads considered	Scenario 1: 25% of scenario loads Scenario 2: 100% of scenario loads
Initial diesel generator size	OKV: 1 x 250-kW generator HVN: 1 x 500-kW generator
Diesel capacity	Unlimited
Assumed battery SOC when outage begins	70%
Mean time to failure of diesel generator	1,100 hours
Operational availability of diesel generator	99.5% of time steps
Failure to start diesel generator	0.94% of time steps
Operational availability of solar PV	97% of time steps
Operational availability of battery	97% of time steps

5.6 Winchester Regional Airport Results

This section compares results for the future scenarios ET2 and ET2+, which use electric aircraft loads. Results for the baseline OKV scenarios are available in Appendix B**.**

5.6.1 Impact of Electric Vehicle Supply Equipment Loads

Table 27 describes the expected electricity consumption and the electricity cost from the projected EVSE loads at OKV. The annual grid electricity consumption metrics in this table represent the energy drawn from the grid so they include an EVSE efficiency of 90%. No new on-site generation systems or battery storage are assumed in this calculation. The estimated energy consumption and costs for all OKV buildings as a single node are also given for comparison. Note that these energy consumption, peak demand, and electricity costs are substantially higher than the estimated electricity costs of 10 existing buildings and the new terminal at OKV, making the EVSE electric loads a substantial electrical expense at OKV. Because these EVSE loads are new loads, an underground cable from the existing airport electrical distribution system to the EVSE will also need to be priced as part of the techno-economic analysis. The annual peak demand for each charging scenario was used with line upgrade costs for the underground lines from Table 25 to arrive at the anticipated new line costs. Note that the EVSE loads have a load factor <8%. The load factor is the ratio of energy consumed at the site over the maximum possible energy consumption at that site, and it is representative of how peaky a load is (*Understanding Load Factor*, n.d.). Intuitively, an electric utility must build enough capacity to serve the maximum possible EVSE loads, but the EVSE loads use <8% of this available capacity. Building loads at OKV have a load factor of 39%, i.e., a typical load profile that peaks during the day.

Table 27. Cost Impacts of New ET2 EVSE Loads at OKV

Load Types	Annual Grid Electricity Consumption	Annual Peak Demand	Load Factor (%)	Year 1 Cost of Energy ($k)	Year 1 Cost of Demand ($k)	Anticipated New Line Costs ($k)
UAM only	487 MWh	707 kW	7.9%	32.9	83.3	$90
RAM only	527 MWh	796 kW	7.6%	35.6	93.8	$90
Trainer only	133 MWh	290 kW	5.2%	9.0	34.2	$90
All EVSE	1,147 MWh	1,768 kW	7.4%	77.4	191	$91.5
All EVSE + All Buildings	1,400 MWh	1,800 kW	8.9%	94.4	195	$91.5
All OKV buildings as one node	252 MWh	74 kW	39%	23.3	1.98	N/A

The forecasted ET2+ loads at OKV have substantially higher energy consumption at similar peak power draw as the ET2 loads (as presented in Table 28). Again, the annual grid electricity consumption metrics in this table represent the energy drawn from the grid so they include an EVSE efficiency of 90%. No new on-site generation systems or battery storage are assumed in this calculation. Electricity costs and consumption for all OKV buildings as a single node are provided for comparison. The cost to build a new line from the existing airport distribution infrastructure to the EVSE would be nearly $90,000 irrespective of the load types served.

Table 28. Cost Impacts of New ET2+ EVSE Loads at OKV

Load Types	Annual Grid Electricity Consumption	Annual Peak Demand	Load Factor (%)	Year 1 Cost of Energy ($k)	Year 1 Cost of Demand ($k)	Anticipated New Line Costs ($k)
UAM only	645 MWh	707 kW	10.4%	43.6	83.3	$90
RAM only	625 MWh	796 kW	9.0%	42.2	92.1	$90
Trainer only	118 MWh	290 kW	4.6%	7.97	34.2	$90
All EVSE	1,389 MWh	1,752 kW	9.1%	93.7	185	$91.5
All EVSE + All Buildings	1,641 MWh	1,790 kW	10.5%	111	188	$91.5
All OKV buildings as one node	252 MWh	74 kW	39%	23.3	1.98	N/A

Given the similarity between the ET2 and ET2+ loads in their magnitudes and resulting electricity costs, subsequent sections of this report focus only on the results with the more refined ET2+ EVSE loads. Results for the ET2 loads can be found in Appendix B.

5.6.2 Reducing Electric Vehicle Supply Equipment Bill Impacts Using On-Site Distributed Energy Resources

This section presents the REopt-identified cost-optimal system sizes for each load type that maximizes electric utility bill savings across project life cycle (see Table 29). These results do not include any line upgrade implications of building on-site generation and laying an underground line to transport power to the loads. A battery storage system is the only solution that is cost-effective given the underlying electric tariff. Solar PV is not identified as cost-effective across these load types at the price points considered. The presence of up-front grants or an investment tax credit could make solar PV financially cost-effective. On-site BESS systems might provide substantial savings on demand charges at the expense of slightly higher energy charges due to losses in the BESS' energy transfer systems. The absence of any on-site energy generation sources results in the BESS charging from the grid and increasing the overall grid electricity consumption while reducing the overall peak demand across load types. Compared to smaller ET2 loads, the ET2+ results identify a smaller battery than the ET2 results because the load factor of the ET2+ EVSE loads is greater than that of the ET2 loads. This results in the model perform more aggressive peak shaving for the ET2 loads than the ET2+ loads.

Table 29. REopt-Identified Cost-Optimal Results for OKV (ET2+)

Load Type	New BESS System Sizes	NPV of Cost Savings	Internal Rate of Return	Simple Payback	Installed Costs	Annual Grid Energy Reduction	Annual Peak Demand Reduction
UAM only	25 kW/ 8 kWh	$8,300	7.0%	15 yrs	$28,000	-0.04%	3.54%
RAM only	155 kW/ 58 kWh	$48,000	6.7%	15 yrs	$179,000	-0.42%	19.47%
Trainer only	14 kW/ 6 kWh	$3,900	6.4%	16 yrs	$17,000	-0.07%	4.48%
All EVSE	394 kW/ 188 kWh	$78,000	5.9%	16 yrs	$476,000	-0.09%	22.49%
All OKV buildings	N/A	N/A	N/A	N/A	N/A	N/A	N/A
All EVSE + All Buildings	395 kW/ 191 kWh	$79,000	5.9%	16 yrs	$478,000	-0.08%	22.07%

Table 30 presents the Year 1 identified electric utility bill costs and savings given the REopt-identified on-site generation systems. The presence of on-site BESS can provide demand charge savings when the ET2+ EVSE loads are served while causing very small increases in the total energy costs because the BESS also charges from the grid. For example, in the All EVSE load type, the BESS unlocks $45,000 in demand charge reduction while negligibly increasing the energy costs by $100. In general, the ET2+ load types provide modest utility bill savings in isolation, but aggregating EVSE loads or aggregating building and EVSE loads provides considerably more savings.

Table 30. Electric Utility Bill Savings From Cost-Optimal DERs (ET2+)

Load Type	BAU Energy Charges	BAU Demand Charges	OPT Energy Charge (% Reduction)	OPT Demand Charges (% Reduction)	Utility Bill Savings
UAM only	$43,600	$83,300	$43,600 (0%)	$80,400 (3%)	2.29%
RAM only	$42,100	$92,100	$42,400 (-1%)	$73,800 (20%)	13.41%
Trainer only	$7,970	$34,200	$7,970 (0%)	$32,500 (5%)	4.03%
All EVSE loads	$93,700	$185,000	$93,800 (~0%)	$140,000 (24%)	16.11%
All EVSE + All BLDG loads	$111,000	$188,000	$111,000 (0%)	$143,000 (24%)	15.05%

The results presented thus far identify cost savings that could be unlocked with new on-site energy assets, but they do not factor in the cost of the new distribution line upgrades that would be required to electrically connect the assets. Table 31 presents the net cost savings over 25 years after the line upgrade costs are factored in. Under the Grid-Only scenario, the line upgrade costs for the EVSE are sunk costs. When a BESS is installed, it does not reduce the EVSE power consumption enough to downsize the cable that would be required to energize the EVSE, resulting in no cost savings in EVSE line upgrades. Under the All EVSE and All EVSE + All Buildings load types, the REopt-identified battery-provided cost savings nearly break even (costs of $11,000 and $12,000 over 25 years, respectively) with the line upgrade cost for the battery if the EVSE line is considered a sunk cost.

Table 31. Savings After Line Costs From DERs at OKV (ET2+)

Load Type	EVSE Line Upgrades (Sunk Cost)	BESS Line Costs	NPV From BESS Before Considering Line Costs	NPV With All Line Upgrades	NPV With All Line Upgrades Minus Sunk Cost
UAM only	$90,000	$90,000	$8,300	-$172,000	-$82,000
RAM only	$90,000	$90,000	$48,000	-$132,000	-$42,000
Trainer only	$90,000	$90,000	$3,900	-$176,000	-$86,000
All EVSE	$91,500	$90,000	$78,000	-$103,000	-$12,000
All EVSE + All Buildings	$91,500	$90,000	$79,000	-$102,000	-$11,000

5.6.3 Resilience Benefits of On-Site Generation Assets

Table 32 presents the probability of surviving outages of varying durations using the on-site generation systems identified under the Cost-Optimal scenario by REopt and a backup diesel generator. These results can detail the ability of purely cost-effective systems to sustain critical loads at OKV (both building and EVSE loads).

Table 32. OKV System Sizes for Resilience Assessments

Load Type	Battery (ET2+)	Backup Generator (Same for ET2/ET2+)
Existing OKV buildings	0	250 kW (1)
New terminal	0	250 kW (1)
UAM only	25 kW/8.5 kWh	250 kW (1)
RAM only	155 kW/58 kWh	250 kW (1)
Trainer only	14 kW/6 kWh	250 kW (1)
All EVSE	394 kW/188 kWh	250 kW (1)
All OKV buildings	0	250 kW (1)
All EVSE + All Buildings	394 kW/191 kWh	250 kW (1)

Table 33 presents the probability of surviving outages of varying durations using backup generators and on-site generation from Table 32 when only 25% of the building loads are considered critical. These results were only computed for the existing OKV buildings, the new terminal, and a combination of these two profiles. Note that the building-only scenarios do not identify any storage; hence, their resilience results only consider the backup generator. In general, the backup generator can provide 92% or better confidence of surviving outages for up to 72 hours.

Table 33. Probability of Surviving Outages Serving 25% of OKV Building Loads

Load Type	8 Hours	12 Hours	24 Hours	72 Hours
Existing OKV buildings	97.8%	97.5%	96.4%	92.3%
New terminal	97.9%	97.5%	96.4%	92.3%
OKV buildings + New terminal	97.7%	97.5%	96.4%	92.3%

Next, Table 34 shows similar resilience results across the OKV load scenarios where 100% of the site load (including the EVSE loads) were deemed critical and must be served using the identified on-site generation system sizes. Note that the probability of outage survival does not change for scenarios with only building loads compared to assessments assuming only 25% of critical loads. When the EVSE loads are considered, the UAM-only scenario has an approximate 53% chance of surviving 8-hour outages at best, with confidence dropping to less than 7% for 72-hour outages. In comparison, the Trainer-only scenarios perform better due to larger identified battery systems or the annual peak being less than the dispatchable power from the battery and the backup generator. When the EVSE loads are aggregated, the outage survival probability reduces because the critical loads are larger than the backup generator, and the REopt-identified battery, sized for cost savings, cannot sustain these loads. Survival percentages for scenarios with ET2+ loads are overall marginally worse off than scenarios with ET2 loads.

Table 34. Probability of Surviving Outages Serving 100% of OKV Loads

Load Type	8 Hours	12 Hours	24 Hours	72 Hours
Existing OKV buildings	97.8%	97.5%	96.4%	92.3%
New terminal	97.9%	97.5%	96.4%	92.3%
UAM only (ET2+)	53.9%	40.6%	22.8%	6.7%
RAM only (ET2+)	32.1%	18.0%	8.4%	0.2%
Trainer only (ET2+)	98.8%	98.3%	97.0%	92.3%
All EVSE (ET2+)	28.4%	12.1%	4.1%	0.2%
All EVSE (ET2+) + All buildings	23.4%	9.0%	3.1%	0.1%

5.6.4 ÆNodes Results

The results presented in this section consider the airport as an energy node. Table 35 presents the ÆNode results assuming the Allowed PV or Maximum PV capacity for all the OKV building loads and all the projected ET2+ EVSE loads modeled as a single node. The Allowed PV and Maximum PV scenarios have a large PV system and a large battery. These systems might provide reductions in annual grid electricity consumption, but they do not provide any substantial peak demand reduction across scenarios because these peaks occur overnight (the peak with the ET2+ loads in the Maximum PV scenario occurs at 18:45 on Aug. 23). Both scenarios result in considerable electric utility bill savings. The very large PV system maximizes the on-site generation at the airport and can allow the airport to become grid neutral, whereas installing PV systems that are sized only for annual consumption can offset a portion of the billed energy charges. Due to the load factor of the forecasted loads, batteries can provide a higher peak demand reduction for the ET2 loads than the ET2+ loads. The primary purpose of the battery is monthly peak shaving, which is why the battery maintains SOC levels of nearly 90% or better in all scenarios. Under the Maximum PV scenario, the system only exports enough electricity to break even with the net grid electricity imports at the airport. The remainder of the PV production is curtailed.

Across both scenarios, the NPV of the cost savings is negative, ranging from -$0.719 million to $21.6 million. If the electricity exported to the grid under the ET2+ Allowed PV scenario were compensated at an additional $0.07/kWh than the modeled export rates, the total export benefit could make this scenario cost neutral. Similarly, all exports and curtailments from solar PV would need to be valued at an additional $0.09/kWh more than the current export rates (curtailment has no value in the current results) to break even with the negative NPVs for the ET2+ Maximum PV scenarios. This calculation considers the total export or curtailment over 25 years from solar PV and the negative NPV (also over the 25-year time horizon) to arrive at these add-on break-even compensation thresholds. These calculations assume that all exported or curtailed electricity could be used at or outside the airport, and they do not factor in any line upgrade costs associated with getting the electricity from the airport. These rates could be compared against the value of lost load at an airport, at a large load, or at critical loads surrounding an airport that could benefit from these exports to justify the investment. The airport and its utility could also come to an agreement on exporting power to the grid based on market signals that can be lucrative and use the airport to add flexibility when the regional grid is under stress.

Table 35. ÆNode Results for OKV

Output	ET2+ Allowed PV	ET2+ Maximum PV
New solar PV	618 kW	8,300 kW
New battery kW/kWh	376 kW/205 kWh	409 kW/219 kWh
BAU life cycle cost	$5.26 million	$5.26 million
Life cycle cost w/DERs	$5.97 million	$26.8 million
NPV	-$0.719 million	-$21.56 million
Initial capital costs	$2.04 million	$21.6 million
Grid to load MWh	1,288 MWh	677 MWh
Grid to battery MWh	6.44 MWh	9.07 MWh
Total grid consumption	1,295 MWh	686 MWh
Peak demand BAU	1,791 kW	1,791 kW
Peak demand w/DERs	1,411 kW	1,327 kW
Year 1 energy cost BAU	$111,000	$111,000
Year 1 energy cost	$87,400	$46,300
Year 1 demand cost BAU	$188,000	$188,000
Year 1 demand cost	$140,000	$131,000
Annual PV energy produced	762 MWh	10,232 MWh
PV LCOE	$0.156/kWh	$0.156/kWh

Output	ET2+ Allowed PV	ET2+ Maximum PV
PV to load kWh	343 MWh	876 MWh
PV to battery kWh	3.67 MWh	89 MWh
PV to export kWh	415 MWh	686 MWh
Year 1 export benefit	$28,000	$46,200
PV curtailed MWh	0	8,581 MWh
Battery to load MWh	9.14 MWh	88.3 MWh
Calculated battery efficiency	90.4%	90.0%
Average battery SOC	97.6%	93%
Additional compensation for exported and curtailed solar PV to break even with negative NPV	$0.07/kWh	$0.09/kWh

Figure 16 presents the dispatch plot for OKV's Allowed PV scenario over 3 days in August. This plot represents how on-site assets should be operated to maximize cost savings. The BESS cycles regularly to shave EVSE charging peaks and cycles from 100% to 20% to shave the peak demand on Sept. 5. PV exports to the grid occur during the day and are presented in pink.

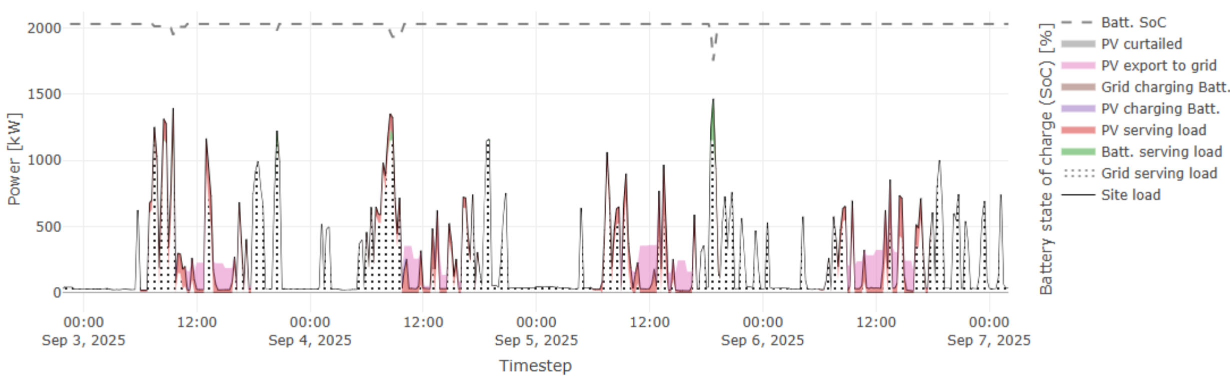

Figure 16. Dispatch for 3 days in September, Allowed PV scenario.

Note: The battery SOC trace (secondary y-axis) was scaled down to minimize the overlap with the dispatch plot. This trace varies between 100% and 20%.

5.6.5 When Does Solar Export Power to the Grid?

REopt's optimal dispatch provides a time series of when surplus solar energy from the ÆNodes scenario might be available for export to the grid under the optimal dispatch strategy. Outputs from REopt were used to calculate the expected values of the PV production surplus (in the form of exports to the grid or curtailment) for all hours of the year. Figure 17 presents the expected value of the surplus PV energy and power that could typically be available at each hour of the day for the Allowed PV system with ET2+ loads. The system has no PV curtailments, but it can be expected to export up to 154 kWh at 12 p.m., peaking at approximately 223 kW exported energy between 11 a.m. and 12 p.m. The exports dip in early afternoon, possibly due to scheduled flights that need charging, and resume in the early evening.

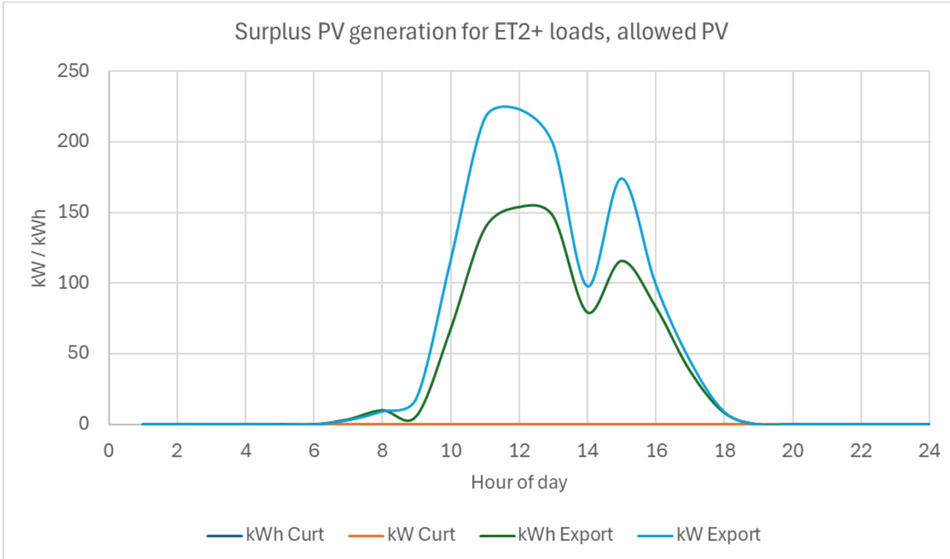

Figure 17. Expected energy and power export, Allowed PV scenario

The Maximum PV scenario produces a lot of surplus PV energy, thereby exporting power to the grid and curtailing production throughout the day. This system can be expected to curtail up to 3.6 MW of power between 12 p.m. and 1 p.m. (resulting in 2,500 kWh curtailed between 12 p.m. and 1 p.m.). Exports to the grid are substantially lower and are expected to peak at approximately 700 kW/200 kWh in the afternoon between 12 p.m. and 1 p.m. (shown in Figure 18).

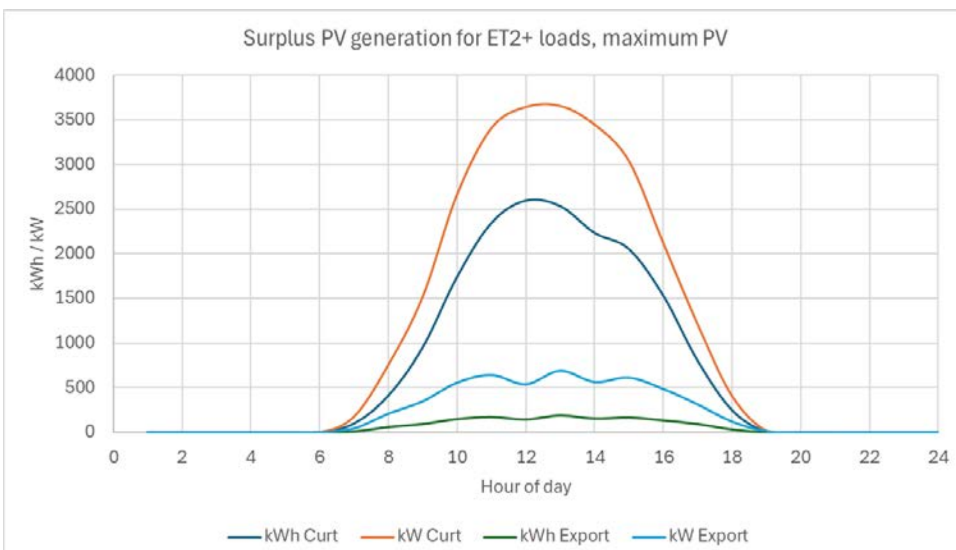

Figure 18. Expected surplus energy and power, Maximum PV scenario

5.6.6 Resilience Value of ÆNode Systems

Table 36 presents the likelihood of surviving an outage of varying durations with the REopt-identified system sizes for the Allowed PV and Maximum PV scenarios. When critical loads are limited to 100% of the building loads only, the identified system mix and existing 250-kW backup diesel generator can provide 99% or greater likelihood of surviving outages of up to 72 hours.

Table 36. Likelihood of Surviving an Outage at OKV With Buildings Only

	Solar PV	Battery	Backup Generator	8 Hours	12 Hours	24 Hours	72 Hours
All buildings	618 kW	646 kW/ 375 kWh	250 kW (1)	99.9%	99.9%	99.9%	99.8%
All buildings	8,300 kW	646 kW/ 375 kWh	250 kW (1)	99.9%	99.9%	99.9%	99.8%

Table 37 provides the probability of surviving outages with 100% of the buildings and the projected OKV EVSE loads. A single 250-kW generator can provide very minimal odds of surviving outages of 8 hours. If the airport were to install two generators, the odds of surviving outages of 8 hours and 12 hours increase to 65% and 53%, respectively, with the system giving a 9% chance of surviving a 72-hour outage. The Allowed PV system with one generator performs slightly worse than the two-generator system. If the airport were to have two backup generators with the Allowed PV system and a battery, it would have a greater than 90% chance of sustaining outages of up to 12 hours. After this, the outage survival dips to an approximately 65% chance of sustaining a 72-hour outage. The larger Maximum PV system results in modest improvements in outage survival compared to the limited Allowed PV system.

Results with the ET2+ loads and all the building loads identified smaller batteries than the ET2 load results. This reduces the ability to sustain outages compared to the ET2 results (as detailed in Table 37). At best, the Maximum PV system and the associated battery along with two backup generators can support the ET2+ loads and the OKV building loads with 89% confidence for outages lasting 8 hours or longer.

Table 37. ET2+ Probability of Surviving Outages With All OKV Buildings and EVSE Loads

	Solar PV	Battery	Backup Generator	8 Hours	12 Hours	24 Hours	72 Hours
Buildings + EVSE	618 kW	376 kW/ 205 kWh	250 kW (1)	36.6%	17.7%	7.58%	1.45%
Buildings + EVSE	618 kW	376 kW/ 205 kWh	250 kW (2)	76.5%	66.2%	46.5%	16.1%
Buildings + EVSE	8,300 kW	409 kW/ 219 kWh	250 kW (1)	60.8%	45.4%	16.5%	3.18%
Buildings + EVSE	8,300 kW	409 kW/ 219 kWh	250 kW (2)	89.5%	84.8%	73.2%	46.3%

5.6.7 Robust Design Results at Winchester Regional Airport

An in-depth description of the REopt-Insight results and analysis is included in Appendix A. These complete results have been condensed to specific design guidance given in Section 5.6.8. This section includes an abbreviated example of some results.

The uncertainties with the greatest effect on HVN are the demand charge in the electric tariff, the electricity cost escalation rate, the discount rate, and the capital cost of solar. Assumptions around these values will have an outsized impact on the optimal sizing and potential returns of an on-site generation and storage system. Figure 19 shows the impact of these parameters on the NPV of the system after 25 years. At OKV, although some systems can provide a positive return, this benefit is small and well within the error bars. Only in the case of a continuously high energy escalation rate does the system reliably pay for itself and produce significant revenue.

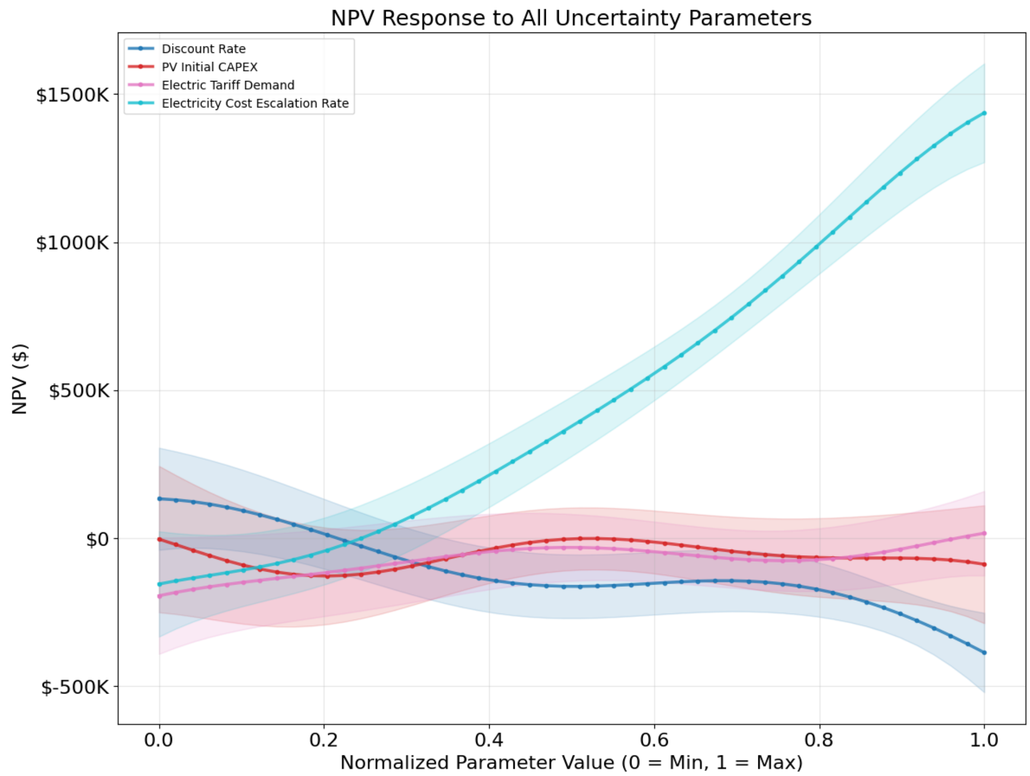

Figure 19. Sensitivity for fixed system size (PV: 0 kW, BESS: 583 kW/531 kWh)

Figure 20 shows how optimal design sizes vary against some of these uncertainty sensitivities. This analysis has been completed for each impactful uncertainty in the appendix. Solar PV should be considered only if the electricity escalation rate exceeds 5% or if the PV system can be purchased for less than $1,250/kW. A large battery system is only optimal if the energy escalation rate is high.

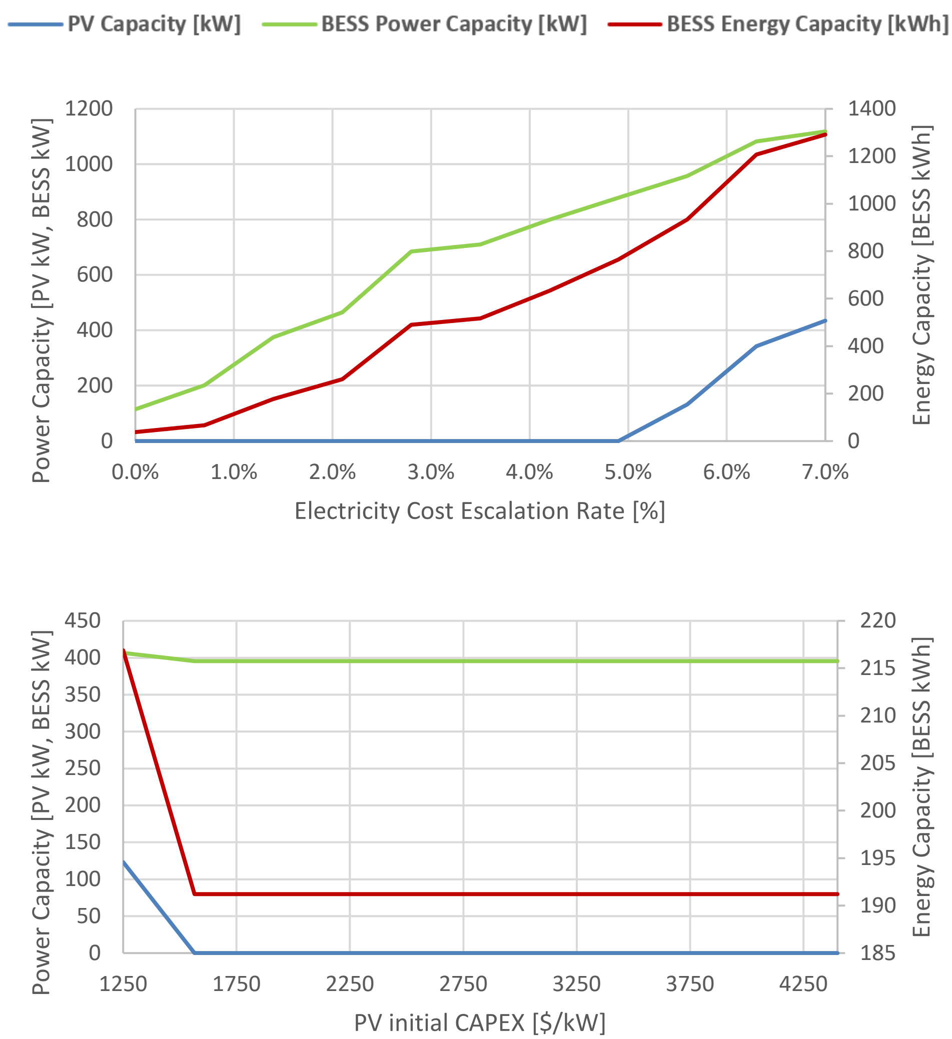

Figure 20. OKV optimal design sizes for varying uncertainty parameters

Figure 21 and Figure 22 depict the designs that strike the optimal balance between cost and resilience. Each data point has a 90% chance of surviving a utility outage that lasts for the survival resilience period (SRP) given on the x-axis. For each SRP, several thousand systems were tested using REopt-Insight, and the system that had the highest NPV while achieving the stated resilience criteria is depicted here. These data can be used to devise a cost-effective resilience investment strategy by selecting how many hours the site wants to build for and finding the recommended system sizes in the plots.

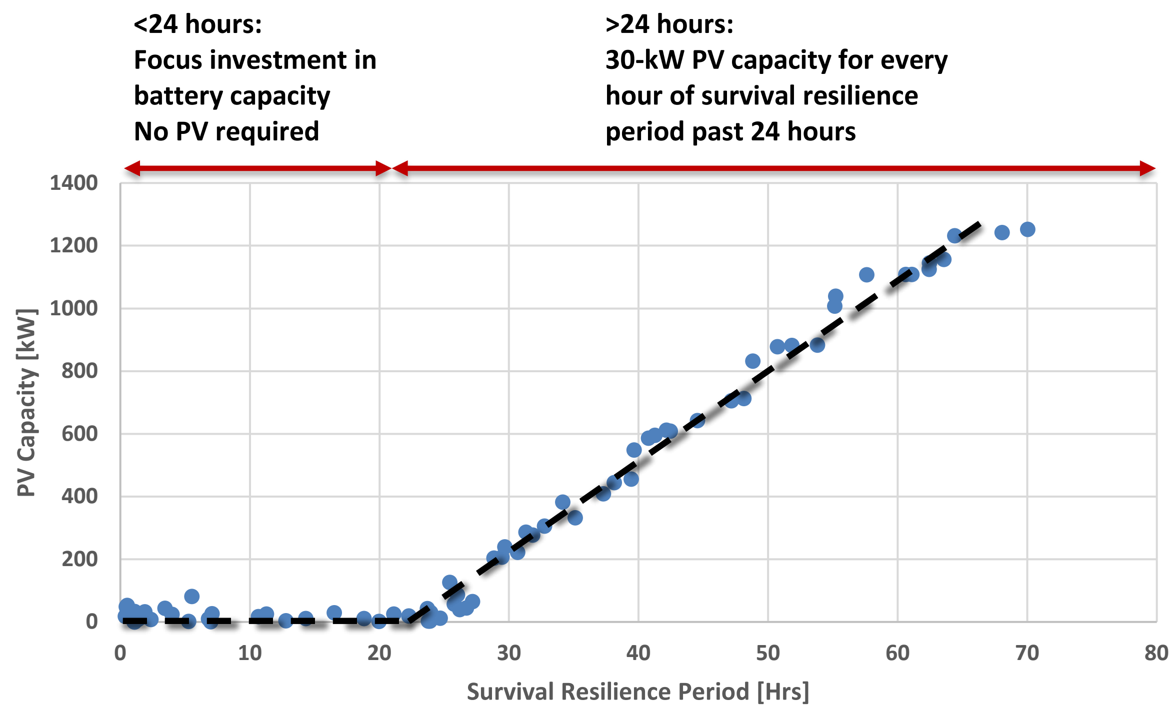

Figure 21. OKV pareto optimal designs: PV system sizes

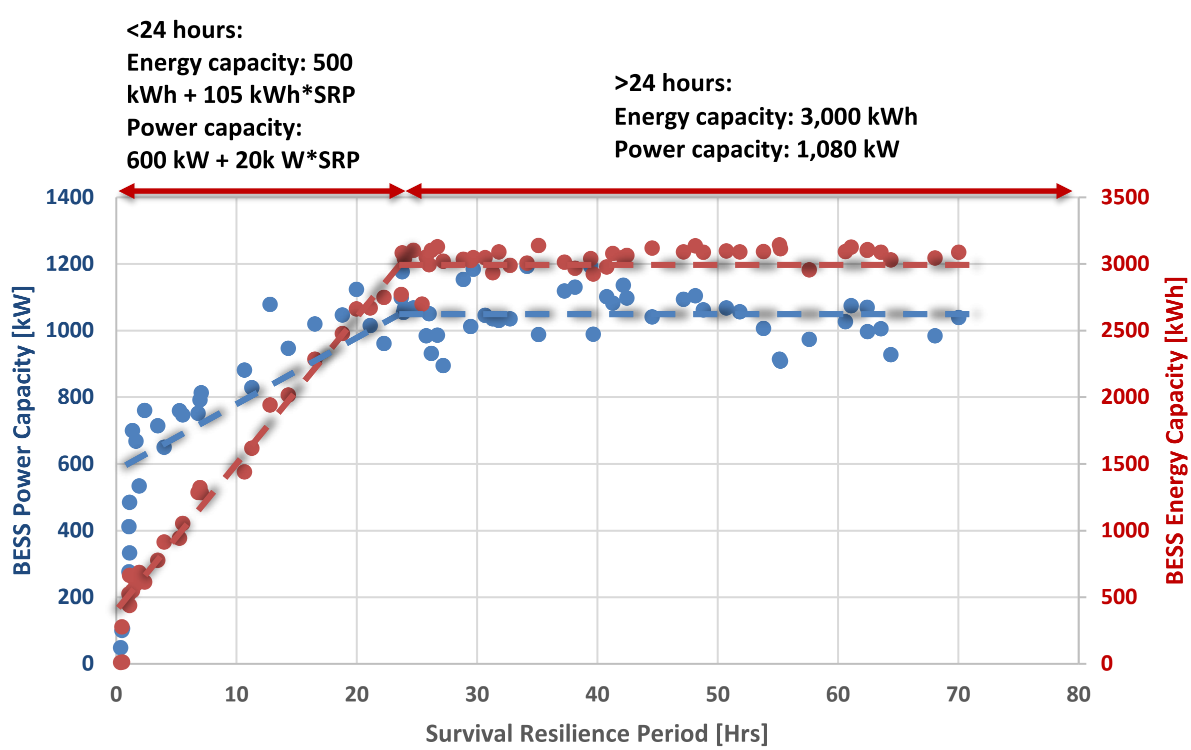

Figure 22. OKV pareto optimal designs: BESS system sizes

5.6.8 Robust Design Guidance for Winchester Regional Airport

REopt-Insight was used to look at the financial trends and optimal investment strategies for OKV. The high-level insights are given here. The detailed methodology and results of the analysis at OKV are in Appendix A.

- Local generation and storage assets can provide resilience benefits, but it is unlikely they will provide significant utility savings.
  - PV provides limited value under most conditions: PV capacity rarely appears in cost-optimal solutions. It should be invested in only if the system can be purchased for less than $1,565/kW or if electricity cost escalation rates are expected to be extremely high (>5% nominal annual escalation over the next 25 years).
  - BESS can be cost-effective, but significant savings occur only under market conditions that are particularly well suited to on-site generation. Under base conditions, only small batteries break even, with small and uncertain NPVs. Under adverse market conditions, no on-site storage design is financially viable. Only when future electricity prices rise faster than discounting effects do batteries deliver strong economic returns. For this reason, they should not be viewed as an economic investment, but they can provide resilience benefits.
- Resilience provided by PV and BESS will cost roughly $47,000 per hour of desired outage survival: The analysis shows a consistent trade-off of roughly $47,000 NPV per hour of outage that the system can survive (this estimate includes no estimate for the value of lost load on the site). This assumes that an ideal system design is chosen for the desired length of the outage survival, and a fixed set of assumptions was used for the uncertainty parameters. Table 38 shows the cost-optimal investment strategy for investing in resilience assuming no diesel generators. The SRP denotes the outage duration that the system has a 90% chance of surviving with no loss of load. To choose a system size, select the number of hours that the site needs to be able to survive, and enter this into Table 38.

Table 38. Optimal Investment Strategies for Resilient Energy Systems at OKV

Parameter	Up to 24 Hours	Beyond 24 Hours
PV capacity (kW)	No PV is needed.	30 kW × (SRP–24 h)
BESS energy capacity (kWh)	500 kWh + 105 kWh × (SRP)	3,000 kWh
BESS power capacity (kW)	600 kW + 20 kW × (SRP)	1,080 kW

* SRP: outage length (in hours) that the site is hoping to survive

- Future economic conditions dominate system performance.
  - Factors encouraging on-site energy investment: Discount rate and electricity cost escalation rate were the most influential parameters, highlighting that long-term financial uncertainty, not equipment pricing, drives project risk at OKV.

Considering that airports are less profit driven than private companies, an assumption of a low discount rate might be reasonable. Additionally, data center related load growth and electrification trends might result in increased energy costs. This suggests that on-site generation systems might be more cost-effective than our analysis suggests.

- Factors discouraging on-site energy investment: Market volatility increases investment risk. Because on-site generation cost-effectiveness heavily depends on uncertain future financial conditions, any revenue from on-site generation assets at OKV are inherently unpredictable. Although such systems might turn a profit, they cannot be considered a reliable investment.

5.7 Tweed New Haven Airport Results

Results for the baseline HVN scenarios are available in Appendix B.

5.7.1 Impact of Electric Vehicle Supply Equipment Loads

The electricity usage and cost implications of the ET2 EVSE loads are presented in Table 39. Forecasted EVSE electricity consumption at HVN could be as high as 1,449 MWh with an added peak demand of 1,728 kW. In comparison, all HVN buildings together could consume as much as 4,062 MWh with a peak demand of 1,345 kW. The estimated energy consumption and costs for all HVN buildings as a single node are also given for comparison. Note that added EVSE-related energy consumption and peak demand could be less than the eventual electricity consumption at the HVN buildings.

Table 39. Cost Impacts of New ET2 EVSE Loads at HVN

Load Type	Annual Grid Electricity Consumption	Annual Peak Demand	Year 1 Cost of Energy ($k)	Year 1 Cost of Demand ($k)
UAM only	398 MWh	707 kW	46.0	73.2
RAM only	955 MWh	791 kW	117	67.8
Trainer only	96.3 MWh	290 kW	11.1	30.1
All EVSE	1,449 MWh	1,728 kW	174	146
All EVSE + All buildings	5,511 MWh	2,586 kW	768	574
All HVN buildings as one node	4,062 MWh	1,345 kW	559	326

The forecasted ET2+ loads at HVN have substantially higher energy consumption at similar peak power draw than the ET2 loads (as presented Table 40). Electricity costs and consumption for all HVN buildings as a single node are provided for comparison.

Table 40. Cost Impacts of New ET2+ EVSE Loads at HVN

Scenario	Annual Grid Electricity Consumption	Annual Peak Demand	Year 1 Cost of Energy ($k)	Year 1 Cost of Demand ($k)
UAM only	666 MWh	705 kW	76.0	73.3
RAM only	1,075 MWh	793 kW	133	70.1
Trainer only	91.7 MWh	290 kW	10.3	30.0
All EVSE	1,833 MWh	1,673 kW	220	149
All EVSE + All buildings	5,895 MWh	2,457 kW	823	592
All HVN buildings as one node	4,062 MWh	1,345 kW	559	326

Given the similarity between the ET2 and ET2+ loads in their magnitudes and the resulting electricity costs, subsequent sections of this report focus only on the results with the more refined ET2+ EVSE loads. Results for the ET2 loads can be found in Appendix B.

5.7.2 Reducing Electric Vehicle Supply Equipment Bill Impacts Using On-Site Generation

Table 41 presents the cost-optimal REopt results with the identified on-site generation system sizes that can help save money on electric utility bills at HVN for existing building loads, new terminal loads, and forecasted ET2+ EVSE loads. Scenarios with both building and ET2+ EVSE were modeled with UI's GSTD rate with Direct Energy's day-ahead market rate, which facilitates the buildout of large PV and modest battery systems. UI's GSTEVSE tariff was used to model EVSE-only load types. This tariff had considerable energy charges but did not have high enough demand charges, resulting in the buildout of large PV systems but very small (negligible) batteries.

For comparison, EVSE-only load types were also modeled using UI's GSTEVSE rate with Direct Energy's energy charges. With this electric tariff combination, the model identified no on-site generation solutions as cost-effective for the EVSE-only load types. When built, on-site generation can provide a substantial reduction in grid energy. Due to the nature of electric tariffs, solar PV can provide more value than battery systems for the ET2+-only load types. Like ET2+, on-site generation solutions were not cost-effective for the ET2-only load types when using the GSTEVSE rate with the day-ahead market rate from Direct Energy.

Table 41. REopt-Identified Cost-Optimal Results for HVN (ET2+)

Load Type	New System Sizes	NPV of Cost Savings	Internal Rate of Return	Simple Payback (Years)	Installed Costs	Annual Grid Energy Reduction	Annual Peak Demand Reduction
UAM only	PV: 550 kW Battery: 26 kW/9 kWh	$444,000	7.3%	11.5 yrs	$1,459k	19.2%	3.8%
RAM only	PV: 889 kW	$710,000	7.3%	11.3 yrs	$2.3 million	23.7%	0.0%
Trainer only	PV: 76 kW Battery: 21 kW/7 kWh	$63.3,000	7.1%	12 yrs	$221,000	13.7%	7.8%
All EVSE	PV: 1,515 kW	$1.3 million	7.5%	11.1 yrs	$3.9 million	32.5%	1.9%
All HVN buildings	PV: 335 kW Battery: 60 kW/154 kWh	$148,000	5.9%	13.5 yrs	$1 million	6.8%	5.1%
All EVSE + All buildings	PV: 1183 kW Battery: 965 kW/1011 kWh	$2.15 million	8.7%	11 yrs	$4.5 million	34.0%	28.3%

Table 42 describes the possible electric utility cost savings through cost-optimal on-site generation systems. In line with the identified system sizes, on-site generation can provide considerable energy charge reductions across load types. Note the small demand charge savings in the EVSE-only load type scenarios, which is a result of smaller identified batteries due to the nature of the EVSE rate structure. Like ET2+, scenarios with ET2 load types also provide considerable energy charge reductions, but demand charge savings are only realized when building loads are included and the GSTEVSE tariff is not applicable.

Table 42. Electric Utility Bill Savings From Cost-Optimal On-Site Generation Solutions (ET2+)

Scenario	BAU Energy Charges	BAU Demand Charges	OPT Energy Charge (% Reduction)	OPT Demand Charges (% Reduction)	Utility Bill Savings
UAM only	$127,000	$79,100	$101,000 (20.5%)	$75,200(5%)	14.51%
RAM only	$200,000	$76,700	$150,000 (25%)	$75,700 (1%)	18.43%
Trainer only	$18,400	$32,300	$15,800 (14%)	$29,700 (8%)	10.26%
All EVSE loads	$345,000	$162,000	$233,000 (32%)	$155,000 (4%)	23.47%
All EVSE + All BLDG loads	$823,000	$592,000	$621,000 (24%)	$281,000 (52%)	36.25%

5.7.3 Resilience Benefits of On-Site Generation

The results presented in this sub-section quantify the likelihood of various HVN load types surviving outages of varying durations given a backup diesel generator and the REopt-identified on-site generation systems. Table 43 summarizes the REopt-identified system sizes by load type for the ET2+ load categories.

Table 43. HVN System Sizes for Resilience Assessments

Load Type	Battery (ET2+)	Backup Generator (Same for ET2/ET2+)
Existing HVN buildings	Same as ET2	500 kW (1)
New terminal	Same as ET2	500 kW (1)
UAM only	PV: 550 kW Battery: 26 kW/9 kWh	500 kW (1)
RAM only	PV: 889 kW	500 kW (1)
Trainer only	PV: 76 kW Battery: 21 kW/7 kWh	500 kW (1)
All EVSE	PV: 1,515 kW	500 kW (1)
All HVN buildings	PV: 335 kW Battery: 60 kW/154 kWh	500 kW (1)
All EVSE + All buildings	PV: 1,183 kW Battery: 965 kW/1,011 kWh	500 kW (1)

Table 44 presents the results for the load types associated with building loads where 25% of the loads were deemed critical and had to be served. Given the on-site generation configuration, building loads could be sustained for 72 hours or more with 92% or greater confidence.

Table 44. Likelihood of Serving 25% Building Loads at HVN Using REopt-Identified On-Site Generation

Load Type	8 Hours	12 Hours	24 Hours	72 Hours
Existing HVN buildings	98.4%	97.9%	96.8%	92.6%
New terminal	98.0%	97.6%	96.6%	92.4%
HVN existing + New terminal	98.0%	97.6%	96.5%	92.4%

Next, the probability of sustaining outages given the systems identified in Table 45 were assessed across load types. All loads for a scenario was deemed critical and had to be served.

Table 45. Probability of Surviving Outages Serving 100% HVN Loads

Load Type	8 Hours	12 Hours	24 Hours	72 Hours
Existing HVN buildings	97.9%	97.5%	96.4%	92.3%
New terminal	46.1%	29.7%	0.5%	0
HVN existing + New terminal	38.6%	22.2%	0.2%	0
UAM only (ET2+)	94.8%	92.7%	86.8%	66.4%
RAM only (ET2+)	41.4%	20.8%	8.5%	0
Trainer only (ET2+)	99.0%	98.7%	97.5%	93.4%
All EVSE (ET2+)	33.2%	13.5%	4.3%	0
All EVSE (ET2+) + All buildings	33.9%	14.4%	2.9%	0

5.7.4 ÆNodes Results

Table 46 presents the ÆNodes results assuming the Allowed PV or Maximum PV capacity for all HVN building loads and all projected ET2+ EVSE loads modeled as a single node. The Allowed PV and Maximum PV load types were modeled with a relevant PV system and a REopt-identified battery. For the ET2+ loads, the identified systems provide substantial reductions in annual grid electricity consumption and peak electricity consumption from the grid. The same applies for scenarios with the ET2 load type.

When maximizing on-site generation at the airport, the very large PV system can allow the airport to become grid neutral, whereas installing PV systems sized for annual consumption can offset large portions of the billed energy charges. Unlike OKV, the batteries identified for these scenarios maintain an average SOC of 55.9% and 56.7% for the Allowed PV and Maximum PV load types, respectively. Figure 23 presents the dispatch plot for HVN's Allowed PV scenario to show how on-site assets are used to minimize operational costs. Under both the Allowed PV and Maximum PV scenarios, the battery is dispatched in the evening hours and charges overnight/early morning for energy arbitrage on day-ahead market prices. During the day, surplus on-site PV serves a large majority of the loads. The Maximum PV scenario has a larger battery than the Allowed PV scenario, which results in its battery's average annual SOC being fractionally higher than the battery from the Allowed PV scenario.

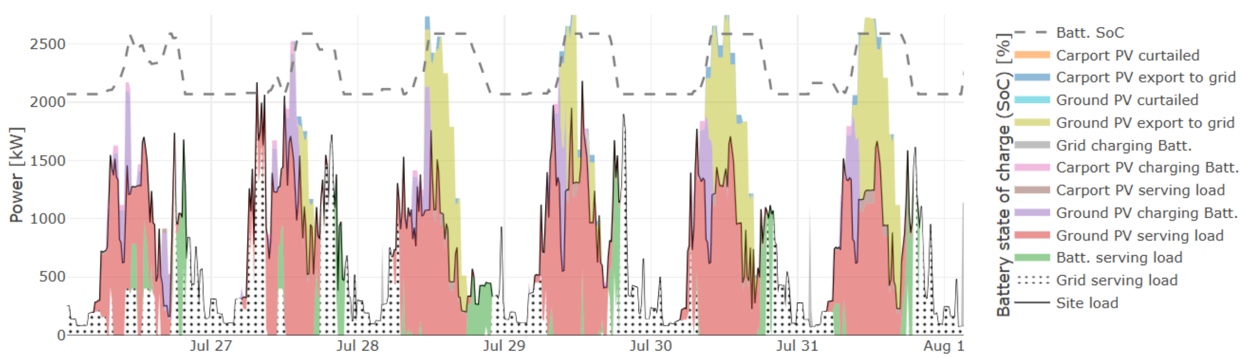

Figure 23. Dispatch plot for HVN's Allowed PV scenario

Under the Maximum PV scenario, the system only exports enough electricity to break even with the net grid electricity purchased at the airport. The remainder of the PV production is curtailed. If the grid exports in the Allowed PV scenarios are compensated at an additional $0.011/kWh, this scenario could become cost neutral. For the maximized PV scenario, if the exports and curtailment are valued additionally at $0.072/kWh, the scenarios would become cost neutral. This compensation rate can be compared against the value of lost load at an airport, at a large load, or at critical loads surrounding an airport. HVN could work with its electric utility to push surplus power to the grid in response to price signals or consider avenues such as virtual net metering or selling solar RECs to generate additional revenue from exports and curtailments from on-site solar. This back-of-the-envelope calculation also assumes that all solar exports and curtailments can be pushed to the grid and compensation is received over 25 years to break even with the NPV.

Table 46. ÆNode Results for HVN

Output	ET2+ Allowed PV	ET2+ Maximum PV
New solar PV	4,308 kW	5,129 kW
New battery kW/kWh	1,061/1980	1,169/2,469
BAU life cycle cost	$21.34 million	$21.34 million
Life cycle cost w/on-site generation	$21.78 million	$27.22 million
NPV	-$0.44 million	-$5.88 million
Initial capital costs	$13.40 million	$20.13 million
Initial capital costs after incentives	$13.40 million	$20.13 million
Grid to load MWh	2,159 MWh	1,674 MWh
Grid to battery MWh	270 MWh	392 MWh
Total grid consumption	2,429 MWh	2,065 MWh
Peak demand BAU	2,457 kW	2,457 kW
Peak demand w/DERs	2,088 kW	2,089 kW
Year 1 energy cost BAU	$823,000	$823,000
Year 1 energy cost	$338,000	$286,000
Year 1 demand cost BAU	$592,000	$592,000
Year 1 demand cost	$169,000	$116,000
Annual PV energy produced	5,211 MWh	7,222 MWh
PV LCOE		
PV to load kWh	2,967 MWh	3,203 MWh
PV to battery kWh	586 MWh	741 MWh
PV to export kWh	1,659 MWh	2,065 MWh
Year 1 export benefit	$105,000	$131,000
PV curtailed MWh	0	1,213 MWh
Battery to load MWh	769 MWh	1,018 MWh

Output	ET2+ Allowed PV	ET2+ Maximum PV
Calculated battery efficiency	89.8%	89.8%
Average battery SOC	55.9%	56.7%
Break-even compensation	$0.011/kWh	$0.072/kWh

5.7.5 When Does Solar Export Power to the Grid?

This section explores when HVN's Allowed PV and Maximum PV systems export power to the grid. Outputs from REopt were used to calculate the expected values of PV production surplus (in the form of exports to the grid or curtailment) for all hours of the year. Figure 24 presents the expected value of the surplus PV energy and power that could typically be available at each hour of the day for the Allowed PV system with the ET2+ loads. The system has no PV curtailments, but it can be expected to export up to approximately 604 kWh between 10 a.m. and 12 p.m., with a peak power export of approximately 1,000 kW around 11 a.m. and 12 p.m. The exports dip in the early afternoon, possibly due to scheduled flights that need charging, and they resume in the early evening.

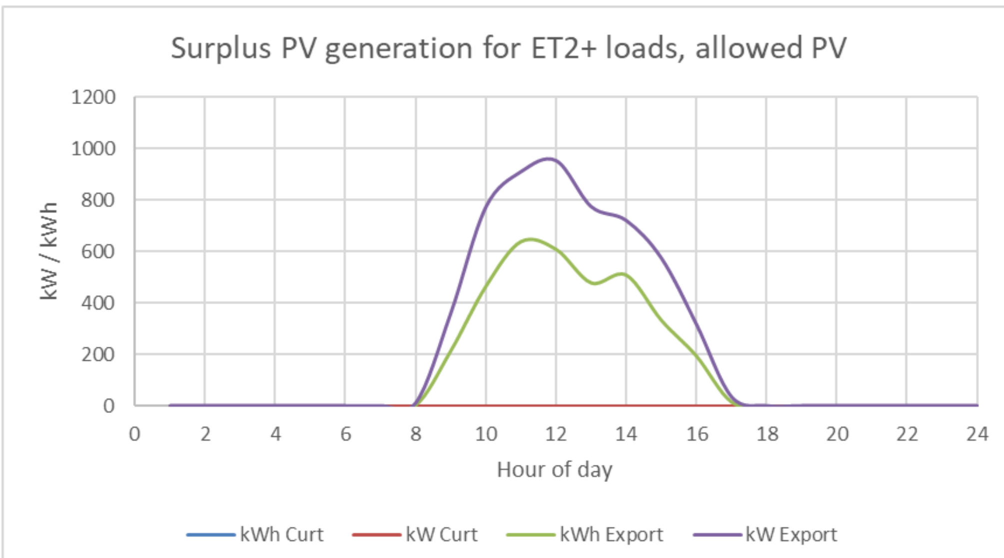

Figure 24. Expected energy and power export, Allowed PV scenario

Figure 25 plots the surplus PV generation for the Maximum PV buildout scenario. The Maximum PV system produces a lot of surplus PV energy, thereby exporting power to the grid and curtailing production throughout the day. This system can be expected to curtail up to 779 kW of power (at most approximately 387 kWh) between around 11 a.m. and 1 p.m. Exports to the grid are substantially higher and are expected to peak at approximately 1,387 kW/779 kWh between 11 a.m. and 12 p.m. OKV is a smaller airport, and the curtailments were substantially higher than the grid exports because the system would only export enough power to make the site grid neutral. The system does not make a site an exporter to the grid. At HVN, the airport itself is modeled to have high electricity consumption, allowing for more exports than curtailment without making HVN an exporter of PV power.

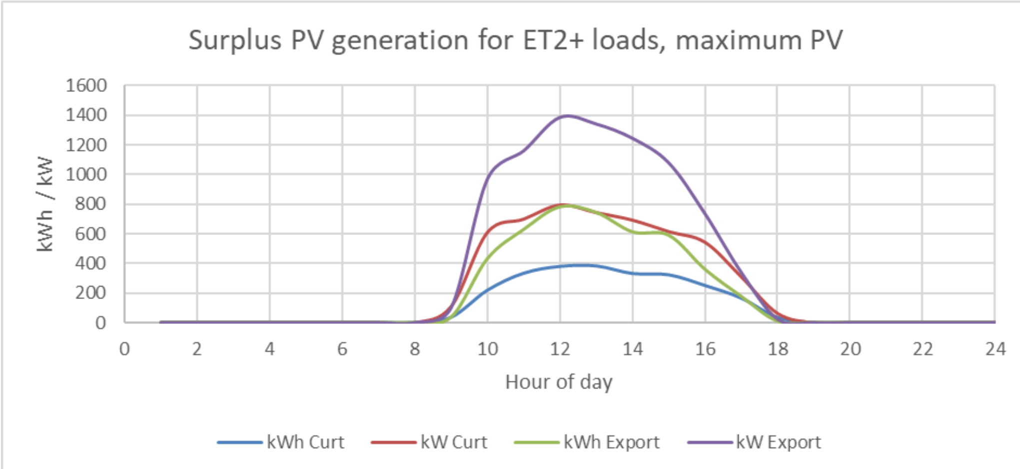

Figure 25. Expected surplus energy and power, Maximum PV scenario

5.7.6 Resilience Value of ÆNodes Systems

Table 47 presents the likelihood of surviving an outage of varying durations with the REopt-identified system sizes for the Allowed PV and Maximum PV scenarios at HVN. When critical loads are limited to building loads only, the identified system mix and a 500-kW backup diesel generator can provide a 92% or greater likelihood of surviving outages of up to 72 hours.

Table 47. Likelihood of Surviving an Outage at All HVN Buildings

	Battery	Backup Generator (Quantity)	8 Hours	12 Hours	24 Hours	72 Hours
All buildings (PV = 4,308 kW)	1,169 kW/ 3,973 kWh	500 kW (1)	97.7%	96.8%	95.6%	92.6%
All buildings (PV = 5,129 kW)	1,233 kW/ 3,949 kWh	500 kW (1)	97.7%	96.8%	95.6%	92.5%
All buildings (PV = 4,308 kW)	1,367 kW/ 3,927 kWh	500 kW (1)	97.6%	96.7%	95.5%	92.2%
All buildings (PV = 5,129 kW)	1,367 kW/ 3,927 kWh	500 kW (1)	97.7%	96.7%	95.6%	92.5%

Table 48 presents the likelihood of surviving outages of varying durations when HVN's building loads and ET2+ loads are considered along with the ÆNodes systems. The presence of a redundant backup generator plays a key role in prolonging the outage survival likelihood for 24- and 72-hour outage duration data points.

Table 48. Likelihood of Surviving an Outage at All HVN Buildings (ET2+)

	Battery	Backup Generator	8 Hours	12 Hours	24 Hours	72 Hours
Buildings + EVSE (PV = 4,308 kW)	1,367 kW/3,927 kWh	500 kW (1)	94.6%	91.3%	78.7%	53.7%
Buildings + EVSE (PV = 4,308 kW)	1,367 kW/3,927 kWh	500 kW (2)	97.6%	97.0%	96.5%	94.7%
Buildings + EVSE (PV = 5,129 kW)	1,367 kW/3,927 kWh	500 kW (1)	95.0%	92.3%	82.3%	59.4%
Buildings + EVSE (PV = 5,129 kW)	1,367 kW/3,927 kWh	500 kW (2)	97.6%	97.1%	96.6%	95.1%

5.7.7 Robust Design Results at Tweed New Haven Airport

An in-depth description of the REopt-Insight results and analysis is included in Appendix A. These complete results have been condensed to specific design guidance given in Section 5.7.8. This section includes an abbreviated example of some results.

The uncertainties with the greatest effect on HVN are the demand charge in the electric tariff, the electricity cost escalation rate, the discount rate, the capital cost of solar, and the capital cost for the battery energy capacity. Assumptions around these values will have an outsized impact on the optimal sizing and potential returns of an on-site generation and storage system. Figure 26 shows the impact of these parameters on the NPV of the system after 25 years. Although the system delivers a positive NPV in almost all future scenarios, the size of this return varies from hundreds of thousands to tens of millions.

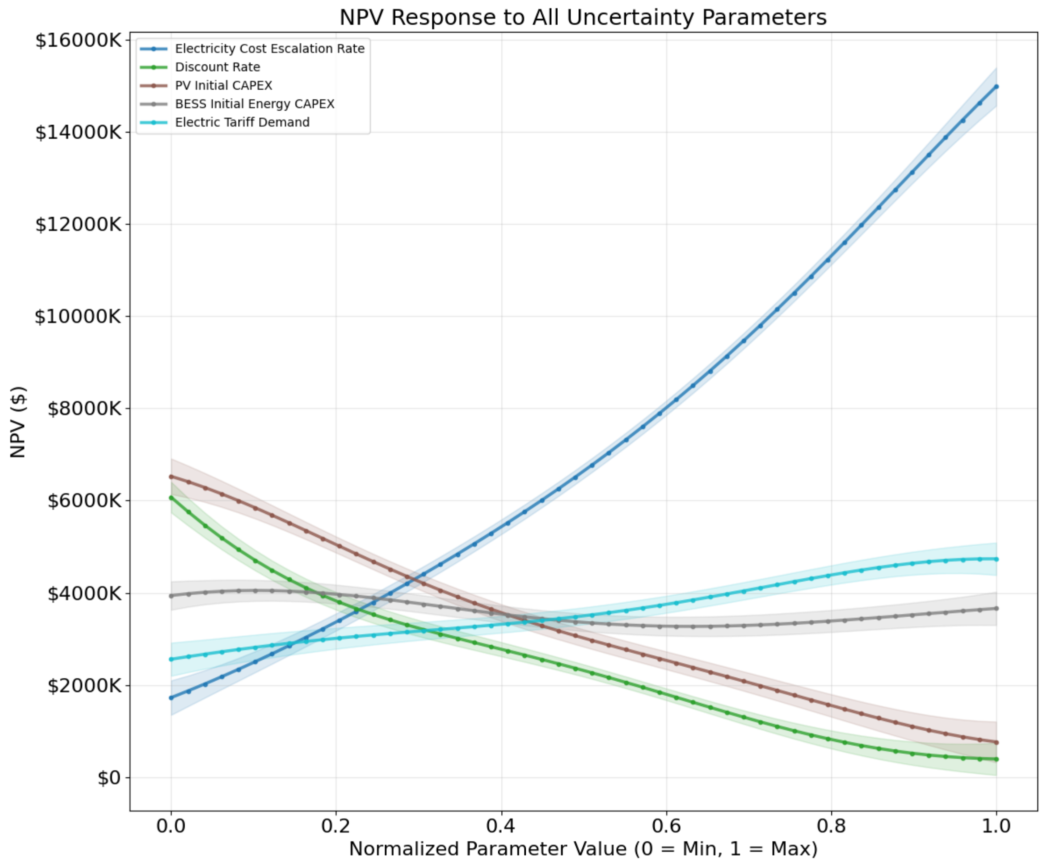

Figure 26. Sensitivity for fixed system size (PV: 1,572 kW, BESS: 1,291 kW/2,146 kWh)

Figure 27 shows how optimal design sizes vary against these uncertainty sensitivities. High escalation rates and low solar costs will justify the extended buildout of PV capacity and BESS energy capacity. The optimal amount of solar capacity drops to zero for very expensive systems. Approximately 1,000–1,500 kW of battery power will consistently provide strong returns across future scenarios.

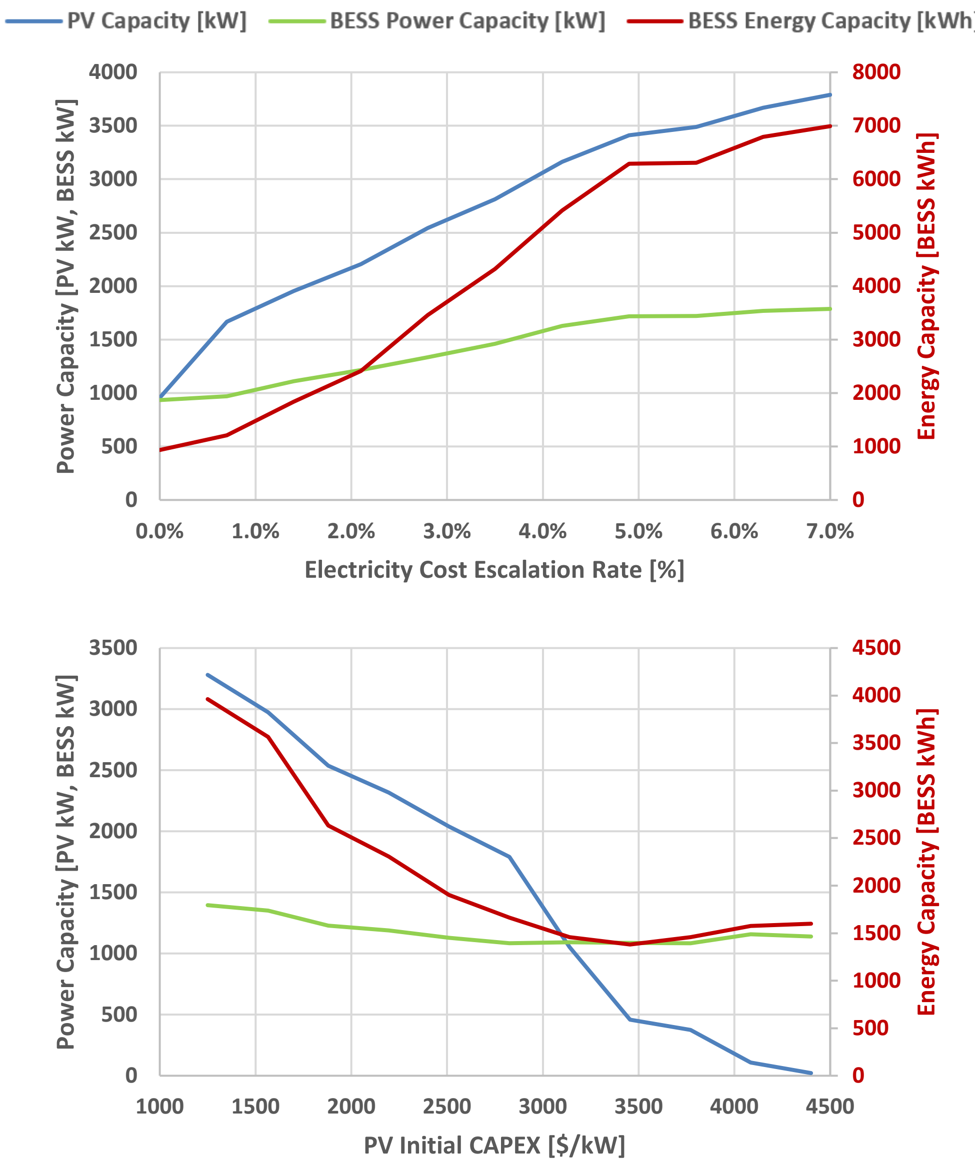

Figure 27. HVN optimal design sizes for varying uncertainty parameters

Figure 28 and Figure 29 depict the designs that strike the optimal balance between cost and resilience. Each data point has a 90% chance of surviving a utility outage that lasts for the SRP given on the x-axis. For each SRP, several thousand systems were tested using REopt-Insight, and the system that had the highest NPV while achieving the stated resilience criteria is depicted here. These data can be used to devise a cost-effective resilience investment strategy by selecting how many hours the site wants to build for and finding the recommended system sizes in the plots.

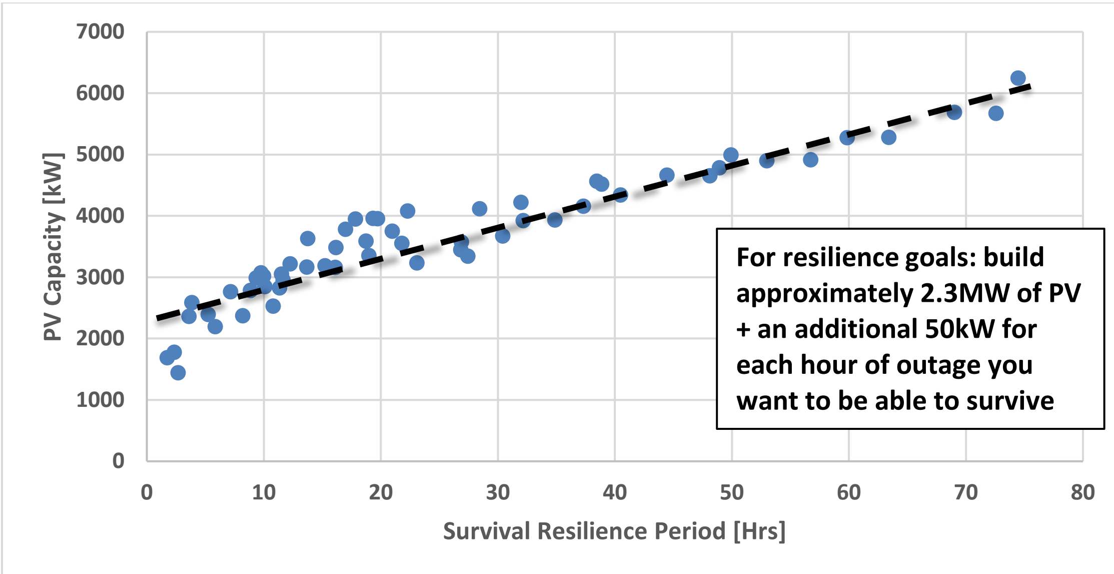

Figure 28. HVN pareto optimal designs: PV system sizes

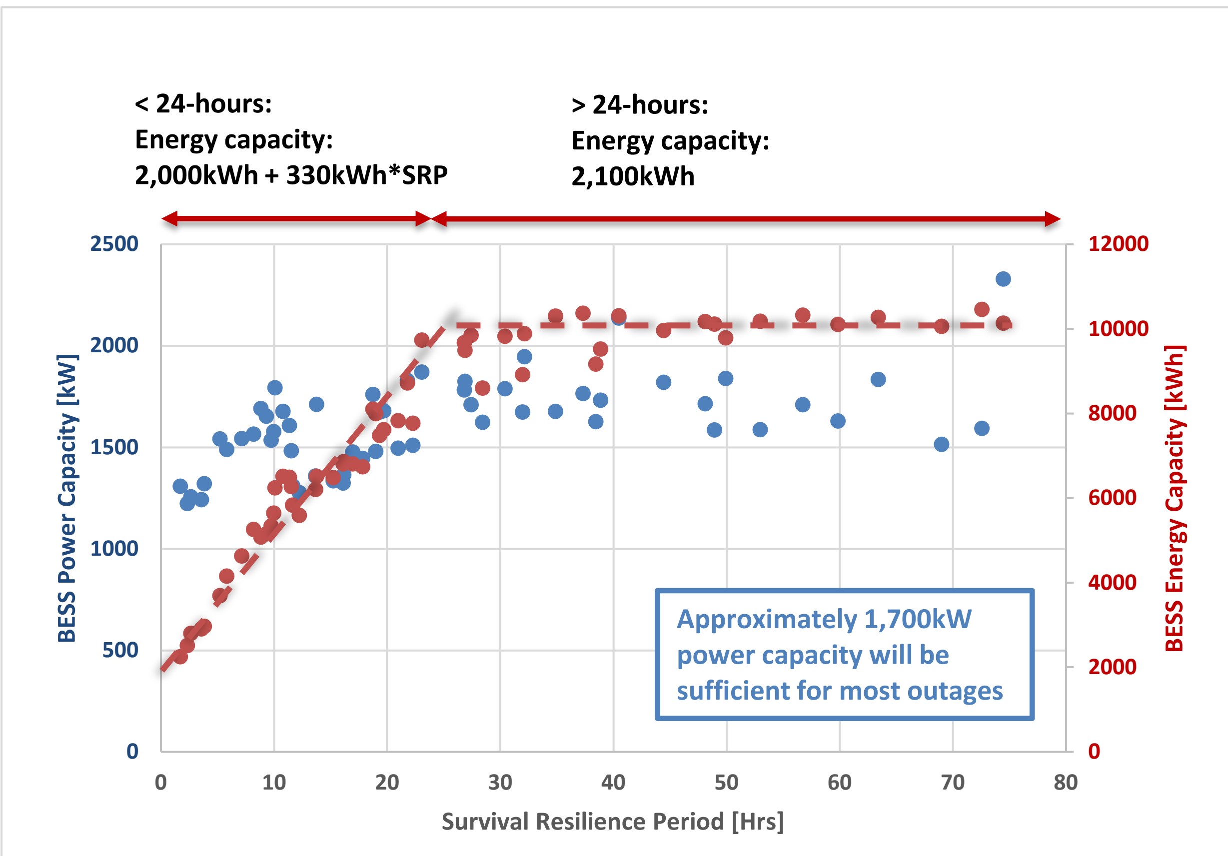

Figure 29. HVN pareto optimal designs: BESS system sizes

5.7.8 Robust Design Guidance for Tweed New Haven Airport

REopt-Insight was used to look at the financial trends and optimal investment strategies for HVN. The high-level insights are given here. The detailed methodology and results of the analysis at HVN are in Appendix A.

- On-site generation and storage investments at HVN can provide cost-effectiveness under almost all market conditions. The following systems will achieve a positive NPV in all but extremely poor economic scenarios where multiple adverse conditions are compounded:
    - PV: PV capacity of 1,500–2,500 kW will be close to cost-optimal in most scenarios.
    - BESS power capacity: The optimal amount of electrical storage power capacity stays consistent in almost all scenarios at 1,000–1,400 kW. Any system within this range is likely to be close to cost-optimal.
- One potential system (PV: 1,572 kW, BESS: 1,291 kW, 2,146 kW) achieved a positive NPV after 25 years across all sensitivities with a minimum of $680,000 and a maximum of $15,000,000.
- Resilience provided by PV and BESS will cost approximately $110,800 per hour of desired outage survival. The analysis shows a consistent trade-off of roughly $110,800 NPV per hour of outage. This does not account for any savings derived from avoiding lost load during an outage. This assumes that an ideal system design is chosen for the desired length of the outage survival, and a fixed set of assumptions was used for the uncertainty parameters. Table 49 shows the cost-optimal investment strategy for investing in resilience assuming no diesel generators. The SRP denotes the outage duration that the system has a 90% chance of surviving with no loss of load. To choose a system size, select the number of hours that the site needs to be able to survive, and enter this into Table 49.

Table 49. Optimal Investment Strategies for Resilient Energy Systems at HVN

Parameter	Up to 24 Hours	Beyond 24 hours
PV capacity (kW)	2,300 kW + 50 kW × (SRP)	2,300 kW + 50 kW × (SRP)
BESS energy capacity (kWh)	2,000 kWh + 330 kWh × (SRP)	10,000 kWh
BESS power capacity (kW)	>1,700 kW	>1,700 kW

* SRP: outage length (in hours) that the site is hoping to survive

- Although cost-optimal systems will almost always pay for themselves, the scale of returns is heavily influenced by some external uncertainties. A fixed system (PV: 1,572 kW, BESS: 1,291 kW, 2,146 kW) demonstrated the following trends:
    - Discount rate: NPV decreases by approximately $830,000 per percentage point increase in discount rate.

- Electricity cost escalation rate: The NPV increases by approximately $1.83 million per percentage point increase in electricity cost escalation rate.
- PV initial CAPEX: The NPV decreases by approximately $158,000 per $100/kW increase in PV cost.
- BESS initial energy CAPEX: The NPV decreases by approximately $210,000 per 100/kWh for the BESS energy cost.
- Electric tariff demand charge: The NPV increases by approximately $55,000 per percentage point increase in demand charges.

5.8 Break-Even Cost of Charging

As discussed in previous sections of this report, installing and operating EVSE at an airport could result in new electric utility costs for the airport. These costs could be reduced by on-site generation assets. In addition to serving the electric load, the airport must also spend money on grid infrastructure upgrades and the installation of the EVSE. The break-even cost of charging (BCOC) estimates the all-inclusive cost of serving EVSE loads in a $/kWh basis. An airport could use this number to know what rate of energy could be charged to vehicles using EVSEs to break even on their investment. Because BCOC is an all-inclusive cost, it considers the following costs associated with EVSE installation and utilization:

1. Electric utility bills—which reflect cost of powering the EVSE
2. On-site generation installed costs—meant to primarily offset electric utility bills and save money
3. On-site generation operations and maintenance costs
4. EVSE installed costs—the all-in cost of installing the EVSE units
5. EVSE replacement costs
6. Grid infrastructure costs—an estimate of the all-in cost of adding underground distribution lines to serve EVSE and any on-site energy systems.

This analysis uses the formula for levelized cost of energy (LCOE) for the calculation of BCOC:

$$BCOC\left[\frac{\$}{kWh}\right] = \frac{FCR * TCC + FOC}{AEU}$$

And:

$$FCR = \frac{1}{\sum_{n=1}^{25} \frac{1}{(1+i)^n}}$$

Here, *FCR* is the fixed charge rate and represents the total amount of money that must be recouped for each dollar invested. *AEU* is the annual energy used in the system. *TCC* is the total capital cost, and *FOC* is the fixed operating cost. The present value of all on-site generation, EVSE, and infrastructure upgrade costs over the time horizon (n = 25 years) will be considered under the *TCC* and annualized using the *FCR*. The required return on investment, *I*, is 6.38% (per Table 22).

Table 50 presents the calculations of BCOC for all building and ET2+ EVSE load types at HVN and OKV. The total annual electricity usage for this load type varies by a factor of 3.6 times between airports. Because both airports have the same discount rate and time horizon, FCR is calculated as 0.08107. The EVSE's installed cost is used in year 0, and the EVSE is considered to be replaced every 10 years after that. The EVSE's year 0 capital costs are inflated to years 10 and 20 and then discounted to the present value. No salvage value is assumed for the EVSE in year 25. At HVN, the EVSE soft costs are assumed to be 150% of the initial estimates because EVSE for training loads are expected to be placed separately from RAM and eVTOL EVSE. This will result in additional costs than at OKV, where the EVSE are colocated. Grid infrastructure is assumed to have a 40-year total life, resulting in 62.5% of year 0 grid costs being attributed to the BCOC calculations.

This analysis considers only new line additions and does not consider existing line upgrades at HVN. The development of HVN's digital twin could help include any existing line upgrade costs in HVN's BCOC calculations. Installed costs for batteries and PV along with the present value of the battery replacement costs and the yearly PV operations and maintenance costs are used for the capital cost calculations related to the on-site generation. Electric utility costs from the REopt results are used for the utility account to factor in the impact of the on-site energy assets. Any export benefits were subtracted from the energy costs.

Table 50. Break-Even Charging Cost Calculations

Cost Item	HVN	OKV
All buildings and EVSE ET2+ loads (*AEU*)	5,895 MWh	1,641 MWh
Discount rate (*i*)	6.38%	6.38%
Time horizon (*n*)	25 years	25 years
FCR	0.08107	0.08107
EVSE	Assumed life: 10 years, full installation in year 0 Only EVSE is replaced in years 10 and 20. All costs are in present value and assume no salvage value of EVSE in year 25.	
EVSE	Year 0 install cost: $967k Year 10 replace cost: 92.7k Year 20 replace cost: $64k Total EVSE cost: $1,124k Annualized: $91.1k	Year 0 install cost: $725k Year 10 replace cost: 92.7k Year 20 replace cost: $64k Total EVSE cost: $881k Annualized: $71.4k
Grid	Assumed life of new grid infrastructure: 40 years Useful life fraction for costs: 25/40 = 0.625	
Grid	Upgrades only for EVSE: $913k ($74.1k annualized) Upgrades for EVSE, PV, BESS: $1,292k ($105k annualized)	Upgrades only for EVSE: $57.2k ($7.42k annualized) Upgrades for EVSE, PV, BESS: $570k ($74k annualized)
On-site PV considered	965 kW ground-mounted PV	618 kW ground-mounted PV

Cost Item	HVN	OKV
On-site battery considered	965 kW/1,011 kWh	376 kW/205 kWh
On-site PV	Installed cost: $3070k (annualized $249k) Year 1 operations and maintenance cost: $22.4k	Installed cost: $1,574k (annualized $127.6k) Year 1 operations and maintenance cost: $11.1k
On-site battery	Installed cost: $1,459k (annualized $118k) Replacement cost: $1,103k (annualized $89k)	Installed cost: $466k (annualized $37.7k) Replacement cost: $230k (annualized $18.7k)
Electric utility	No DERs: $1,415k With DERs: $902k	No DERs: $300.3k With DERs: $200.6k
No on-site generation BCOC (numerator costs are in $k)	$\frac{1415+91.1+74.1}{5{,}895{,}000} = 0.268\frac{\$}{kWh}$	$\frac{300.3+7.42+71.4}{1{,}641{,}000} = 0.231\frac{\$}{kWh}$
BCOC with on-site generation (numerator costs are in $k)	$\frac{902+118+89}{5{,}895{,}000} + \frac{249+22.4+105}{5{,}895{,}000} + \frac{91.1}{5{,}895{,}000} = 0.267\frac{\$}{kWh}$	$\frac{200.6+37.7+18.7}{1{,}641{,}000} + \frac{11.1+127.6+74}{1{,}641{,}000} + \frac{71.4}{1{,}641{,}000} = 0.3296\frac{\$}{kWh}$

Based on these calculations, HVN would need to make at least $0.268/kWh to recoup all costs associated with supporting the EVSE loads. Due to the large electric utility bill savings provided by the on-site generation, HVN's BCOC reduces by $0.01 /kWh with on-site generation. Any on-site generation at HVN could support the airport and EVSE loads during outages, thereby offering reliability benefits at no added cost per useful kWh. At OKV, the electric tariff is cheaper than at HVN, and therefore the airport would need to charge $0.231/kWh to recoup its investment to support the forecasted EVSE loads with the grid only scenario. The addition of on-site generation provides cost savings, but the resulting BCOC is higher than the Grid-Only case by approximately 9.86–10 cents/kWh (at $0.3296/kWh); therefore, to financially break even with any outage survival benefits of these on-site generation assets, OKV would need to charge $0.0986/kWh more, a higher rate, than the Grid-Only base case. This difference could be compared against the value of the lost load at OKV's buildings or at flights that would like to charge during an outage and recouped as best as possible.

5.9 Discussion

The results presented in the preceding section explore the implications of additional forecasted EVSE loads at two regional airports in the United States in addition to exploring the reliability and resilience benefits of on-site energy systems at these airports. OKV is a representative small airport where forecasted EVSE loads can eclipse its annual electricity consumption. It is important for airports like OKV to plan for how to effectively serve forecasted EVSE loads in a cost-effective way to manage the electric utility bills and the load growth associated with the new loads. Airports like OKV could also pay attention to projected peak demand from EVSE loads because this number can directly influence the infrastructure costs associated with powering EVSEs. EVSE peaks can be substantially larger than such airports' own peak demand. HVN is representative of an airport one order of magnitude larger than OKV because its airport buildings are expected to consume more energy than the forecasted EVSE loads. The added demand from the forecasted EVSE loads can be equivalent to the entire airport building stock and does not dwarf the airport's peak as it did with OKV. Both OKV and HVN have the option of either serving the forecasted EVSE loads with the electric grid or using on-site generation, whichever is more cost-effective.

Opting to rely on the grid to serve EVSE loads could be cost-effective if the underlying electricity cost is low. Alternatively, an airport could choose to build on-site generation to help shave peak demand and save money on electric utility bills. If it is cost-effective, on-site generation could save airports money over their entire useful life. The use of on-site generation can also shield airports from expected rises in electric utility rates. If the electricity costs escalate more quickly than expected, any on-site generation can offset more expensive electricity from the grid, thereby shielding the airport from electric rate volatility. There can be cases where on-site generation is found to be very cost-effective or not cost-effective at an airport. The electric tariff's rate structure dictates when on-site generation can provide economic value to cost-compete against the grid. If the electric tariffs are very low in general, on-site generation would not make financial sense. OKV is an example of an airport where the energy rate is not high enough for solar PV to provide value, but demand charges justify an on-site battery. HVN is an airport where the electric tariff is high enough to allow the buildout of solar PV and a battery system; however, UI's GSTEVSE rate, which is designed to serve EVSE loads, currently has minimal demand charges and does not allow batteries to provide value. This rate would allow solar to provide cost savings, but it would not allow for considerable peak demand reduction using batteries, thereby not avoiding higher infrastructure costs. Time-of-use demand charges can allow the buildout of large batteries that do not shave any demand at an airport because the battery would not have any financial incentive to reduce demand when there are no demand charges[12]; therefore, the structure of an electric tariff is very important in determining the cost of serving electric loads and whether on-site generation can provide any cost savings by offsetting grid consumption and peak demand shaving.

Besides cost savings, on-site generation can also augment existing backup reliability assets for serving critical loads at and around airports. Though such a system might not be cost-effective if it is sized with a resilience goal in mind, the up-front cost of these systems can be justified by estimating the value of the lost load for the load served during outages. For example, an airport might lose money on an on-site generation installation, but if it can survive multiday outages with confidence, the up-front cost can be compared against what customers would have paid on a

[12] For example, a prior study focused on quantifying possible electric utility cost savings from on-site generation at Albuquerque International Sunport (Morris et al., 2025). Although solar PV and BESS could save the airport $3 million in electricity costs over 25 years, peak demand from the grid would not reduce despite the identification of substantial battery capacity. This was due to the time-of-use nature of the demand charges in the applicable tariff at Albuquerque International Sunport.

per-kWh basis to have access to the airport's services during that outage. It is important for an airport to set bounds on how long it would like to sustain outages. As shown in OKV and HVN's resilience results, confidently sustaining EVSE and building loads for long durations might require larger batteries or multiple diesel generators, which can be costly up front. An airport that is aware of how it intends to handle outages (routine and major events) while safely adapting its operations could opt to purchase generators or batteries that can serve EVSE loads and critical building loads for enough time to react to power outages.

An airport can also choose to act as an energy node where it would aim to use as much of its available land as possible to host on-site generation. For example, the airport could build batteries at different land parcels or maximize solar PV capacity. There are various pros and cons of becoming an energy node.

- Pros:
    - Serving airport loads or forecasted EVSE loads would become easier as the airport would be able to rely on oversized on-site generation assets. Such a system would lead to large electric utility bill savings.
    - There could be large amounts of surplus generation—for example, OKV and HVN's ÆNode scenarios had large amounts of grid exports and curtailed solar PV. Airports such as HVN that have a state renewable portfolio standard with a solar carve-out can choose to be compensated for exported energy and its REC value. The airport could also opt to perform virtual net metering where it offsets consumption for other congested eligible entities in the area to realize utility bill savings across a portfolio of buildings.
    - An airport can benefit from large on-site DERs by sustaining its critical loads for longer, by augmenting its existing on-site backup generation system during outages, and by sustaining critical loads within its vicinity. Becoming an ÆNode can be very useful in areas that are prone to natural disasters where airport buildings can act as a community shelter for people to seek refuge. OKV is surrounded by a variety of important loads (such as a U.S. National Guard site, a U.S. Army Corps of Engineers site, and Costco) all of which can serve critical functions in a community and would benefit from OKV becoming an ÆNode. The value of the benefit provided by such a system during outages could be tough to estimate and compare against the up-front cost of the entire system.
    - Airports can choose to work with their electric utility and any nearby large loads (such as data centers) to offer flexibility or access to generation from airport-owned resources.[13] Data centers would like to interconnect with the local utility system quickly and avoid delays in securing sufficient reliable generation or infrastructure upgrades. An energy node could offer to ramp up exports to the grid during times of grid stresses, thereby providing flexibility to a colocated large-load neighbor. Alternatively, an energy node could enter an arrangement with its

[13] Large loads such as data centers are coming online at a quicker rate than electricity generation capacity can be constructed to serve these loads. This scarcity in the supply of power (and spare capacity) and rising demand is resulting in skyrocketing prices for capacity and could prolong interconnection times for data centers (Howland, 2026).

large-load neighbor to offer firm electricity generation as a service. Such arrangements could involve the airport, a large-load entity, and the local electric utility to ensure that agreements can be reached that allow cost-effective power supply to new EVSE loads, provide peak demand reduction for the airport, establish time frames when on-site resources are used as "capacity" for the large load, and work out an order of dispatch during grid outages (small or large). An ideal example of this could be an airport that welcomes EVSE loads to be colocated with data centers.

  - As presented in Figure 30, the Maximum PV scenario at OKV might be able to export 4 MW of power to the grid typically around noon (this is what could make OKV an ÆNode). This solar PV system could produce sufficient power during the day to offset certain daytime community loads and help the utility manage load growth in OKV's distribution branch. Such an asset might be able to help Rappahannock Electric Cooperative postpone desired infrastructure upgrades in response to anticipated load growth around the airport, allowing it to prioritize more critical grid component upgrades.

- Cons:
  - The system might not have a positive net present value for the airport, but an ÆNode energy node should not aim to recoup its investment as quickly as it can given the resilience that it provides.
  - For an airport such as OKV or HVN to act as a true energy node, it would need to export power to the grid in the right amounts and at the right times when exporting power would be valuable to the grid. If we use real-time hourly locational marginal prices (PJM, 2025) as a proxy of stress on the local grid, most surplus PV generation occurs during daytime hours that coincide with lower market rates. For example, OKV's Maximum PV system (with ET2+ loads) could generate approximately 525 kW of surplus power for export to the grid or curtailment between 5 p.m. and 6 p.m. But the probability of the system exporting or curtailing power at this time step is only 23% and 56%, respectively; therefore, despite having surplus solar production during the day, an expected decline in solar production during evening hours can prohibit the airport from supporting its utility in offsetting the generation ramp-up to support the evening peak loads. The presence of a properly sized BESS or a long-duration energy storage system at an up-front cost might be able to assist in storing large amounts of energy when possible and exporting firm power to the grid when necessary. HVN (Figure 31) is similar to OKV (Figure 30) when the day-ahead market rate peaks right after 6 p.m., but the Maximum PV exports are likely to happen during the day.

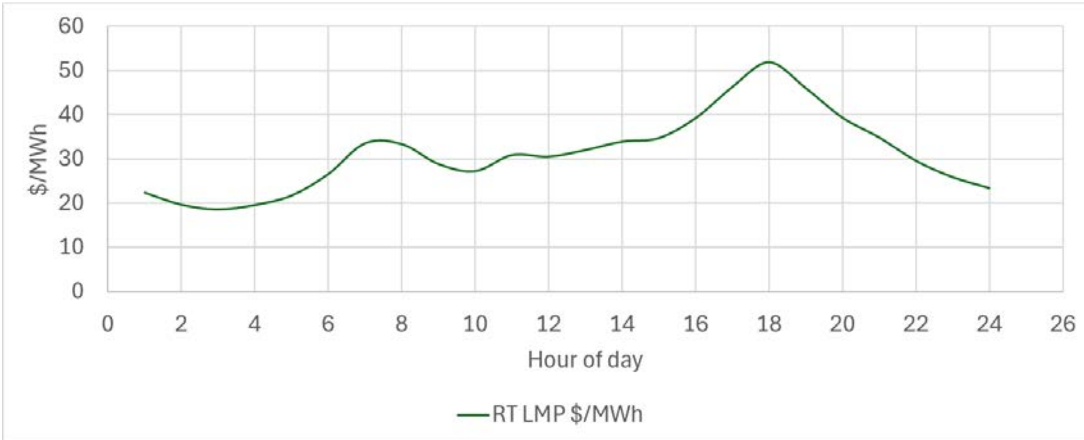

Figure 30. Average real-time hourly locational marginal prices for OKV

Costs are hourly average values for PJM's AEP load zone

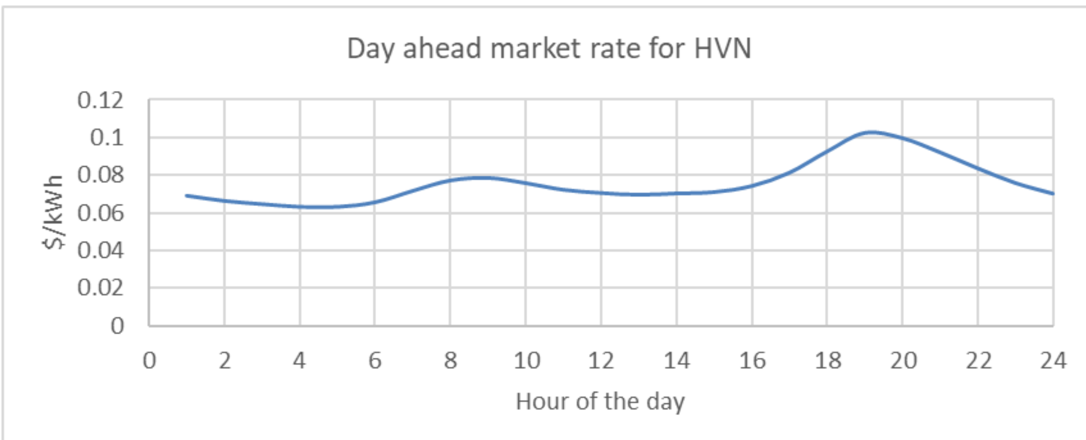

Figure 31. Average real-time hourly locational marginal prices for HVN

Costs are hourly average values for Independent System Operator New England's Connecticut load zone

The robust design guidance at both sites demonstrates the variability in the economic performance of on-site energy systems depending on the location and the economic parameters. OKV's bottom line will rarely benefit from more than a modest battery system except in very specific economic conditions. This is primarily due to the low cost of energy in the area. On the other hand, HVN can expect significant returns in a well-designed generation and storage system. Under specific economic conditions, the returns from such a system could reach upward of $10 million.

Both systems show similar optimal investment strategies in building for resilience. In each case, if the site is only concerned with outages that last less than 24 hours, battery capacity should be of primary concern. For multiday outages, storage becomes too expensive to be the sole provider of resilience, and the site should focus investment in on-site generation, such as PV. A more specific breakdown of investment guidance can be found in sections 5.7.7 and 5.8.7. Appendix A gives a full analysis of the performance of each site.

This analysis uses BCOC as an estimated cost that the airport must charge any flights to recoup all the electric utility and infrastructure costs related to serving the EVSE loads. BCOC costs were calculated for one scenario with and without on-site generation at both OKV and HVN to understand how the calculated costs might differ. Rather than using a traditional LCOE to determine the marginal cost of an investment, this analysis relies on a variation instead. The LCOE calculation relies on determining the dollars per the useful kWh cost of each investment asset, and it is typically used for energy-producing assets. The inclusion of batteries would complicate calculations and require combining LCOE with the levelized cost of storage to get a meaningful $/kWh value. Within this context, we would like to consider the all-inclusive costs required to serve a fixed amount of energy per year. Our context includes the costs of grid electricity purchases, depreciating assets such as EVSE, and grid infrastructure and assets such as battery systems and PV systems; therefore, the analysis had to use the LCOE formula but with a fixed volume of useful energy across all costs that could be incurred to install cost-effective EVSE-supporting systems at HVN and OKV.

Despite the similarity in formulas, HVN and OKV's BCOCs cannot be compared at their face values because the data used as the basis for the BCOC vary across the nation. Aspects such as electricity costs and grid infrastructure costs vary nationwide, and EVSE installation costs depend on the cost of shipping equipment and local labor rates. On-site DERs can provide cost savings, but their sizes can also vary drastically per electric tariff. EVSE costs could also see variations. This analysis used six 350-kW (or 2.1-MW) chargers for $881,000, but (Cox et al., 2023) considered one 3-MW EVSE at a cost of $900,000. Further, forecasted EVSE load variations across scenarios and locations could directly impact the denominator of the BCOC calculations, thereby causing variations in costs for similar airports. Spare capacity requirements could also vary by utility and therefore could directly influence the BCOC. The BCOC values could be normalized for cross-project comparisons. For example, the load factor of an EVSE system could be used to scale infrastructure costs to not penalize low-load-factor EVSE schedules. Further work on this topic could explore avenues to compare BCOCs across airports and scenarios in a more seamless manner.

The Allowed PV and Maximum PV scenarios quantify the amount of energy that can be generated at OKV to best use the available land at the airport. Once this energy is generated, any surplus energy can be used to serve critical loads in and around the airport during an outage if the airport infrastructure has sufficient capacity to transfer up to 6.3 MW of generation from the airport for its vicinity to use. If the critical loads do not require such magnitude of power, energy generation assets at the airport can be sized to remove any excess curtailment. Knowledge of community-based critical loads can also enable detailed resilience assessments to quantify the likelihood of serving critical airport and community loads for varying outage durations.

6 Validating Sizing and Placement of Generation and Electric Vehicle Supply Equipment Scenarios Using an Airport Digital Twin

6.1 Overview of the Digital Twin

A digital twin of an airport electrical system can provide real-time, physics-based, and data-driven emulation of the electrical network and power system assets, enabling advanced monitoring, analysis, control, and decision-making capabilities. The major feature of a digital twin is that it is continuously updated and synchronized with real-world data, enabling stakeholders to test scenarios virtually and get reliable insights for dynamic response and decision support. This minimizes operational risks and improves efficiency, creating tangible economic and strategic value. The digial twin facilitates more informed investment decisions and supports sustainability goals by optimizing resource utilization.

Although traditional simulations have long been used to study the behavior of power systems, digital twins extend this capability by establishing a more realistic, dynamic, data-driven connection to the physical asset. Offline conventional simulations typically rely on predefined models with fixed assumptions and boundary conditions. After the study is complete, their predictive accuracy decreases when the real-world system diverges from the underlying modeling assumptions under various conditions. A digital twin, in contrast, has the ability to integrate operational data, ensuring that predictions, diagnostics, and performance assessments remain accurate under changing conditions.

Ditial twins bridge the gap between design and real-world operation. This means that the insights gained from the field data can be fed back into the model to continuously refine its accuracy, a feature absent in stand-alone simulations. Although conventional simulations are effective for controlled, preoperational analysis, such as contingency studies and capacity planning, digital twins extend this capability into the operational phase. Digital twins continuously update with actual system data, enabling a shift from periodic offline analysis to the real-time representation of the physical system.

6.1.1 Role of Digital Twins in Modern Airport Infrastructure

As airports progressively electrify—introducing high-power charging for aircraft, electrified building systems (HVAC), fully electric ground support fleets, large-scale battery systems, and renewables integrated into a smart microgrid—their behavior will become far more dynamic, tightly coupled, and uncertain than in today's largely predictable infrastructure. Anticipating and managing this future requires a digital twin that does more than replicate current layouts; it must embody a fundamentally different architecture that can represent multidomain interactions (electrical, operational, thermal, and cyber), integrate real-time data from heterogeneous sensors, and support scenario-based simulations of emerging technologies and operating concepts. Such an architectural shift enables planners and operators to explore "what if" futures—e.g., the impact of widespread e-aircraft adoption, new charging strategies, or grid constraints—before committing to costly physical changes, thereby de-risking the transition and ensuring that next-generation airports are designed, validated, and digitally optimized before they are realized in the physical world.

To address this, a digital twin base framework was developed for airport microgrids that is generic, modular, and scalable. The airport digital twin base framework models airport-specific loads, sources, interconnections, and other relevant assets, such as transformers and line capacity. The framework can be customized to accommodate the high-fidelity modeling of any specific small to midsize airport microgrid. Specifically, the airport digital twin can be used to validate investment decisions and capacity constraints and to ensure that the system stability is maintained with the introduction of new loads and resources. Further, the airport digital twin can provide tailored insights and scope for optimization based on the unique operational needs of the airport. The airport digital twin serves as a high-fidelity, data-augmented virtual platform to perform "what if," "what is," and "what will be" assessments associated with the expected future electric needs of the airport.

The digital twin developed for this project integrated operational data provided by the utility for the airport. It provides a generic framework to seamlessly integrate future operational data and accommodate network reconfigurations. The first digital twin was developed based on OKV, which is a midsize airport that handles approximately 120 flights per day. The electricity supply to the airport comes from the grid through a substation. The utility shared electrical network data comprising associated sources, loads, and lines. In addition, smart meter data corresponding to certain categories of the airport loads were available. These smart meter data were integrated into the virtual airport digital twin along with other network parameters. The high-fidelity digital representations of the current and future physical assets were developed and integrated into the airport digital twin. The airport digital twin encompasses models of EVs, BESS, DERs, and other potential future airport assets.

6.1.2 Architecture Topologies

Before initiating the OKV digital twin development, NLR first established a generic digital twin (GDT) concept as a foundational starting point. The airport GDT has been designed as an adaptable framework that can be reconfigured for different airports without extensive work, effectively serving as a library that supports plug-and-play components. Various distribution network architectures can be used to model this GDT, including radial, loop, and zonal-mesh configurations. Details on the different architectural topologies are provided in Appendix C.1.

NLR's goal was to develop a generic framework that promptly adapts to any airport microgrid architecture while being ready for any "what if" scenario evaluation. In addition, it can be used to evaluate grid modernization initiatives that target resilience enhancement. Among different configurations, the zonal-mesh architecture offers several advantages and can be readily reconfigured into either radial or loop layouts; therefore, the GDT was developed based on the zonal-mesh architecture.

6.1.3 Zonal-Mesh-Based Generic Digital Twin

The framework for the zonal-mesh-based GDT exhibiting modularity is depicted in Figure 32. Widely adopted on-site generation assets have been modeled, including PV systems. Additionally, a BESS is incorporated to represent energy storage capabilities, while a diesel generator is included as a conventional nonrenewable backup source. These energy assets are selected based on their predominant use within airport infrastructures. Along with the energy assets, loads are assigned within each zone and categorized as critical (C), noncritical (NC), or semicritical (SC).

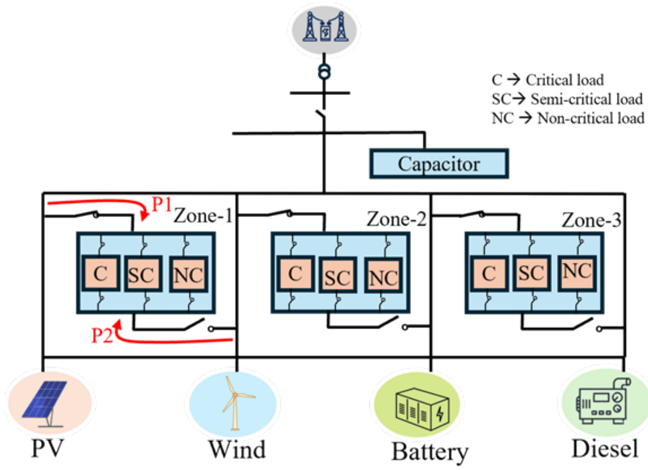

Figure 32. Generic zonal-mesh digital twin

The representative zonal division of loads for a typical zonal-mesh-based GDT is shown in Figure 33, where HIES and PCC represent the hydrogen-based integrated energy system and the point of common coupling, respectively. The utility grid is also integrated to reflect the grid-connected/islanded operations. The status of the switches shown in Figure 32 can be configured to adapt the zonal-mesh-based GDT to any other architecture (e.g., radial based, loop based), enabling plug-and-play capability. Due to the modular and plug-and-play nature of the proposed zonal-mesh-based GDT, stakeholders can seamlessly integrate additional assets, enabling customized studies and analysis tailored to specific airport requirements. The detailed physics-informed model of each asset can be found in Appendix C.2.

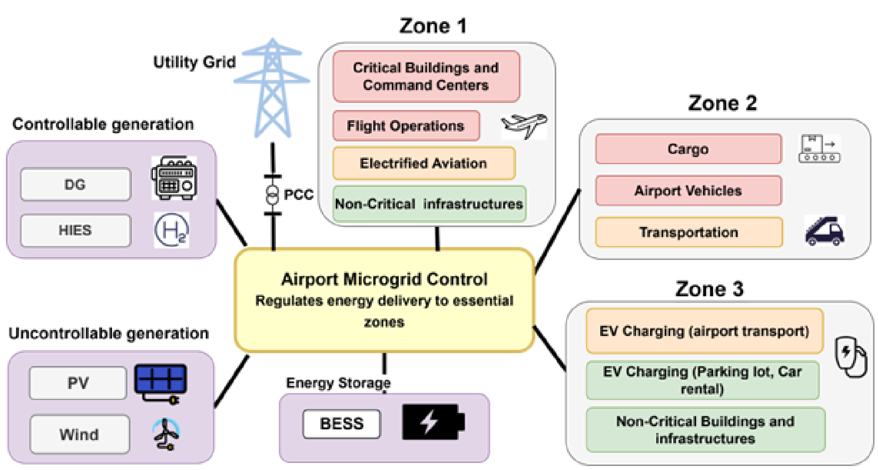

Figure 33. Representative zonal division of loads and on-site energy resources for a typical airport microgrid

6.2 Digital Twin Development of Winchester Regional Airport Microgrid

Following the development of the zonal-mesh-based GDT and the evaluation of different operational scenarios (Poudel et al. 2025), the zonal-mesh-based GDT was deployed as a prototype designed to adapt to a wide range of airport microgrids. NLR adapted and reconfigured it to replicate the microgrid of an actual midsize airport, OKV, which handles approximately 120 flights per day.

As part of the reconfiguration and validation, NLR collected the airport distribution network information. The utility provided a model of the Greenwood Substation (GSS), which supplies power to the airport, as well as detailed system parameters, such as meter geographic locations, line lengths and spans, transformer ratings, capacities, and voltage levels, among others. Additionally, SCADA data for each meter within the airport distribution network were obtained from the utility, reflecting the existing radial configuration of the system. This section explains the steps of extracting information to develop a digital twin.

6.2.1 System Parameter Extraction From Utility-Provided Model

The process began by identifying the service locations associated with each installed meter. The utility provided meter identifiers and their corresponding service locations. Using the utility-supplied network model, we collected connectivity information describing how each load is tied to the distribution system, including the line segments linking specific service locations. Geographic mapping was then performed using latitude and longitude coordinates for nodes and line segments to locate each meter spatially.

After establishing the meter locations, the substation supplying the airport distribution network was identified. Feeder paths from the substation to each service location were then traced using the utility-provided model, which specifies the sending and receiving buses, the line code (conductor type), and the length of each line segment. These attributes were used to construct the electrical and topological connections that link all the service locations back to the substation.

Because the conductor type is available for each span, the corresponding electrical parameters—resistance, inductance, and capacitance—were extracted from the provided line information and applied to refine the distribution network model. Following this workflow, a complete digital twin of the airport distribution system was developed directly from the utility data. Additional procedural details are provided in Appendix C.3. To protect sensitive information, detailed model descriptions and network identifiers are omitted from this report; only a generalized one-line diagram of the developed digital twin is included, depicted in Figure 34.

The SCADA data were fed to the developed radial digital twin of the airport, and the emulated results were compared with the real meter readings to check for accuracy. To ensure the feasibility of running the model in the real-time digital simulation (RTDS) platform, where 1 second of simulation corresponds to 1 real-world second, the full year of SCADA meter data was appropriately down-sampled. This step was necessary due to the impracticality of emulating an entire year's worth of data in real time. The mean square error between the actual SCADA meter data and the output of each meter in the reconfigured radial digital twin was observed to range between 3% and 8%. Some graphs of the validation are depicted in Figure 35.

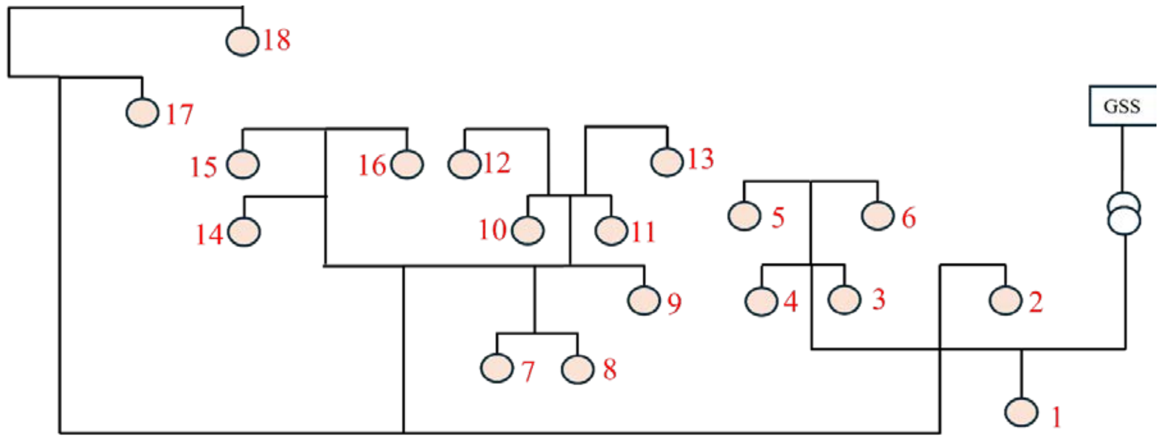

Figure 34. Meter IDs with locations relative to the airport network topology

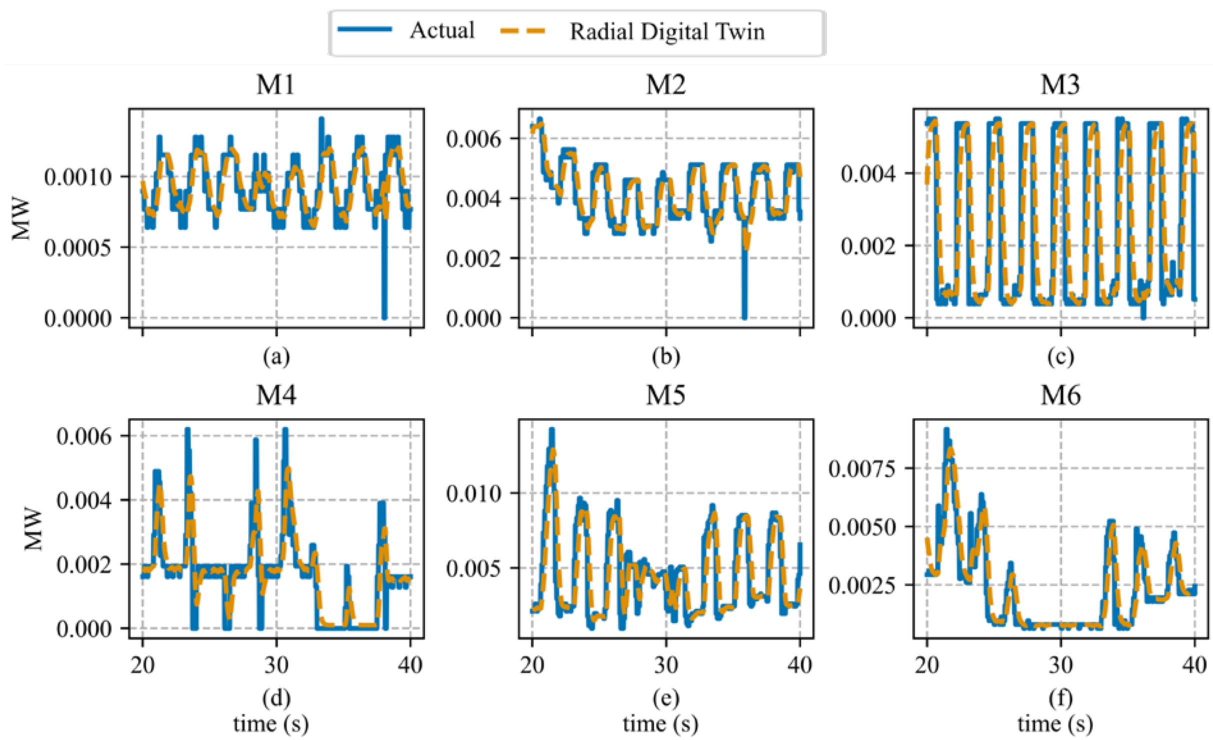

Figure 35. Validation of SCADA data from each meter in the digital twin

Because the physics-informed digital twin of the airport with a radial distribution architecture is developed using actual conductor specifications, transformer nameplate data, field sensor measurements, and geospatial coordinates, its behavior has been rigorously aligned with the real system to support accuracy validation. As a result, we have a high degree of confidence in using this digital twin to perform a wide range of "what if" scenario studies because the airport distribution network represented in the RTDS reproduces the operational behavior of the physical system with sufficient fidelity to safely explore diverse operating conditions and control strategies.

6.3 Smarter Capital Cost Planning and De-Risking Infrastructure Investments Through REopt-Digital Twin Synchronization for OKV

After developing the airport digital twin, the REopt analysis was integrated with it to establish a synchronized planning–operations workflow (the overall framework is shown in Figure 36). The upper portion of the framework—the baseline digital twin development and validation—had already been completed by developing a physics-informed model using real conductor and transformer data and then feeding resampled SCADA meter measurements over a full year to verify the steady-state and quasi-dynamic behavior. Building on this validated baseline, REopt is configured with decision variables for candidate generation and storage assets, an economic objective function, and a set of technical and operational constraints. The tool then returns the optimal asset sizes and associated time-series trajectories (e.g., battery dispatch, net load) that are technically feasible and cost-effective for airports.

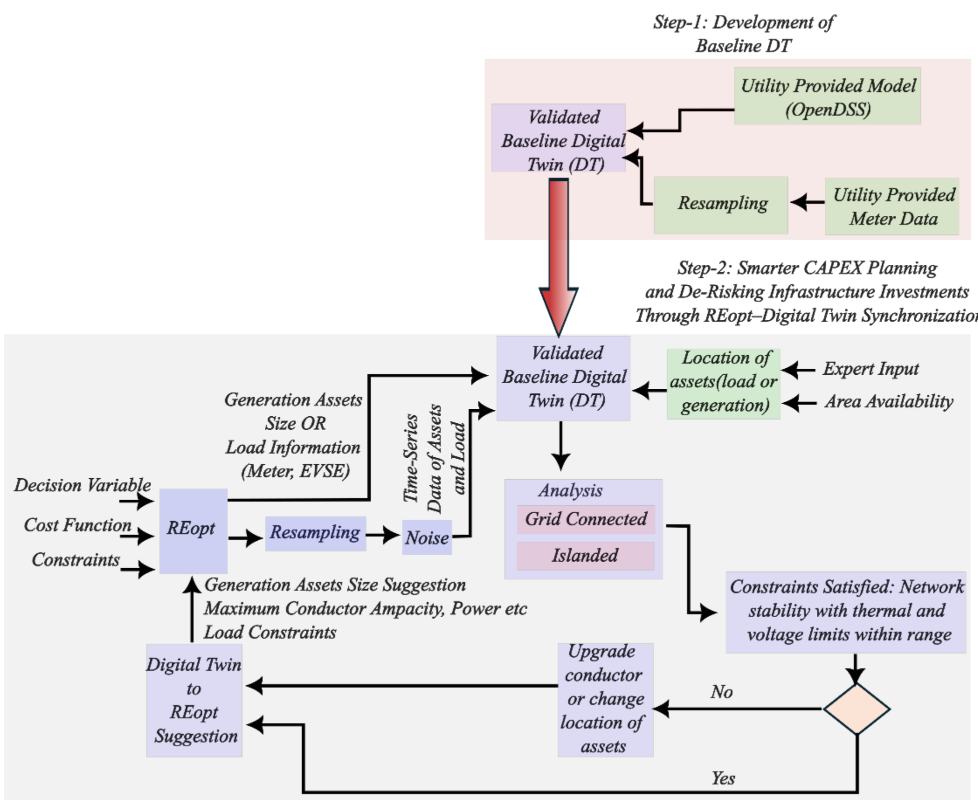

Figure 36. REopt and digital twin workflow

To stress-test these REopt solutions in the digital twin, we focus on a worst-case operating day extracted from the yearlong validation dataset—specifically, the day when the airport meter recorded its maximum demand. For this day, REopt provides the optimal asset portfolio; the corresponding meter and ET2+ time-series data; and the 15-minute profiles for the RAM, UAM, and Trainer meters as well as the battery dispatch set points. These 15-minute series are first resampled to a 5-minute resolution, and stochastic noise is deliberately added to emulate forecast errors and ambient uncertainty, thereby making the test conditions more representative of real-world operations. The resulting 5-minute data are then down-sampled such that each 5-minute interval is mapped to 1 second in the RTDS-based digital twin. This temporal compression is necessary because simulating a full 24-hour period at a 50-µs time step would otherwise produce prohibitively large datasets, while numerical experiments confirm that the down-sampled profiles preserve the salient power, energy, and congestion patterns. This REopt-digital twin synchronization gives us strong confidence that the airport digital twin can reliably replay optimized operational strategies and serves as a credible platform for de-risking asset sizing and operational decisions before field deployment. Figure 37 shows the framework for the integration of the real-world data to emulate the dynamic system behavior for validation, innovation, and de-risking the deployment of new technologies.

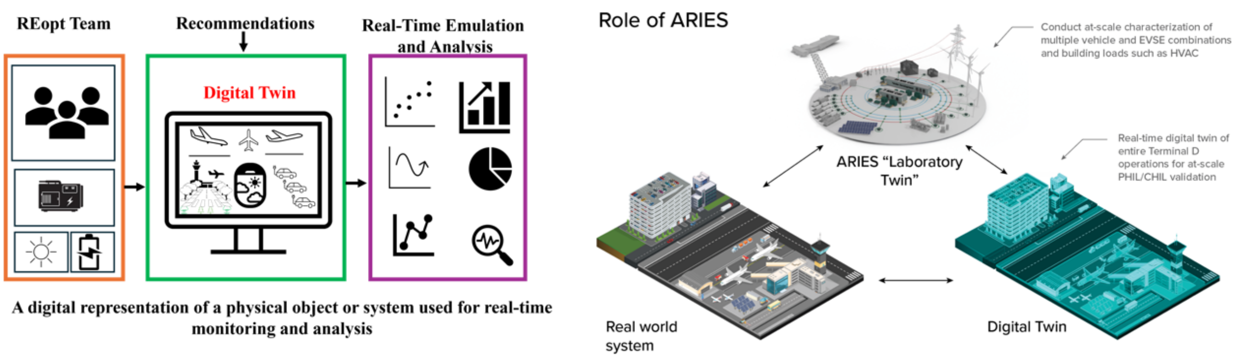

Figure 37. Emulation framework for validation and de-risking the deployment of new technologies

6.3.1 Evaluation Scenarios

We developed three broad scenarios for the evaluation of the REopt-digital twin synchronization, summarized in Table 51. The following sections discuss the results for each scenario.

Table 51. Scenarios Under Consideration

Scenario	Sub-Scenarios	Potential Outcomes
1: Baseline: All loads without PV, BESS, GEN	(a) Buildings (b) All ET2+ & Building (c) All ET2+ & Community	Baseline condition to check the impact of the addition of load To ensure the existing system can handle the addition of the load
2: Scenario 1(c) with PV/BESS (grid connected)	(a) With only PV (b) With PV + BESS	How DERs improve the system operational conditions (e.g., voltage, loading of line)
3: Scenario 2 in islanding mode (resilience scenario)	With PV, BESS, and distributed generation	Validating DERs can sustain the potential outage.

6.3.1.1 Scenario 1

Scenario 1 validates the existing electrical system by implementing a baseline digital twin in the RTDS environment. All building loads within the airport are modeled explicitly. Scenario 1 (a) represents the present-day operating condition (baseline airport demand), while Scenario 1 (b) evaluates whether the existing system can accommodate incremental load growth with the addition of ET2+.

A key modeling challenge is the limited availability of metering data for loads outside the airport boundary. For the studied feeder ("airport circuit"), additional community loads are supplied from the same circuit that serves the airport. Details of the community loads outside the airport boundary can be found in Appendix C.4. Although detailed time-series measurements for these external loads are not available, the airport engineer provided the maximum feeder loading (approximately 7 MVA) and the circuit capacity, which were used to upper bound and parameterize the representation of the off-airport demand. Accordingly, aggregated community loads are represented in the digital twin, as illustrated in Figure 38. Three community load equivalents—Community Load 1, Community Load 2, and Community Load 3—are used to capture the demand from three distinct community sections served by the feeder. Because the analysis focuses on the system-level impacts of integrating ET2+ on the airport circuit, the ET2+ load is also modeled as a prospective (future) demand component as considered in Scenario 1 (c).

Overall, Scenario 1 (c) acts as the baseline digital twin for the "what if" analysis, which includes (1) all airport metered building loads, (2) aggregated community load contributions represented at three feeder sections to capture the non-airport demand served by the airport circuit, and (3) the ET2+ load as the primary future load scenario.

To avoid confusion for the reader regarding digital twin notations, such as "Junction to BC-Connector," note that the variables used in the digital twin are synchronized with those of the physical system currently in place. For example, "Junction to BC-Connector" refers to a conductor associated with a specific location within the airport. Appendix C.5 provides the correspondence between the digital twin variables and the actual physical assets. As illustrated, "Junction to BC-Connector" appears in both Figure 38 (digital twin) and Appendix C.5 (physical system currently in place), where it represents that specific line, and other variables follow accordingly.

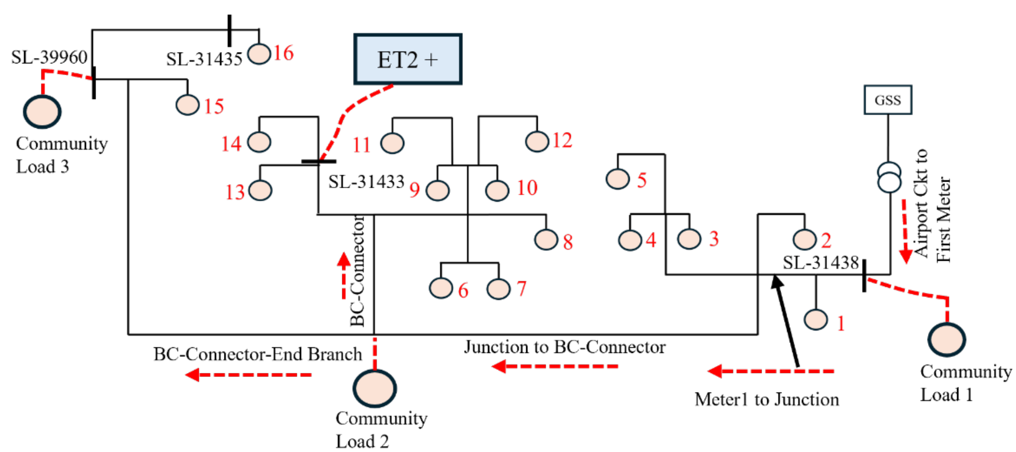

Figure 38. Digital twin representation of the airport circuit with community load

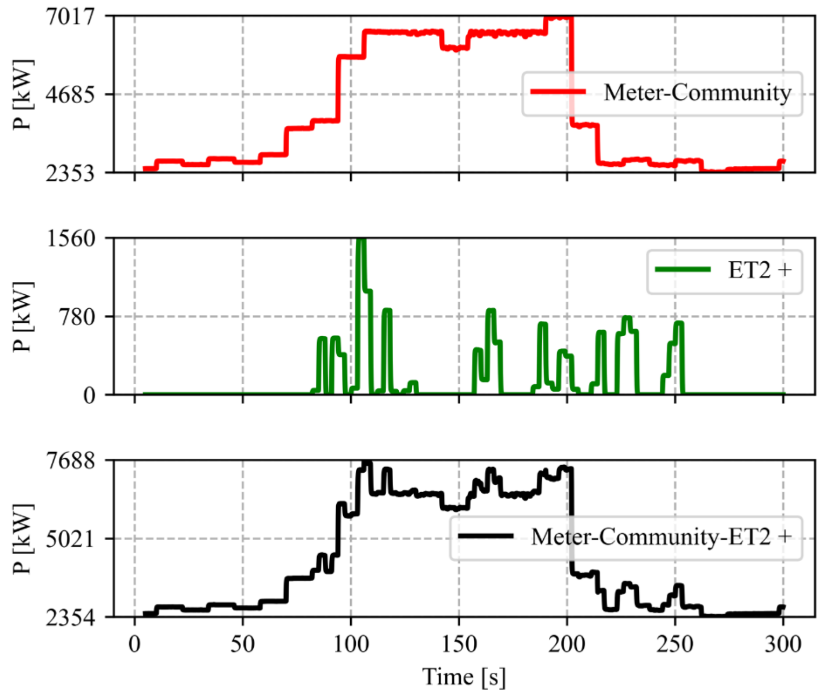

Figure 39. Time-varying demands of community loads, airport loads, and prospective ET2+ future loads for Scenario 1 (c)

6.3.1.2 Scenario 2

Scenario 2 builds on the baseline digital twin (Scenario 1 (c)) by incorporating PV generation and a BESS. Scenario 2 is designed to quantify how on-site generation can enhance feeder operating conditions, particularly by reducing line loading, improving voltage profiles, and mitigating other performance constraints, such as transformer overloading, voltage fluctuations, and power quality. In addition to assessing the operational benefits, this scenario is used to systematically evaluate where on-site generation should be sited to maximize its impact on the airport circuit.

Because feeder performance is location dependent, Scenario 2 explicitly examines on-site generation placement sensitivity. For example, installing PV generation at a downstream node with high local demand might yield a larger reduction in upstream power transfer, thereby decreasing the current flow and apparent power (kVA/MVA) loading on critical line segments; however, the more fundamental driver is the line impedance between the generation node and the substation. In contrast, PV placed at a less influential node might provide limited relief to the most constrained sections of the feeder. Similarly, BESS can be positioned to target specific operational objectives: charging during low-demand periods and discharging during peak or contingency conditions can reduce peak feeder loading, support voltage regulation, and relieve thermal stress on overloaded components. Scenario 2 also enables a power-flow-based interpretation of how on-site generation reshapes net demand on the circuit. PV offsets real power import during daylight hours, while storage provides dispatchable support that can be tuned to reduce peak power transfer, improve voltage stability, and smooth ramps driven by load variability. Collectively, these analyses provide practical guidance on on-site generation siting and dispatch strategies, helping to identify configurations that deliver the greatest reduction in line loading and the most significant voltage improvement while clarifying trade-offs among competing objectives (e.g., peak reduction versus voltage support). The digital twin representations of the airport circuit corresponding to Scenario 2 (a) are shown in Figure 40 and Figure 41. Note that in the digital twin, PV placements were kept at two distinct locations: the upstream node and the downstream node.

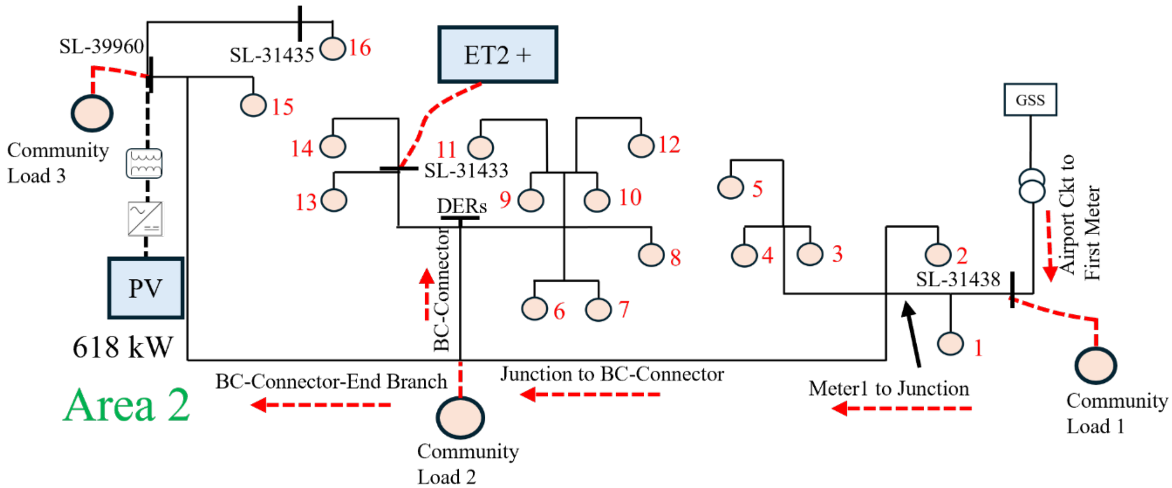

Figure 40. Digital twin representation of airport Area 2 corresponding to Scenario 2 (a)

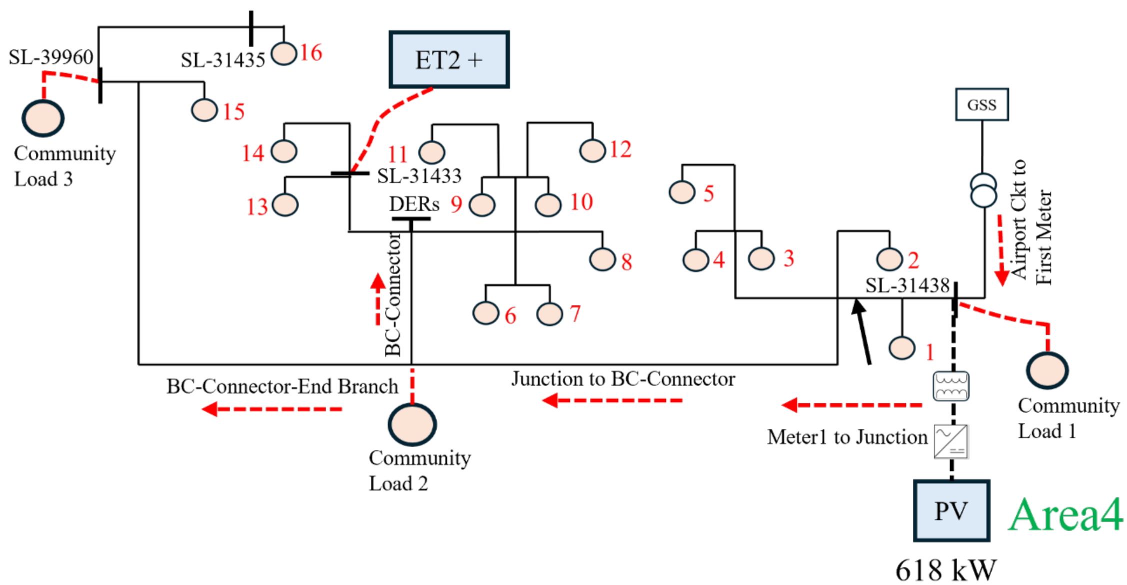

Figure 41. Digital twin representation of airport Area 4 corresponding to Scenario 2 (a)

Based on the REopt results, a 618-kW PV system was identified as the economically optimal capacity for OKV; therefore, the next step was not to resize the PV but to determine where along the existing distribution circuit this capacity should be installed to maximize the technical benefits and minimize adverse impacts. Using the validated airport digital twin running on RTDS, we evaluated multiple candidate locations within the airport circuit. As an initial screening and informed by the available physical space and expert input from the airport stakeholders, two practical siting options—Area 2 and Area 4—were selected and implemented in the digital twin. (See Appendix C.5 for Area 2 and Area 4.)

With the PV system deployed at the optimal location (Area 2; see Section 6.3.2 for the site-selection rationale), the REopt-recommended optimal BESS capacity of 205 kWh for this case was implemented in the digital twin using a physics-informed battery model, and the resulting digital twin configuration is shown in Figure 42 (representation of Scenario 2b). Because the utility grid is available in this scenario, the BESS operates in grid-following (GFL) mode: The grid establishes voltage and frequency, while the BESS charges or discharges according to its dispatch schedule.

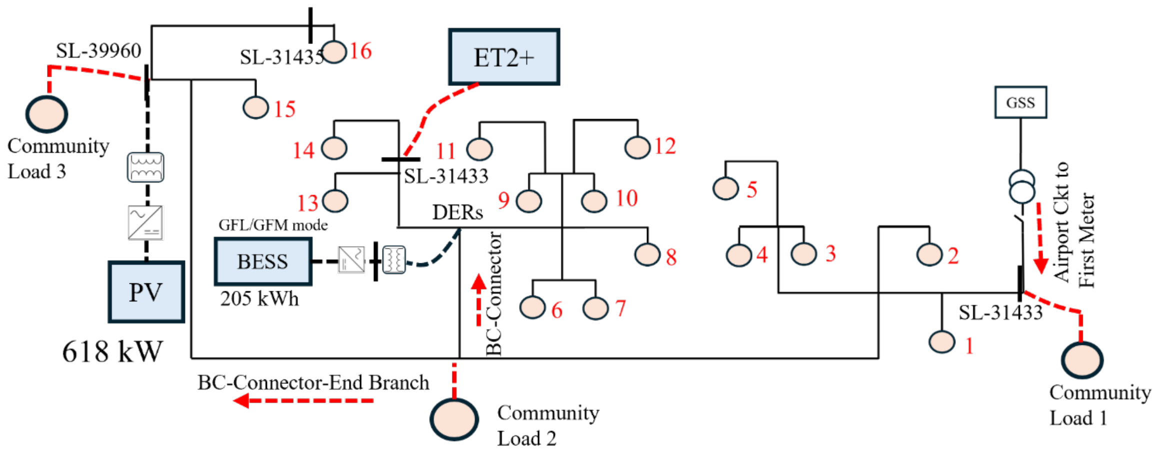

Figure 42. Digital twin representation of the airport circuit corresponding to Scenario 2 (b)

6.3.1.3 Scenario 3

Scenario 3 extends Scenario 2 by incorporating a dispatchable distributed generator to enable islanded operation during utility outages. The objective is to assess whether the on-site DER portfolio (PV, BESS, and diesel generator) can sustain airport service under the loss-of-grid conditions while enforcing a hierarchical load-prioritization strategy: critical loads are served first, followed by semicritical loads as capacity permits, and noncritical loads only when a sufficient margin remains.

Upon the occurrence of a contingency, the initial operational action is to shed the community load to preserve the available generation and storage capacity for airport operations. Support to off-airport loads is considered only if surplus capacity remains after meeting the airport critical demand, creating an explicit trade-off between maintaining full airport functionality and supplying external critical services. Where feasible, the curtailment of selected noncritical airport loads could free capacity for external critical loads, subject to feeder constraints and utility operational policies.

This scenario also accounts for practical interconnection constraints. The ability to export power from the airport microgrid to community critical loads depends on the utility authorization and the location of the fault on the feeder. If transfer over existing utility conductors is not permitted or is electrically infeasible due to the faulted section, additional infrastructure (e.g., a dedicated conductor/feeder segment) might be required to supply off-airport critical loads.

The islanding sequence is modeled as follows: immediately after the grid loss, the BESS transitions to grid-forming (GFM) mode to regulate voltage and frequency and provide fast dynamic support during the distributed generation startup. Once synchronized and online, the distributed generation assumes the primary GFM role, and the BESS transitions to GFL operation, dispatching power according to the set points issued by the airport control center. PV always operates in GFL mode.

For the extreme-event island case, the airport is assumed to be fully separated from the bulk grid. The initial isolation boundary, Airport Isolation-1, is implemented at switch S1 (Figure 43); however, isolation at S1 is operationally infeasible because the downstream feeder segment also supplies non-airport loads (Community Loads 1, 2, and 3), preventing the selective energization of the airport without simultaneously energizing external customers. To establish an airport-only microgrid, an additional conductor segment is introduced (New Conductor 1 in Figure 43), and the isolation boundary is redefined at Airport Isolation-2, implemented at switch S4, which electrically separates the airport loads from the remainder of the distribution network. The digital twin variables Airport Isolation-1 and Airport Isolation-2, which correspond to the actual physical assets, can be found in Appendix C.6. Because most airport loads are electrically clustered within the designated airport region, the distributed generation and BESS are colocated at the primary aggregation point, and the conductor extension is routed accordingly. A natural question arises as to why meters 1–5 are not energized in this islanded configuration. Although it is technically feasible to extend conductors to supply these loads, a yearlong data analysis of their metered demand showed that their aggregate energy and peak demand are very small relative to the rest of the airport. From a resilience- and CAPEX-focused perspective, these loads were therefore deemed noncritical, and their exclusion from the islanded microgrid during contingencies was considered acceptable, especially given the additional infrastructure that would be required to include them. Instead, a new conductor is extended to supply meters 15 and 16, which serve a larger and more operationally relevant portion of the airport. This new conductor (New Conductor 1) also provides a local sink and flexibility path for PV power during contingencies, preventing overloading the upstream segments and enabling better utilization of local generation.

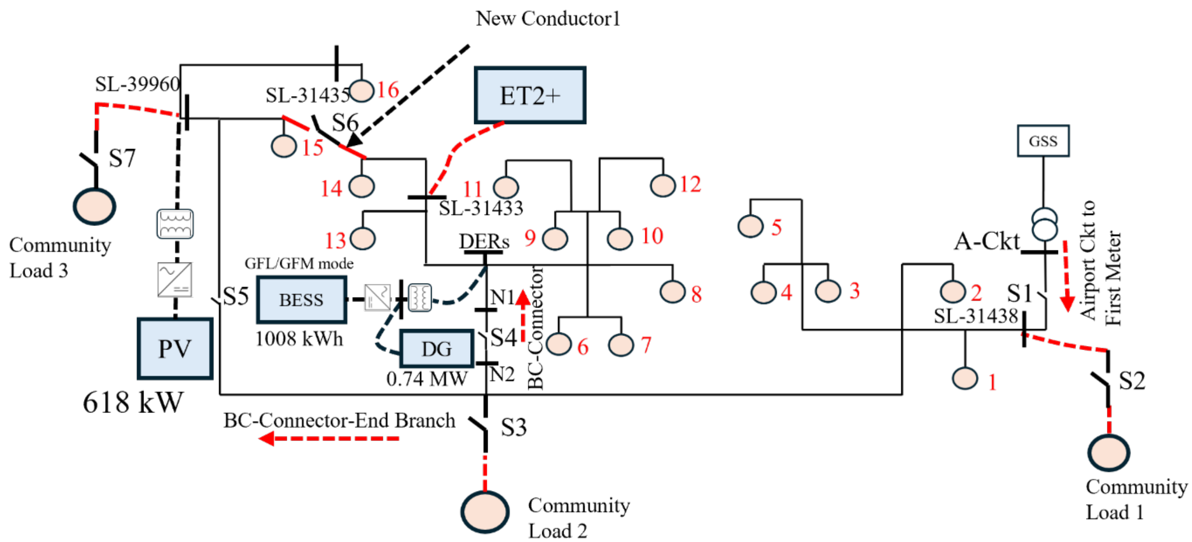

Figure 43. Digital twin representation of airport circuit corresponding to the islanding in Scenario 3

Under normal grid-connected operation, switches S1, S2, S3, S4, S5, and S7 are closed and S6 is open, allowing the upstream utility source to supply both airport and adjacent community loads. During an extreme contingency, the system transitions to an airport-only island through a coordinated switching sequence: S1 is opened at Airport Isolation-1 to disconnect the feeder from the bulk grid; S2, S3, and S7 are opened to fully isolate the community loads; S4 and S5 are opened at Airport Isolation-2 to refine the airport island boundary; and S6 is closed to reconfigure the network into a self-contained airport microgrid supplied exclusively by on-site PV, distributed generation, and BESS.

The sizes of the on-site generation assets in the islanded scenario (PV, BESS, and diesel generator) are obtained from REopt and implemented in the digital twin accordingly. The BESS and distributed generation are intentionally placed at the node where most of the airport meters are electrically clustered, maximizing their effectiveness in supporting critical loads, mitigating line loading, and maintaining voltage stability throughout the islanded microgrid.

6.3.2 Evaluation Scenario Results

6.3.2.1 Scenario 2 (a) Results

To ensure realistic generation behavior, the PV model in the digital twin is driven by measured irradiance and ambient temperature data for the OKV region, obtained from NLR's National Solar Radiation Database (NSRDB) at an hourly resolution. These data are resampled to 5-minute intervals and processed using Gaussian smoothing with added stochastic noise to approximate short-term variability and forecast errors, thereby better reflecting real-world operating conditions. The resulting irradiance and temperature profiles, found in Appendix C.7, are fed into a physics-informed PV model, and the digital twin is then exercised under the combined effect of the individual meter loads, the ET2+ loads, the community load, and the 618-kW PV injection.

For each candidate siting configuration described earlier, time-series power flow simulations are executed, and the resulting voltage profiles and conductor loadings (ampacities) are examined. In all cases, the integration of PV at either Area 2 or Area 4 reduces the line loading relative to the no-PV baseline (denoted "WO PV" in Figure 44), demonstrating a generally beneficial effect on the existing infrastructure.

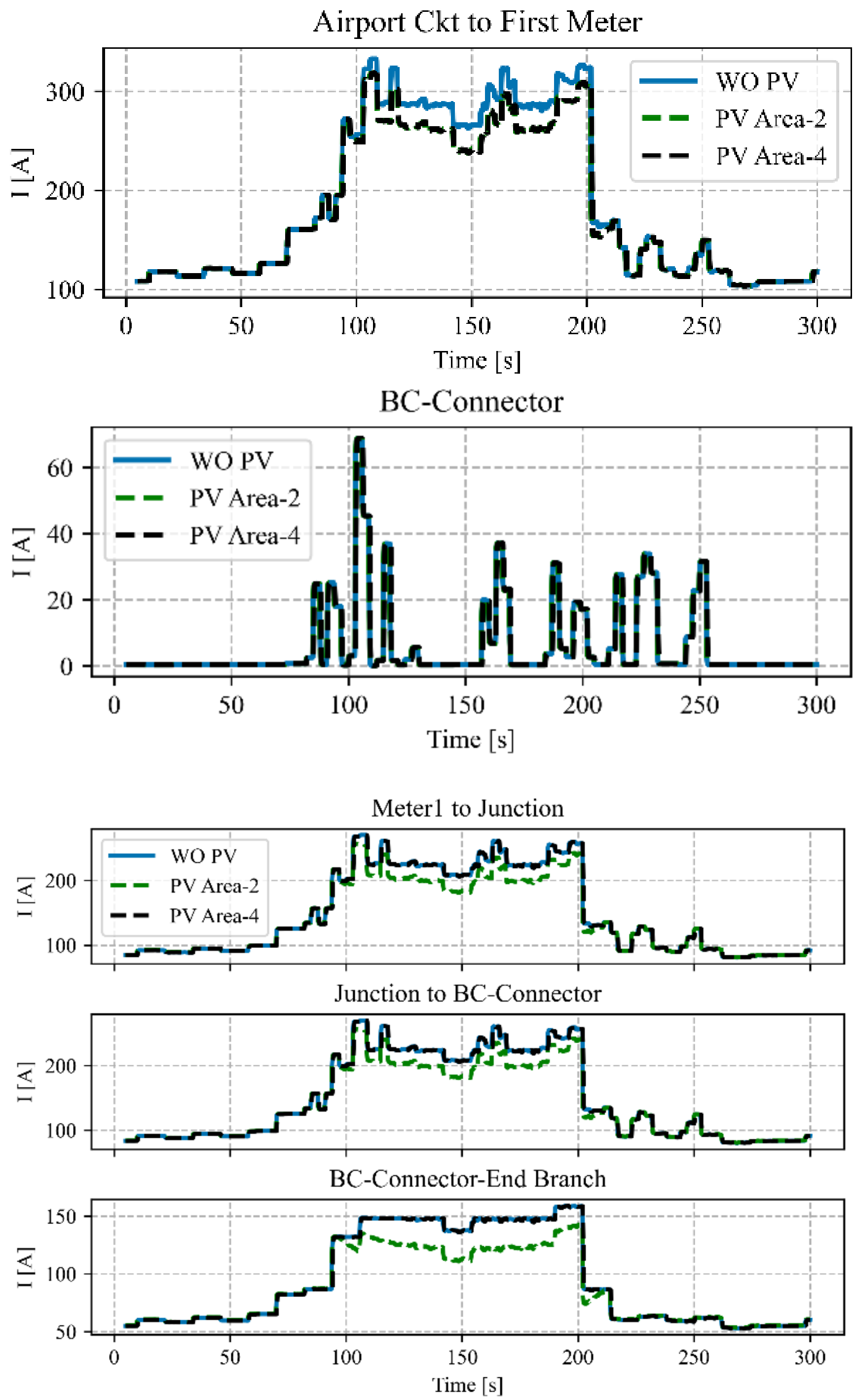

Figure 44. Current profiles at different branches corresponding to Scenario 2

A more granular comparison, however, reveals a clear advantage for siting the PV at the electrically farthest location (Area 2). In this case, the PV installation produces a systematic reduction in current on all upstream conductors—from the airport circuit breaker to the first meter, from the first meter to the junction, from the junction to the BC-connector, and from the BC-connector to the end branch. By contrast, installing the same PV capacity at Area 4 does not reduce the current on the segments from meter 1 to the junction, from the junction to the BC-connector, and from the BC-connector to the end branch, as illustrated in Figure 45 . Beyond the BC-connector, where the branch is strictly load-serving and does not host generation, line loading remains essentially unchanged between the PV and no-PV scenarios, which is consistent with the radial nature of the configuration.

Collectively, these results indicate that for a fixed PV capacity, siting the asset deeper in the feeder (Area 2) delivers more effective relief upstream of the thermal constraints (modeled as maximum conductor ampacities) and improves the utilization of the existing conductors. This, in turn, provides valuable evidence to support smarter CAPEX allocation and more informed PV siting decisions within the airport distribution network.

Node voltages were also monitored for each siting case. With PV installed, a slight improvement in voltage magnitude is observed; however, the change is small and remains well within the 1-p.u. band shown in Figure 45 (a), and therefore it can be considered negligible from a voltage-regulation perspective. This indicates that the existing transformer capacity is adequate and that the bus voltages already remain within the acceptable limits, even in the absence of PV.

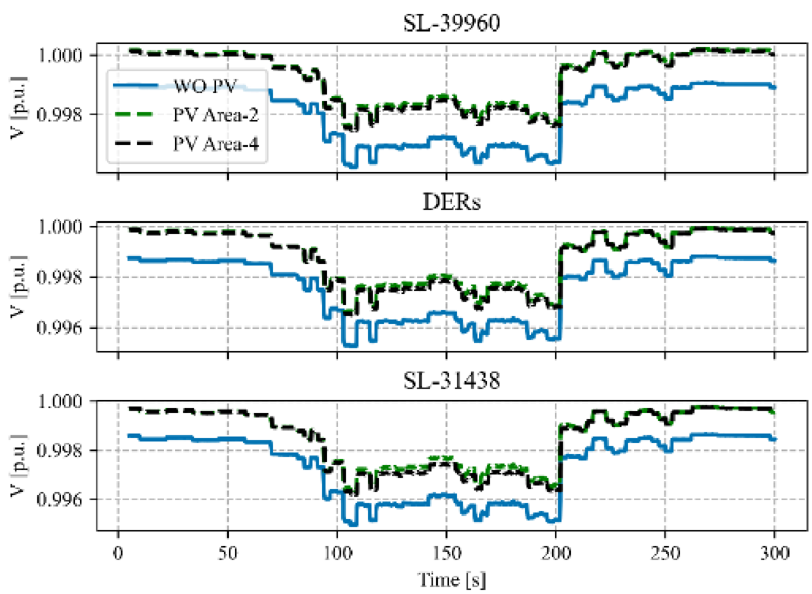

(a)

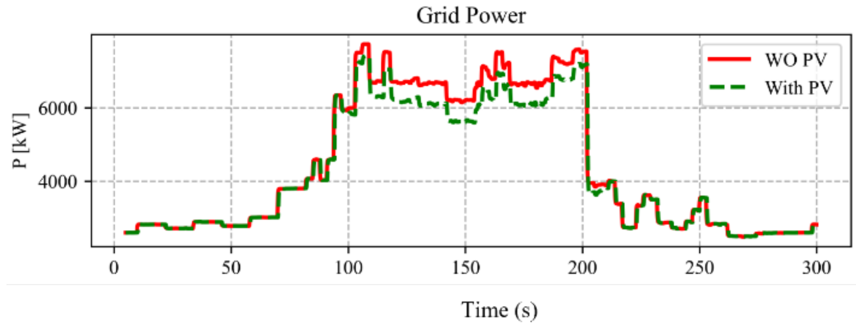

(b)

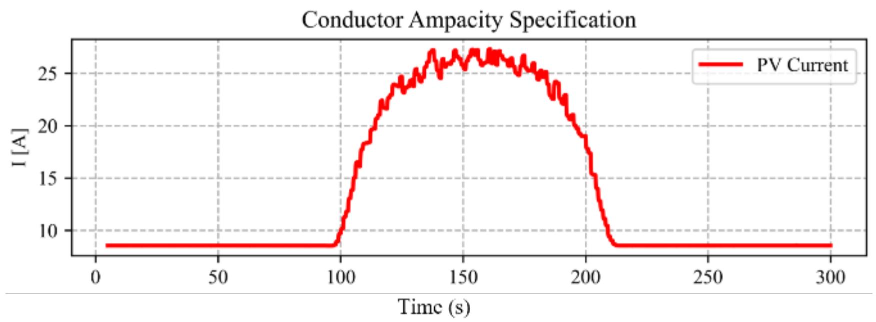

(c)

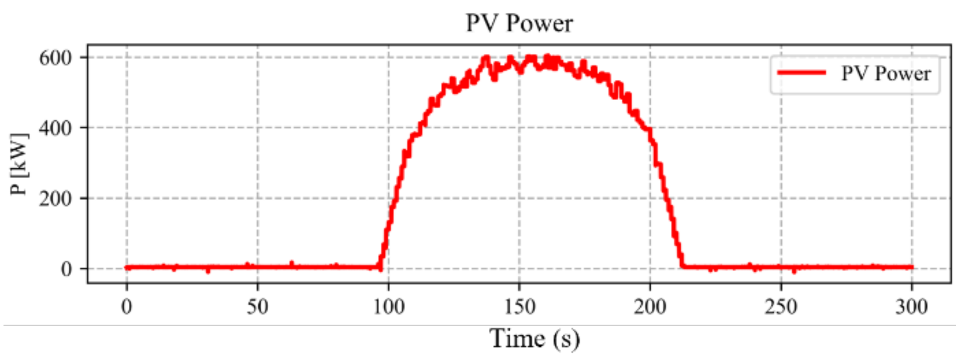

(d)

Figure 45. (a) Voltage, (b) grid power, (c) conductor ampacity, and (d) PV power profiles corresponding to Scenario 2

Consequently, the primary operational benefit of the PV installation manifests in conductor loading rather than voltage support. PV generation effectively underloads the conductors during daytime hours, creating additional thermal headroom for future load additions. From a planning standpoint, this suggests that new loads should be preferentially scheduled or interconnected such that their dominant operation coincides with daytime periods when the PV output is highest, thereby leveraging the available capacity unlocked by the PV generation. In parallel, grid power imports were recorded for both cases—with and without PV, as shown in Figure 45 (b). As expected, the presence of PV reduces the daytime power consumption from the grid, thereby decreasing energy purchases during periods of high solar output and lowering operational costs over the long term. The required conductor's ampacity to host the PV installation was also quantified by monitoring the current in the line segment interfacing with the PV point of interconnection. The resulting minimum ampacity requirement for that conductor is summarized in Figure 45 (c), and the resulting PV power output is depicted in Figure 45 (d). Scenario 2 (a) for different time periods is explained in Table 52.

Yet, a complete assessment must also account for the capital cost of the PV system and balance-of-system upgrades; thus, the economic benefit of reduced grid purchases needs to be evaluated against the up-front and life cycle costs of PV deployment on a case-by-case basis, ideally through an integrated techno-economic analysis.

Table 52. Scenario 2 (a) Explanation at Different Time Periods

Time Period	Analysis
0–100 sec (approx. 12 a.m. to 7 a.m.)	Irradiance is effectively zero (nighttime conditions), so the PV system produces no active power. Consequently, there is no noticeable impact on the conductor’s ampacity or node voltages.
100–220 sec (approx. 7 a.m. to 6 p.m.)	Irradiance and ambient temperature vary, driving PV power production. During this interval, the PV injection substantially reduces the line loading, thereby freeing the thermal headroom and enabling the accommodation of additional load.
220–300 sec (approx. 6 p.m. to 12 a.m.)	Irradiance again drops to zero (nighttime), and the PV system ceases to produce power. As in the initial interval, there is no significant influence on the conductor’s ampacity or voltage profiles.

6.3.2.1.1 Contingency Scenario: Scenario 2 (a) But PV Is Driven by Cloudy Irradiance

To evaluate the impact of cloud transients, a “cloudy” scenario was developed by reducing the irradiance driving the PV model over a selected interval. The resulting effect on conductor loading is shown in Figure 46 (a). In this experiment, the cloud event is imposed between 160 seconds and 200 seconds (Figure 46 (b)), during which the reduced irradiance leads to a corresponding drop in PV power output. Relative to the clear-sky PV case (Scenario 2, with a 618-kW PV installation at Area 4) (Figure 46 (a and c))), the cloudy interval exhibits increased line loading and a modest rise in grid power imports because the deficit in PV generation must be supplied by the upstream utility source. A small deterioration in node voltages is also observed, although the deviations remain minor and within the acceptable limits (Figure 46 (d)).

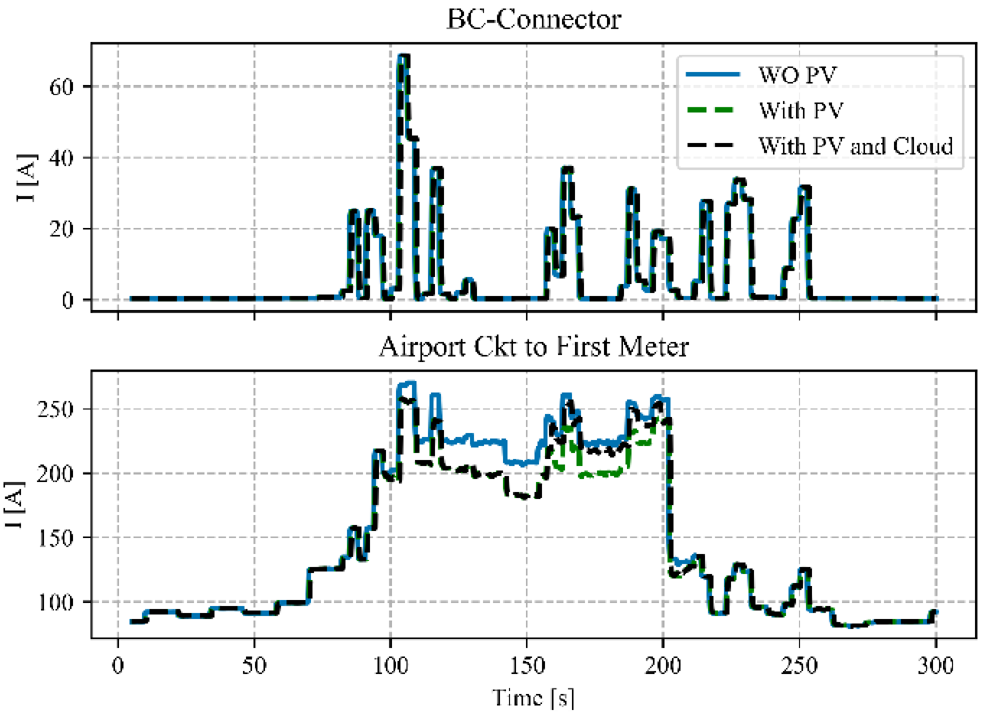
BC-Connector
WO PV
With PV
With PV and Cloud
I [A]
0
20
40
60
Airport Ckt to First Meter
I [A]
100
150
200
250
0
50
100
150
200
250
300
Time [s]

(a)

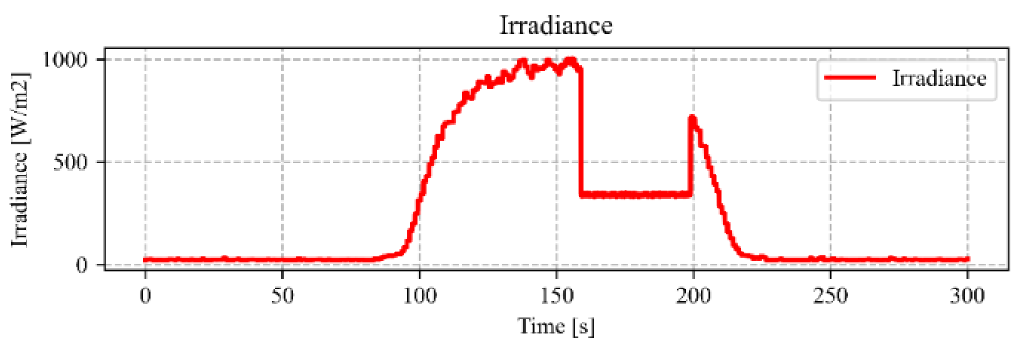
Irradiance
Irradiance
Irradiance [W/m2]
0
500
1000
0
50
100
150
200
250
300
Time [s]

(b)

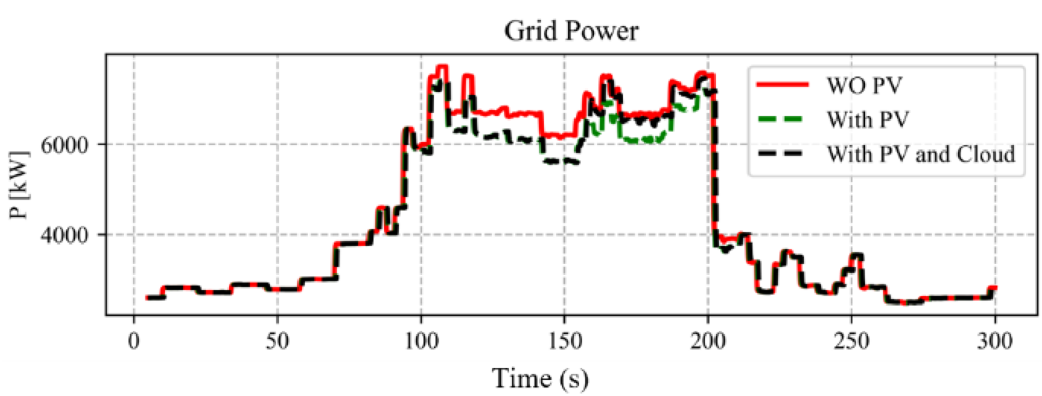
Grid Power
WO PV
With PV
With PV and Cloud
P [kW]
4000
6000
0
50
100
150
200
250
300
Time (s)

(c)

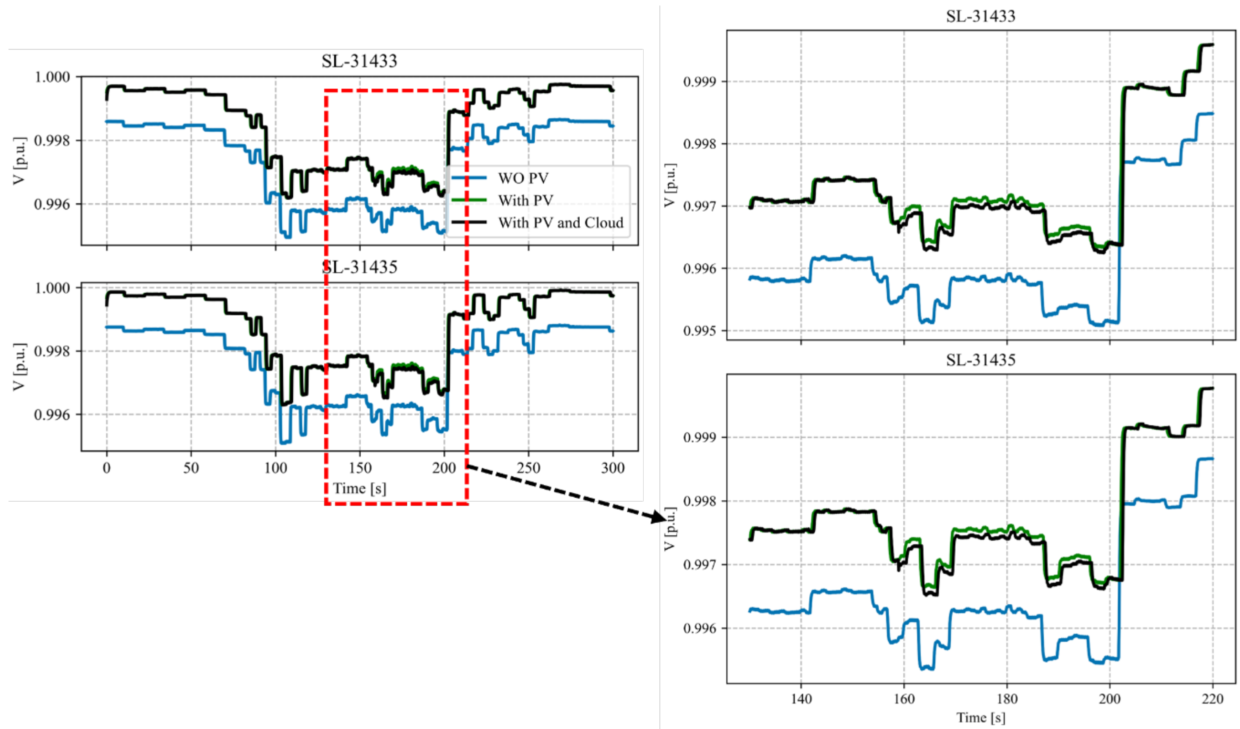

(d)

Figure 46. (a) Conductor ampacities, (b) irradiance, (c) power, and (d) voltage profiles corresponding to Scenario 2 with PV driven by cloudy irradiance

Overall, the cloud event primarily manifests as temporarily higher conductor loading and increased grid energy consumption, while the voltage impacts are comparatively limited, as shown in Figure 46. In other words, although PV provides beneficial unloading of the lines and reduces grid purchases under clear-sky conditions, short-duration cloud passages partially erode these benefits over the affected period and should be accounted for in planning and operational studies.

6.3.2.1.2 Maximize PV Buildout to All Available Airport Area

REopt also identified the maximum feasible PV capacity that could be installed within the airport footprint, yielding several candidate capacity values based on the available area and system constraints. In the digital twin, these PV configurations were instantiated with the corresponding capacities and driven by the same irradiance and temperature time series used in previous studies. The overarching objective of this analysis was to assess whether fully using the available PV siting area would have any adverse impacts on the existing conductor loading or voltage performance. The resulting digital twin configuration used for this scenario is illustrated in Figure 47, and the PV maximum power output is summarized in Table 53.

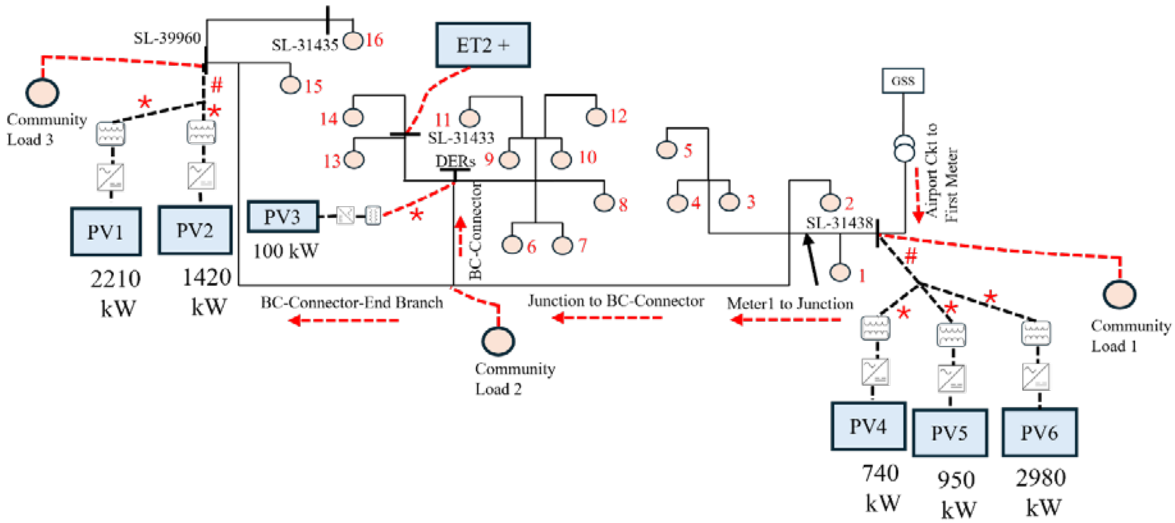

Figure 47. Digital twin representation of the airport circuit corresponding to the scenario with maximum utilization of the available area

Table 53. PV Maximum Power for Different Areas in the Digital Twin

Area	Maximum Power
1	2,210 kW
2	1,420 kW
3	100 kW
4	740 kW
5	950 kW
6	2,980 kW

Using this enhanced PV deployment scenario, we evaluated line loading, grid power consumption, and node voltages over the simulated period. As anticipated, the higher PV capacity produces a substantial reduction in conductor loading along multiple segments of the airport distribution network and significantly decreases the grid power imports during daytime hours. Voltage magnitudes in Figure 48 (a) exhibit only minor improvements and remain within the nominal 1-p.u. band, reinforcing the conclusion that the principal technical benefit of additional PV capacity is thermal rather than voltage support. The corresponding line-loading profiles are computed and analyzed to confirm that even at maximum PV deployment, the conductor ampacities remain within the acceptable limits, thereby demonstrating that the system can accommodate an aggressive PV buildout without triggering thermal violations.

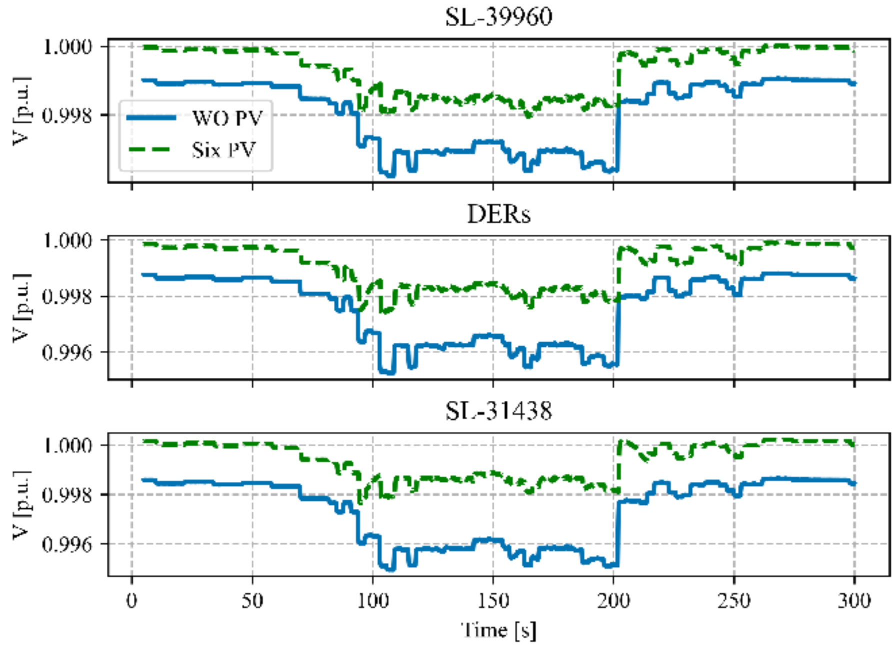

SL-39960
1.000
0.998
V [p.u.]
WO PV
Six PV
DERs
1.000
0.998
0.996
V [p.u.]
SL-31438
1.000
0.998
0.996
V [p.u.]
0
50
100
150
200
250
300
Time [s]

(a)

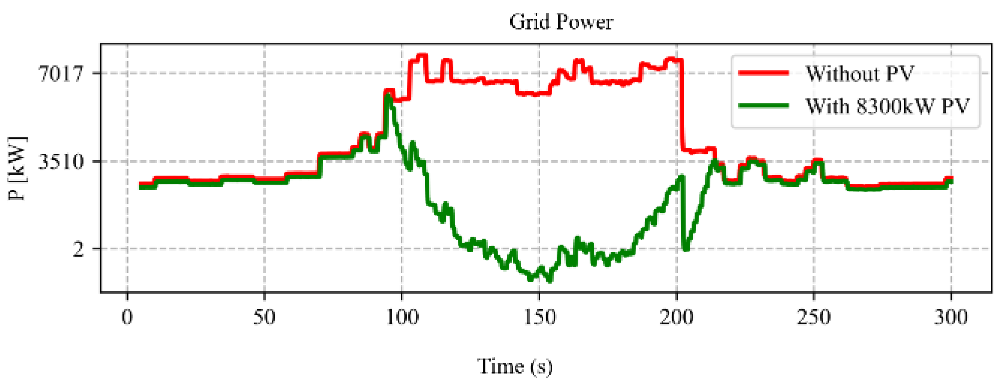

Grid Power
7017
3510
2
P [kW]
Without PV
With 8300kW PV
0
50
100
150
200
250
300
Time (s)

(b)

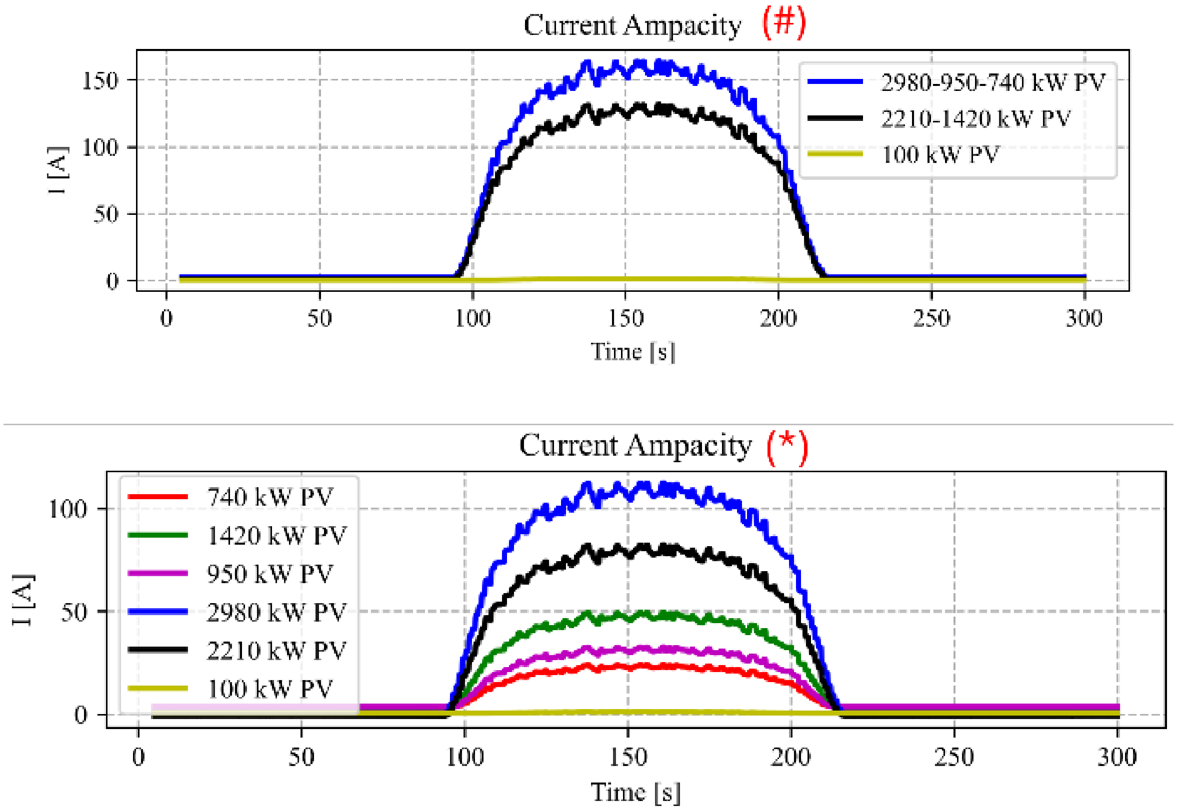

(c)

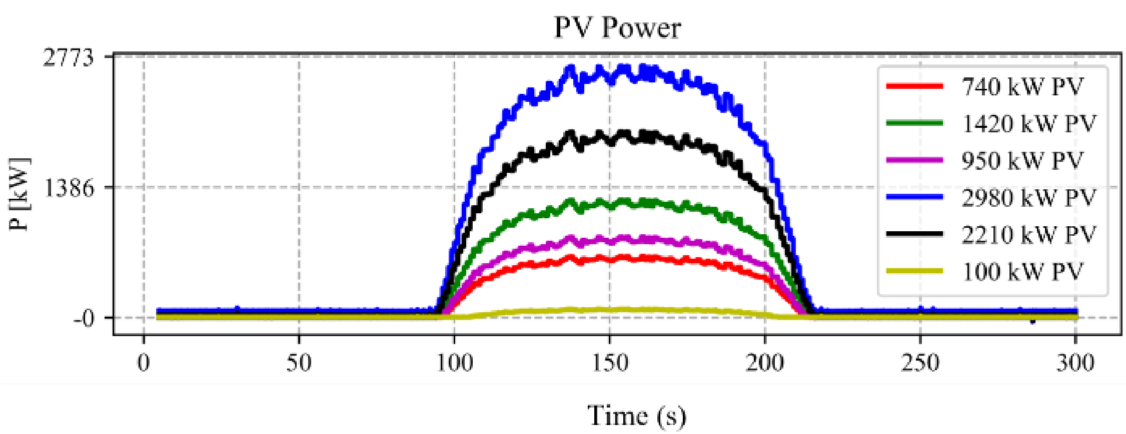

(d)

Figure 48. (a) Voltage, (b) grid power, (c) conductor ampacity, and (d) PV power profiles corresponding to the scenario with maximum utilization of the available area

In parallel, grid power imports were recorded for both cases, with and without PV, as shown in Figure 48 (b). As expected, the presence of PV reduces the daytime power consumption from the grid, thereby decreasing energy purchases during periods of high solar output and lowering operational costs over the long term. The required conductor's ampacity to host the PV installation was also quantified by monitoring the current in the line segment interfacing with the

PV point of interconnection. The resulting minimum ampacity requirement for that conductor is summarized in Figure 48 (c), and the resulting PV power output is depicted in Figure 48 (d).

6.3.2.2 Scenario 2 (b) Results

In this scenario, we examined the impact of BESS charging and discharging on the line loading and nodal voltages. REopt identifies the optimal on-site energy asset dispatch strategy that maximize cost savings. Battery charging set point and battery discharging set point from the REopt-identified dispatch strategy were used to drive the BESS system of Scenario 2 (b). The resulting charging profile is depicted in Figure 49.

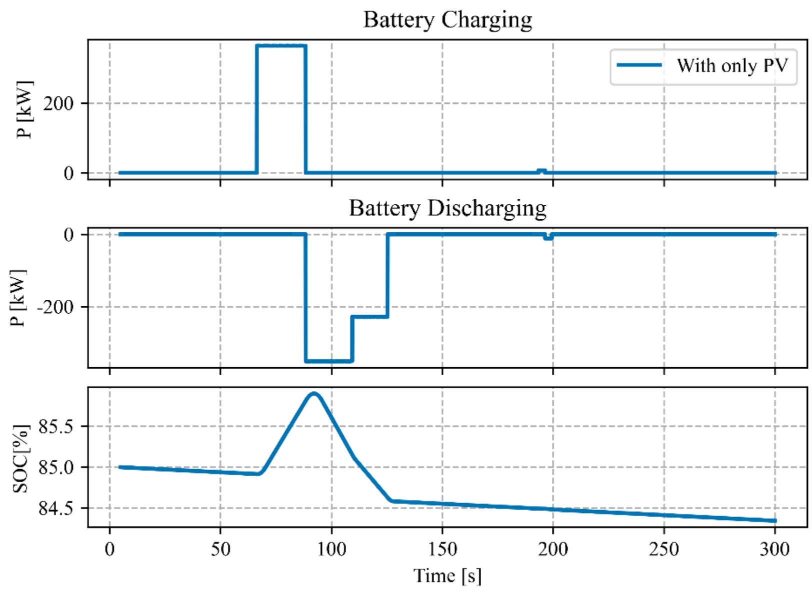

Figure 49. Charging and discharging dynamics of the BESS

The results in Figure 49, indicate that the BESS charging increases current flows and thus elevates the conductor loading and stress while also causing a slight reduction in the voltage magnitudes, which is consistent with the BESS behaving as an additional load. Conversely, during discharging intervals, the BESS operates as a local source, reducing the line loading on the upstream conductors and providing modest voltage support, as shown in Figure 50. These dynamics are mirrored in the SOC trajectory: SOC increases during charging, decreases during discharging, and exhibits gradual self-discharge during idle periods, as shown in the SOC profile in Figure 50. Collectively, these findings underscore the dual role of the BESS as both a flexible load and a local supply resource and highlight the importance of coordinated PV-BESS operation to exploit conductor unloading and voltage support benefits while managing line-stress during charging periods.

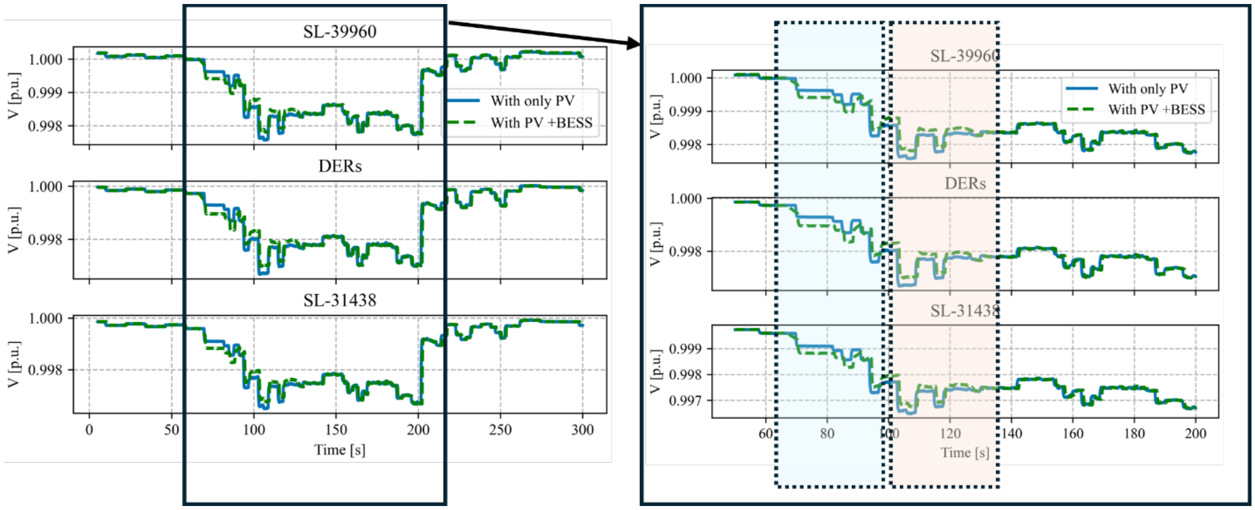

(a)

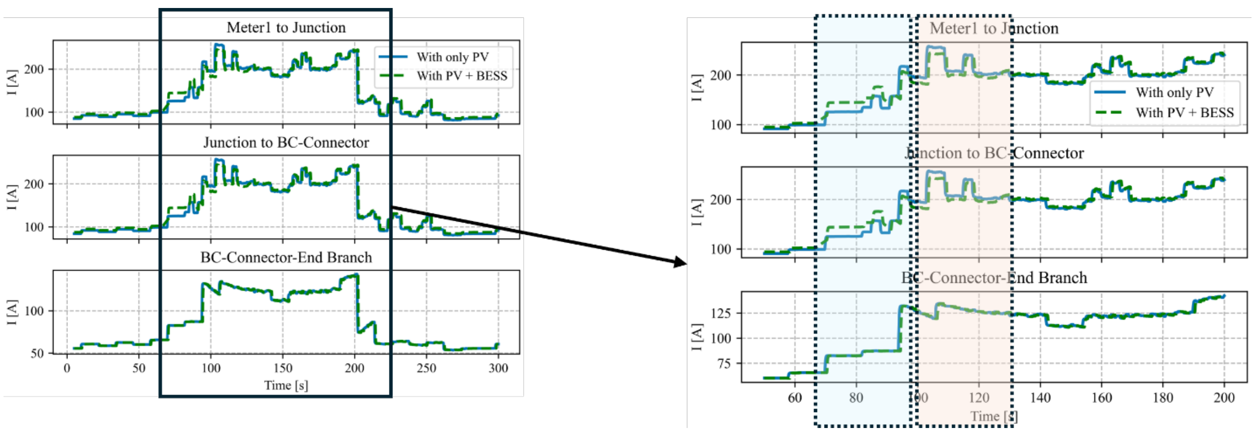

(b)

Figure 50. Nodal (a) voltage and (b) current profiles during charging and discharging of BESS

6.3.2.3 Scenario 2 (c) Results of Islanding Scenario

In this scenario, we evaluated whether the on-site generation portfolio (PV, BESS, and diesel generator) can maintain airport service during a loss-of-grid event. The digital twin configuration used to simulate this case is described in the previous section (Scenario 1 (c)). We used the REopt-provided capacities to execute the scenario. Although REopt initially recommended a 1-MWhr BESS (1-MW converter), time-domain simulations in the islanded Airport Isolation-1 microgrid revealed that this rating was insufficient to maintain acceptable frequency performance under the worst-case loading condition of approximately 1.4 MW (Figure 51 (c)), which violates the frequency deviation. In particular, the 1-MW converter could not provide enough active power support and inertial/frequency response during large disturbances, leading to frequency excursions outside the desired bounds. To address this limitation, the BESS converter rating was increased to 1.6 MW in the digital twin while preserving the REopt-recommended energy capacity. The resulting operational performance, along with the power/current, voltage, and frequency, are shown in Figure 51 (a), Figure 51 (b), and Figure 51 (c), respectively, and the time-series explanations are summarized in Table 54.

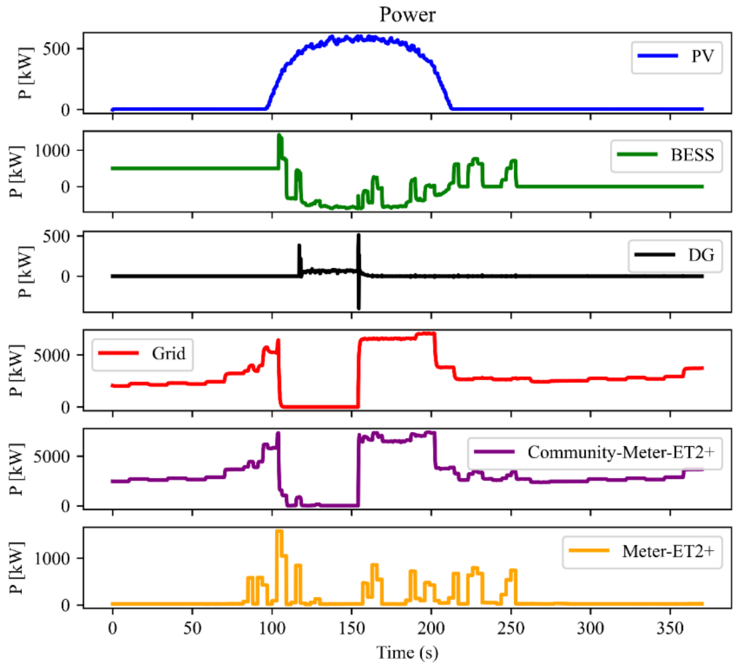
Power
PV
BESS
DG
Grid
Community-Meter-ET2+
Meter-ET2+
P [kW]
Time (s)

(a)

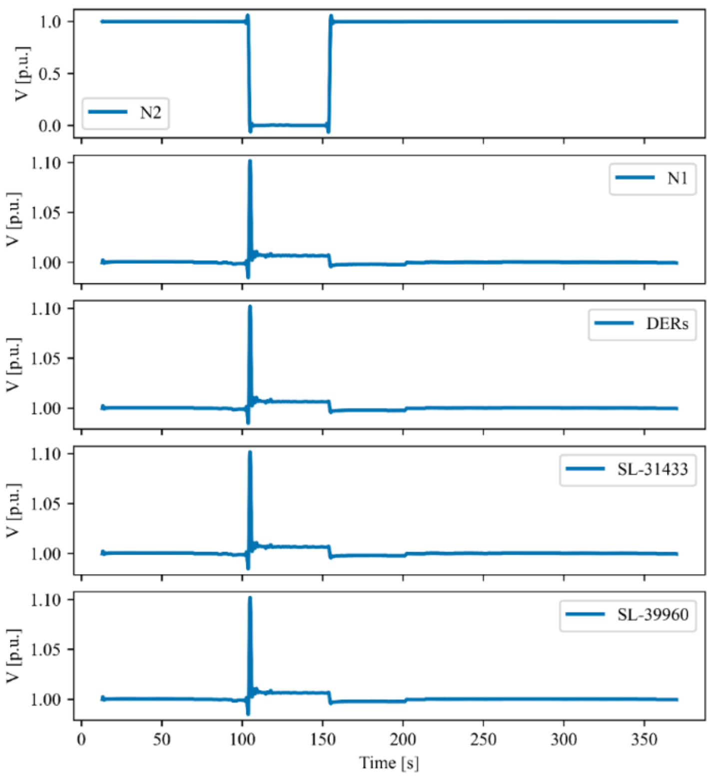
N2
N1
DERs
SL-31433
SL-39960
V [p.u.]
Time [s]

(b)

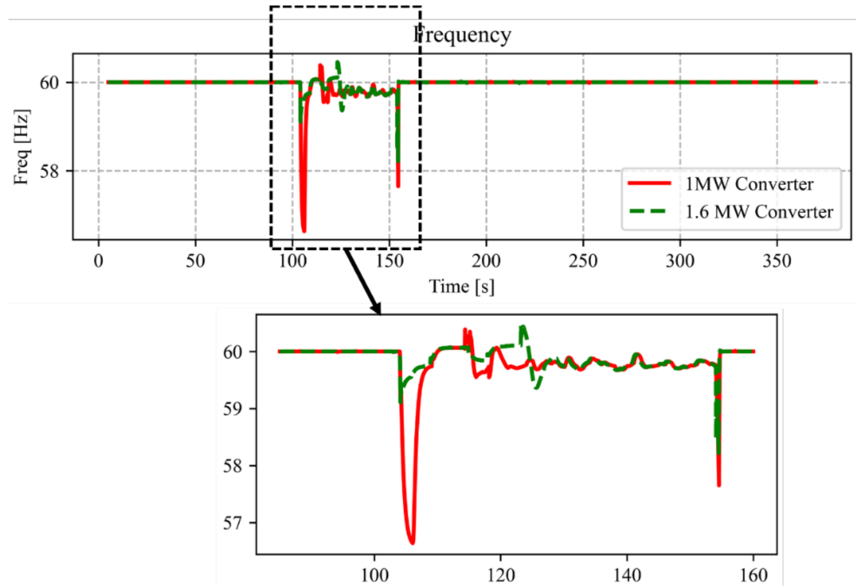

(c)

Figure 51. Operational performance of the (a) power, (b) voltage, and (c) frequency of the islanding Scenario 3

Table 54. Results Correspond to a 1.6-MW BESS Converter Scenario

Time Period	Result and Analysis
0–105 sec	The system operates in normal grid-connected mode: Switches S1, S2, S3, S4, S5, and S7 are closed, while S6 remains open. During this interval, it is effectively nighttime (no PV output), so the BESS is scheduled to discharge, supplying part of the airport load. The remaining demand from the airport meters and the ET2+ loads, together with the community load, are supplied by the upstream grid.
106 sec	The combined Airport + ET2+ demand reaches its peak, which is selected as the worst-case operating point. This instant is used as the trigger to drop the grid and transition to islanded operation. The rationale is that if the DER portfolio can sustain the system at this maximum demand condition, it will be sufficient for all less severe operating points.
106–155 sec	Immediately after the grid disconnection, switches S1, S2, S3, S4, S5, and S7 are opened, and S6 is closed. The BESS initially assumes a GFM role to maintain voltage and frequency because the diesel generator requires a finite startup time before it can contribute. During this interval, the load is supported by a combination of BESS and PV. When the PV generation exceeds the instantaneous load, the surplus is used to charge the BESS. Once the diesel generator is fully online, it transitions to GFM operation, and the BESS switches from GFM to GFL mode, injecting or absorbing power relative to the diesel generator-established voltage and frequency.
155 sec	The fault/contingency is considered clear, then S1, S2, S3, S4, S5, and S7 are closed, S6 is opened, and the resynchronization process between the islanded airport microgrid and the main grid is initiated. For safe reconnection, the voltage magnitude difference between nodes N1 and N2, the frequency deviation, and the phase angle difference are continuously monitored. When these parameters fall within the predefined tolerances, the resynchronization command is issued, and the intertie is reclosed. We observed that the frequency dip remains larger than expected, even in the case with the 1.6-MW converter in operation. As part of future work, we will investigate the sensitivity of the response to the allowable phase angle difference at the breaker closing and confirm whether a tighter

Time Period	Result and Analysis
	synchronization window mitigates the observed dip. In addition, we will verify that the breaker closing occurs at the intended electrical conditions and that the post-synchronization converter response is modeled correctly.
155 sec to 350+ sec	The system returns to a quasi-steady post-contingency regime. Within the airport, the BESS continues to supply power, and surplus PV generation is again used to recharge the battery. The community load is reconnected and served by the grid. Although the grid could also fully supply the airport loads during this phase, the control strategy prioritizes using stored energy in the BESS to reduce the utility energy purchases and exploit the available flexibility. At the end of this interval, the islanded scenario is considered complete, having demonstrated a successful ride-through, autonomous operation, and controlled resynchronization under a worst-case disturbance.

The enhanced rating enables the BESS to supply a sufficient power margin during islanded operation and to stabilize the frequency even at the peak demand. This finding effectively feeds back a dynamic-operability constraint into the planning process, suggesting that REopt (or similar tools) should incorporate additional constraints or post-processing steps to ensure that the BESS power ratings are not only economically optimal but also adequate for frequency support in worst-case islanded scenarios.

6.3.2.3.1 Islanded Scenario (Maximum Utilization of PV)

Scenario 3 was conducted to quantify the airport feeder's contingency resilience and its ability to sustain critical community loads under credible fault events. The network was augmented with a 10-MWh BESS (operated under grid support controls, such as voltage-frequency droop and fast frequency response) and 4 MW of dispatchable diesel generator to provide firm capacity and inertial/primary-like support. In parallel, PV generation was expanded to the maximum developable area to represent the upper bound of the on-site renewable penetration. The resulting digital twin configuration is shown in Figure 52.

To emulate realistic disturbance conditions, a line-to-ground (L–G) fault was imposed at a representative location on the airport distribution circuit, serving as a proxy for contingency scenarios (e.g., feeder faults or segment outages). System performance was evaluated by continuously monitoring the bus voltage profiles, frequency deviations (nadir and settling behavior), and overall dynamic stability during and after the event, as shown in Figure 53. The time-series results summarized in Table 55 indicate that the proposed on-site generation portfolio—10-MWh BESS + 4 MW of diesel generation with fully used PV—maintains acceptable voltage and frequency response and is therefore sufficient to ride through and mitigate the modeled contingencies, supporting the targeted community load without violating key operational limits.

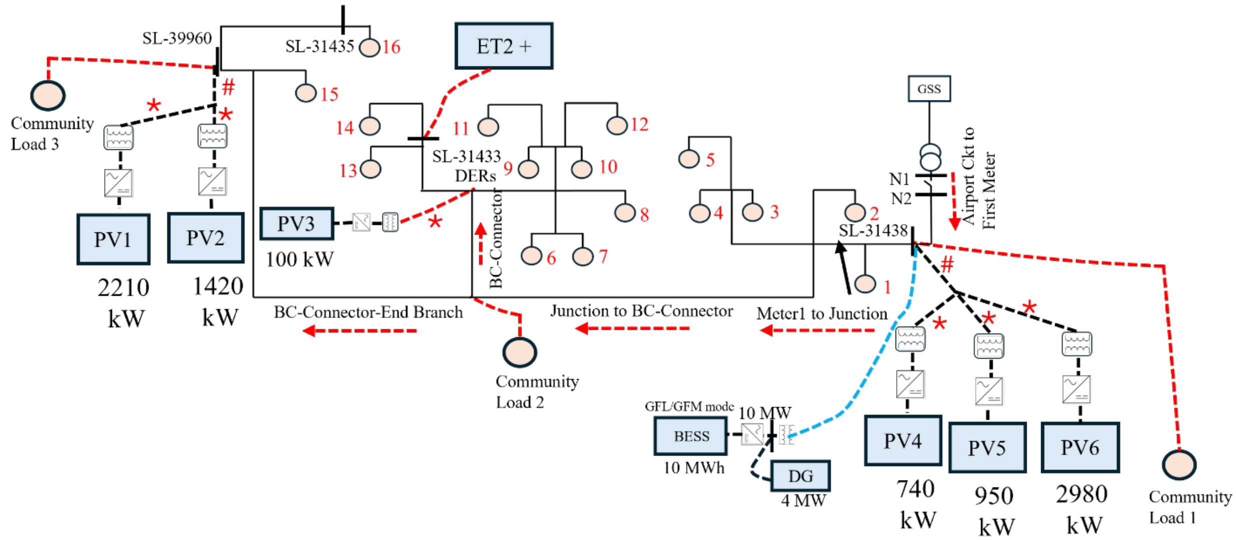

Figure 52. Digital twin representation of the airport circuit corresponding to the islanding Scenario 3 with maximum utilization of PV

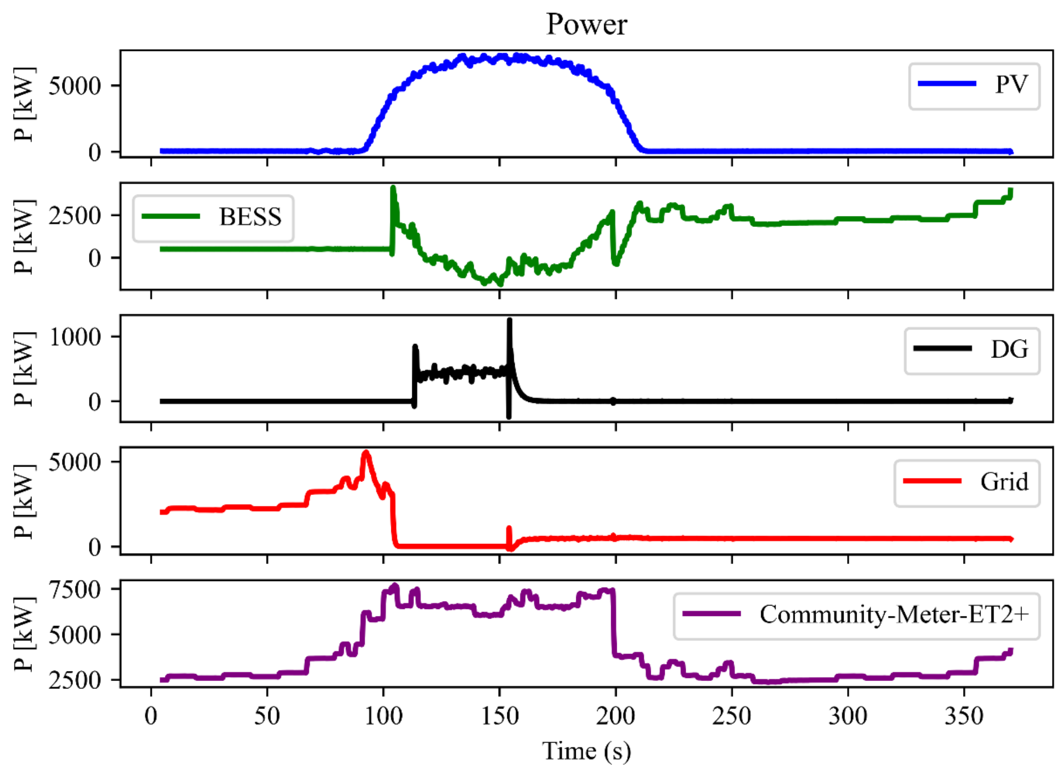

(a)

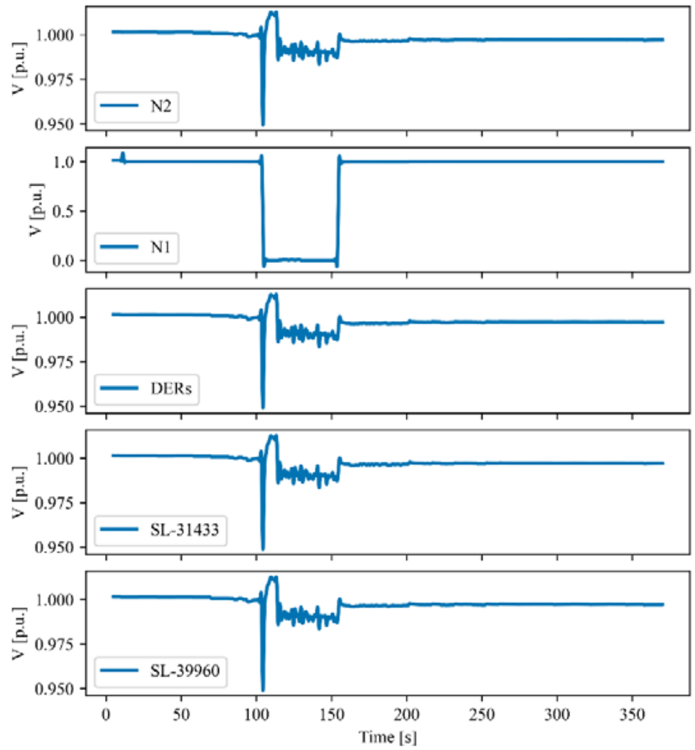

(b)

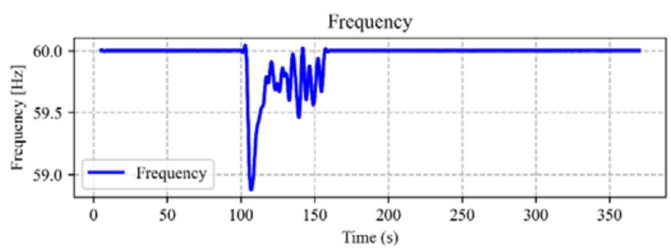

(c)

Figure 53. Operational performance of the (a) power, (b) voltage, and (c) frequency of the islanding Scenario 3 with maximum utilization of PV

Table 55. Results Corresponding to Scenario 3 With Maximum Utilization of PV

Time Period	Result and Analysis
0–105 sec	The system operates in normal grid-connected mode. During this interval, PV output is mostly zero, so the BESS is scheduled to discharge, supplying part of the airport load. The remaining demand from the airport meters and ET2+ loads, together with the community load, is supplied by the upstream grid.
106 sec	The combined Airport + ET2+ demand reaches its peak, which is selected as the worst-case operating point. This instant is used as the trigger to drop the grid and transition to islanded operation. The rationale is that if the DER portfolio can sustain the system at this maximum demand condition, it will be sufficient for all less severe operating points.
106–155 sec	Immediately after the grid disconnects, the BESS initially assumes a GFM role to maintain voltage and frequency because the diesel generator requires a finite startup time before it can contribute. During this interval, the load is supported by a combination of BESS and PV. When the PV generation exceeds the instantaneous

Time Period	Result and Analysis
	load, the surplus is used to charge the BESS. Once the diesel generator is fully online, it transitions to GFM operation, and the BESS switches from GFM to GFL mode, injecting or absorbing power relative to the diesel generator-established voltage and frequency.
155 sec	The fault/contingency is considered clear, and the resynchronization process between the islanded airport microgrid and the main grid is initiated. For safe reconnection, the voltage magnitude difference between nodes N1 and N2, the frequency deviation, and the phase angle difference are continuously monitored. When these parameters fall within the predefined tolerances, the resynchronization command is issued, and the intertie is reclosed.
155 sec to 350+ sec	The system returns to a quasi-steady post-contingency regime. Within the airport, the BESS continues to supply power, and while surplus PV generation is available, it is used to recharge the battery. The community load is reconnected and served by the grid. Although the grid could also fully supply the airport loads during this phase, the control strategy prioritizes using stored energy in the BESS to reduce the utility energy purchases and the exploit the available flexibility. At the end of this interval, the islanded scenario is considered complete, having demonstrated successful ride-through, autonomous operation, and controlled resynchronization under a worst-case disturbance.

6.4 Discussion

A modular, scalable GDT framework was developed using a zonal-mesh architecture to support plug-and-play reconfiguration, allowing the same framework to be adapted to different airport microgrid layouts—including radial, loop, and mesh configurations—with minimal rework. Building on this, a physics-informed digital twin of the OKV airport distribution network was constructed using utility-provided topology, conductor specifications, transformer data, and geospatial coordinates, establishing a high-fidelity baseline that is suitable for planning and operational studies while omitting sensitive identifiers. The digital twin was subsequently validated against utility SCADA smart meter measurements, with a meter-level mean square error of approximately 3–8%, indicating acceptable agreement between the digital twin outputs and the field data.

A synchronized REopt-digital twin workflow was implemented to connect the techno-economic planning with the time-domain operational verification, enabling de-risking of CAPEX decisions by stress-testing optimized DER portfolios and dispatch strategies in the digital twin prior to deployment. The analysis of the PV integration revealed that its primary system benefit comes through conductor unloading, by creating thermal headroom, rather than through voltage regulation, as the voltage changes remained minor while the line-loading reductions created capacity for future load growth. PV siting location was found to significantly affect the system benefits, with deeper placement providing broader upstream relief by reducing the conductor currents across more segments; however, PV variability, such as cloud transients, was shown to temporarily reduce these benefits, with conductor loading and grid imports increasing during reduced irradiance intervals, underscoring the importance of accounting for variability in both planning and operations.

High PV buildout across the available airport areas was found to be technically accommodable without introducing major violations, with aggressive deployment further reducing grid imports and line loading while maintaining acceptable voltage and ampacity limits in the simulations. BESS operation exhibited a dual effect: charging increased line loading, while discharging reduced upstream loading and provided modest voltage support, highlighting the need for coordinated PV-BESS scheduling to maximize benefits while avoiding unnecessary conductor stress.

Island operation was shown to be feasible with coordinated PV, BESS, and diesel generator, but it requires architecture-aware switching and a dedicated island boundary to avoid energizing non-airport loads. This indicates that additional conductor and switching changes might be necessary for practical airport-only islanding. Finally, dynamic digital twin simulations provided critical feedback to the planning results: In the worst-case demand islanding conditions, the REopt-recommended 1-MW BESS converter proved insufficient for frequency performance, with approximately 1.6 MW required, motivating the inclusion of dynamic-operability constraints alongside purely economic recommendations.

7 Conclusions

Electricity costs can be significant at airports, especially at smaller airports like OKV and HVN. Airports can choose to engage their electric utility to serve existing loads and any anticipated future loads, such as forecasted EVSE loads or new loads from related CAPEX; however, solely relying on the utility might not be the least-cost way of serving these electric loads. Rapid increases in electricity costs due to load growth and geopolitical factors can also result in electricity costs rising quicker than expected. These cost increases directly influence the airports' operational costs. Forecasted EVSE loads can be equivalent to or greater than the existing electric loads at small or midsize airports, and they can double the electricity bills at smaller airports. The power demanded by AAM can result in large peaks that can grow with the needs of AAM aircraft and the increasing flight scheduling complexity that comes with increasing AAM adoption. Energy usage for charging is significant, especially for smaller airports like OKV and HVN, and it will grow with the adoption rate. Table 56 shows the percentage change in energy usage from the ET2 projections to the ET2+ projections. Note that this is in terms of MWh, so there can be significant energy need changes as the usage changes.

Table 56. Percentage Change in Energy Needs per Aircraft Between ET2 and ET2+

	HVN	OKV
RAM	11.2%	18.6%
eGA	-4.8%	-11.5%
eVTOL	67.5%	32.4%

Therefore, it is critical that airports proactively work with their utilities to learn about electric tariff options and other programs that could provide cost savings. Choosing to wait to settle on the electricity supply for new EVSE loads can lock in the airport to excessively high electric utility bills and distribution infrastructure upgrade costs. Electrical utility connection issues can also arise that delay EVSE projects by many years, so advanced infrastructure planning can help to alleviate that. Airports can choose to consider on-site generation systems to unlock cost savings on their electric utility bills. In addition to financial savings, various other benefits of on-site generation systems were discussed in the report and are summarized.

This study considered the financial feasibility and resilience benefits of on-site generation systems at OKV and HVN. Results indicate that very small on-site generation systems could be cost-effective at OKV, whereas these systems could provide a lot more financial value at HVN. OKV could place a larger battery system to offset the new demand introduced by the forecasted EVSE loads and save a modest amount of money over 25 years; therefore, this airport would need to consider the added benefits of on-site generation, such as outage survival, to justify investments. HVN is the opposite because on-site generation systems are very lucrative there if the loads are aggregated for billing purposes. OKV would need to rely on resilience value to justify investments in maximizing on-site generation if it were to consider becoming an ÆNode. HVN, on the other hand, can rely on financial savings and resilience benefits to justify the costs associated with becoming an ÆNode.

The financial feasibility of on-site generation depends on the electric tariffs, which can vary across the nation. It could be that an airport's existing electric tariff is not conducive for on-site generation to provide cost savings, but an alternate tariff could be viable. Note that the REopt results presented in this report are based on a static set of techno-economic assumptions. In the real world, these assumptions have uncertainty and can change over time. For example, financial feasibility can vary with changes in capital costs, incentives, and electricity cost escalation rates. Results from REopt-Insight identify the parameters that can make on-site generation more viable or less viable at either OKV or HVN. When it comes to serving forecasted EVSE loads, airports could incur the cost of EVSE and the cost of local grid upgrades in addition to the electricity costs. This report presents the BCOC, which is an all-inclusive $/kWh cost of serving EVSE loads. (BCOC does not factor in any resilience or capacity benefits provided by on-site generation systems.) This cost can be compared against the equivalent cost of jet fuel that would be required to serve the forecasted EVSE loads to obtain a purely financial comparison. Electric tariffs can play a crucial role in BCOCs, as shown in the results for OKV and HVN. More favorable electricity rates at HVN could result in a reduction in BCOC when on-site generation is installed compared to solely relying on utility power.

In addition, financial viability, on-site generation systems provide the ability to withstand outages at airports, making airports an energy node for their communities. Enabling local community members to use an airport's facilities during an outage can be invaluable and could justify modest or poor economic projections from on-site generation systems. Airports can also choose to maximize generation on their grounds to act as an energy source. Such a system can dispatch substantial power to the local grid either during outages or during times of high electricity demand and help critical local facilities remain online. Again, the value of lost load for a nearby hospital, supermarket, or law enforcement center can be impossible to quantify for comparison against the cost incurred for the installation of a very large on-site generation system at airports.

Using a digital twin of OKV provided an accurate sandbox to test the effectiveness of the on-site generation sources to scenarios like those described here. It helped not only to determine the effectiveness of the energy system but also to answer questions such as where the generation resources should be placed, what electric meter to connect them to, and what, if any, network upgrades would be required to achieve the stated goal—all without buying a piece of equipment or breaking ground on construction.

This effort found that a modest cost increase of $0.01/kWh to $0.09/kWh from the local community for the exported and curtailed on-site generation could make energy generation systems cost neutral at both OKV and HVN. Additionally, surplus generation from an airport installation can add flexibility in power generation to the local distribution feeder. The additional capacity at the airport can help reduce demand for electrical capacity in the community and allow electric utilities to bring large-load customers (such as data centers) online faster compared to constructing new power plants.

References

Anderson, K., Olis, D., Becker, B., Casson, L., Laws, N., Li, X., Mishra, S., Kwasnik, T., Jeffrey, A., Elgqvist, E., Krah, K., Cutler, D., Zolan, A., Muerdter, N., Eger, R., Walker, A., Hampel, C., Tomberlin, G., Farthing, A., … Pullatasig, B. (n.d.). *The REopt Web Tool User Manual*. National Renewable Energy Laboratory. Retrieved https://reopt.nrel.gov/tool/reopt-user-manual.pdf

Borer, N. (n.d.). *Airports as Energy Nodes: Sustainable Energy Hubs to Benefit AAM Users and Local Communities*. Retrieved September 5, 2025, from https://ntrs.nasa.gov/citations/20230002407

Borer, N. K., Blaesser, N. J., Denham, C. L.-A., Hallock, T. J., Patterson, M. D., Fernandez, X. C., Lvovich, V. F., Malone, B. P., Klopp, H., & Mccormick, A. (2025). *Airports as Energy Nodes Activity Summary*.

Brancucci, C., Cutler, D., & Jenkins, J. (2025). *Flexible Data Centers: A Faster, More Affordable Path to Power*. Camus, encoord, and Princeton ZERO Lab. https://cdn.prod.website-files.com/60dbdcca2e4b1919e8894fa5/6930abf1be0f36db6fc27157_Whitepaper%20-%20With%20Appendix.pdf

Cox, J., Harris, T., Krah, K., Morris, J., Li, X., & Cary, S. (2023). Impacts of Regional Air Mobility and Electrified Aircraft on Airport Electricity Infrastructure and Demand. *Renewable Energy*.

Cutler, D., Olis, D., Elgqvist, E., Li, X., Laws, N., DiOrio, N., Walker, A., & Anderson, K. (2017). *REopt: A Platform for Energy System Integration and Optimization* (Technical

Report NREL/TP-7A40-70022). National Renewable Energy Laboratory (NREL), Golden, CO (United States). https://docs.nrel.gov/docs/fy17osti/70022.pdf

DiGangi, D. (2025, December 4). *Flexible connections and BYOC could reduce data center burden: Report*. Utility Dive. https://www.utilitydive.com/news/flexible-grid-connections-byoc-data-centers-utilities/807047/

Grid Status. (2025, April 18). Byte Blackouts: How large data center loads are surfacing new issues. *Batteries*. https://blog.gridstatus.io/byte-blackouts-large-data-center-loads-new-issues-pjm/

Horowitz, K. (2019). *2019 Distribution System Upgrade Unit Cost Database Current Version* (No. 101) [Dataset]. https://doi.org/10.7799/1491263

Howland, E. (2026, January 7). *Data centers were 40% of PJM capacity costs in last auction: Market monitor*. Utility Dive. https://www.utilitydive.com/news/data-centers-pjm-capacity-auction/808951/

Justin, C. Y., Payan, A. P., & Mavris, D. N. (2022). Integrated fleet assignment and scheduling for environmentally friendly electrified regional air mobility. *Transportation Research Part C: Emerging Technologies*, *138*, 103567. https://doi.org/10.1016/j.trc.2022.103567

Kneifel, J. D., & Lavappa, P. D. (2024). *Energy Price Indices and Discount Factors for Life-Cycle Cost Analysis – 2024* (NIST Interagency Report NIST IR 85-3273-39; p. 1). National Institute of Standards and Technology. https://doi.org/10.6028/NIST.IR.85-3273-39

Morris, J., Rathod, B., Kim, A., Robby, K., Leddy, L., Harris, T., Grue, N., & Cary, S. (2025). *Colorado Alternatively Powered Aircraft Airport Infrastructure Study* (NREL/TP-5R00-

91144; p. 47). National Renewable Energy Laboratory (NREL), Golden, CO (United States). https://docs.nrel.gov/docs/fy25osti/91144.pdf

National Institute of Standards and Technology. (n.d.). *NIST Energy Escalation Rate Calculator*. EERC. Retrieved https://pages.nist.gov/eerc/

National Renewable Energy Laboratory. (n.d.-a). *Electricity Annual Technology Baseline (ATB) Data Download* (Version 2024) [Dataset]. Retrieved https://atb.nrel.gov/electricity/2024/data

National Renewable Energy Laboratory. (n.d.-b). *NREL's PVWatts® Calculator*. PVWatts Calculator. Retrieved https://pvwatts.nrel.gov/

OFFICE OF ELECTRICITY. (2023). *Communications with the Grid Edge* [White Paper]. U.S. DEPARTMENT OF ENERGY. https://www.energy.gov/sites/default/files/2023-07/Communications%20with%20the%20Grid%20Edge%20-%20Unlocking%20Options%20for%20Power%20System%20Coordination%20and%20Reliability_0.pdf

PJM. (2025, September 4). *Real-Time Hourly LMPs*. Data Miner 2. https://dataminer2.pjm.com/feed/rt_hrl_lmps/definition

Public Utilities Regulatory Authority. (n.d.). *Connecticut Renewable Portfolio Standard*. Renewable Portfolio Standards Overview. Retrieved September 2, 2025, from https://portal.ct.gov/pura/rps/renewable-portfolio-standards-overview

RAPPAHANNOCK ELECTRIC COOPERATIVE. (2023, October 25). *SCHEDULE NEM-10A NET ENERGY METERING RIDER*. https://myrec.coop/sites/default/files/documents/Governance%20Center/NET%20ENERGY%20METERING%20RIDER%202023.pdf

RAPPAHANNOCK ELECTRIC COOPERATIVE. (2024a, October 2). *LARGE POWER SERVICE SCHEDULE LP-1*. https://myrec.coop/sites/default/files/documents/Electric%20Rates/Large%20Power%20Service%20LP-1.pdf

RAPPAHANNOCK ELECTRIC COOPERATIVE. (2024b, October 2). *SMALL GENERAL SERVICE SCHEDULE B-1*. https://myrec.coop/sites/default/files/documents/Electric%20Rates/SGS%20B-1.pdf

RAPPAHANNOCK ELECTRIC COOPERATIVE. (2024c, October 2). *SMALL GENERAL SERVICE SCHEDULE B-3*. https://myrec.coop/sites/default/files/documents/Governance%20Center/Schedule%20B%203r.pdf

UI: An Avangrid company. (2026). *Pricing*. Pricing - UI. https://www.uinet.com/account/understandyourbill/pricing

Understanding Load Factor. (n.d.). Austin Energy. Retrieved January 16, 2025, from https://austinenergy.com/-/media/project/websites/austinenergy/rates/pdfs-and-files/understandingloadfactor.pdf

United States Department of Energy. (2024). *Large Power Transformer Resilience* (pp. 5, 12). United States Department of Energy. https://www.energy.gov/sites/default/files/2024-10/EXEC-2022-001242%20-%20Large%20Power%20Transformer%20Resilience%20Report%20signed%20by%20Secretary%20Granholm%20on%207-10-24.pdf

US Army Corps of Engineers. (n.d.). *Cost Engineering*. Retrieved January 16, 2025, from https://www.usace.army.mil/Missions/Cost-Engineering/

US Energy Information Administration. (2023, June 21). *As solar capacity grows, duck curves are getting deeper in California*. As Solar Capacity Grows, Duck Curves Are Getting Deeper in California. https://www.eia.gov/todayinenergy/detail.php?id=56880

US Energy Information Administration. (2025, May 13). *After more than a decade of little change, U.S. electricity consumption is rising again*. After More than a Decade of Little Change, U.S. Electricity Consumption Is Rising Again. https://www.eia.gov/todayinenergy/detail.php?id=65264

Appendices

Appendix A. REopt-InSight Methodology and Results

Identifying robust designs that have a high likelihood of achieving the required performance must overcome the following difficulties:

1. **High dimensionality:** The combined space of design parameters and uncertain inputs can exceed 25 variables, making exhaustive sampling infeasible.
2. **Computational burden:** REopt® runs are slow, usually 1–5 minutes, so exploring the full uncertainty space for each possible design is not practical.
3. **Decision confidence needs:** Stakeholders benefit from investment guidelines rather than a specific system to invest in. Identifying ranges of system configurations that meet financial and resilience thresholds with high statistical confidence can provide significantly more insight than just a single "best estimate" scenario.

The following methodology describes a process that combines parameter screening, space mapping, and surrogate modeling to produce a fast, flexible tool for robust energy system design evaluation. This workflow has been developed to achieve the following:

- Reduce the dimensionality of the uncertainty space.
- Efficiently map the combined design/uncertainty space.
- Provide a fast, queryable surrogate for REopt results.
- Quantify not just expected performance but also confidence intervals, enabling robust design recommendations.

Step 1: Uncertainty Parameter Filter (Taguchi Method)

This step reduces the dimensional space of the solution by removing any input parameters that do not have a significant effect on the system design (Atkinson, Donev, & Tobias, 2007).

1. Begin with a superset of uncertainty parameters as shown in Table 57.
2. Assign three levels to each parameter: low, medium, and high. These levels are informed through market analysis to encompass the maximum and minimum assumptions that may be seen in current market conditions.
3. Using a Taguchi array, multiple test cases of the site are generated with the uncertain input parameters varied across their three levels. The Taguchi array ensures the set of test cases captures first- and second-order variance contributions.
4. Run REopt for each Taguchi case and perform an analysis of variance (ANOVA) on the resulting performance metrics (e.g., net present value [NPV], optimal photovoltaics/battery energy storage system [PV/BESS] sizing).
5. Sum of squares (SS) quantifies parameter influence by measuring how much variation in an output indicator is attributable to changes in each parameter. It is calculated as:

$$ss = \sum_{i=l,m,h} n_i(\overline{y_i} - \bar{Y})^2$$

where i indexes the low, medium, and high parameter cases; n_i is the number of observations in each case; $\bar{y}_i$ is the mean output for that case; and $\bar{Y}$ is the overall mean output across all cases. Larger SS values indicate a stronger impact of the parameter on the output variation.

6. The parameter's percentage contribution toward the variation of each output indicator is calculated to determine the most significant uncertainty parameters. Examples of this can be seen in Table 57 and Table 59.
7. The four to five parameters that have the most significant effect on system sizes and life cycle costs are included in the second stage of this analysis for further investigation. The remaining parameters are fixed because their variation has a smaller impact on outputs.
8. **Outcome:** Reduced uncertainty space, typically fewer than five parameters.

Table 57. Testing Levels for Uncertainty Parameters in Taguchi Analysis

Parameter	Low	Mid	High
Financial | Discount Rate	3%	6%	9%
Financial | Electricity Cost Escalation Rate	0%	2.5%	7%
Financial | Inflation Rate	0%	2.5%	5%
PV | ITC Incentive	0%	1.5%	3%
PV | Initial CAPEX	1250 $/kW	2500 $/kW	4400 $/kW
PV | Azimuth*	135°	180°	225°
PV | Tilt*	10°	15°	20°
PV | O&M Annual Cost	15$	17.5$	20$
BESS | Initial Energy CAPEX	289 $/kW	455 $/kW	686 $/kW
BESS | Initial Power CAPEX	578 $/kWh	910 $/kWh	1372 $/kWh
BESS | Replacement Energy CAPEX	202 $/kWh	339 $/kWh	480 $/kWh
BESS | Replacement Power CAPEX	454 $/kW	766 $/kW	1078 $/kW
BESS | Minimum SOC	15%	22.5%	30%
BESS | ITC Incentive	0%	15%	30%
Electric Tariff | Energy**	80%	100%	120%
Electric Tariff | Demand**	80%	100%	120%

ITC = investment tax credit; CAPEX = capital expenditure; O&M = operations and maintenance; SOC = state of charge

* PV azimuth, tilt, and BESS min SOC are often under the designer's control and could be considered design parameters. However, during REopt style scoping analyses, these inputs are often unknown and may change with roof tilt or wind loading requirements and so are considered uncertainty parameters during this step.

** The energy and demand charges are changed proportionally to the current tariff the site is on. Such charges, although known at the time of this work, are changed regularly by the utility provider.

Step 2: Mapping the Design + Uncertainty Space (Latin Hypercube Sampling)

This step aims to select a second set of test cases to be run through REopt. These will have fixed design sizes (PV/BESS) rather than using REopt's optimizer to select optimal sizing.

1. Combine the screened uncertainty parameters (U) with the chosen design parameters (D).
    - Example:
        - Uncertainty parameters = {Financial | Discount Rate, PV | Initial CAPEX, BESS | Initial CAPEX, Electric Tariff | Energy, Electric Tariff | Demand}
        - Design Parameters = {PV | Capacity, BESS | Energy Capacity, Bess | Power Capacity}
2. Use Latin hypercube sampling (Mckay, Beckman, & Conover, 1979) to generate a representative set of points in the high-dimensional D+U space (random number generator seed of 1234 used for point generation).
3. Generate enough REopt cases to accurately map the D+U space (~10,000 cases).
4. Sampled points will be run through REopt to create a training dataset.

Step 3: Surrogate Modeling (Gaussian Process Regression)

This step will use the training data to generate multiple Gaussian processes across the D+U space (Neal, 1997). One Gaussian process will be generated for each output of interest.

9. Train a Gaussian process on the REopt results to create a predictive model for any combination of D and U parameters.
10. The Gaussian process provides both mean predictions and standard deviations—the latter serving as an interpolation error metric.
11. If the interpolation error is too high, increase the number of training samples or investigate statistical methods that may be more suitable to your dataset.

In this analysis, two Gaussian processes are constructed. One maps the NPV of system designs; the other maps the resilience achieved by those systems. The resilience was modeled using REopt's Energy Resilience Performance (REopt-ERP) tool. This tool was used to evaluate a survival resilience period for a system, i.e., how long a system can provide continuous operation at a site during a utility outage. REopt-ERP accounts for weather patterns, load variation, and hardware failure to predict a likelihood of survival. The survival resilience period was calculated as the maximum duration outage for which the system has a greater than 90% chance of survival.

Step 4: Robust Design Evaluation

The data available through the Gaussian process mapping of the space allow rapid testing of system designs and sensitivities. Figure 54 illustrates the robust design workflow. Examples of how to use these data include the following:

- **Safe harbor analysis:** Select a cut-off requirement and confidence interval above which you consider an acceptable design (for example: 95% likelihood that a design will have an NPV greater than $100,000). Sample the design space to find this boundary. This can be combined with multiple criteria (e.g., can provide energy during an 8-hour outage, peak demand of less than 1 megawatt [MW], 50% on-site generation). By finding the overlap in these safe harbors, multiple objectives can be achieved.
- **Design sensitivity to specific uncertainty parameters:** When a design has been selected, a sensitivity analysis can easily be run to show how the design performance varies against any or all of the modeled uncertainty parameters.
- **Pareto fronts:** By accurately modeling multiple objectives across the design space, Pareto fronts can be mapped to aid in design selection.

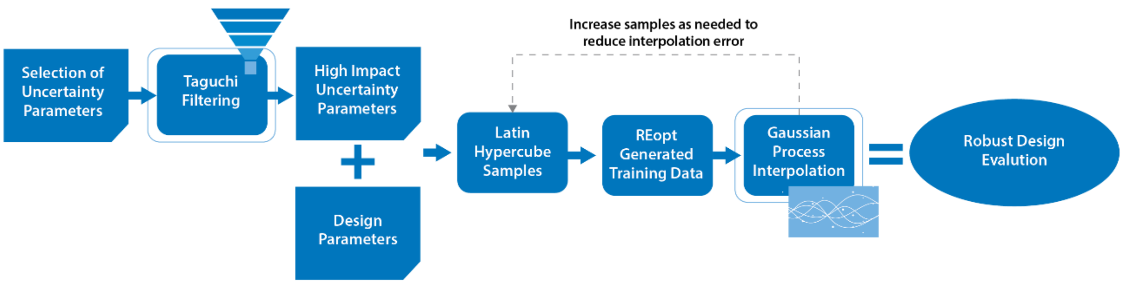

Figure 54. Robust design analysis workflow

Robust Design Results and Analysis

The following sections provide the results and conclusions from using REopt-Insight to analyze Winchester Regional Airport (OKV) and Tweed New Haven Airport (HVN). The first step—Taguchi filtering—will narrow down which uncertainties have the most significant effect on the system performance. The second step—the Gaussian process interpolation—is used to map the design space, which allows the user to investigate trends in the system performance.

Because of the significant computational effort required to generate the Gaussian processes for each scenario, only one scenario was modeled for each site. For both HVN and OKV, the selected scenario included all aggregated charging loads and conventional electric loads. As a result, the findings are most applicable when all loads and on-site generation assets at a site can be interconnected within a single microgrid. Nevertheless, the underlying principles regarding the influence of uncertainty variables and the implications for system resilience sizing remain broadly relevant and can serve as useful guidelines for evaluating performance.

The robustness analysis tool is inherently less exact than REopt because of interpolation error during the Gaussian process mapping. The results presented in this section may differ slightly from other results in this report. Results from this tool should be taken as indicative of trends surrounding market behaviors and system designs as opposed to the exactly optimal results produced by REopt.

OKV

Taguchi Analysis

Table 58 shows the results of the ANOVA analysis performed on OKV. Columns sum to 100%, with data points denoting how much an input parameter contributes to the variation between runs of the output parameter. The dominant factors influencing system outcomes were the demand charge in the electric tariff, the electricity cost escalation rate, the discount rate, and the capital cost of solar. Notably, the demand charge had a substantially greater impact on BESS sizing than solar CAPEX. Both system sizing and life cycle cost were highly sensitive to the discount rate and electricity cost escalation rate, indicating future economic conditions—rather than current equipment prices—play the most significant role in determining the optimal design.

This sensitivity underscores the considerable uncertainty associated with developing a system at OKV. Long-term market conditions are difficult to forecast with confidence, so on-site generation investment decisions at this site inherently carry greater risk and less predictable savings.

Table 58. Results of ANOVA Analysis at OKV

Parameter	PV Capacity	BESS Power Capacity	BESS Energy Capacity	Life Cycle Cost
BESS | Initial Power CAPEX	1.57	6.78	4.30	1.53
BESS | Initial Energy CAPEX	0.72	3.43	5.09	0.63
BESS | Replacement Power CAPEX	0.02	2.29	1.46	0.34
BESS | Replacement Energy CAPEX	0.09	0.80	0.88	0.15
BESS | Minimum SOC	0.79	0.10	0.13	0.13
BESS | ITC Incentive	0.01	2.36	1.82	0.66
Electric Tariff | Demand	1.31	9.58	9.75	2.02
Electric Tariff | Energy	3.23	0.42	0.04	3.63
Financial | Electricity Cost Escalation Rate	26.94	55.26	47.53	48.43
Financial | Discount Rate	12.83	17.22	19.92	39.04
Financial | O&M Escalation Rate	6.36	0.14	1.54	0.31
PV | Azimuth	2.91	0.89	0.59	0.37
PV | ITC Incentive	3.37	0.36	1.98	0.06
PV | Initial CAPEX	26.11	0.13	1.73	2.21
PV | O&M Annual Cost per kW	1.44	0.00	0.16	0.11

Parameter	PV Capacity	BESS Power Capacity	BESS Energy Capacity	Life Cycle Cost
PV | Tilt	12.17	0.19	3.08	0.35

* Parameters in yellow were considered the most influential and selected to be included in Gaussian process modeling.

Latin Hypercube Mapping

Following the Taguchi filtering step, the seven-dimensional parameter space was mapped using a Latin hypercube sampling approach to generate input sets for the REopt runs used as training data for the Gaussian process model.

Mapped parameter dimensions were as follows:

- Financial | Discount Rate
- Financial | Electricity Cost Escalation Rate
- PV | Initial CAPEX
- Electric Tariff | Demand Charge
- PV | Capacity
- BESS | Energy Capacity
- BESS | Power Capacity.

Gaussian Process Analysis

Three market conditions were selected first to examine breakeven scenarios, i.e., the subset of designs that have an NPV > 0 (Table 59):

- Scenario A: Base conditions. Best estimate of the real-world value of uncertainty variables. Assumptions are based on historical data. These values are the same as those used in the traditional REopt section of this report.
- Scenario B: Favorable for on-site energy resources. Current and future market conditions are well suited to on-site generation investment.
- Scenario C: Adverse for on-site generation. Current and future market conditions are poorly suited to on-site generation investment.

Table 59. Market Condition Scenarios: OKV

Parameter	A	B	C
Financial | Discount Rate*	4.5%	3.0%	6.0%
Financial | Electricity Cost Escalation Rate	1.5%	4.0%	0.5%
PV | Initial CAPEX	$2,547/kW	$1,500/kW	$3,500/kW
Electric Tariff | Demand Charge	100%	120%	80%

* A discount rate is the interest rate used to convert future money into its value today, reflecting the idea that money is worth more now than the same amount later. This is because of inflation, risk, and investment opportunities. A higher discount rate makes future cash worth less in today’s terms, whereas a lower rate makes it worth more.

Scenario A: Base Conditions

Under base assumptions, there is minimal financial benefit. PV systems are almost never viable. There is a small selection of battery sizes that achieve an NPV > 0 after 25 years, which are shown in Figure 55. The breakeven system centered around the origin can be considered noise because the origin point (i.e., building zero on-site generation) is, by definition, going to break even. The grouping of batteries clustered around the point of 580 kW/530 kWh denotes the viability of a small energy storage system.

Example breakeven-design-performing system sizing:

- PV capacity: 0 kW
- BESS capacity: 580 kW/530 kWh
- NPV: $18,319
- Maximum outage length for which the system achieves a 90% chance of survival: 1.9 hours.

Note: System sizes and NPV differ from optimal sizing produced by REopt. This is because of the difficulty in mapping multidimensional space and in interpolation error introduced when generating the Gaussian process. This error averages approximately 5% of the life cycle cost of the system.

Such a system would reduce demand charges. However, the total savings from these systems provide only a small amount of value across 25 years.

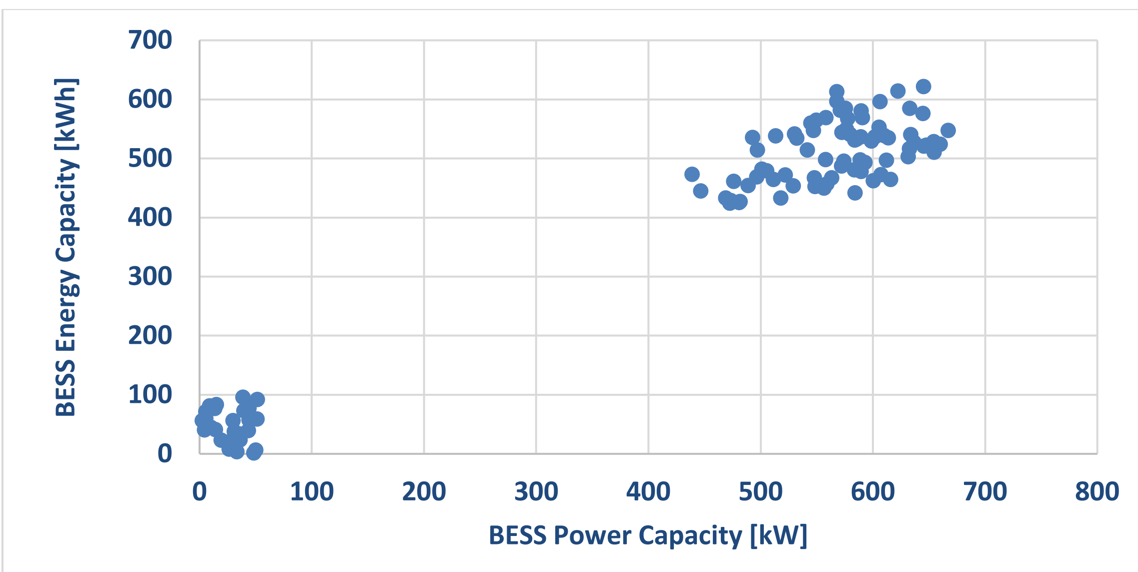

Figure 55. Scenario A: Breakeven battery sizes

Scenario B: Favorable for On-Site Generation

Essentially all DER systems become profitable within the tested range with NPVs up to $1.5 million. This situation is unlikely but demonstrates under favorable market conditions on-site generation have a positive NPV.

High-performing system sizing:

- PV capacity: 1,104 kW
- BESS capacity: 1,236 kW/1,126 kWh
- NPV: $1,463,871
- Maximum outage length for which the system achieves a 90% chance of survival: 10.5 hours.

Scenario C: Adverse for On-Site Generation

No breakeven systems. There is no financial benefit to on-site generation investment because systems will never pay back their initial cost.

Sensitivity Analysis

Scenario A and Scenario B provided two possible optimal design configurations for consideration at OKV. In Figure 56 and Figure 57, the uncertainty variables are fixed at base conditions (Scenario A) and varied one at a time across their ranges as presented in Table 60. This demonstrates the changes necessary to allow these systems to provide strong economic returns. Error margins are included to account for interpolation error in the Gaussian process. Uncertainty parameters have been normalized to compare the impact of their variation on a single graph.

Table 60. Market Condition Variable Ranges

Parameter	Fixed Point	Min	Max
Financial | Discount Rate	4.5%	3.0%	9.0%
Financial | Electricity Cost Escalation Rate	1.5%	0.0%	7.0%
PV | Initial CAPEX	$2,547/kW	$1,500/kW	$4,400/kW
Electric Tariff | Demand Charge	100%	80%	120%

The battery-only system (PV: 0 kW, BESS: 583 kW/531 kWh) from Scenario A and investigated in Figure 56 achieves a small NPV of $18,319 after 25 years. This value is well within error margins. The system demonstrated breakeven NPV under the following conditions:

- Electricity cost escalation rate > 1.8%. Escalation rates above these criteria show a high likelihood of a breakeven NPV.
- Discount rate < 4.2%. This parameter has a much weaker effect than electricity escalation rates on the system, and any positive NPV may not be guaranteed because it is less than interpolation error across the full range of tested discount rates.
- Initial CAPEX of PV has no effect because no PV is included. Any variation in the system can be considered noise.
- Electric tariff demand charges seem to have a slight effect on cost-effectiveness. However, the maximum tested demand rate (120% of the current demand rate structure) is insufficient to reliably make the system cost-effective.

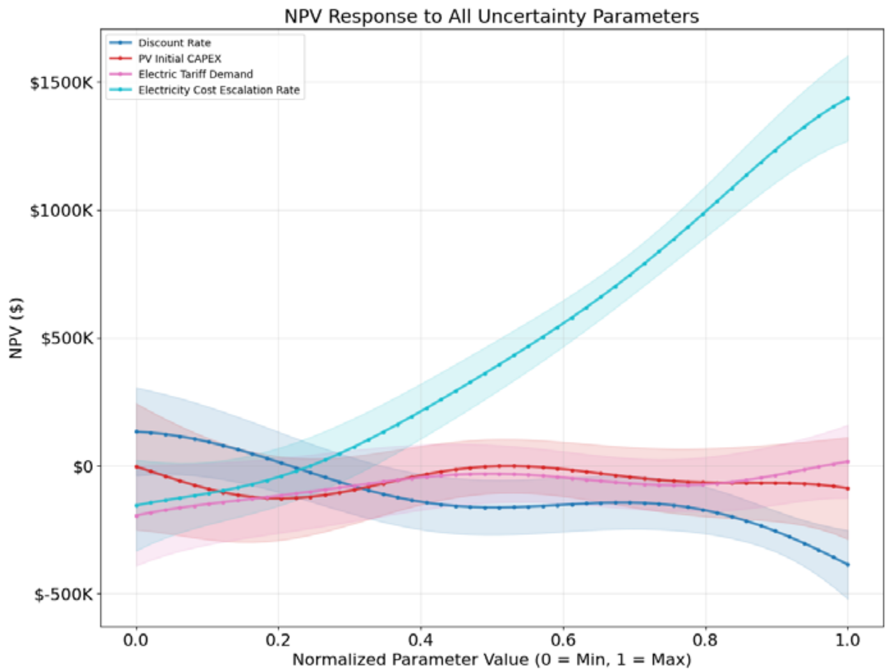

Figure 56. Sensitivity for fixed system size (PV: 0 kW, BESS: 583 kW/531 kWh)

Figure 57 demonstrates the performance of a larger PV and storage system (PV: 1,104 kW, BESS: 1,236 kW/1,126 kWh). This system is the optimal size under favorable conditions for on-site generation as described in Scenario B previously. However, under our base assumptions, this system will almost never achieve breakeven, except for an electricity cost escalation rate greater than 5.1%. Such a system requires the compounding effect of low PV CAPEX, high demand charges, low discount rates, and high electricity escalation rates to reliably break even. This is a very unlikely scenario.

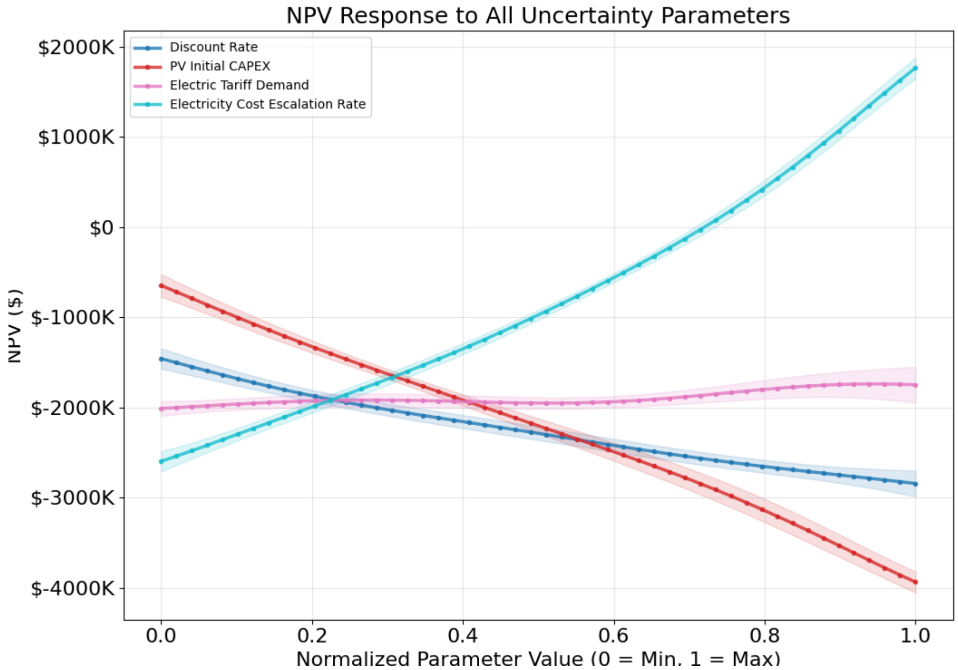

Figure 57. Sensitivity for fixed system size (PV: 1,104 kW, BESS: 1,236 kW/1,126 kWh)

Optimal Design Sensitivity

Traditional REopt was used to generate the sensitivity analyses shown in Figure 58. Each uncertainty was tested across its range whereas the rest of the uncertainties were fixed according to Table 60. The analysis shows how the optimal system changes in relation to uncertainties. REopt was used here to avoid the effects of interpolation error introduced by the Gaussian process. Optimal system sizes will differ slightly from REopt-Insight results because of interpolation error incurred during the Gaussian process generation. The following trends are evident:

- **BESS:** A small battery system (300–500 kW/200–350 kWh) may provide some nominal savings over 25 years under most conditions. A low discount rate or high electricity cost escalation rate may justify a larger battery.
- **PV:** Solar becomes cost-effective only for systems with extremely high electricity cost escalation rates (>5%) or extremely low initial PV cost (<$1,565/kW).

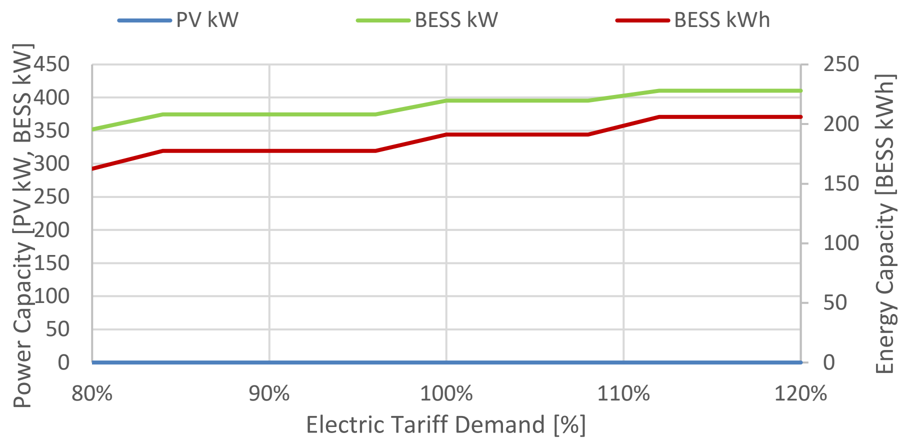
PV kW
BESS kW
BESS kWh
Power Capacity [PV kW, BESS kW]
Energy Capacity [BESS kWh]
0
50
100
150
200
250
300
350
400
450
0
50
100
150
200
250
80%
90%
100%
110%
120%
Electric Tariff Demand [%]

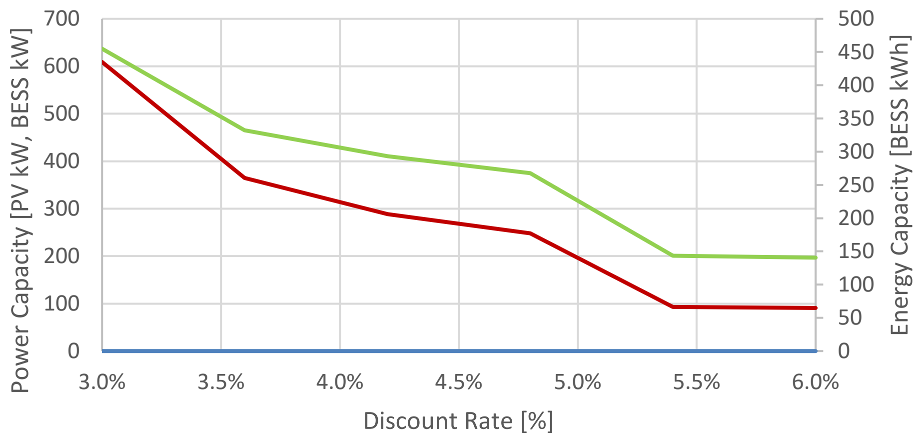
Power Capacity [PV kW, BESS kW]
Energy Capacity [BESS kWh]
0
100
200
300
400
500
600
700
0
50
100
150
200
250
300
350
400
450
500
3.0%
3.5%
4.0%
4.5%
5.0%
5.5%
6.0%
Discount Rate [%]

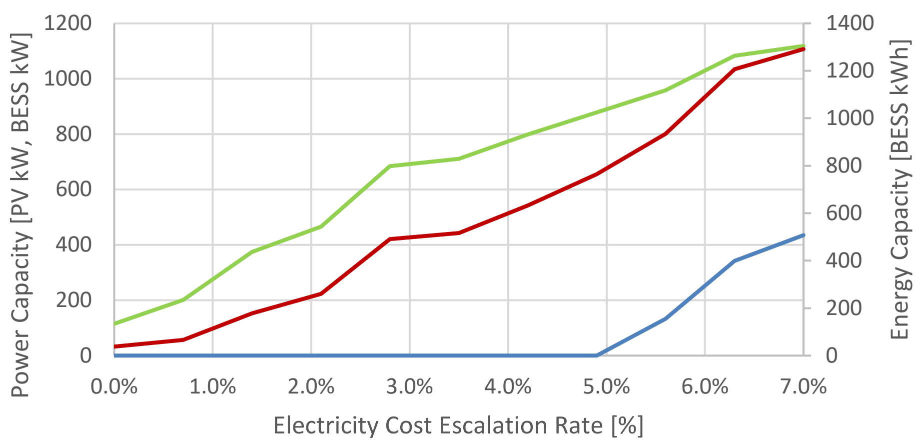
Power Capacity [PV kW, BESS kW]
Energy Capacity [BESS kWh]
0
200
400
600
800
1000
1200
0
200
400
600
800
1000
1200
1400
0.0%
1.0%
2.0%
3.0%
4.0%
5.0%
6.0%
7.0%
Electricity Cost Escalation Rate [%]

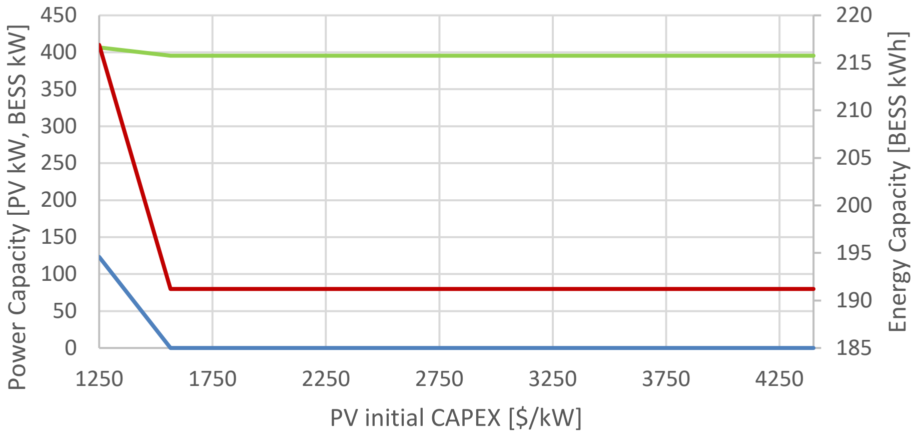

Figure 58. OKV: Optimal design sizes for varying uncertainty parameters

Pareto Front Analysis

Figure 59 demonstrates the Pareto front between the NPV and the resilience of the system. The resilience is quantified by survival resilience period—the maximum duration outage for which the system has a greater than 90% chance of survival. This accounts for hardware failure, weather patterns, and the variable load across the year. The Pareto front shows a quasi-linear relationship between cost and resilience with a drop in NPV of approximately $47,000 per hour of resilience (assuming base condition assumptions for uncertainty parameters used in Scenario A previously). Although the dollar value of this relationship may differ under various uncertainty inputs, the trends relating to optimal system sizes stayed consistent under most assumptions. Figure 60 and Figure 61 show the Pareto optimal system sizes.

Because of its poor financial performance, PV is not Pareto optimal up to 24 hours of resilience. A survival resilience period of less than 24 hours shows a linear increase in the energy capacity of the battery. At 24 hours, the requirements transition to a multiday outage. Here, PV becomes more beneficial because the PV can provide enough energy to recharge the battery. The optimal PV increases linearly across this range. The battery system's required power capacity is less consistent because of the highly variable, "peaky" behavior of electric vehicle supply equipment (EVSE) chargers and a limitation in our modeling approach. The outage-resilience model evaluates every possible outage scenario throughout the year and sizes the system to achieve a 90% probability of surviving an outage. Although peak loads can reach up to 2,500 MW, these events are extremely short-lived and infrequent. As a result, the model sizes the battery for the load level that occurs 90% of the time, which is significantly lower. In practice, however, sites should determine the BESS power capacity based on the number of chargers they intend to operate simultaneously during an outage. If they plan to run fewer than the total installed chargers, they can manage the load by adjusting charging schedules accordingly. The optimal investment strategy is provided in Table 61.

This Pareto analysis was conducted for Scenarios A–C as described previously. Only Scenario A is presented here. This is because although the NPV of the systems changed under various market conditions, the sizing of PV and BESS stayed largely consistent. The deviation from this was under favorable conditions for on-site generation (Option B). Here, PV was inherently cost-effective, which changed the calculus to include PV for shorter-duration outages. This scenario was considered highly unlikely and so should not drive the decision of system sizing.

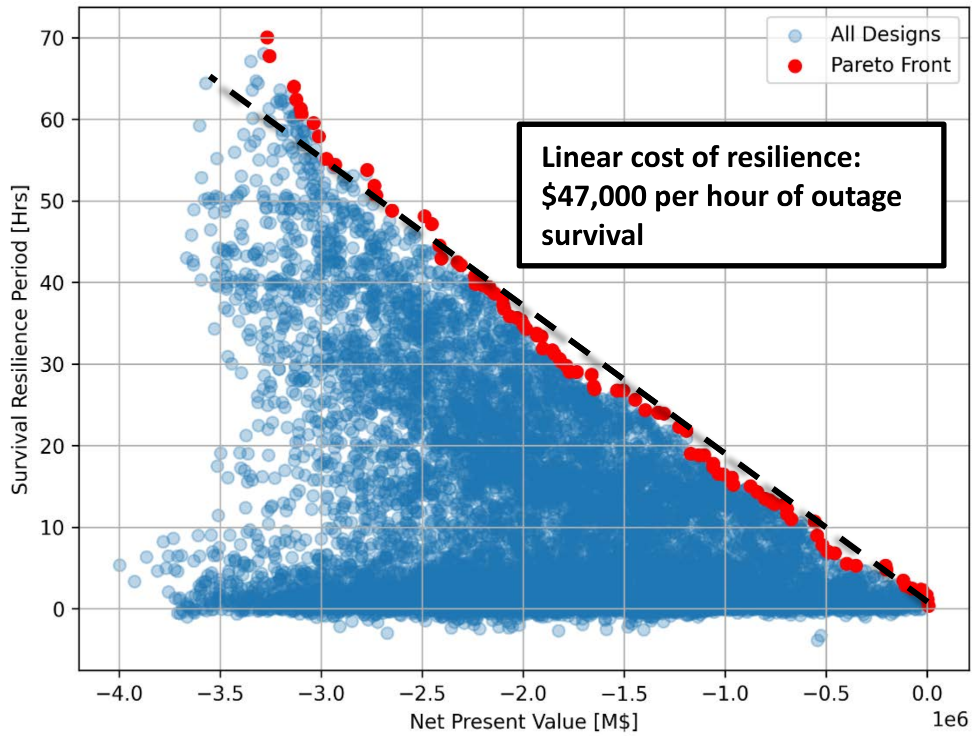

Figure 59. OKV Pareto optimal designs: Financial vs. resilience

Figure 60 and Figure 61 show the survival resilience period with respect to PV and BESS capacity, respectively.

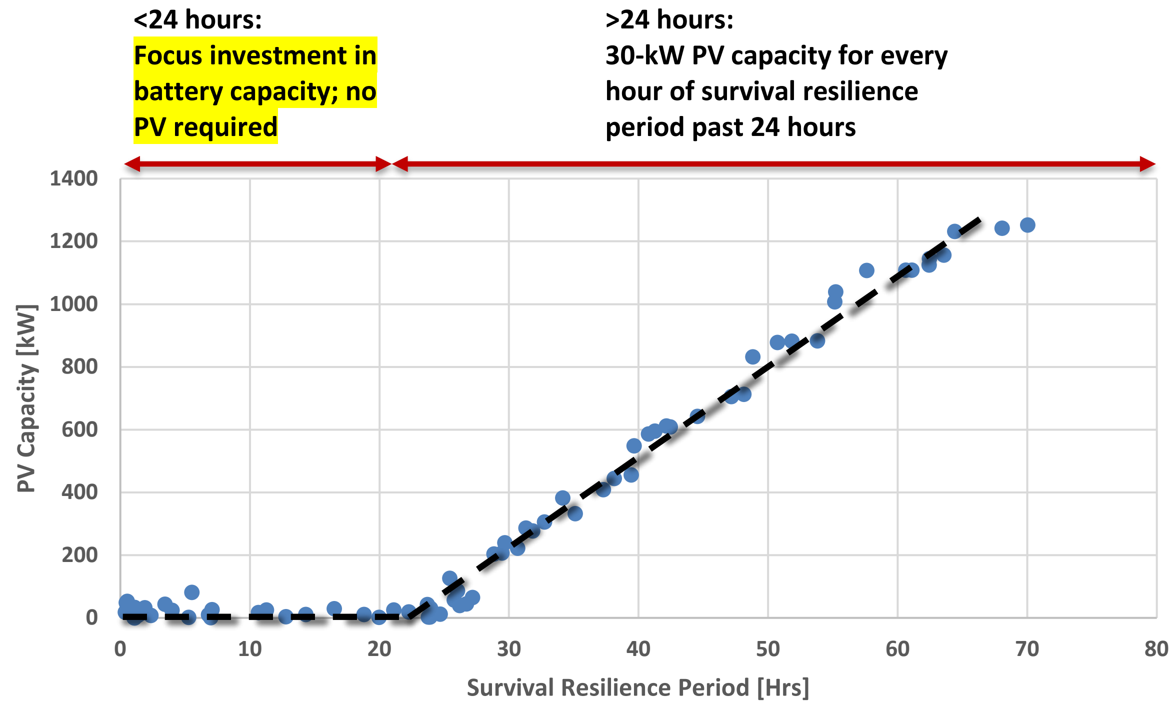

Figure 60. OKV pareto optimal designs: PV system sizes

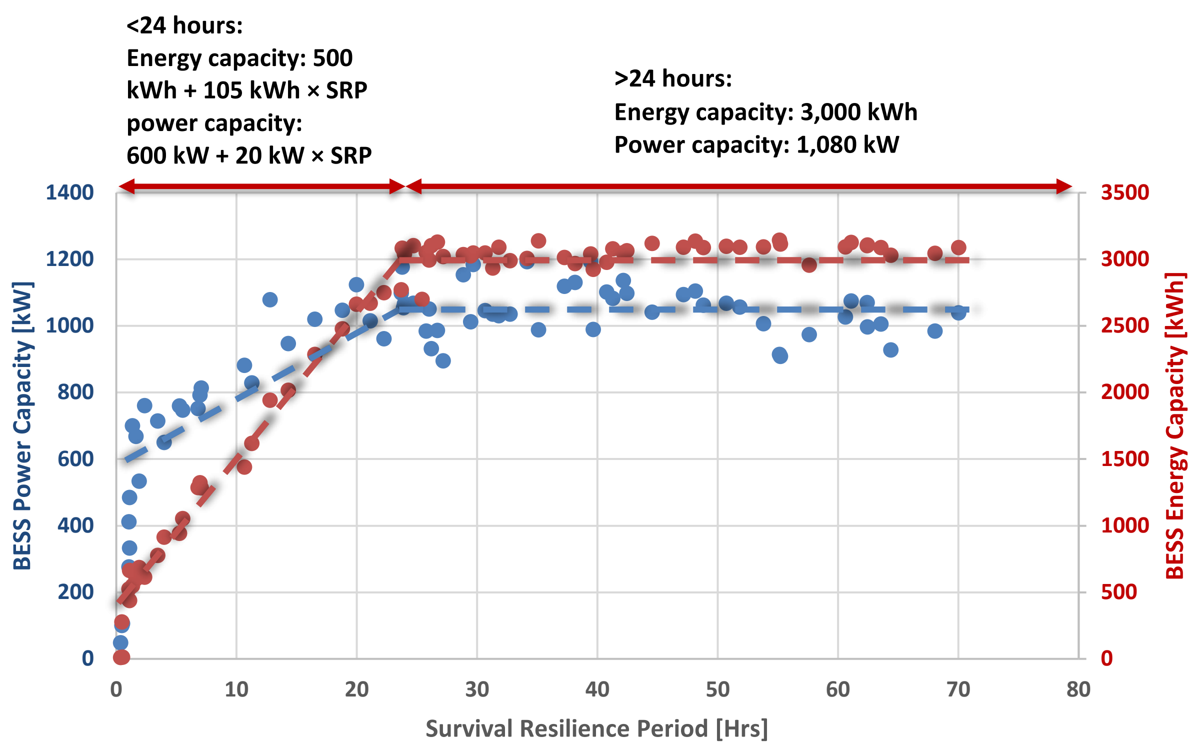

Figure 61. OKV pareto optimal design: BESS system sizes

SRP = survival resilience period

Table 61. Optimal Investment Strategies for Resilient Infrastructure at OKV

Parameter	Up to 24 Hours	Beyond 24 hours
PV Capacity (kW)	No PV is needed	30 kW × (SRP – 24 hr)
BESS Energy Capacity (kWh)	500 kWh + 105 kWh × survival resilience period (SRP)	3,000 kWh
BESS Power Capacity (kW)	600 kW + 20 kW × SRP	1,080 kW

HVN

Table 62 shows the results of the ANOVA analysis performed on HVN. Columns sum to 100%, with data points denoting how much a parameter contributes to the variation between runs of the output parameter. The dominant factors influencing system outcomes were the demand charge in the electric tariff, the electricity cost escalation rate, the discount rate, the capital cost of solar, and the capital cost for battery energy capacity. Like OKV, electricity cost escalation rate and discount rate dominate the life cycle costs. However, the other uncertainty parameters have a large effect on system sizing.

Table 62. Results of ANOVA Analysis at HVN

Parameter	PV Capacity	BESS Power Capacity	BESS Energy Capacity	Life Cycle Cost
BESS | Initial Power CAPEX	0.09	1.43	0.77	0.93
BESS | Initial Energy CAPEX	0.48	10.10	13.44	1.61
BESS | Replacement Power CAPEX	0.40	0.74	0.59	0.25
BESS | Replacement Energy CAPEX	0.71	1.54	2.50	0.22
BESS | Minimum SOC	0.02	0.25	1.04	0.23
BESS | ITC Incentive	0.14	1.69	1.14	0.69
Electric Tariff | Demand	1.02	9.49	8.06	0.07
Electric Tariff | Energy	6.90	1.67	1.86	4.57
Financial | Electricity Cost Escalation Rate	35.31	54.07	51.15	33.88
Financial | Discount Rate	13.59	14.45	14.70	34.88
Financial | O&M Escalation Rate	0.09	1.42	0.90	0.86
PV | Azimuth	0.23	0.55	0.46	2.08
PV | ITC Incentive	2.30	0.41	0.08	0.23

Parameter	PV Capacity	BESS Power Capacity	BESS Energy Capacity	Life Cycle Cost
PV | Initial CAPEX	38.06	1.45	2.95	18.89
PV | O&M Annual Cost per kW	0.54	0.28	0.12	0.22
PV | Tilt	0.07	0.47	0.23	0.21

* Parameters in yellow were considered the most influential and selected to be included in Gaussian process modeling.

Latin Hypercube Mapping

Following the Taguchi filtering step, the eight-dimensional parameter space was mapped using a Latin hypercube sampling approach to generate input sets for 10,000 REopt runs. The results of these runs were then used as training data for the Gaussian process model.

Mapped parameter dimensions were as follows:

- Financial | Discount Rate
- Financial | Electricity Cost Escalation Rate
- PV | Initial CAPEX
- Electric Tariff | Demand Charge
- BESS | Initial Energy CAPEX
- PV | Capacity
- BESS | Energy Capacity
- BESS | Power Capacity.

Gaussian Process Analysis

On-site generation assets are significantly more cost-effective at HVN than at OKV. Figure 62 shows the impact of the uncertainty parameters on a fixed design configuration. This design was selected because it performs well under the same uncertainty conditions used throughout the basic REopt analyses. Each uncertainty parameter is varied across its tested range whereas the other values are fixed as shown in Table 63. The design always produced a positive return on investment. These relationships show a close to linear relationship with the following slopes:

- **Discount rate:** NPV decreases by approximately $830,000 per percentage point increase in discount rate.
- **Electricity cost escalation rate:** NPV increases by approximately $1.83M per percentage point increase in electricity escalation rate.
- **PV initial CAPEX:** NPV decreases by approximately $158,000 per $100/kW increase in PV cost.
- **BESS initial energy CAPEX:** NPV decreases approximately $210,000 per 100/kWh for BESS energy cost.
- **Electric tariff demand charge:** NPV increases by approximately $55,000 per percentage point increase in demand charges.

Table 63. Tested Parameter Ranges and Fixed Points

Parameter	Fixed Point	Min	Max
Financial | Discount Rate	4.5%	3.0%	9.0%
Financial | Electricity Cost Escalation Rate	1.5%	0.0%	7.0%
PV | Initial CAPEX	$2,547/kW	$1,500/kW	$4,400/kW
Electric Tariff | Demand Charge	100%	80%	120%
BESS | Initial Energy CAPEX	$455/kWh	$289/kWh	$686/kWh

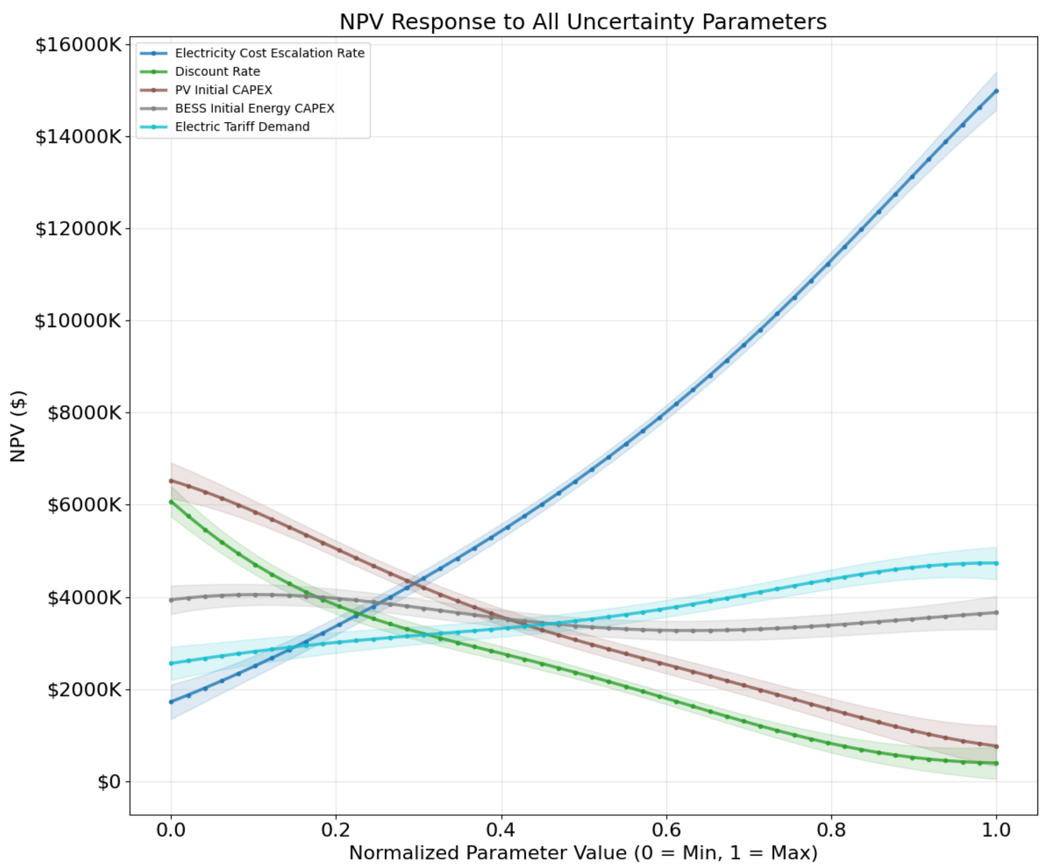

Figure 62. Sensitivity for fixed system size (PV: 1,572 kW, BESS: 1,291 kW/2,146 kWh)

Optimal Design Sensitivity

Figure 54 portrays the optimal design sizes that should be built under variation of the uncertainty parameters. One data point for each curve was varied whereas the four remaining points were fixed according to Table 63. Although Figure 63 demonstrates how a system will be affected by an uncertainty parameter, Figure 64 shows how HVN could consider changing its on-site energy investments depending on how uncertainty parameters change. The following trends can be ascertained:

- **PV:** PV capacity of 1,500–2,500 kilowatts (kW) will be close to cost-optimal in most scenarios with some rare exceptions. If the electricity cost escalation rate is especially high (>4%) or PV can be purchased extremely cheaply (<$2,000/kW), the site should consider purchasing up to 3,500 kW of PV. If the initial PV CAPEX is extremely high (>$4,000/kW), PV may not be cost-effective and the site might consider not purchasing any solar capacity.
- **BESS power capacity:** The optimal amount of electrical storage power capacity stays consistent in almost all scenarios at 1,000–1,400 kW. Any system within this range is likely to be close to cost-optimal.
- **BESS energy capacity:** The optimal amount of electrical storage energy capacity is highly dependent on market conditions and may vary between 500 kWh and 7,000 kWh. A minimum of 1,000 kWh will be cost-effective in most scenarios. Beyond that, the optimal configuration is difficult to predict. As we will see in the next section, BESS energy capacity sizing is central to the resilience of the system. Given the variability of the cost-optimal sizing, resilience criteria may be a more appropriate tool for selecting energy capacity.

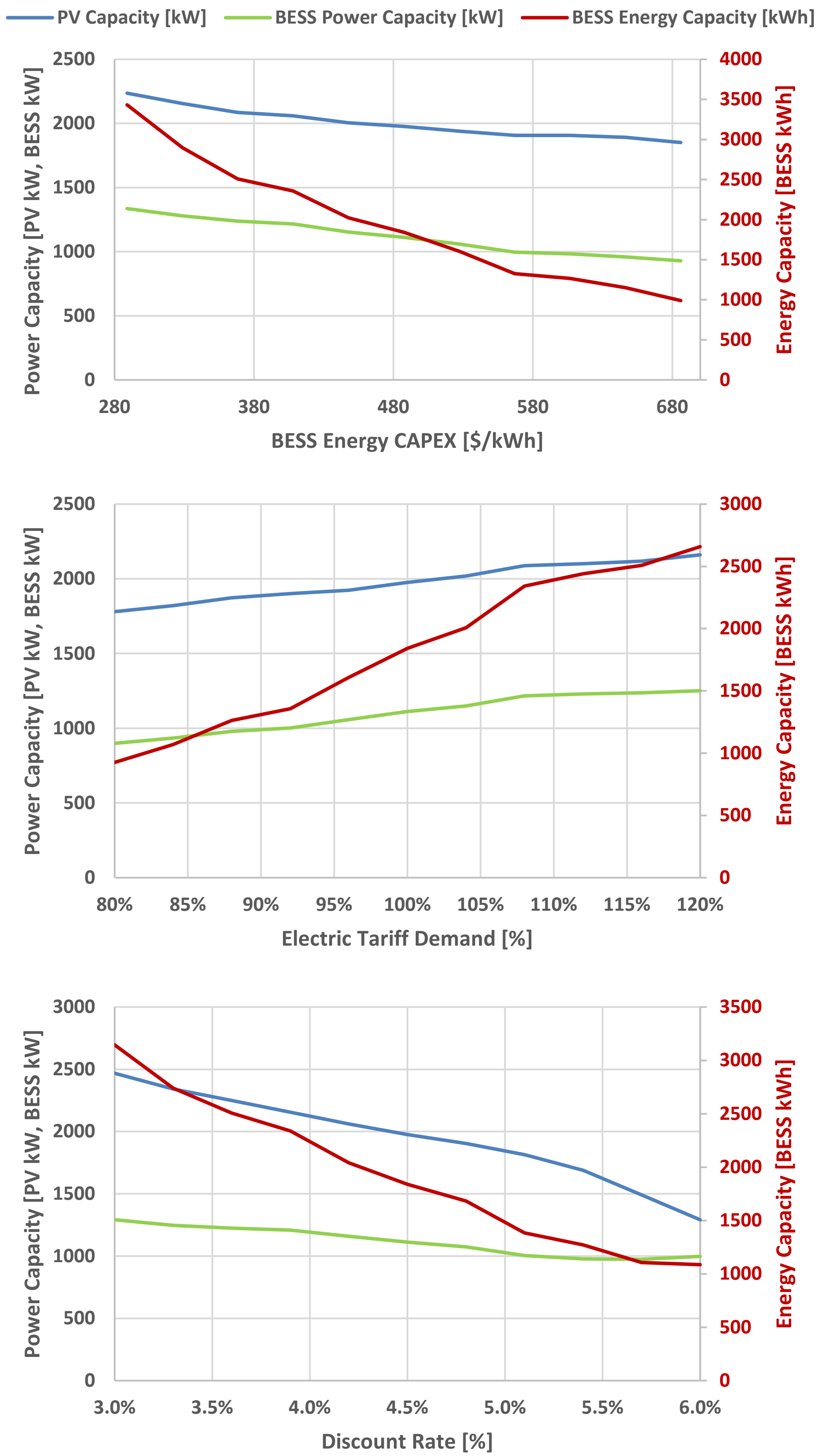

PV Capacity [kW]
BESS Power Capacity [kW]
BESS Energy Capacity [kWh]
Power Capacity [PV kW, BESS kW]
Energy Capacity [BESS kWh]
2500
2000
1500
1000
500
0
4000
3500
3000
2500
2000
1500
1000
500
0
280
380
480
580
680
BESS Energy CAPEX [$/kWh]
Power Capacity [PV kW, BESS kW]
Energy Capacity [BESS kWh]
2500
2000
1500
1000
500
0
3000
2500
2000
1500
1000
500
0
80%
85%
90%
95%
100%
105%
110%
115%
120%
Electric Tariff Demand [%]
Power Capacity [PV kW, BESS kW]
Energy Capacity [BESS kWh]
3000
2500
2000
1500
1000
500
0
3500
3000
2500
2000
1500
1000
500
0
3.0%
3.5%
4.0%
4.5%
5.0%
5.5%
6.0%
Discount Rate [%]

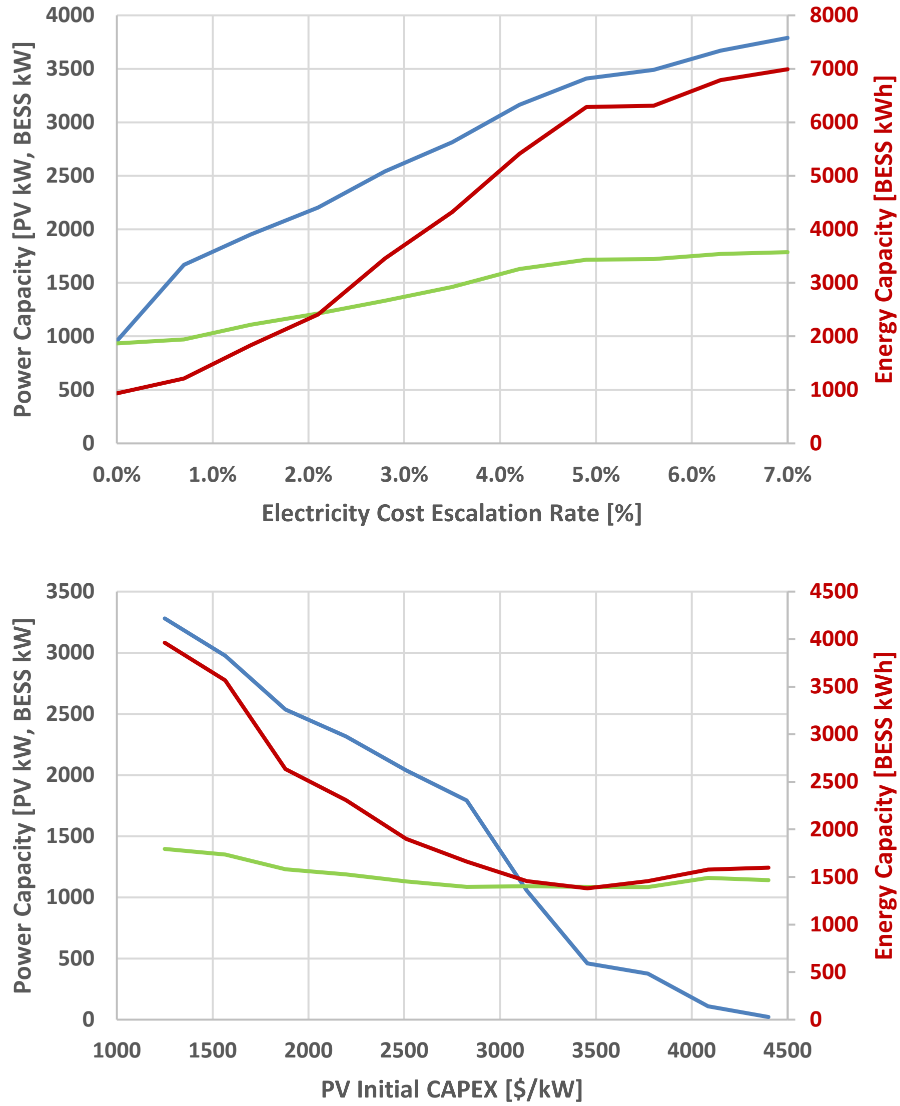

Figure 63. HVN optimal design sizes for varying uncertainty parameters

Pareto Front Analysis

A Pareto front analysis was conducted for using the HVN Gaussian process. The details of this process are the same as for OKV and are explained previously. Again, there is a quasi-linear relationship between resilience and NPV for an optimized system. If systems are sized appropriately, HVN can extend the length of outage that can be survived with a reduction to the NPV of $110,800/hour (assuming the base condition assumptions denoted by the fixed-point uncertainty inputs in Table 63).

Figure 65 and Figure 66 show the optimal investment strategy HVN could use to build out its on-site energy assets to extend outage survival time. Optimal PV sizing has a quasi-linear relationship with survival resilience period. Approximately 3,000 kW of solar is needed to survive a 10-hour outage, and 50 kW should be added for every extra hour. BESS capacity is slightly less straightforward. In almost all cases, the battery should be rated to 1,500–2,000 kW.

It requires at least this much power capacity to power most loads on-site. The energy capacity linearly increases up to approximately 10,000 kWh to supply for a 24-hour outage. After that point, it is more economical to invest in a solar system that can refill the battery daily. These trends are shown in Table 64.

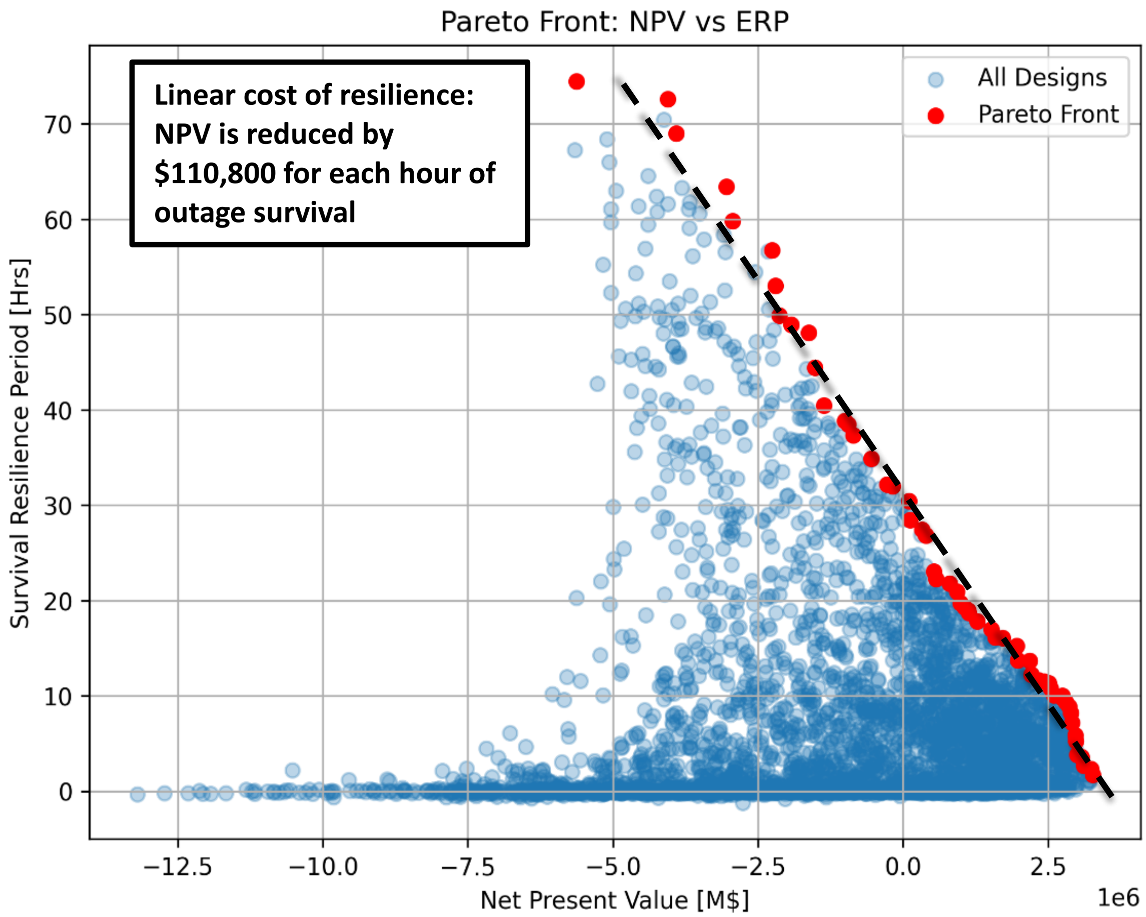

Figure 64. HVN Pareto optimal designs: Financial vs. resilience

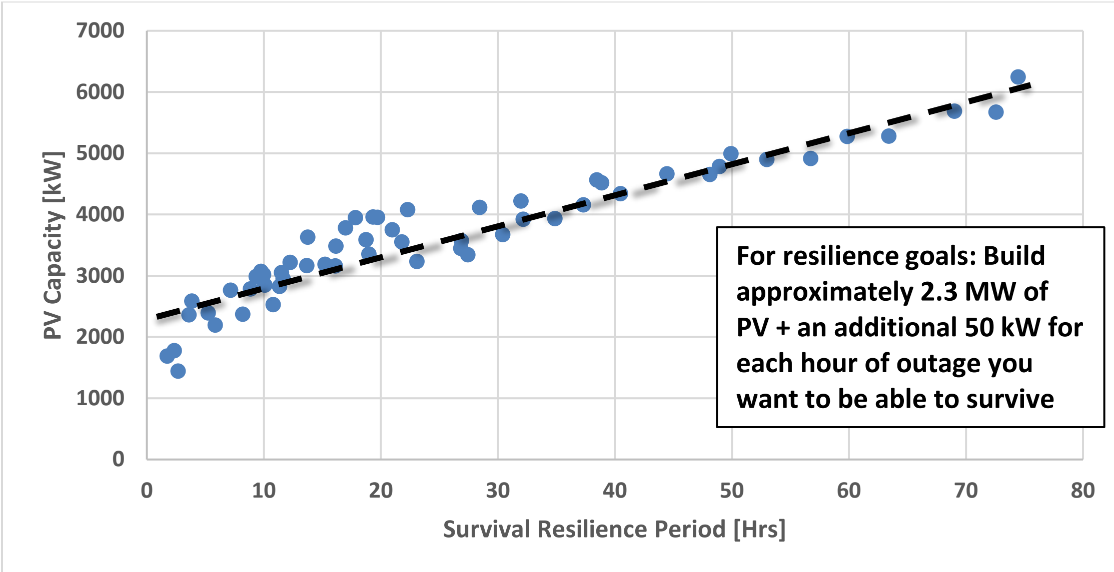

Figure 65. HVN Pareto optimal designs: PV system sizes

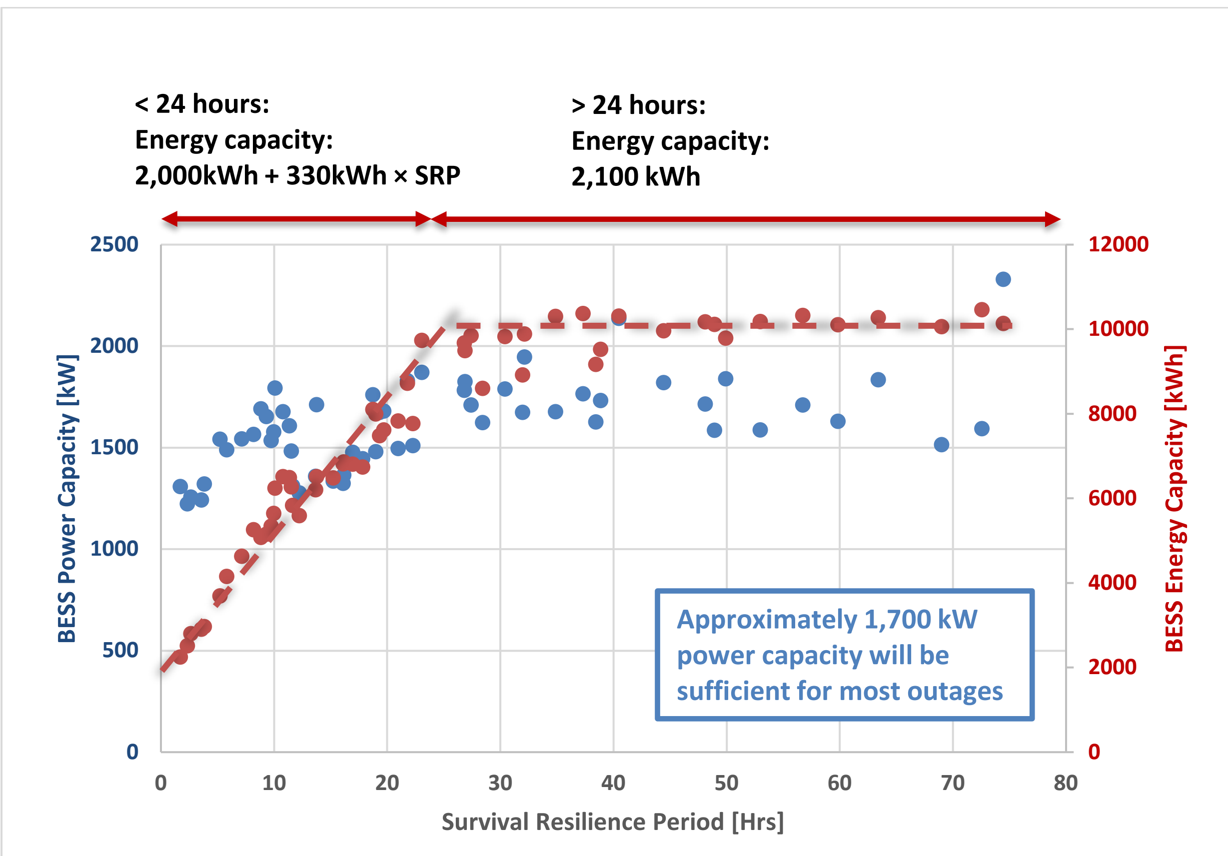

Figure 66. OKV Pareto optimal designs: BESS system sizes

Table 64. HVN Energy Resilience Trends

Parameter	Up to 24 Hours	Beyond 24 hours
PV Capacity (kW)	2,300 kW + 50 kW × SRP	2,300 kW + 50 kW × SRP
BESS Energy Capacity (kWh)	2,000 kWh + 330 kWh × SRP	10,000 kWh
BESS Power Capacity (kW)	>1,700 kW	>1,700 kW

Appendix B. Baseline and ET2 REopt Results

REopt Input Details and ET2 Results

Table 65 provides a breakdown of United Illuminating's (UI's) electricity tariffs used in the analysis.

Table 65. UI's Electricity Tariffs Used in the Analysis

	General Service (GS)	General Service Demand (GSD)	General Service Time of Use (GST)	General Service Time-of-Use Demand (GSTD)	General Service Time-of-Use-Electric Vehicle (GST-EV)
Electricity Delivery Charges					
Energy assistance costs	\$0.032/kWh	\$0.032/kWh	\$0.032/kWh	\$0.032/kWh	\$0.032/kWh
Energy efficiency programs	\$0.006/kWh	\$0.006/kWh	\$0.006/kWh	\$0.006/kWh	\$0.006/kWh
Renewable energy investment	\$0.001/kWh	\$0/kWh	\$0.001/kWh	\$0.001/kWh	\$0.001/kWh
New England grid operator costs	\$0.002/kWh	\$0.44/kW	\$0.001/kWh	\$0.45/kW	\$0.06/kW
State-mandated energy purchases	\$0.012/kWh	\$2.03/kW	\$0.028/kWh	\$2.07/kW	\$0.30/kW
Customer-produced energy	\$0.009/kWh	\$1.57/kW	\$0.022/kWh	\$1.6/kW	\$0.23/kW
Miscellaneous and other mandates	\$0.009/kWh	\$1.67/kW	\$0.023/kWh	\$1.7/kW	\$0.24/kW
Transmission	\$0.058/kWh	\$9.76/kW	\$0.198/kWh	\$11.6/kW	\$1.66/kW
Distribution charge	\$0.082/kWh	\$0.014/kWh	\$0.035/kWh	\$0.026/kWh	\$0
Distribution demand	\$0/kW	\$11.78/kW	\$0/kW	\$4.77/kW	\$0.68/kW
Fixed charges (\$/month)	\$16.98	\$53.2	\$30.95	\$85.35	\$85.35
Electricity Supply Charges: *These charges are in addition to UI's charges and are provided in the main report.*					

OKV ET2 On-Site Generation Results

Considering Existing OKV Buildings

The baseline results for the 10 existing meters were similar (within 2.5%) to the billed cost of electricity, indicating the REopt model has been calibrated to OKV airport and key site data have been accounted for. Complete data were received only for these 10 existing meters. The existing terminal building was excluded from baseline results because it was decommissioned and rebuilt during this analysis. Comparison between billed and modeled costs and electricity consumption across the existing buildings is provided in Table 66. Based on preliminary data received from Rappahannock Electric Cooperative, the new OKV terminal building is being served under Rappahannock Electric Cooperative's B33 rate tariff. Electric consumption data for this building were received from January to June 2025 and were mirrored to create a representative year-long load profile. Based on these inputs, the new terminal is expected to have a peak demand of 47 kW. If all OKV buildings were metered together, they would have a peak demand of 74 kW.

Table 65. Comparing Billed and Modeled Costs at OKV

Data Point	Billed	Modeled
Existing 10 OKV Buildings		
Annual electricity consumption	127 MWh	121 MWh
Electric tariffs	Renewable energy credits (RECs) B1, B33, B31	RECs B1, B33, B31
Billed cost of electricity	$22.4k	$20.8k
Blended rate of electricity	$0.1764/kWh	$0.1719/kWh
Difference in billed cost of electricity		-2.55%
New Terminal Building		
Annual electricity consumption	N/A	132 MWh
Electric tariffs	N/A	B33
Billed cost of electricity	N/A	$14.2k
Blended rate of electricity	N/A	$0.1076/kWh
All OKV Buildings		
Annual electricity consumption	N/A	252 MWh
Electric tariffs	N/A	B33
Billed cost of electricity	N/A	$26.1k
Blended rate of electricity	N/A	$0.1036/kWh

Considering Existing OKV Buildings and ET2 Loads

Information presented in this subsection (Table 67 through Table 75) details the results for ET2 forecasted loads. These results follow the same format and similar takeaways as the ET2+ results presented in the OKV Results section of this report. Please refer to this section for a detailed explanation and discussions from these results.

Table 66. REopt Identified Cost-Optimal Results for OKV (ET2)

Load Type	New System Sizes	NPV of Cost Savings	Internal Rate of Return	Simple Payback (years)	Installed Costs	Annual Grid Energy Reduction	Annual Peak Demand Reduction
Existing OKV buildings	None identified	N/A	N/A	N/A	N/A	N/A	N/A
New Terminal	None identified	N/A	N/A	N/A	N/A	N/A	N/A
Urban air mobility (UAM) only	24 kW/ 8 kWh	$8.3k	7.0%	15 yrs	$27k	-0.03%	3.39%
Regional air mobility (RAM) only	190 kW/ 63 kWh	$63k	6.9%	15 yrs	$216k	-0.90%	23.87%
Trainer only	11 kW/ 3.5 kWh	$3.6k	7.0%	15 yrs	$12k	-0.04%	3.45%
All EVSE	766 kW/ 455 kWh	$103k	5.4%	17 yrs	$968k	-0.43%	43.33%
All OKV buildings	None identified	N/A	N/A	N/A	N/A	N/A	N/A
All EVSE + all buildings	743 kW/ 439 kWh	$98k	5.4%	17 yrs	$937k	-0.31%	41.28%

Table 67. Electric Utility Bill Savings From Cost-Optimal On-Site Generation (ET2)

Scenario	Business-as-Usual (BAU) Energy Charges	BAU Demand Charges	OPT Energy Charge (% reduction)	OPT Demand Charges (% reduction)	Utility Bill Savings
All existing OKV buildings	$11.0k	$3.5k	$11.0k (0%)	$3.5k (0%)	0.00%
New terminal	$12.2k	$1.2k	$12.2k (0%)	$1.2k (0%)	0.00%
All OKV buildings	$23.3k	$2.0k	$23.3k (0%)	$2.0k (0%)	0.00%
UAM only	$21.5k	$40.9k	$21.5k (0%)	$39.1k (4%)	2.88%
RAM only	$17.2k	$58.6k	$17.5k (-2%)	$33.9k (42%)	32.19%
Trainer only	$6.5k	$33.3k	$6.5k (0%)	$30.7k (8%)	6.53%
All EVSE loads	$45.2k	$107.6k	$45.2k (0%)	$80.9k (25%)	17.47%

Scenario	Business-as-Usual (BAU) Energy Charges	BAU Demand Charges	OPT Energy Charge (% reduction)	OPT Demand Charges (% reduction)	Utility Bill Savings
All EVSE + all building loads	$62.2k	$111.0k	$62.2k (0%)	$84.5k (24%)	15.30%

Table 69. REopt Identified Cost-Optimal Results With Prime Generator, for OKV (ET2)

Load Type	New DER System Sizes	NPV of Cost Savings	Internal Rate of Return	Simple Payback (years)	Installed Costs
New terminal	Prime generator: 17.5 kW	$37k	10%	8.93	$55.8k
All EVSE	Battery: 266 kW/ 104 kWh Prime generator: 100 kW	$11k	4.4%	16.7	$587k
All OKV buildings	Prime generator: 30 kW	$76k	11%	8.27	$96.5k
All EVSE + all buildings	Battery: 325 kW/ 163 kWh Prime generator: 100 kW	$116k	5.7%	15.1	$673k

Note: Only load types where the prime generator was cost-effective are presented.

Table 70. Savings After Line Costs From On-Site Generation at OKV (ET2)

Load Type	EVSE Line Upgrades (sunk cost)	BESS Line Cost	NPV From BESS Before Considering Line Costs	NPV From BESS Before Considering Line Costs	NPV With All Line Upgrades Minus Sunk Costs
UAM only	$90k	$90k	$8.3k	-$172k	-$82k
RAM only	$90k	$90k	$63k	-$117k	-$27k
Trainer only	$90k	$90k	$3.6k	-$176k	-$86k
All EVSE	$91.5k	$90k	$103k	-$77k	***$14k***
All EVSE + all buildings	$91.5k	$90k	$98k	-$83k	***$8k***

Note: Italicized net savings values refer to load types where on-site generation could provide enough cost savings to pay for underground lines to connect battery storage (assuming new EVSE line cost is a sunk cost).

Table 68. OKV System Sizes for Resilience Assessments

Load Type	Battery (ET2)	Backup Generator (same for ET2/ET2+)
Existing OKV buildings	0	250 kW (1)
New terminal	0	250 kW (1)
UAM only	24 kW/8 kWh	250 kW (1)
RAM only	190 kW/63 kWh	250 kW (1)
Trainer only	11 kW/4 kWh	250 kW (1)
All EVSE	766 kW/455 kWh	250 kW (1)
All OKV buildings	0	250 kW (1)
All EVSE + all buildings	742 kW/438 kWh	250 kW (1)

Table 69. Probability of Surviving Outages Serving 25% OKV Building Loads

Load Type	8 Hours	12 Hours	24 Hours	72 Hours
Existing OKV buildings	97.8%	97.5%	96.4%	92.3%
New terminal	97.9%	97.5%	96.4%	92.3%
OKV buildings + new terminal	97.7%	97.5%	96.4%	92.3%

Table 70. Probability of Surviving Outages Serving 100% OKV Loads

Load Type	8 Hours	12 Hours	24 Hours	72 Hours
Existing OKV buildings	97.9%	97.5%	96.4%	92.3%
New terminal	97.9%	97.5%	96.4%	92.3%
UAM only (ET2)	64.5%	52.7%	32.0%	8.4%
RAM only (ET2)	47.0%	32.7%	10.6%	0%
Trainer only (ET2)	97.7%	96.8%	94.3%	86.2%
All EVSE (ET2)	60.5%	42.7%	16.8%	0.3%
All EVSE (ET2) + all buildings	52.1%	32.7%	9.8%	0.2%

Table 71. ÆNode Results for OKV

Output	ET2 Allowed PV	ET2 Maximum PV
New solar PV	618 kW	8,300 kW
Battery kW/kWh	646 kW/375 kWh	646 kW/375 kWh
BAU life cycle cost (LCC)	$5.09M	$5.09M
LCC with On-Site Generation	$5.73M	$26.9M
NPV	-$0.645M	-$21.8M

Output	ET2 Allowed PV	ET2 Maximum PV
Initial capital costs	$2.39M	$21.9M
Initial capital costs after incentives	$2.39M	$21.9M
Grid to load MWh	1,062 MWh	516 MWh
Grid to battery MWh	14.8 MWh	14 MWh
Total grid consumption	1,076 MWh	530 MWh
Peak demand BAU	1,800 kW	1,800 kW
Peak demand with On-Site Generation	1,143 kW	1,042 kW
Year 1 energy cost BAU	$94.4k	$94.4k
Year 1 energy cost	$72.6k	$35.7k
Year 1 demand cost BAU	$195k	$195k
Year 1 demand cost	$113k	$108k
Annual PV energy produced	762 MWh	10,232 MWh
PV levelized cost of energy (LCOE)	$0.156/kWh	$0.156/kWh
PV to load kWh	314 MWh	749 MWh
PV to battery kWh	12.4 MWh	136 MWh
PV to export kWh	436 MWh	530 MWh
Year 1 export benefit	$29.4k	$35.7k
PV curtailed MWh	0	8,817 MWh
Battery to load MWh	24.5 MWh	135 MWh
Calculated battery efficiency	90.1%	90.0%
Average battery SOC	96.6%	89.6%
Breakeven compensation	$0.06/kWh	$0.09/kWh

Table 72. ET2 Probability of Surviving Outages With All OKV Buildings and EVSE Loads

	Battery	Backup Generator	8 Hours	12 Hours	24 Hours	72 Hours
Buildings + EVSE (PV = 0 kW)	0 kW/0 kWh	250 kW (1)	18.2%	6.1%	2.0%	0%
Buildings + EVSE (PV = 0 kW)	0 kW/0 kWh	250 kW (2)	65.1%	53.0%	33.9%	8.85%
Buildings + EVSE (PV = 618 kW)	646 kW/375 kWh	250 kW (1)	65.1%	50.3%	26.3%	5.15%
Buildings + EVSE (PV = 618 kW)	646 kW/375 kWh	250 kW (2)	94.3%	91.8%	84.9%	65.5%
Buildings + EVSE	646 kW/375 kWh	250 kW (1)	78.6%	69.2%	46.2%	17.1%

	Battery	Backup Generator	8 Hours	12 Hours	24 Hours	72 Hours
(PV = 8,300 kW)						
Buildings + EVSE (PV = 8,300 kW)	646 kW/375 kWh	250 kW (2)	97.1%	95.8%	92.2%	80.3%

HVN ET2 On-Site Generation Results

Considering Existing HVN Buildings

Required data were received for 12 of HVN's existing buildings for inclusion as building loads in the analysis. Meter-specific rate tariffs were used for comparison against billing data to calibrate REopt with HVN. However, for simplification, all existing buildings were modeled using Direct Energy's day-ahead energy supply rate in downstream analysis. Like OKV, HVN is also an evolving airport. The airport is constructing a new terminal building for which limited information was shared with the research team. The new terminal is expected to consume 3,200 MWh of electricity annually, and its simulated load profile was provided by the airport. The analysis assumes the new terminal building will be billed according to the utility's general service time-of-use demand (GSTD) rate with Direct Energy's day-ahead market rate. Going forward, buildings-related results for HVN include all existing buildings and the new terminal building. To take a more conservative approach, the analysis included the new terminal only as a load and did not include any backup generators or on-site generation that may be built along with the new terminal building. Table 76 shows a comparison of billed and modeled electricity consumption and costs across 12 existing HVN meters. Data reveal the modeled costs to be 2.9% higher than the billed costs, which is an acceptable difference. The observed difference can be attributed to electric tariff changes over time. The modeled results use the latest tariff information; frequent changes could widen the gap between modeled and billed costs.

Table 73. Comparing Billed and Modeled Costs at HVN

Data Point	Billed	Modeled
Existing 12 HVN Buildings		
Annual electricity consumption	844 MWh	847 MWh
Electric tariffs	UI's GS, GSD, GST, GSTD rates with Direct Energy's day-ahead market rate tariff.	UI's GS, GSD, GST, GSTD rates with Direct Energy's day-ahead market rate tariff
Billed cost of electricity	$139k	$143k
Blended rate of electricity	$0.165/kWh	$0.169/kWh
Difference in billed cost of electricity		-2.9%
New Terminal Building		
Annual electricity consumption	N/A	3214 MWh
Electric tariffs	N/A	UI's GSTD for transmission and distribution, Direct Energy day-ahead market rates for energy supply

Data Point	Billed	Modeled
Billed cost of electricity	N/A	$734k
Blended rate of electricity	N/A	$0.228/kWh
All HVN Buildings		
Annual electricity consumption	N/A	4062 MWh
Electric tariffs	N/A	UI's GSTD for transmission and distribution, Direct Energy day-ahead market rates for energy supply
Billed cost of electricity	N/A	$886k
Blended rate of electricity	N/A	$0.218/kWh

Considering Existing HVN Buildings and ET2 Loads

Information presented in this subsection (Table 77 through Table 83) details the results for ET2 forecasted loads. These results follow the same format and similar takeaways as the ET2+ results presented in the HVN Results section of this report. Please refer to this section for a detailed explanation and discussions from these results.

Table 74. REopt Identified Cost-Optimal Results for HVN (ET2)

Load Type	New System Sizes	NPV of Cost Savings	Internal Rate of Return	Simple Payback (years)	Installed Costs	Annual Grid Energy Reduction	Annual Peak Demand Reduction
Existing HVN buildings	None identified	N/A	N/A	N/A	N/A	N/A	N/A
New Terminal	PV: 273 kW Battery: 47 kW/116 kWh	$105k	5.7%	13.6	$810k	11%	8%
UAM only	PV: 329 kW Battery: 4 kW/1 kWh	$267k	7.6%	11.2	$858k	13.1%	0.6%
RAM only	PV: 789 kW Battery: 1.27 kW/0.42 kWh	$628k	7.3%	11.4	$2,050k	23.2%	0.2%
Trainer only	PV: 80 kW Battery: 3 kW/1 kWh	$70.5k	7.6%	11.2	$210k	13.2%	1.0%
All EVSE	PV: 1198 kW Battery: 20 kW/6.5 kWh	$1,082k	7.6%	11	$3,131k	29.6%	7.7%

Load Type	New System Sizes	NPV of Cost Savings	Internal Rate of Return	Simple Payback (years)	Installed Costs	Annual Grid Energy Reduction	Annual Peak Demand Reduction
All HVN buildings	PV: 335 kW Battery: 60 kW/154 kWh	$148k	5.9%	13.5	$1,002k	7.2%	4.8%
All EVSE + All buildings	PV: 1484 kW Battery: 730 kW/839 kWh	$2,209k	8.5%	11	$4,971k	43.1%	32.3%

Table 75. Electric Utility Bill Savings From Cost-Optimal On-Site Generation Solutions (ET2)

Scenario	BAU Energy Charges	BAU Demand Charges	OPT Energy Charge (% reduction)	OPT Demand Charges (% reduction)	Utility Bill Savings
All existing HVN BLDGs	$121k	$53k	$121k	$53k	0%
New terminal	$438k	$295k	$393k (10%)	$271k (8%)	9.41%
All HVN buildings	$559k	$326k	$503k (10%)	$294k (10%)	9.94%
UAM only	$76.2k	$79k	$65.9k (13%)	$77.9k (1%)	7.35%
RAM only	$178k	$74.2k	$134k (25%)	$73.4k (1%)	17.76%
Trainer only	$19.4k	$32.5k	$16.8k (13%)	$31.7k (2%)	6.55%
All EVSE loads	$274k	$159k	$189k (31%)	$147k (7%)	22.40%
All EVSE + all building loads	$768k	$574k	$520k (32%)	$279k (51%)	40.46%

Table 76. OKV System Sizes for Resilience Assessments

Load Type	Battery (ET2)	Backup Generator (same for ET2/ET2+)
Existing HVN buildings	PV: 68 kW Battery: 32 kW/62 kWh	500 kW (1)
New terminal	PV: 273 kW Battery: 47 kW/116 kWh	500 kW (1)
UAM only	PV: 329 kW	500 kW (1)

Load Type	Battery (ET2)	Backup Generator (same for ET2/ET2+)
	Battery: 4 kW/1 kWh	
RAM only	PV: 789 kW Battery: 1.27 kW/0.42 kWh	500 kW (1)
Trainer only	PV: 80 kW Battery: 3 kW/1 kWh	500 kW (1)
All EVSE	PV: 1198 kW Battery: 20 kW/6.5 kWh	500 kW (1)
All HVN buildings	PV: 335 kW Battery: 60 kW/154 kWh	500 kW (1)
All EVSE + all buildings	PV: 1484 kW Battery: 730 kW/839 kWh	500 kW (1)

Table 80. Likelihood of Serving 25% Building Loads at HVN Using REopt Identified On-Site Generation

Load Type	8 Hours	12 Hours	24 Hours	72 Hours
Existing HVN buildings	98.4%	97.9%	96.8%	92.6%
New terminal	98.0%	97.6%	96.6%	92.4%
HVN existing + new terminal	98.0%	97.6%	96.5%	92.4%

Table 77. Probability of Surviving Outages Serving 100% OKV Loads

Load type	8 Hours	12 Hours	24 Hours	72 Hours
Existing HVN buildings	97.9%	97.5%	96.4%	92.3%
New terminal	46.1%	29.7%	0.5%	0
UAM only (ET2)	97.3%	96.2%	93.1%	81.4%
RAM only (ET2)	65.2%	50.4%	16.9%	0.4%
Trainer only (ET2)	99.1%	98.7%	97.6%	93.5%
All EVSE (ET2)	52.5%	34.2%	12.1%	0.5%
HVN existing + new terminal	38.6%	22.2%	0.2%	0
All EVSE (ET2) + all buildings	39.7%	20.2%	6.7%	0.2%

Table 78. ÆNode Results for HVN

Output	ET2 Allowed PV	ET2 Maximum PV
New solar PV	4,308 kW	5,129 kW
Battery kW/kWh	929/1,852	991/1,980
BAU LCC	$20.24M	$20.24M
LCC with on-site generation	$20.69M	$26.55M
NPV	-$0.45M	-$6.14M
Initial capital costs	$13.21M	$19.72M
Initial capital costs after incentives	$13.21M	$19.72M
Grid to load MWh	1,913 MWh	1,569 MWh
Grid to battery MWh	239 MWh	323 MWh
Total grid consumption	2,152 MWh	1,892 MWh
Peak demand BAU	2,585 kW	2,585 kW
Peak demand with On-Site Generation	2,078 kW	2,078 kW
Year 1 energy cost BAU	$768k	$768k
Year 1 energy cost	$299k	$264k
Year 1 demand cost BAU	$574k	$574k
Year 1 demand cost	$161k	$123k
Annual PV energy produced	5,211 MWh	7,222 MWh
PV LCOE		
PV to load kWh	2,878 MWh	3,096 MWh
PV to battery kWh	561 MWh	617 MWh
PV to export kWh	1,772 MWh	1,892 MWh
Year 1 export benefit	$112k	$120k
PV curtailed MWh	0	1,616 MWh
Battery to load MWh	720 MWh	845 MWh
Calculated battery efficiency	90%	89.8%
Average battery SOC	57.16%	57.64%
Breakeven compensation	$0.01/kWh	$0.07/kWh

Table 79. Probability of Surviving Outages With All HVN Buildings and ET2 EVSE Loads

	Battery	Backup Generator	8 Hours	12 Hours	24 Hours	72 Hours
Buildings + EVSE (PV = 0 kW)	0 kW/0 kWh	500 kW (1)	13.5%	1.9%	0	0
Buildings + EVSE (PV = 0 kW)	0 kW/0 kWh	500 kW (2)	27.1%	11.2%	2.2%	0
Buildings + EVSE (PV = 4,308 kW)	1,169 kW/ 3,973 kWh	500 kW (1)	95.3%	92.9%	83.7%	64.1%
Buildings + EVSE (PV = 4,308 kW)	1,169 kW/ 3,973 kWh	500 kW (2)	97.7%	97.2%	96.8%	95.4%
Buildings + EVSE (PV = 5,129 kW)	1,233 kW/ 3,949 kWh	500 kW (1)	95.6%	93.5%	86.1%	69.3%
Buildings + EVSE (PV = 5,129 kW)	1,233 kW/ 3,949 kWh	500 kW (2)	97.8%	97.2%	96.8%	95.7%

Appendix C. Digital Twin Architecture

Distribution Network Configuration: Radial, Loop, and Zonal Mesh

Airports are often modeled as dedicated distribution-level systems, reflecting their role as self-contained electrical networks with diverse, critical, and high-density loads. These systems are designed to function like microgrids, often with medium-voltage feeders supplying different airport zones, such as terminals, runways, hangars, and ground operations. Airport electrical distribution systems are predominantly configured using a radial network topology.

The radial topology typically follows a single-source distribution model with a tree-like branching structure, as illustrated in Figure 67. Power flows unidirectionally from source to the loads. In terms of reliability, this architecture is less dependable because any fault along the radial line results in power loss for downstream loads. Redundancy is minimal in this topology, because backup sources, if present, do not actively supply power. One key advantage of radial topology is the low investment cost, and it is preferred mainly because of this.

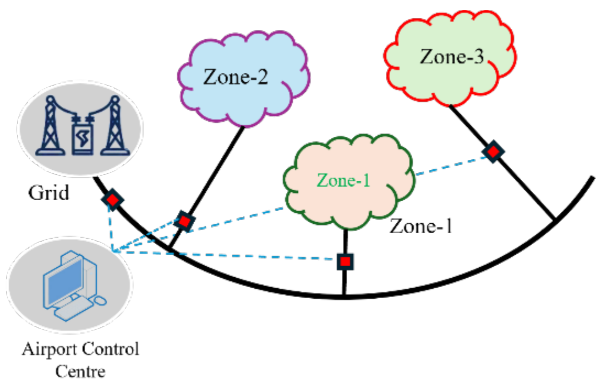

Figure 67. Radial network configuration

The loop architecture is based on a closed-loop configuration, allowing loads to receive power from two directions, as illustrated in Figure 68. Power flows bidirectionally and can be rerouted during a path failure. In terms of reliability, this architecture offers moderate dependability because it can isolate faults while maintaining power supply. Compared to radial architecture, it provides greater redundancy; however, its reliability is still constrained by its dependence on a single loop.

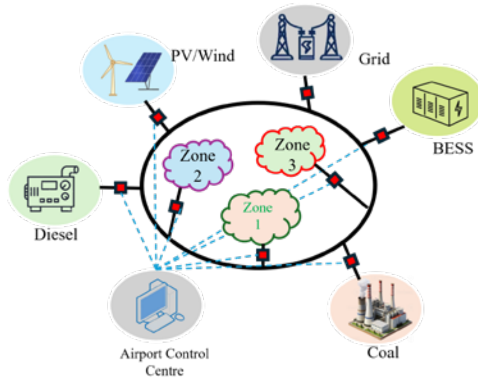

Figure 68. Loop network configuration

The zonal mesh architecture shown in Figure 69 comprises multiple interconnected zones. These zones are defined by aggregating a set of loads and generation sources based on the operational need and to make the system resilient. Each zone is connected to the grid through a breaker/switch to protect or reconfigure the network based on resiliency-oriented scenarios. The loads in the zones can be categorized as critical or noncritical, and their dispatch status can be decided based on the protection and resiliency needs. Furthermore, multiple zones are connected in a redundant mesh architecture offering higher reliability and scope for topological reconfiguration oriented to resiliency.

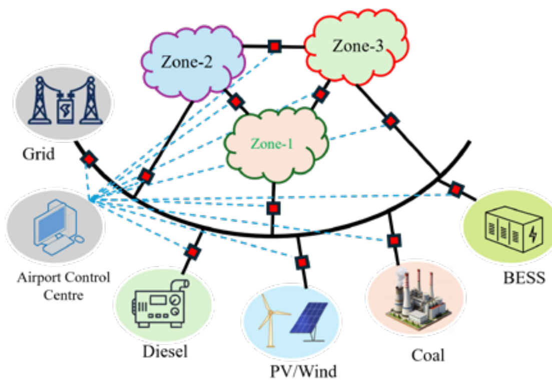

Figure 69. Zonal mesh network configuration

Simulation Platform

Traditional simulation software for power systems can become slow and less accurate as the complexity of the model increases, leading to discrepancies between the simulated and real-time behavior. These tools often struggle with real-time performance and may require time compression or simplifications that compromise accuracy, especially in transient stability and dynamic response.

To address this, the proposed zonal mesh-based generic digital twin (GDT) for the airport microgrid was developed on the real-time digital simulation platform, which ensures accurate synchronization with real-world data, enables hardware-in-the-loop testing, and facilitates the integration of field measurements. Real-time digital simulation also provides flexibility for analyzing system dynamics at the microsecond level, allowing simulations with a resolution of

50 microseconds. This capability allows the study of various effects, such as inverter dynamics, which operate at control switching frequencies from a few kilohertz to several megahertz.

Physics-Informed Modeling of Assets

The generation assets—solar PV, BESS, and generators—are represented in the GDT using physics-based models that capture their underlying electromechanical and control dynamics. In contrast, the representative loads in each zone are currently modeled in a data-driven manner, where their behavior is inferred from historical and synthetic profiles rather than explicitly derived from first principles. Nevertheless, each of these representative loads could, in principle, be reformulated as physics-informed models (e.g., aggregations of thermostatically controlled loads, EV charging, or power-electronic interfaced end use) to better capture their dynamic response under abnormal or stressed operating conditions. This section therefore focuses on the physics-based modeling framework adopted for the generation assets within the GDT, implemented on a real-time digital simulation platform with microsecond-level time steps, which enables high-fidelity hardware-in-the-loop experimentation and grid-edge control prototyping.

Grid Generation

The grid at the point of common coupling is modeled as an infinite source. However, the power factor associated with the airport feeder head, based on the steady-state power flow results of the larger electrical network, were incorporated for a more faithful digital twin representation. The validation considers the varying power factor and voltage profile. The grid characteristics are assumed to follow the recommended IEEE standards for voltage/frequency tolerance (C84.1), DER interconnection (1547), power quality (1159), and reliability (1366).

Diesel Generator

A diesel generator comprises units such as diesel engine, alternators, fuel system, and cooling system. To understand diesel generators in the context of power system dynamics and control, it is important to focus on the three critical control subsystems as shown in Figure 70. Here, E_f is the field voltage, V_m is the machine voltage, w_m is the machine's rotational speed, T_m is the mechanical torque, w_{ref} is the reference speed, and V_{pss} is the reference voltage from the power system stabilizer. The system components include a speed governor system (Figure 71), a power system stabilizer (Figure 72), and an excitation system (Figure 73). The main function of the speed governor system is to control the speed of the engine and ultimately the frequency of the generated power. Any changes in the machine's rotational speed caused by a change in load is detected, and the fuel valve is opened or closed based on the change in the load to maintain a constant speed. The main role is to maintain the steady frequency to help in primary frequency regulation. The control scheme for the speed governor system is shown in Figure 71, where R is the droop gain and P_{ref} is the load reference. The power system stabilizer is used to dampen low-frequency oscillations that can occur after a disturbance; it senses the rotor speed deviation and adds a stabilizing signal to counteract the oscillations in generator speed. The control loop for the power system stabilizer is shown in Figure 72. The excitation system regulates the generator field voltage by controlling the current of the alternator. Any deviation on the voltage is sensed by the automatic voltage regulator, and the field excitation current is adjusted accordingly to correct the terminal voltage. The excitation system control scheme is depicted in Figure 73.

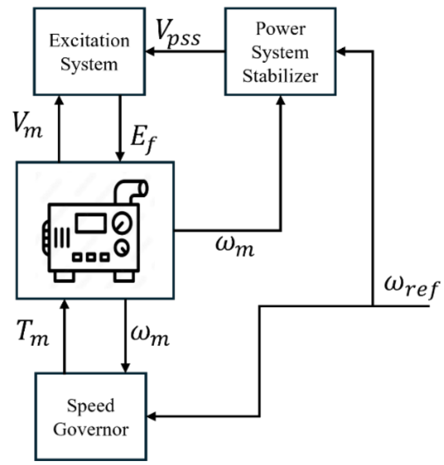

Figure 70. Physics-informed model of a diesel generator

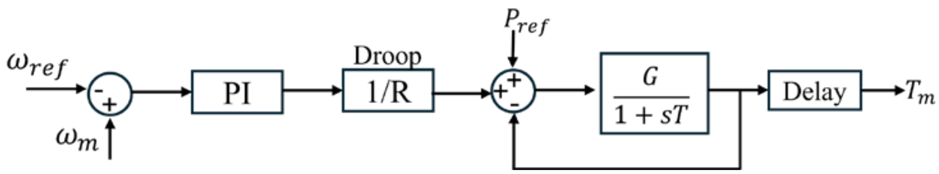

Figure 71. Speed governor

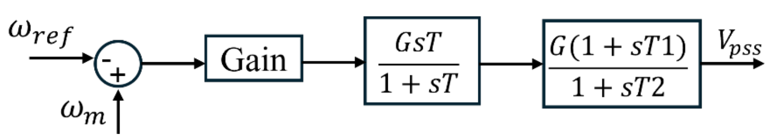

Figure 72. Power system stabilizer

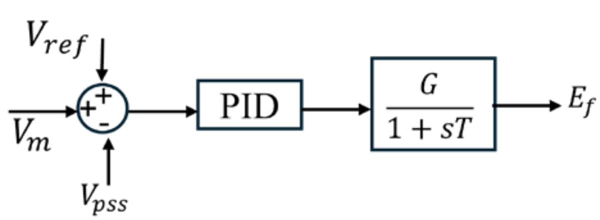

Figure 73. Excitation system

BESS and Photovoltaic System

The RSCAD block diagram representing the physics-informed models of BESS and PV systems are shown in Figure 74 and Figure 75, respectively.

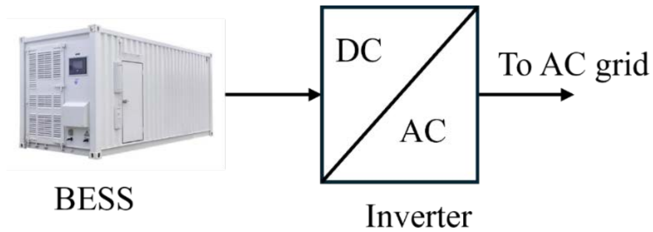

Figure 74. BESS block diagram

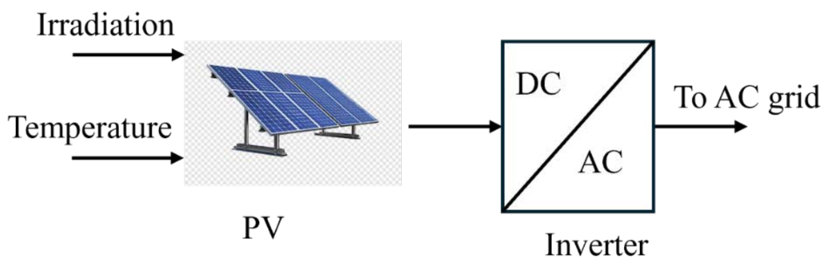

Figure 75. PV system block diagram

Inverter: Modes of Operation

BESS and PV operate in various modes depending on their interaction with the grid and system requirements. The two primary modes are grid-following (GFL) and grid-forming (GFM) mode. In GFL mode, the inverter synchronizes with the existing grid voltage and frequency, acting as a current source that injects power based on grid conditions. In GFM mode, the inverter establishes the voltage and frequency, behaving as a voltage source and actively contributing to grid stability. These modes determine how inverter-based resources respond to disturbances, share power with other generators, and interact with grid dynamics. The physics-informed modeling of BESS and PV inverters are considered grid following. Therefore, the GFL control scheme is explained in this section.

Grid-Following Inverters

GFL is a control method used by inverters in energy systems such as solar, wind, or battery setups. It ensures synchronization between the inverter's output and the grid's voltage and frequency. In simple terms, GFL inverters work as current sources, adjusting their output to match the grid's angle and magnitude. This enables them to manage the absorption or injection of active and reactive power. However, GFL inverters depend on the utility grid for consistent voltage and frequency reference and cannot operate independently in off-grid or island scenarios.

Grid-Following Control Dynamic Model

GFL inverters are typically represented as configurable PQ nodes, with the inner control loops mostly ignored. This section discusses the real control strategies used in GFL inverters as well as the modeling of two GFL control components: phase-locked loop (PLL) and current control loop.

Modeling of Phase-Locked Loop

The purpose of PLL modeling is to estimate the grid voltage's phase angle. The PLL uses a proportional-integral controller to adjust the component of the grid voltage on the q-axis, V_{gq}, to zero by increasing or decreasing the virtual angular frequency ($\Delta\omega$). The integration of $\Delta\omega$ yields the estimated phase angle (θ_{PLL}). K_p and K_i represent the PLL controller's proportional and integral gains, respectively. The schematic diagram for modeling the control block of the PLL is shown in Figure 76.

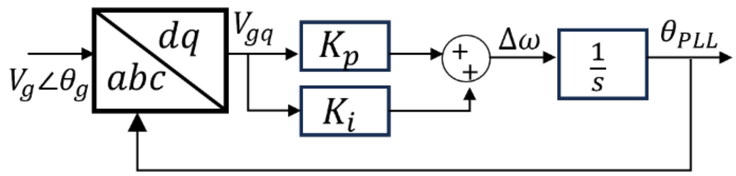

Figure 76. PLL control block

Modeling of Current Control Loop

The purpose of the current control loop is to regulate the active and reactive currents injected into the grid by rapidly adjusting the inverter internal voltage ($E\angle\theta$). The grid voltage $\left(V_g\angle\theta_g\right)$ and current $\left(I_g\angle\delta_g\right)$ are transferred from the abc to dq frame based on the phase angle θ_{PLL} obtained from the PLL control block as shown in the following equation. If P_{ref} and Q_{ref} are the references of the active and reactive power injected into the grid, reference current (I_{g_ref}) is calculated as:

$$I_{g\_ref} = \left(\frac{P_{ref}+Q_{ref}}{V_g}\right)^*$$

Where, $I_{ga\_ref} = I_{g\_ref}$,

$I_{gb\_ref} = \alpha^2 I_{g\_ref}$ and

$I_{gc\_ref} = \alpha I_{g\_ref}$, respectively.

Here, I_{ga_ref}, I_{gb_ref}, and I_{gc_ref} are the A phase, B phase, and C phase reference current, respectively, and $\alpha = e^{j\frac{2\pi}{3}}$. In some applications, the output current of each phase is independently controlled in the dq frame through the proportional-integral controller. However, for most of the applications, I_{g_ref} is transferred from the abc to dq frame using synchronous reference frame transformation based on the phase angle θ_{PLL} obtained from the PLL control block as shown in Figure 68. The dq component of I_{g_ref}, V_g, and I_g acts as an input to the current control loop with the proportional-integral controller. As an output, the current control loop provides the inverter internal voltages in the dq frame: e_{gd} and e_{gq}. The e_{gd} and e_{gq} are then transferred into the abc reference frame to regulate the active and reactive current into the grid as depicted in Figure 77.

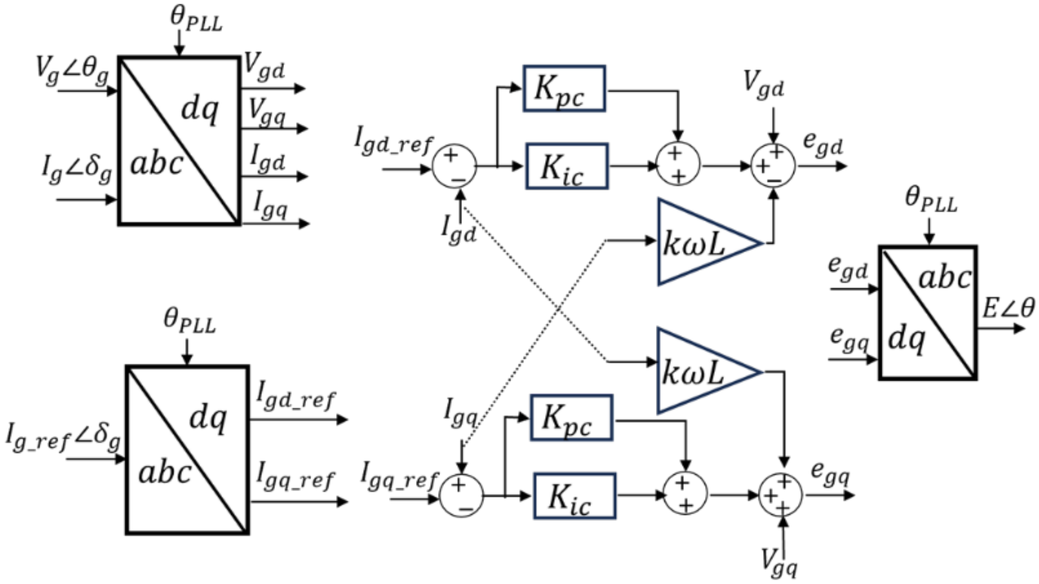

Figure 77. Current controller of grid-following inverter

In recent years, several auxiliary controls for GFL inverters have been presented with the goal of providing voltage and frequency support, such as volt-var, frequency-watt, and synthetic inertia. These controllers function as outer control loops, modifying P_{ref} and Q_{ref}. Because the outer control loops are limited by the bandwidth of the inner control loops, their response is often slow.

Digital Twin Development Procedure

The process began by identifying the service locations where each meter is installed. The utility provided the meter names along with their corresponding service locations. In the utility-provided model, information about each load's connection to the network—including which lines connect to which service locations—was collected. To map these locations geographically, latitude and longitude coordinates for each node and lines were used to pinpoint meter locations.

When the meter locations were identified, the next step was to determine the coordinates of the substation feeding the airport distribution network. From there, the feeder lines connecting the substation to each service location are traced. The utility-provided model gives the line information details about these connections, including the sending and receiving buses, the line code (or conductor type), and the length of each line segment. These data are used to link all service locations to the substation.

Because the conductor type is specified for each span, the corresponding electrical parameters, resistance, inductance, and capacitance were derived from the available data and used to calibrate the model. Through this procedure, a complete digital twin of the distribution network was developed based on utility-provided information. The implementation relies on utility-supplied network data files containing system topology, line geometry, and load information.

The utility-provided system model is presented in Figure 78. Consistent with the utility's workflow and underlying data structure, we first adopted the as-provided feeder representation and determined the distribution circuit serving the airport (Figure 71). We then traced the point of common coupling and confirmed the metering location used for billing and operational monitoring (Figure 80), ensuring the electrical boundary of interest matches the measurement boundary available for model verification. Finally, we extracted conductor and line-segment attributes—such as line identifiers, phase configuration, approximate segment lengths, and network connectivity—to reconstruct the primary distribution topology relevant to airport operations (Figure 73). For clarity, the label “1” in Figure 73 corresponds to meter ID 31438, and the remaining numeric labels map to their respective elements in the same manner.

To improve interpretability and enable rapid engineering use, we synthesized these electrical attributes into an airport aerial view highlighting the distribution network, which overlays the inferred feeder routing and key nodes on a geographic depiction of the airport, as shown in Figure 73. This consolidated view provides a practical, system-level interface for subsequent digital twin activities—supporting streamlined circuit verification, asset-to-topology mapping, and scenario definition (e.g., on-site interconnections, load growth, and operational reconfiguration). Overall, this step establishes a traceable foundation that bridges the utility’s as-operated model with an engineering-friendly representation, reducing ambiguity in network boundaries and accelerating model-based analysis and validation. Using this comprehensive information, the zonal mesh-based GDT was reconfigured into a radial digital twin reflecting the Airport-1 distribution network.

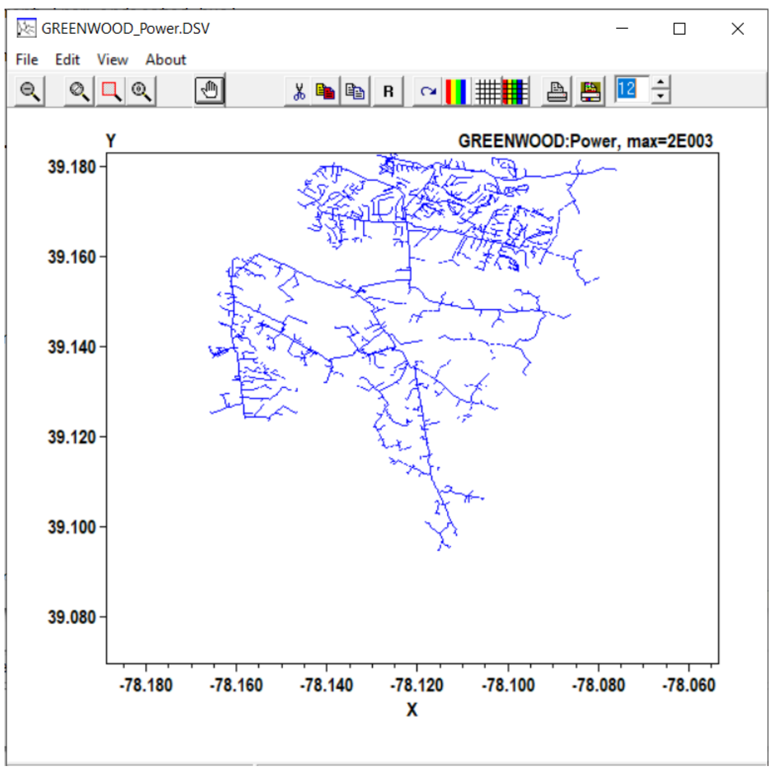

Figure 78. Utility-provided network model in OpenDSS

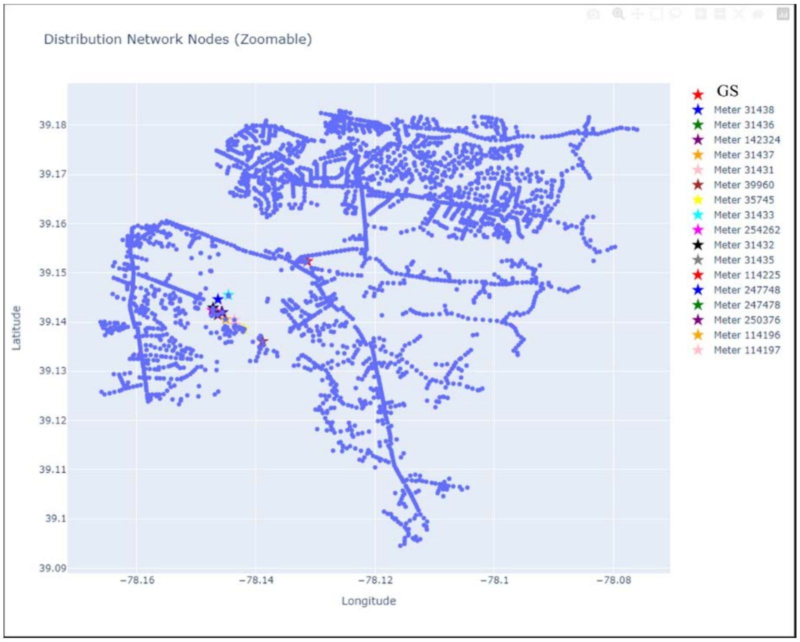

Figure 79. Meter identification in OpenDSS

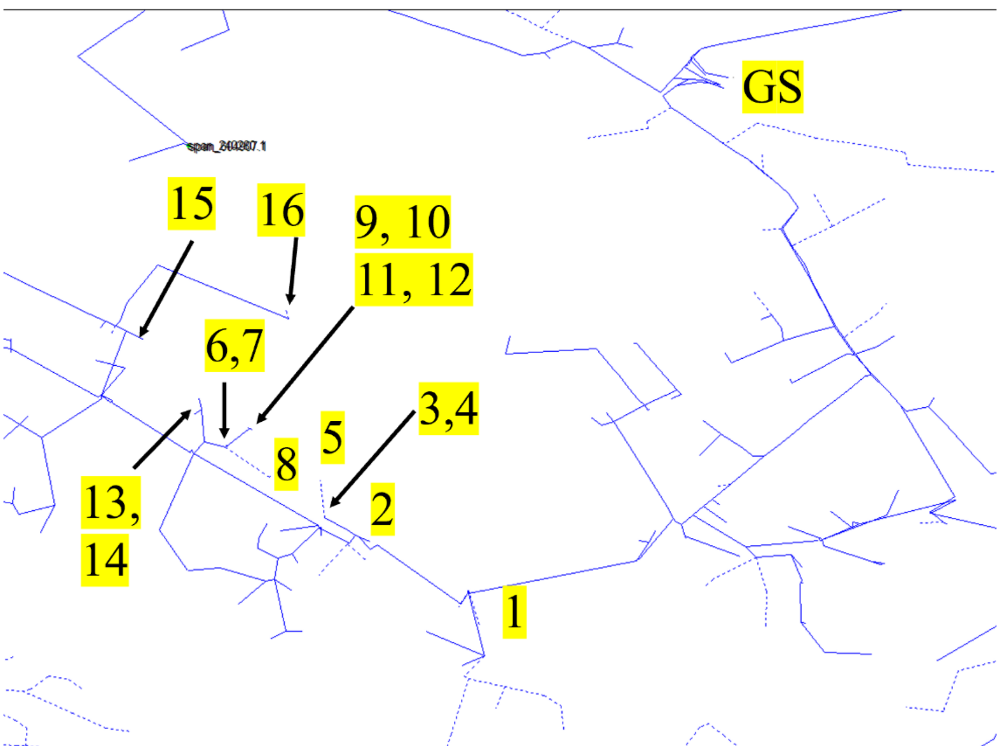

Figure 80. Extraction of line parameters from OpenDSS model

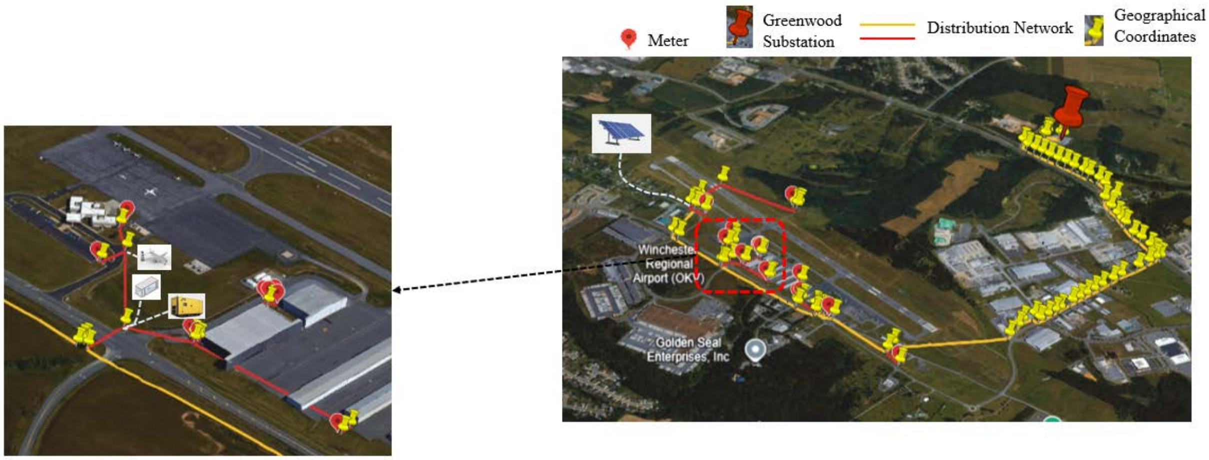

Figure 81. Airport aerial view highlighting distribution network

Community Loads Outside the Airport Boundary

Figure 82 shows the airport feeder layout with three identified community load zones around the airport area. The colored shaded regions represent Community Load-1, Load-2, and Load-3, while the yellow markers indicate distribution feeder/load points connected along the network. This layout helps visualize how community loads are geographically distributed for feeder modeling and load analysis.

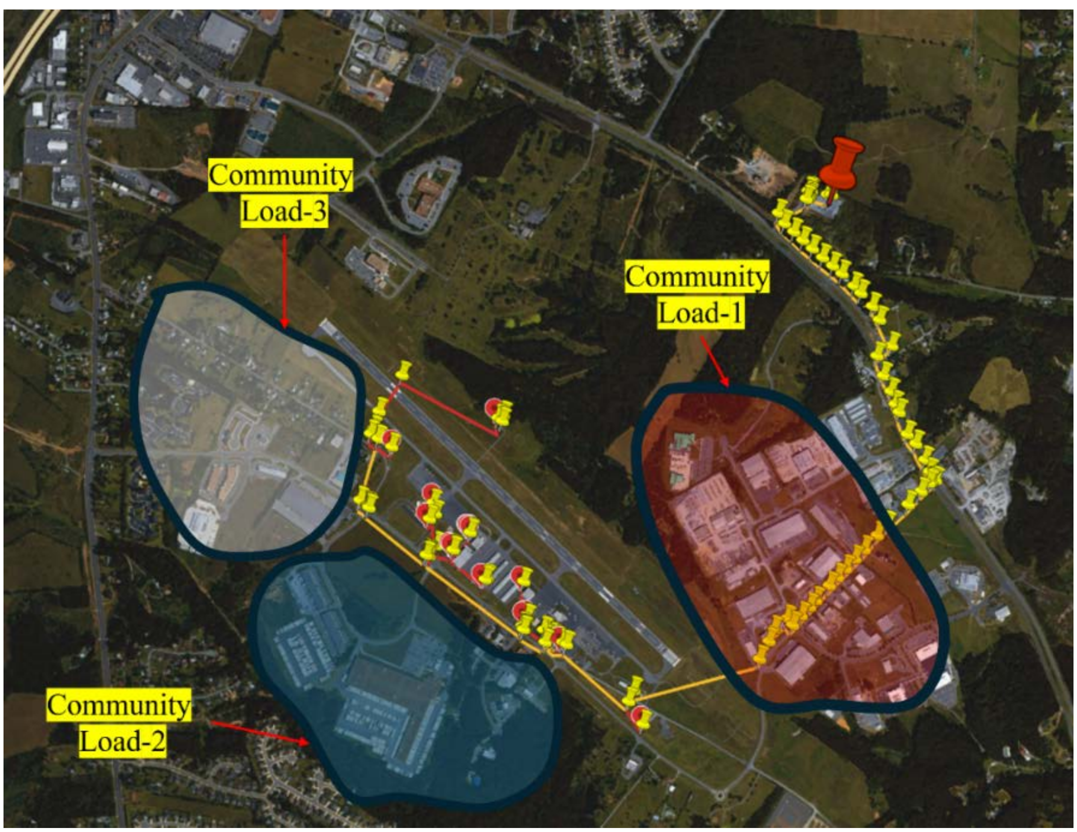

Figure 82. Community load fed by the airport circuit

Synchronization of DT Variables With the Physical Airport Circuit Topology

Figure 83 shows the synchronization of DT variables with physical airport circuits. The segment labeled "Airport Circuit to First Meter" in the DT (Figure 38) explicitly maps to the corresponding portion of the line in the geographic circuit layout shown in Figure 83; the same mapping procedure is applied to all remaining line segments.

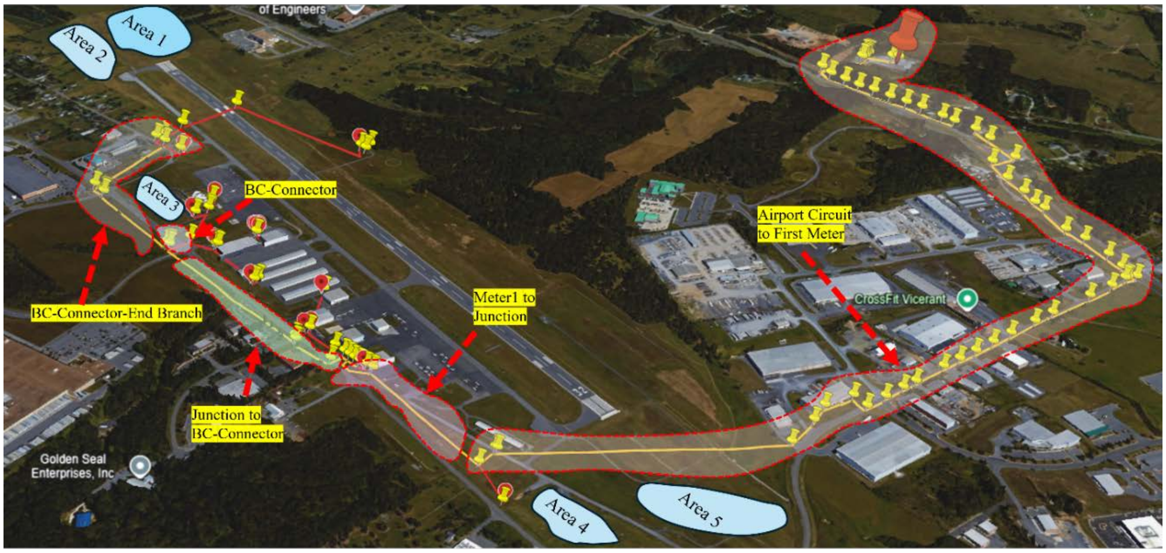

Figure 83. Synchronization of digital twin variables with the physical airport circuit topology

Representation of Isolation Points During Contingencies

Figure 84 shows the modified airport distribution network with added new conductors to improve connectivity and provide alternative power paths. The dashed red region highlights the airport isolation contingency area, showing how the network can be reconfigured during outage or isolation events. It presents the overall feeder layout connected from the Greenwood Substation to the airport area, with meters, distribution lines, and geographical coordinates marked. The zoomed section highlights the airport network where local loads, PV/BESS components, and feeder connections are modeled for detailed analysis.

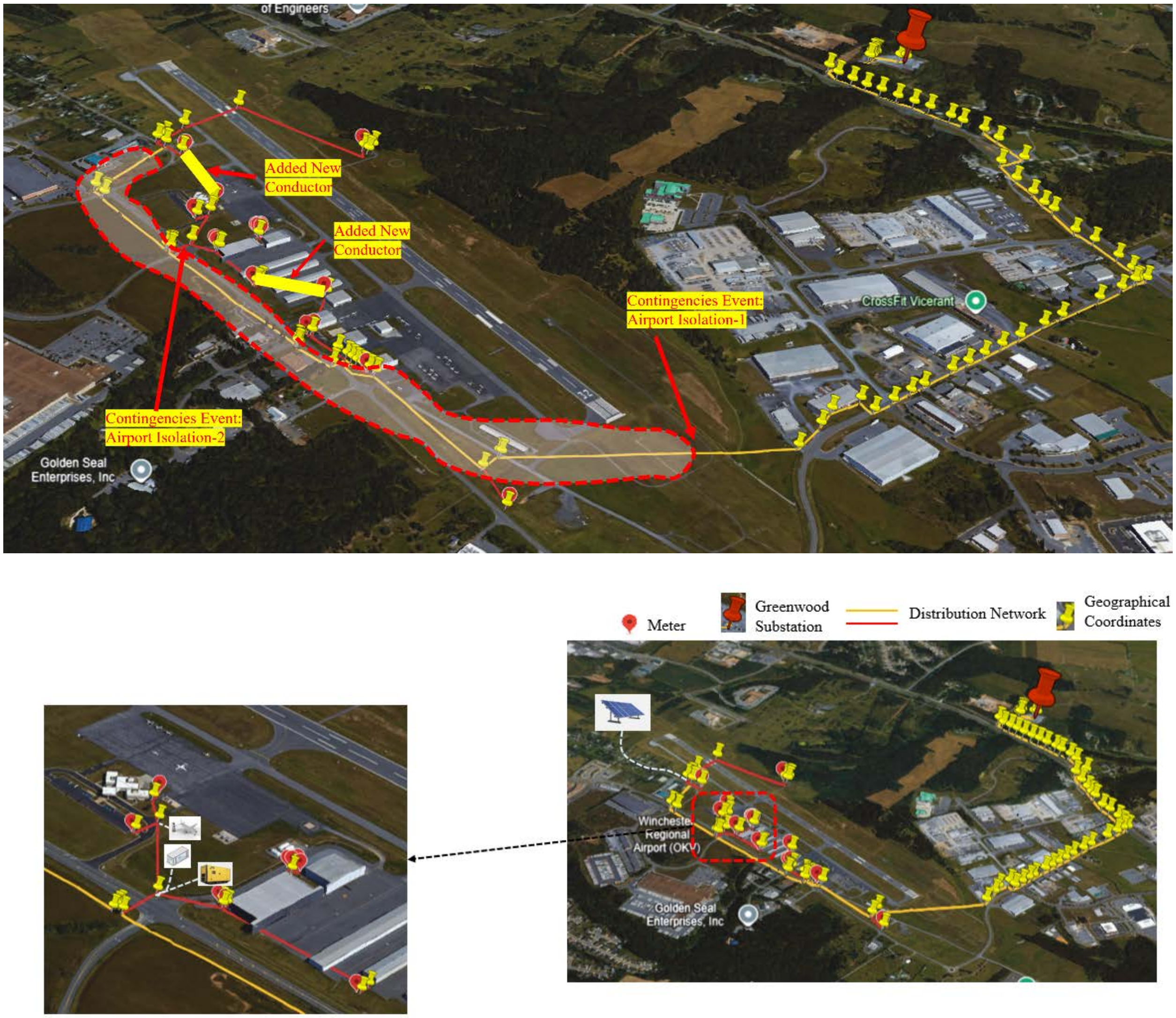

Figure 84. The airport circuit isolation for Scenario 3

Irradiation and Temperature

Figure 85 shows the conversion of hourly irradiance and temperature profiles into minute-level data for PV/load simulation. The left plots represent the original hourly profiles, the middle plots show the stepwise minute-based conversion, and the right plots show the final smoothed minute-resolution profiles. This process helps create more realistic weather inputs for detailed time-series PV power modeling.

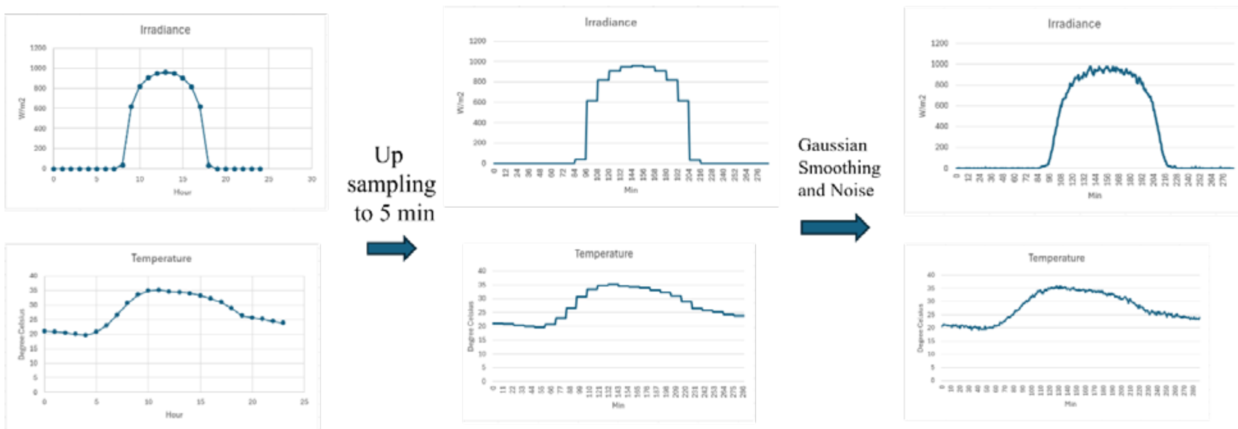

Figure 85. Irradiance and temperature profile for PV

Appendix D. Energy Technologies

This appendix details the energy technologies that were considered during the scoping stages of these analyses.

Enabling Technologies

A microgrid is a localized, intelligent energy system that integrates and controls on-site power generation, storage, loads, and critical infrastructure to ensure efficient operation of the site. A microgrid can comprise various components, including energy generation sources, reciprocating engines, energy storage systems, various types of loads, advanced metering infrastructure, and power conversion equipment—all operating under a controller that can coordinate and optimize dispatch. In addition, microgrids require switching infrastructure to enable automatic or manual islanding from the utility. Section 3 discusses potential energy assets and how they might be deployed at an airport. Although they can improve resilience at the site, these assets will not guarantee operation during an emergency. Microgrids enhance resilience by providing energy surety (i.e., ensuring loads have access to energy) and survivability (i.e., ensuring this access is maintained through unforeseen events, such as utility outages).

Microgrids offer additional benefits. Coordination of on-site loads and generation resources allows these assets to be run at their optimal operating point, which increases efficiency and can minimize utility costs. BESS or dispatchable assets such as natural gas turbines can be employed to minimize utility load during times of high demand charges, which can reduce the site's energy bill. Additional value can be accessed if the site can use its energy resources to participate in demand response or ancillary markets. A closed-network microgrid with a single point of interconnection to the utility allows increased control of the cybersecurity and physical security of the airport's grid. The disadvantages of microgrids are primarily cost and complexity. Microgrids require an increased up-front CAPEX, which is determined by specific site requirements. In addition, they are complex systems that require specialized skills to maintain and operate.

Energy Storage

Energy storage can provide significant cost savings, especially if a significant fraction of a site's energy bills goes toward demand charges or the site is charged variable energy charges depending on time of use. Energy storage will allow the site to reduce its peak monthly demand and offset energy usage during peak times. In addition, storage can be a valuable tool to improve resilience on the airport by providing dispatchable power during outages.

Electrical Storage

BESS is a viable option at most airports because of its potential to offset peak electricity demand, provide critical backup power during outages, and facilitate a more effective integration of intermittent energy resources such as solar PV. Lithium-ion technology—the most mature option available—offers numerous advantages, including high efficiency, commercial maturity, rapid response times, and a compact footprint. Emerging alternative battery technologies and chemistries—such as flow batteries (e.g., vanadium redox, iron flow), sodium-ion, and solid-state batteries—promise improvements in safety, energy duration, and cost, but these technologies remain in the early commercialization stages and will require further development before they become widely viable. Airport-based BESS has become increasingly common and demonstrates the practical viability of such investments. For instance, Rome Fiumicino Airport recently implemented a 10-MWh BESS using repurposed electric vehicle batteries, and JFK International Airport is currently constructing a 1.5-MW/3.34-MWh BESS.

Utility-scale lithium-ion BESS currently costs between $400 and $500/kWh. This price has decreased by nearly 90% during the past decade and is projected to decrease an additional 50% by 2050 (Cole, 2023). EVSE chargers generally incur high peak demand but operate infrequently compared to conventional airport loads, such as heating or lighting—potentially leading to substantially higher demand charges. A significant economic benefit of BESS lies in their ability to reduce such demand charges by flattening peak loads and arbitraging electricity prices through strategic charging and discharging. In addition, coupling BESS with intermittent on-site generation energy sources, such as solar PV, allows excess generation to be stored and later discharged during nighttime or periods of low solar output.

Thermal Energy Storage

Thermal energy storage generally involves storing heat or cooling energy for later use in a heating, ventilation, and air conditioning (HVAC) system. This can significantly reduce energy charges by displacing load to low-demand times and improving overall energy efficiency.

Ground-Source Heat Pumps

Ground-source heat pumps represent a particularly promising geothermal solution. These systems do not generate electricity and do not require significant geothermal resources. Instead, they use the earth's consistent temperature as a heat source in winter and a heat sink in summer, coupled with highly efficient heat pump technology. At the Louisville Muhammad Ali International Airport, 648 vertical wells—each 500 feet deep–were installed beneath a 7-acre area. The project's initial CAPEX was approximately $22 million, with projected annual savings of around $400,000 (Cariaga, 2023). When the installation is complete, the land can be paved for parking or used as open space. A ground-source heat pump system could enhance resilience by providing heating and cooling entirely via electricity, with support from backup systems, such as batteries and generators.

Cold Temperature Storage

Cold temperature storage is another cost-effective cooling strategy. It involves the creation of ice or chilled water during off-peak hours (typically overnight). The stored cold energy is then used to provide cooling during peak daytime hours. Airports such as Chicago Midway International, Honolulu International, and Ronald Reagan Washington National Airport have successfully employed these systems. Typically, such installations involve insulated water tanks and high-efficiency chillers, offering a significantly lower cost than lithium-ion batteries. Although thermal energy storage cannot directly produce electricity, it presents a low-risk, affordable, long-term energy-saving solution.

Energy Generation

On-site energy generation resources are critical for providing energy savings and improving resilience. If the levelized cost of energy (LCOE) of a generation source is less than the cost set by the utility, the site can achieve significant savings by reducing the quantity of energy purchased from the grid. In addition, during extended outages, on-site generation can provide enough power to keep the site operating and keep on-site energy storage charged.

Solar Photovoltaics

Solar PV represents a cost-effective option for on-site energy generation, benefiting from significant cost reductions and widespread global adoption. More than 100 airports worldwide have successfully implemented solar energy projects, leveraging the typically large areas available on airport properties (ICAO, 2017). Some major U.S. airports—including Indianapolis, Denver, San Francisco, and Boston Logan—have active solar programs that are either operational or under development.

Typical estimates for ground-based solar range from $1 to $2/Watts direct current (~$10 million for a 10-MW array) in the initial CAPEX (Ramasamy, 2023). Note such an array would likely achieve an annual capacity factor of 15%–25%, leading to a competitive LCOE estimated at $0.05–0.08/kWh. On-site PV generation could not only secure a lower energy rate than a site's current utility but also shield against future utility rate volatility in the next 30 years. Net metering agreements currently offered by many utilities would allow an on-site solar installation to sell energy back to the grid, further offsetting its cost.

Although most airports have access to large areas for potential PV development, detailed studies are required to assess the feasibility and available area for PV. Factors such as glare, obstructions, and roof age could have an impact. The Federal Aviation Administration (FAA) and industry groups have published guidelines to ensure solar arrays do not interfere with flight operations. Specifically, glare mitigation and appropriate structural setbacks have been successfully addressed at numerous airports, providing established best practices that can be leveraged by other sites.

Natural Gas Combined Heat and Power

Combined heat and power (CHP), also known as cogeneration, offers a highly efficient method of on-site energy production by simultaneously generating electricity and capturing waste heat for beneficial use. Using this method, CHP plants can reach an efficiency of up to 80% compared to approximately 50% for modern combined-cycle power plants. At most airports, a CHP plant would likely comprise centrally located gas-fired generators that are connected to both the electricity and heating systems of the site. CHP adoption is common at airports, with notable examples including JFK International Airport, which operates the largest CHP plant in the United States, at 121 MW. This plant fully meets the electrical and thermal needs of the airport.

The value of CHP lies in its high overall efficiency, potential cost savings, and resilience. Although it does not offer the extremely low operating costs of a solar plant, gas prices in most of the country typically remain lower than electricity rates from the grid—potentially resulting in significant long-term operational savings. In addition, an airport could use a CHP plant to participate in demand response programs and capacity markets, further increasing savings. However, CHP systems require significant upfront costs. Cost estimates range from $1,600–$3,400/kW (Desai, 2020). This does not account for the price of interconnection of a gas supply, electrical connections, and district heating connections. CHP was included in early versions of the analysis at OKV and HVN. However, the significant infrastructure required for natural gas transport onto the site significantly outweighed any potential benefits from a plant.

As part of the evaluation of CHP, environmental and regulatory considerations also should be considered. The plant would need to meet the Clean Air Act and local air quality regulations. Gas is relatively clean burning, and modern CHP systems include emissions controls (catalytic converters) to minimize pollutants. In some regions, renewable natural gas is sourced to meet organizational goals—although potentially at a premium. Widespread industry experience with CHP systems and use in critical facility infrastructure provide methodologies to meet common challenges related to emissions management, regulatory compliance, and grid integration.

Geothermal

Geothermal energy can serve as a reliable, dispatchable on-site power generation resource where suitable subsurface conditions exist. Unlike solar PV or wind, geothermal power is not intermittent and can provide continuous baseload electricity, making it particularly valuable for enhancing airport resilience during extended grid outages. Geothermal power plants generate electricity by harnessing heat from the earth's subsurface to produce steam or drive binary-cycle systems, which in turn power electric generators. Because the energy source is constant, geothermal systems typically achieve capacity factors exceeding 90%, comparable to conventional thermal power plants.

The feasibility of geothermal power is highly site-dependent and is generally limited to regions with favorable geothermal gradients or accessible hydrothermal resources. In areas without high-temperature resources, enhanced geothermal systems may be technically feasible, though they remain costly and are still emerging commercially. As a result, geothermal electricity generation is less broadly applicable than solar PV or natural gas CHP for most airports and requires extensive upfront geological surveys, test drilling, and permitting.

When viable, geothermal power offers several advantages, including very low operating costs, long system lifetimes (often exceeding 30–40 years), and minimal fuel price volatility. However, initial CAPEX is substantial and uncertain, with costs driven largely by drilling depth and subsurface risk. Typically installed costs range widely, from $3,000 to more than $6,000/kW for conventional geothermal developments, depending on resource quality and project complexity (US Department of Energy, 2019).

Wind

Airports almost always reject on-site wind because tall turbines violate FAA Part 77 airspace/obstacle-clearance surfaces around runways and taxiways. Their rotating blades can clutter primary/terminal radar, degrade weather radar, and interfere with navigation. Turbines also intrude on critical sight lines for pilots and air traffic control, especially in low-visibility conditions. Finally, turbine wakes add mechanical turbulence where aircraft are taking off and landing.

Hydro, Wave, and Tidal Power

Hydro, wave, and tidal energy are rarely viable for airports because they are intensely location-dependent and airports are seldom located where these resources are strong or accessible. Conventional hydropower requires major elevation changes and impoundments. Wave and tidal power require coastline or estuary sites with high, predictable energy flux. Even for coastal airports, permitting, shoreline protection rules, and marine-safety corridors make interconnection and maintenance impractical. As a result, airports typically pursue site-agnostic options such as those mentioned previously in this section while buying off-site generation if they want marine, hydro, or wind in their energy mix.

Horizon Technologies

Critical infrastructure facilities rely on durable and proven technologies, with robust supply chains and significant workforce available. In contrast, technologies that are accelerating in development and could be included in an airport's energy portfolio within the 50-year planning window but have not yet reached the commercial viability required for such facilities are considered horizon technologies.

Hydrogen

Hydrogen technology is emerging with significant potential to impact airport operations; however, it remains economically and technically nonviable at a large scale. Airports can leverage hydrogen in several ways, including by using fuel cells that efficiently convert hydrogen into electricity, powering hydrogen-fueled combustion turbines or engines, and producing hydrogen on-site through electrolysis for energy storage or vehicle fueling. Hydrogen-powered aircraft (e.g., the ZEROe concept) are being developed by major aerospace manufacturers such as Airbus, underscoring the importance of hydrogen infrastructure readiness at airports in the medium to long term.

Substantial barriers exist for the widespread adoption of hydrogen. There is very little hydrogen delivery infrastructure across the United States, so it would likely need to be generated on-site through electrolysis, which is expensive, or delivered by truck. The regulatory standards around hydrogen safety and storage (e.g., NFPA 2: Hydrogen Technologies Code in the United States) are relatively new and would require close coordination with the FAA and local fire authorities. Current prices far exceed natural gas at \$5–6/kg with electrolyzers costing \$800–1,500/kW (DOE HFTO 2020). These prices are likely to drop with scale.

As a storage technology, hydrogen can provide long-term energy storage, but the roundtrip efficiency (i.e., electricity-hydrogen-electricity) is extremely low compared to battery technologies. Hydrogen should be considered a promising but currently nascent technology for airport energy. Although large-scale investment in hydrogen infrastructure might be premature, sites could benefit from monitoring industry developments and participating in pilot programs, demonstration projects, and/or early deployment in noncritical operations. These initiatives would build valuable institutional knowledge and position the site to adopt hydrogen-based solutions should they become economically and technically viable.

Nuclear: Small Modular Reactors

Small modular reactors (SMRs) are compact, factory-fabricated nuclear reactors designed to offer scalable power generation with enhanced safety and shorter construction times than traditional nuclear plants. SMRs represent a future option to provide constant, reliable power with some designs providing waste heat for thermal loads. A nuclear reactor could meet the bulk of the site's power requirements while requiring only minimal refueling; however, implementing a nuclear reactor at an airport has not yet occurred globally and would carry substantial regulatory, technological, and public acceptance challenges. The U.S. Nuclear Regulatory

Commission has approved only one SMR to date, NuScale's 50-MW reactor module (NRC 2020), which is scheduled to be deployed in 2029. The CAPEX of SMRs is expected to be higher than other generation methods. NuScale's first plant is projected at approximately $6,000/kW, which is expensive compared to other technologies. This number is likely to increase in the face of regulatory and public outreach hurdles. With several designs in development, the widespread commercial availability of SMRs is expected in the 2030s. Although full-sized nuclear reactors typically require a decade or more to license, SMR technology may provide a modular and repeatable licensing process that could be more efficient. Uncertainties in SMR timelines coupled with regulatory, technological, and public outreach challenges make them unlikely to be available with the required workforce, licensing, and price point for airports until the late 2030s or the following decade.

Appendix E. Overview of Incentive and Revenue Opportunities

To improve the cost-effectiveness of some of these systems, state and federal incentive programs can significantly reduce the financial burden on the site. Such programs can vary significantly by region and utility and so should be treated on a case-by-case basis. Following is a nonexhaustive list of some of the programs available to HVN and OKV. Note: This list is not complete and any airport planning on building such a system should complete its own due diligence to ensure it is capturing all available financial benefits. Outside of the investment tax credit, these incentives were not included in the analysis but should be researched by the sites as potential cost-saving measures.

Federal Incentives: Available Across the United States

The following programs are available across the country, but not all sites will necessarily be eligible.

Investment Tax Credit

Originally introduced as part of the Inflation Reduction Act, the ITC is a 30% tax credit accessible by all tax-paying entities (IRS, 2025). Tax-exempt parties (e.g., airports) can also access the savings using an elective payment system to be reimbursed. Examples of technologies that are covered include solar PV, energy storage technology (BESS and thermal), hydropower, marine and hydrokinetic, nuclear, geothermal, and waste energy recovery technologies. For wind and solar technologies to qualify, projects must begin construction by July 5, 2026, or be placed in operation by December 31, 2027. Other technologies, such as energy storage, are not beholden to these reduced timelines.

FAA Grants and Programs

Airport Improvement Program

The Airport Improvement Program (FAA, Airport Improvement Program (AIP), 2025) provides grants to public agencies—and, in some cases, to private owners and entities—for the planning and development of public-use airports. For medium and large airports, this grant covers 75% of eligible costs. For small airports, the grant can cover 90%–95% of eligible costs, based on statutory requirements. Eligible projects include those improvements related to enhancing airport safety, capacity, security, and environmental concerns. Projects to install microgrids are covered under the AIP.

Airport Infrastructure Grant

As part of the Infrastructure Investment and Jobs Act, the Airport Infrastructure Grant program (FAA, 2025) provides $14.5 billion in funding over 5 years starting in Fiscal Year 2022. This includes up to $2.39 billion for primary airports and up to $500 million for nonprimary airports. These funds can be invested in runways, taxiways, and safety and sustainability projects as well as terminals, airport transit connections, and roadway projects.

Voluntary Airport Low Emission Program

The Voluntary Airport Low Emission Program (VALE) (FAA, 2025) improves airport air quality and provides air quality credits for future airport development. Created in 2004, VALE helps airport sponsors meet their state-related air quality responsibilities under the Clean Air Act. Through VALE, airport sponsors can use AIP funds and passenger facility charges to finance low-emission vehicles, refueling and recharging stations, gate electrification, and other airport air quality improvements.

Airport Zero Emission Vehicle and Infrastructure Pilot Program

The Airport Zero Emissions Vehicle and Infrastructure Pilot Program (FAA, 2025) improves airport air quality and facilitates the use of zero emissions technologies at airports. Created in 2012, the program allows airport sponsors to use AIP funds to purchase zero emissions vehicles and to construct or modify infrastructure needed to use them.

State of Virginia Incentives: Local to OKV

Department of Aviation Virginia

To support the continuing growth and operation of this system, the Virginia Aviation Board has developed funding programs to assist sponsors of public-use airports with a variety of improvement activities ranging from planning to construction to promotions:

- Commonwealth Aviation Fund
- Facilities and Equipment Program
- Voluntary Security Program
- Maintenance Program
- Aviation and Airport Promotion Program.

Airports may acquire funds under one or several of these programs for the design, commissioning, construction, and maintenance of their energy systems. Each program includes specific requirements for eligibility (Virginia Department of Aviation, 2024).

Virginia Airport Revolving Fund

Virginia Airport Revolving Fund (VARF) (Virginia Resource Authority, 2026) provides financial assistance for public-use, publicly owned airports. Since 2000, more than $110 million has been invested in airport infrastructure projects throughout the Commonwealth. Any airport-related capital project on an airport's approved layout plan, including revenue–producing projects, are eligible in the VARF. Examples include hangars, terminal buildings, machinery/equipment, land acquisition, roadways, parking facilities, utilities, fueling systems, and runway/taxi improvements. The VARF can also be used for local matching share of projects eligible for funding through other federal and/or state sources.

Virginia Grid Reliability Improvement Program

The objective of the Virginia Grid Reliability Improvement Program (Virginia Department of Energy, 2026) is to enhance the resilience of the electric grid against disruptive events by reducing the duration and frequency of outages caused by events that disrupt normal grid operations. This program will not cover costs associated with new generation constructions, cybersecurity investments, or large-scale BESS facility constructions that are not intended for system resilience enhancement.

State of Connecticut Incentives: Local to HVN

Connecticut Electric Vehicle Charging Program

The Connecticut Electric Vehicle Charging Program (UI, Eversource, 2025) is available for all commercial and industrial Eversource and UI electric service customers who purchase and install qualified EVSE charging stations at facilities throughout the state to support charging for workplaces, light-duty fleets, and the public. Incentives will be either 50% of eligible EVSE charger costs combined with 100% of eligible make-ready installation costs or the per-site maximum rebate ($150,000), whichever is less.

Energy Storage Solutions

Energy Storage Solutions is a voluntary incentive program (Eversource, US, and Connecticut Green Bank, 2024) offered to all residential, industrial, and commercial customers of Eversource or UI. It provides initial incentives for upfront costs ($100–200/kWh for commercial partners) and performance payments similar to demand response programs (summer: $200/kW; winter: $25/kW for power dispatched during an event). Performance payments are optional, and there is no penalty for failing to dispatch storage power to the grid.

Commercial Property Assessed Clean Energy Financing

Commercial Property Assessed Clean Energy is long-term, low-rate assessment-based financing offered by the Connecticut Green Bank (Connecticut Green Bank, 2023). Capital is offered to building owners to make clean energy and resilience improvements on their properties that is paid back over time from a benefit assessment on the building owner's property tax bill. The interest earned from these types of investments, over time, is expected to cover the operational expenses and a return for the Green Bank.

Connecticut Department of Energy and Environmental Protection Climate Resilience Fund

Connecticut Department of Energy and Environmental Protection is making available up to $44.8 million in federal and state funds to protect communities and critical infrastructure in extreme weather (Connecticut Department of Energy & Environmental Protection, 2025). These funds are consistent with the core goal of airports as energy nodes and could provide significant financial support.

Demand Response and Ancillary Service Markets

Airports can participate in demand response and ancillary service programs by leveraging their on-site generation to support grid stability and earn additional revenue. During peak demand or grid stress events, an airport can reduce or shift noncritical energy use (such as HVAC, lighting, or charging systems) or dispatch stored energy to help balance supply and demand. In return, utilities or grid operators compensate participants through capacity payments, energy payments, or performance-based incentives. Airports may also provide ancillary services such as frequency regulation or voltage support by using fast-responding on-site generation or energy storage systems. These programs can generate new income streams while reducing operational costs by lowering demand charges and optimizing energy use. Integrating demand response into operations can improve energy resilience for the surrounding area, enabling the airport to maintain critical systems during outages or emergencies while reducing the stress on the nearby grid. These controls can be automated or handed off to a third-party aggregator, avoiding logistical burden for the airport. Ultimately, demand response participation turns the airport's energy infrastructure into a flexible grid asset, aligning economic, operational, and environmental goals with the local utility. Although these programs may be lucrative, releasing control to an aggregator or utility may make it more difficult to maximize resilience or optimize on-site operations because the airport may be beholden to other stakeholders.